5/1/2023

The conceptual design of a graving dock

Using Life Cycle Analysis to reduce the carbon footprint of a graving dock for Damen Harlingen

Johannes Idsinga
4719646

Image cover page: aquatech diving website, source: https://www.aquatech-diving.com/nieuwbouw-civiel/

The conceptual design of a graving dock

Using Life Cycle Analysis to reduce the carbon footprint of a graving dock for Damen Harlingen

by

Johannes Idsinga
Student number: 4719646

Delft University of Technology
May 2023

Thesis committee:	Prof.dr. H.M. (Henk) Jonkers - Chair	TUDelft
	Dr.Ir. C. (Cong) Mai Van - Member	TUDelft
	Ir. R.E.P. (Richard) de Nijs – Member	TUDelft
	Ir. J.J. (Jan Jacob) Altenburg – Member	Adonin B.V.
	Ing. F. (Frank) Seinen – Member	Damen Harlingen

Department of Hydraulic Engineering
TU Delft
May 2023

Preface

This report present the final thesis for my Master Hydraulic Engineering at the Delft University of Technology. The topic of this report is the conceptual design of a new graving dock for Damen Shiprepair and Conversion B.V. in Harlingen, where the sustainability through minimization of the carbon footprint of the dock is the main focus.

I would like to thank my thesis committee for guiding me throughout this project and providing me with useful feedback and advice during the process of writing this report. A special thanks to Jan Jacob Altenburg, Gert de Vries and the other colleagues at ADONIN B.V. for welcoming me at their office where I could spend time on working on my thesis and have interesting discussions which helped me out tremendously. I would like to thank Frank Seinen of Damen Harlingen for allowing me to have such a broad and interesting thesis topic and his help throughout the process. Finally I would like to thank my girlfriend, friends and family for supporting me, with a special thanks to my dad for his endless support, ideas and enthusiasm during the past months and beyond.

Johannes Idsinga
Bolsward, March 2023

Summary

In order to meet the increasing demand for a larger capacity, Damen Shiprepair and Conversion B.V. in Harlingen is considering to construct a graving dock near its current shipyard. This thesis aims to facilitate this process by developing a conceptual design of the graving dock, where the minimisation of the environmental impact of the whole life-cycle of the dock is crucial due to the vicinity of Natura-2000 areas and the increased importance of sustainability in the construction sector. The design should fit in the current surroundings while all the specified requirements regarding the functionality and structural integrity of the dock are still met.

Between the various types of dock it soon became clear that the dock in question should be a graving dock with a hall on top. The scope of this report is determined in such a way that the focus will not be on the design of the hall structure but the report substantiates this decision by pointing out the benefits that a hall cover where the temperature can potentially be regulated offers for the quality and efficiency of the ship maintenance works, but also for the structural integrity of the dock floor. The location-specific challenges that are presented include the sedimentation of the dock chamber that is expected to be caused by tugboats that stir up the bottom of the harbour, leading to an inflow of sediment into the dock chamber because of the pressure gradient that is created when a vessel enters or leaves the dock. Mitigation measures to prevent this inflow of sediment are presented in order to prevent the cleaning and disposal of the sediment. Another sustainable design alternative that is included focuses on the optimization of the dock floor package by adding a structural function to the underwater concrete floor (UCF) layer that traditionally only has a water retaining function by the addition of fibres to the concrete mixture.

Firstly, a base design is made that includes this traditional floor build-up and does not include any sedimentation reduction strategies. In this way, the dimensions of the base elements of the dock such as the retaining walls, tension piles and dock gate are designed and the effects of applying the sustainable design alternatives can be determined. The Terms of Reference summarizes the main requirements for the graving dock, that needs to be able to dock a design vessel with a length of 135 meters, width of 21.5 meters and a draught of 7 meters. Including sufficient tolerances on either side of the vessel to perform the maintenance works, the total dimensions of the dock chamber have been set at a length of 150 meters, width of 30 meters and depth of 11.8 meters. The ship-carrying block height must be 1.8 meters and the dimension of the covering hall are a minimum length of 155 meters, width of 50 meters and a height of 40 meters. The requirement for the tension piles of the dock foundation is that they must reach the Pleistocene soil layer in order to prevent pile settlement over time that has been known to cause damage nearby.

Eventually, the dock chamber structure consists of a combi-wall profile with GEWI63.5 anchors and tension piles that are installed at a grid of 2.5 by 2.4 meters. The UCF of the base design has a thickness of 1 meter and structural floor with a thickness of 0.5 meters is placed above it. The design gate has a width of 30 meters, a height of 12.8 meters and weighs 270 tons. Using this base design, the environmental hotspots are determined using a life cycle analysis (LCA) and clearly identify the amount of reinforced concrete and the sediment removal process as the two ‘hotspots’ in the total carbon footprint, for which sustainable alternatives are developed. Three design variants are initially created, which each differ on three design aspects: the build-up of the UCF package, the sedimentation reduction strategy and the gate operation type. Variant A has a 800 millimetre thick steel fibre reinforced UCF integrated with a 330 millimetre thick structural floor, saving a considerable amount of concrete compared to the base design. Variant B contains basalt fibres instead of steel fibres, the total thickness of these two variants are equal. Variant C has a 850 millimetre thick reinforced UCF with traditional rebar reinforcements. In the design of these floor variants, it has found that the influence of the thermal load, caused by fluctuations in temperature throughout the year, will lead to significant stresses in the floor and the temperature decrease during winter can lead to cracks in the top fibre of the concrete floor, which further substantiates the idea of placing a

hall on top of the dock where the temperature can be regulated using excess heat from the waste incineration plant since this will increase the durability of the dock floor. As far as the sediment reduction strategies are considered, variant A contains a gated inlet on the opposite side of the chamber that aims to take away the pressure gradient during docking, Variant B has a bubble screen that filters the sediment out of the inflowing water and Variant C aims to make the use of sediment-stirring tugboats redundant by using winches to dock the vessel. Variant A contains a caisson gate, Variant B combines the bubble screen with a sliding gate that is powered by the same hydro jet installation and Variant C has a mitre gate system. The reduction in carbon footprint is first assessed by performing the LCA, where the different design aspects are also assessed separately. This eventually leads to another design Variant D, which is a combination of the most sustainable aspects, namely a basalt fibre reinforced UCF with the gated inlet and caisson gate. In this configuration the total carbon footprint of the dock is reduced by nearly 50% compared to the base design, amounting to roughly 12.500 tons of CO_2-equivalent emissions. The required cost of investment and expected revenues are determined next, where investments of roughly 7.6 million euros and the return of investment is 20 years are found on average. The results of the LCA and cost benefit analysis (CBA) for each design variant are then used to perform a multi criteria analysis (MCA), that also take the ease of operation, ease of maintenance and constructability of the design variants into account. The conclusion of this MCA was that variant D gives the optimal combination of strengths of the different design elements, since the basalt fibre reinforced UCF leads to an optimal combination of construction costs and emission reduction benefits, the use of the gated inlet allows for the most swift and easy operation of the dock and maintenance can easily be performed to the caisson gate. A more general conclusion is that the LCA and Cost Benefit Analysis also proved that sediment reduction strategies should always be a point of emphasis in the design of a graving dock, since it targets one of the main contributors to the carbon footprint, saves a considerable amount of operational costs each year and allows for a faster docking procedure.

Table of contents

Chapter 1: Introduction

In view of the expected development in the maritime industry regarding vessel dimensions and the increasing demand for capacity, Damen Shiprepair and Conversion B.V. in Harlingen potentially wants to construct a graving dock. A graving dock is a permanent dock where construction, repair and maintenance of large vessels can be carried out. After the vessel is manoeuvred inside the dock and placed on blocks, the dock doors will close and the water is pumped out of the dock, exposing the vessel and allowing the maintenance or repair works. The new dock will be constructed on a large piece of unused land next to a waste incineration plant, near the current Shipyard in Harlingen. The new dock is to be constructed on a large piece of unused land next to a waste incineration plant, near the current Shipyard in Harlingen. An overview of the potential construction site is shown in Figure 1 below, which also shows the location of the shipyard and the waste incineration plant. It has to be noted that the red square doesn't represent the dimensions of the graving dock but merely indicates the global position of the building location.

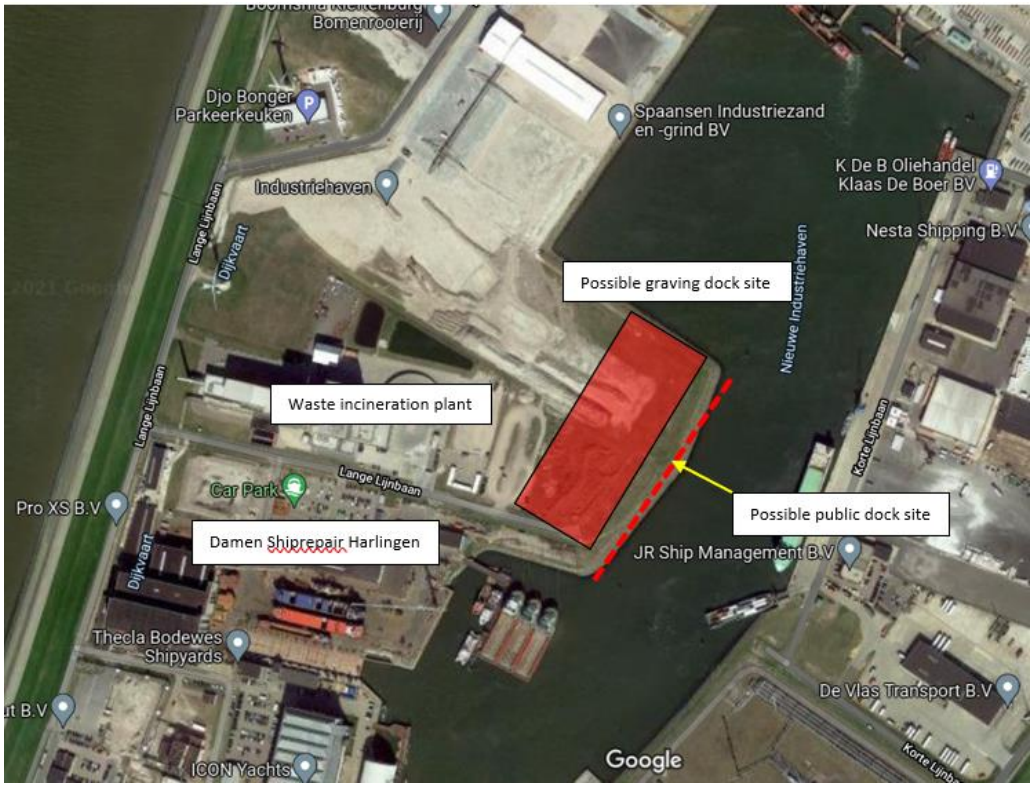

Figure 1: Overview of potential graving dock location

In order to reduce global warming, the Netherlands aims to cut down its CO_2 emissions by 2030 by 49% as determined by the Paris Climate Agreement in 2015 (Rijksoverheid, 2022). In combination with the current nitrogen problems in the Netherlands, where an excess of nitrogen emission leads to deterioration of the flora and fauna, the need for an increased sustainability and subsequently the reduction of environmental impact during construction and operation has become essential for the civil engineering industry (PH bouwadvies, 2022). Therefore, the main objective of this thesis is to develop a conceptual design of the graving dock, where the minimization of the environmental impact of the whole life-cycle (construction, operation and end-of-life) of the dock is key. The design should fit in the current surroundings while all the specified requirements regarding the functionality and structural integrity of the dock will still have to be met.

In order to do so, firstly a literature review will be conducted to investigate all the technical aspects that play a role in the design, construction and operation of a graving dock. Location specific factors such as the sedimentation rate of the dock are researched as well as the structural components that make up a dock. Afterwards, the environmental impact of a graving dock is discussed and the possible reduction strategies are treated. Conclusions from these chapter will be taken into account when setting up the Terms of Reference that serves as a basis for the design and includes all design wishes and requirements given by the client. The boundary conditions such as soil characteristics, water levels and groundwater levels will be determined so that a base design can be made. This base design is a conceptual design that contains the main dock components such as the retaining walls, UCF floor and gate. The sustainable design alternatives are then applied to the base design and design alternatives are developed that focus on reducing the carbon footprint of the base design by looking at the build-up of the floor package, the prevention of inflowing sediment and the different modes of operation for the dock gate.
These design alternatives are evaluated based on their performance in a Life Cycle Analysis that assess the carbon footprint of the base design and design variants to firstly identify and justify the hotspots in the base design and then compare the effects of implementing the different design alternatives. A multi criteria analysis eventually determines the optimal combination of sustainable design options by also considering the required investments (by performing a cost benefit analysis), feasibility and ease of operation.
All in all, this report is build up in the following way. Chapter 2 contains the literature review focusing on the technical details that are involved with the design of a graving dock. Chapter 3 will dive into the environment footprint of a graving dock, Chapter 4 will describe all the requirements as specified by the stakeholders in the Terms of Reference. Here, section 4.2 will describe all the relevant boundary conditions and Section 4.3 will conduct a stakeholder analysis. Chapter 5 then starts the development of design alternatives by making the base design in chapter 5.1. Next, chapter 5.2 starts the develop of design alternatives which are further elaborated in chapter 5.3. In chapter 6 these design variants are evaluated based on their environmental impact (chapter 6.1) and costs (chapter 6.2) and the results are then cooperated in making a decision to determine the optimal design combination in chapter 6.3. Finally chapter 7 shows a final overview of the optimal design combination and chapter 8 gives the conclusions and recommendations.

Chapter 2: Literature review

The aim of this literature study is to introduce ship docks by looking at the types of ship docks that exist, the main components that make up a dock and the desired function. Furthermore, the desired location of the ship dock is analyzed with regards to the external factors that will play a role in the design, the following sub questions are aimed to be answered by this chapter:

- What types of docks exist and which type will form the basis for the design?
- Which location-specific factors will play a role in design of the dock?
- What are the main structural components of a dock?

Answering these questions enables a good preparation for the next phases of the project.

Chapter 2.1: Dock types

Before the various existing dock types are introduced, it is important to understand the mode of operation of a dock, from the moment the ship is preparing to enter the dock until departure of the ship from the dock after the maintenance works are completed.

The most basic description of a dock is a place where a ship can be repaired in a dry environment without having to put the ship on land. In the initial stage of docking, the dock is fully emerged in water and the vessel is maneuvered in the required position, usually with the help of tugging boats. The ship sails into the dock which can be done 'manually' by slowly moving the ship along the bollards using the mooring lines and hauling-in winches on the ship. After the ship is moved into the desired position, the mooring lines are tightened by the winches to keep the vessel steady. Subsequently, the dock doors will close and the water is pumped out of the dock by the docking station until the vessel rests on the blocks. The repair/maintenance works can now take place during which easy access for personnel to the ship hull is important. This can be realized by making sure the blocks have a sufficient height so that workers can walk underneath the vessel and by including access ramps and/or lifts for equipment and personnel to quickly access and leave the dock. After construction works are done, water is drained into the dock again which lifts the ship off of the blocks. The dock doors are opened and the vessels sails out of the dock (Teekay Corporation, 2018).

Now that the docking procedure and mode of operation is known, the various types of docks can be treated, starting off with the floating dock. As the name suggests, floating dock are moveable docks that are able to submerge themselves during docking. The dock is typically a steel U-shaped structure with a set of ballast compartment at the bottom that can be filled up with water at the start of the docking procedure. The ballast compartments slowly fill and pull the dock downward until the draught is sufficient for entry of the ship. As soon as the vessel is manoeuvred into the correct location, the ballast water is pumped out of the compartments and the vessel is slowly exposed, allowing the opportunity for maintenance works to be carried out and when these are finished, the compartments are filled back up and the vessel can sail out of the dock. Advantages of a floating dock include its mobility and efficient space usage, low maintenance costs and flexibility with regards to retrofitting. On the downside, the fact that the steel structure is constantly submerged in salt-water leads to large amounts of corrosion which reduces the structural integrity over time and the influence of the tidal and weather conditions make this dock type less robust.

A picture of one of Damen's former floating docks in operation is visible in Figure 2.

Figure 2: The floating dock before (right) and after (left) the vessel has entered the dock

The other main dock type is a graving dock or permanent dry dock. It is constructed on land and consists of a concrete and steel structure that includes a (re)movable gate, floor and walls. During operation, the vessel is maneuvered into the filled dock and the gates are closed as soon as the vessel is maneuvered on the blocks in the correct position. Pumps are then used to empty the dock and expose the vessel as a result, allowing the maintenance of construction works to take place. Graving docks can also be used for the construction of vessels, as is the case with the graving dock at Icon Yachts in Harlingen. When the gate of the Icon Yachts needs to be opened, it is completely removed by using the cranes that are present at the dock. The pictures below show the dock gate and the rails at the top of the gate that stick out so that the cranes can be moved in the adequate position to remove the gate. The gates of the new dock are expected to be opened more frequently and other solutions for opening the gate will also need to be explored but the option of removing the gate is interesting nonetheless. Furthermore, the graving dock can be split into section by the placement of the intermediate gate, which can also be found on the picture below.

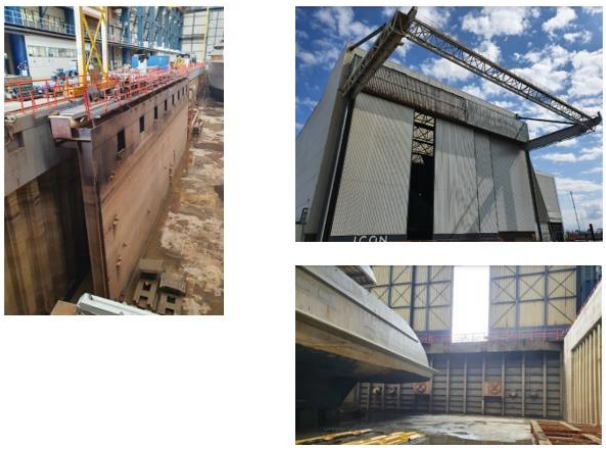

Figure 3: Icon yacht's graving dock, including the intermediate caisson gate (left), the crane rails sticking out of the dock to facilitate removal of the gate (top) and the dock gate seen from inside the dock (bottom)

Advantages of a graving dock include it's long life span and larger capacity. The supply of equipment, personnel and machinery is a lot easier due to the location of the dock near the land and the possibility of placing one or more ramps facilitates this.
On the contrary, the initial construction costs are high and the maintenance costs of the graving dock can become high as the lifetime of the dock increases. Typical docks can have lifetimes of up to 100 to even 200 years and to stay functional, maintenance costs might increase significantly. Furthermore, the presence of a movable gate brings the risk of jamming, mechanical issues or other problems which would make the complete dock non-operational (Marine Insight, 2021).
It is possible to construct a large hall that covers the graving dock which can ensure a controlled environment for performing the maintenance works. The emissions that might occur during the works, such as dust, sand or paint, is trapped inside the dock and prevents it from directly being exposed into the environment which reduces the climate impact. The presence of a hall also adds the possibilities of installing workshops near the dock which prevents the transport of products to and from the vessel and it opens up the possibilities for placement of overhead travelling cranes, as is the case at the Icon Yachts dock (British Standard, 1988). On the contrary, the construction of a hall requires a significant amount of steel which increases the costs of construction and considering the typically large dimensions of such a hall, the magnitude of the wind force will subsequently be significantly large as well.
Other alternatives include a shipping lift, which is currently the way of docking vessels at Damen Harlingen, a closer description of this docking procedure can be found in Appendix K. This lift can only handle ships with a limited dimension and uses large blocks which can move over rails that are installed in the floor of the shipyard to position the vessel on the desired location for the construction works.

Since the client's main wish is to increase the capacity of the shipyard, a graving dock is preferred over a floating dock which is mainly due to the higher future-proofness of a graving dock. Not only can larger vessels be handled in a graving dock, which is desirable considering the development of vessel dimensions in the shipping industry over the last decades (Tran, 2015), but the possibility for placement of an intermediate door(s) allows multiple vessels to be handled simultaneously. Furthermore, the benefits of a hall on top of the dock with regards to the reduction of emissions and consequently the environmental footprint during operation of the dock as well as the opportunities for conducting repair works in a controlled environment leads to the final decision: the dock that will be designed will be a graving dock with a hall on top that covers the dock. This decision will be taken into the Terms of Reference in the next chapter as wish of the client.

Chapter 2.2: Location-specific effects

The location of the graving dock plays a large role in the determination of the design through the boundary conditions of the location. The specifics of these boundary conditions will be collected in the Terms of Reference in the next chapter but here, the concepts behind some of these effects such as the siltation of the dock and the influence of the presence of the Wadden Sea through the Natura 2000 guidelines are introduced.

Section 2.2.1: Siltation of the dock

Inflow of silt during operation of the dock is relatively common for graving docks, this sediment first needs to be removed before the maintenance works can be carried out. In present, the silt is removed manually which is a time-consuming job that increases the cost of operation of the dock through personnel and delays in the work schedule. Furthermore, the silt can be contaminated and disposal of the silt after removal leads to additional unwanted costs and environmental impact. The amount of inflowing silt depends on a number of factors and can be driven by multiple large- and small scale processes. Appendix L treats the larger scale processes that are expected to play a minor role in the sedimentation of the new dock due to its location within the port of Harlingen.

Local processes will play a more prominent role in the sedimentation of a dock, for example the maneuvering of the vessel in the turning circle and entering the dock which will locally increase the inflow of silt caused by exchange due to turbulence and the resulting velocity difference. In fact, the majority of the sediment is expected to enter the dock during the entrance of the ship into the dock chamber and (especially) during the exit of the ship from the chamber. When the vessel is maneuvered into the chamber with help of a tugboat, the propeller jet of the tugboat will stir up the layer of sediment at the bottom of the harbor (port authorities expect a layer of fine sediment or sludge of 0.5 to 1.5 meter at the bottom of the harbor), increasing the turbulence near the bed and sediment concentration of the water near the bed. At this moment in time, the dock chamber is completely filled up with water as the dock gate is opened and the ship is ready to sail into the chamber. As the ship slowly moves into the port, a body of water with the same volume as the displacement of the ship needs to leave the chamber, which creates a return flow out of the chamber along both sides and underneath the vessel that will (partly) wash away the sediment flow but can also leads to the entrance of sediment together with the vessel. This process is illustrated in figure 4, where a side view and top view is drawn as well as an indication of the flow lines of the return flow and the expected location where the increase in turbulence will be.

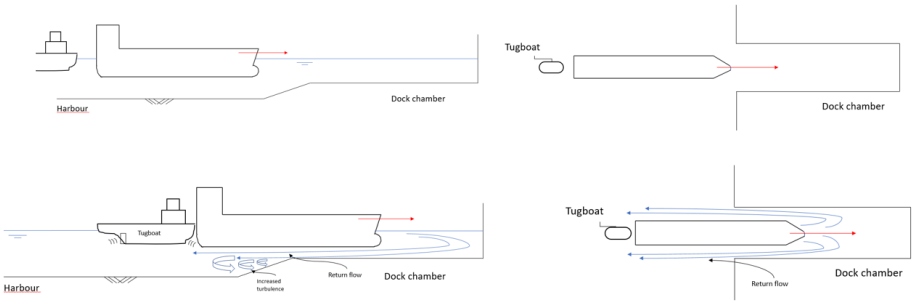

Figure 4: Sedimentation process during docking

When the vessel exits the dock chamber, a flow of water which is equal to the displacement of the vessel will flow into the chamber, through a kind of suction effect. In this situation the flow will take the sediment that has been stirred up by the propeller of the tugboat, that pulls the vessel out, into the dock chamber. This process is illustrated in figure 5 and most of the sediment inflow is expected to occur in this process.

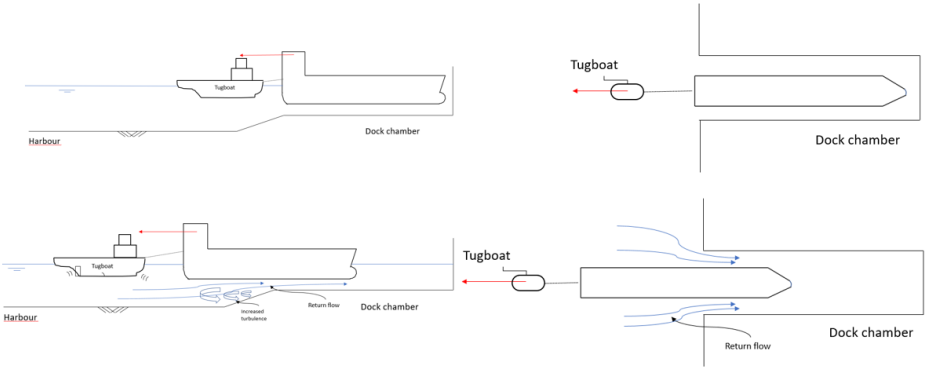

Figure 5: Sedimentation process during undocking

Possible mitigation measures for the sedimentation of the dock chamber are developed in Chapter 5.2.

Chapter 2.2.2: Nitrogen emissions

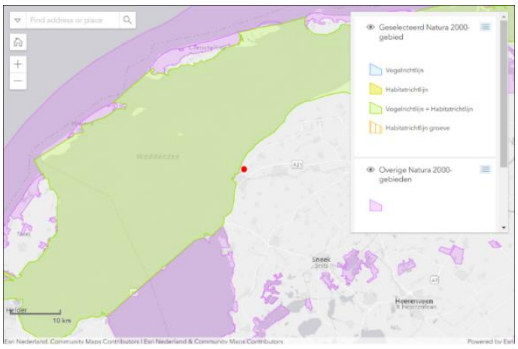

Figure 6: Relative location of Damen shipyard (red dot) with Natura2000 area, source: (Natura2000, 2022)

As visible on Figure 6, the Damen Harlingen Shipyard, highlighted with the red dot, is located at close proximity to the Wadden Sea, which is identified as a Natura 2000 area and is listed under both the Birds Directive and Habitat Directive. This means that active protection guidelines exist to preserve the Wadden Sea habitat and the species that rely on it. In fact, the Wadden Sea is mentioned as the *"biggest and - from an international perspective – most important Natura 2000-area in the Netherlands"* (Natura2000, 2022).

Active protection guidelines are mainly focused on the reduction of emissions, especially CO_2 and nitrogen. Especially the latter is a large cause of concern for the Netherlands and in order to reduce the emissions of these gasses and improve the wellbeing of nature areas in the Netherlands, the government created the 'nitrogen law', called 'Wetsvoorstel stikstofreductie en natuurverbetering', which aims to have the nitrogen level in at least half of the Natura 2000 areas in the country at a safe level by the year 2030 (Rijksoverheid, 2020). This law became active starting from the 1st of July 2021 and contains an exemption for the building sector, the so-called 'Bouwvrijstelling'. This states that the nitrogen emissions during the construction phase for building projects will not count towards determining the effect of the project on the Natura 2000 area. This relies on the temporary nature of the construction works and the relatively small impact of the emissions in the greater picture of the nitrogen problems (Rijksoverheid, 2021). This statement is supported by Figure 7 where the contribution of each sector to the total nitrogen emission can be seen and the contribution of the construction sector is negligibly small (RIVM, 2021).

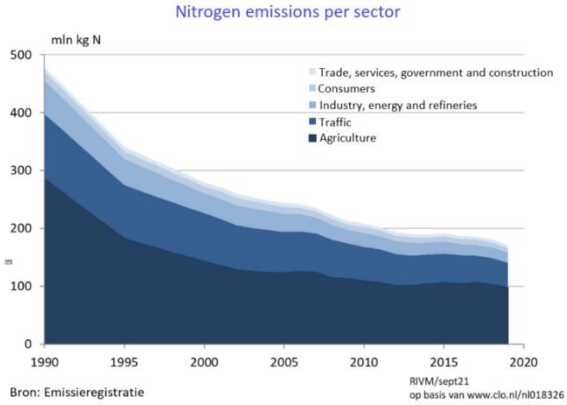

Figure 7: Contribution of different sectors to the total nitrogen emissions

Several options exist for minimization of the emissions during the construction phase of the dock but the main focus should be on the operational phase of the dock. The current laws do not allow for any nitrogen disposal, so 0,00 mol/ha/year during the use phase of the dock (Bij12, 2022). Since the main source of nitrogen dioxide emissions is the combustion of fuels, other zero-emission energy sources need to be applied during the use phase of the dock, appendix L gives more background information regarding this issue.

Chapter 2.3: Main dock components

In this section, the main components for the design of the docks are mentioned and various alternatives are introduced. While these alternatives are more accurately compared and assessment during the design chapter of this report, in order to make an adequate design, it is important to have a clear view of the components that make up a dock and all the sub-systems that need to be present for operation of the dock.

Section 2.3.1: Dock gates

The dock gates mainly have a water retaining function, after the water has been fully pumped out of the dock, the doors need to withstand large (hydrostatic) loads for a considerable amount of time and transfer this to the supports at the lock head, in order to ensure safe conduction of the maintenance/repair works and safety of personnel.

Various dock gate types exist, varying in gate movement, which is often either a translational or a rotational movement. The most frequently applied gate types are described in Appendix M, though it has to be noted that these are the most commonly used lock gates, the requirements for lock gates regarding the water tightness of the door differ from that of a dock door. The most commonly applied lock gate types are mitre gates that move by a rotation around the vertical axis, single leaf gate that operate in a similar way as the mitre gates, sector gates that rotate around either the vertical or horizontal axis, lift gates that use a vertical translation movement to open, rolling- or sliding gates that uses a horizontal translational movement during operation of the dock and finally a caisson gate that is completely removed by cranes or other machinery. Other types exist as well but are less commonly applied in practice, caused by various reasons such as construction costs or complexity of operation. Further details such as the advantages and disadvantages of the gate types are treated in Appendix M, figure 8 shows the operation of a caisson gate for reference.

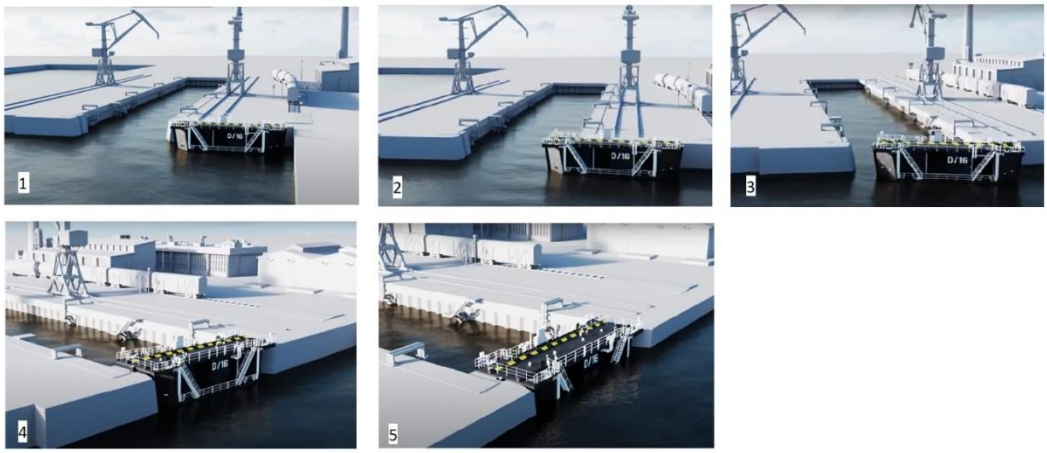

Figure 8: Operation of a caisson dock, source: (Ravestein Shipyard & Construction Company, 2017)

All in all, the main challenges in design of the lock gate is ensuring a relatively fast and efficient operation procedure while keeping the watertightness of the gate intact. Even though a certain leakage discharge is inevitable, this needs to be minimized. Furthermore, the operation of the opening and closure of the gate must be sufficiently robust, so minimization of the probability of jamming or mechanical issues is crucial.

Section 2.3.2: Filling and Emptying system

Two main types of filling and emptying system can be distinguished. The first type is head filling where the gate has valves near the bottom of the gate that will be opened in case the repair works have ended and the gate needs to be opened. The type of filling system is most commonly applied in docks due to its cheap installation and operation. In figure 3 the two valves in the gate of the Icon Yachts dock can clearly be identified.
The second type of filling system is a longitudinal culvert system which can be applied in cases with head differences of up to 25 meters. The inflow of water is distributed over multiple location

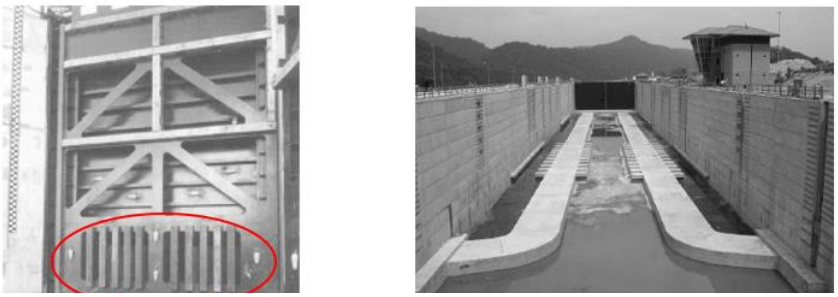

Figure 9: Head filling system (left) with valves and energy-breaking structure circled red and the longitudinal system (right)

along the length of the dock, in this way no turbulent zones will be created in the dock. The large increase in cost of construction is the major downside of this filling and emptying system (Molenaar, Locks, 2020). Figure 9 shows two types of filling and emptying systems.
For the design of the graving dock, the head filling seems to be the most desirable option considering the low costs that are involved with this type of filling system that seem to outweigh the benefits of installing a system with longitudinal culverts. This decision is further supported by the fact that longitudinal culverts are most often applied in cases of extreme head differences which will not be the case in Harlingen.

Section 2.3.3: Dock head structure

The exact layout of the dock head structure heavily depends on the type of dock gate that is applied in the design but in general, three main functions can be distinguished for the dock head structure:

- Accommodate the gate and all the equipment that is necessary for operation of the gate. For example, in case of a rolling or sliding gate, the dock head structure should contain sufficient recess space for the gate to be stored in during opening.
- Water tightness and water retention. Sufficient sealing of the dock gate must be present such that the leakage discharge in closed conditions is minimized. Furthermore, seepage of groundwater underneath and alongside the head structure must be avoided in order to prevent erosion and piping of the structure. The dock head and the dock chamber must be connected in a watertight manner.
- Transfer of loads. The lock head has to transfer the large hydrostatic force during closure of the dock gate towards the foundation.

The most common lock head structure is an open concrete box or U-profile, where the floor of the head is rigidly connected with the walls. Figure 10 shows the most standard U-shaped profile and an example of lock head that has been modified to fit the gate type, which in this case is a mitre gate. As mentioned before, the shape of the dock head will depend on the gate type that is chosen and the required space for equipment and recesses that the gate requires (Molenaar, Locks, 2020).

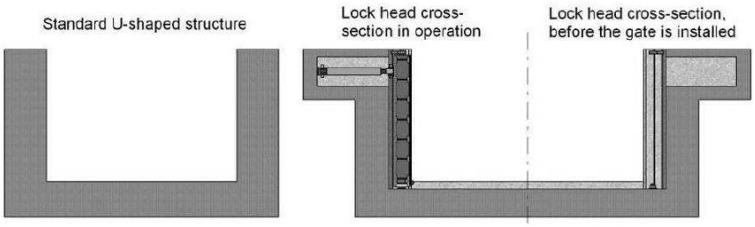

Figure 10: Standard dock head U-shaped profile, source: (Molenaar, Locks, 2020)

Section 2.3.4: Dock ship chamber structure

A dock chamber consists of a combination of walls and a floor that together provide a soil and water retaining function for the dock, and transfers the loads due to the weight of the vessel and all additional equipment to the soil. For the dock chamber walls, the most common configurations are listed.

- A gravity structure that uses its self-weight to ensure stability, which might mean that a large volume of concrete is necessary for equilibrium of horizontal forces. Furthermore, sufficient friction is necessary between the structure and the soil to prevent sliding of the gravity wall.
- Retaining wall structure, for which sheet-pile walls, combi-walls and diaphragm walls can be used. Anchors can be installed to ensure stability and to reduce the bending moments in the wall.
- Walls can be combined with a deep foundation in case the dock chamber has a large depth or if sand layers with a high bearing capacity can only be found at a large depth. With this configuration, the forces acting on the top structure are transferred by foundation piles into the soil.

The floor of the dock chamber needs to transfer the forces of the structure resting on top of it towards the soil. Another important requirement for the floor is the fact that it needs to be impermeable so that there is no risk of water flowing into the chamber during the repair works. A commonly applied floor type is an underwater concrete floor in combination with tension piles that prevent the uplift of the floor.
The selection of the right combination of walls and floor depends on a number of factors such as the required dimensions of the chamber, soil and water level conditions, construction requirements such as the dimensions of the available construction site and the availability of materials and equipment. Naturally, the costs and environmental impact that is involved in the construction of the dock chamber play an important role as well.
An interesting option is the use of a foil construction, or foil polder. This method is often applied in underground infrastructure such as viaducts or tunnels. In principle, a large building pit is dug with a slope of approximately 1:3. On the bottom of this building pit, a watertight plastic foil (PVC or HDPE) of a few millimeters thickness is placed. The building pit is filled with ballast soil and the remaining water is pumped out. In the middle of the building pit, the graving dock can be constructed. The foil layer is impermeable and the ballast soil ensures vertical equilibrium of forces. The main advantage of this type of construction is the fact that a large thick underwater concrete floor is no longer necessary, reducing the costs and climate impact of the design considerably. However, sufficient space has to be available on both side of the graving dock, since the slopes need to be constructed initially.

Chapter 3: Environmental impact of a graving dock

In this chapter, the concept of sustainability and the way in which it can be applied in engineering projects is treated. First of all, the definition of sustainability in design and the relevant philosophies are introduced in chapter 3.1. Afterwards, the way in which the sustainability of a design is determined in practice, namely by performing a Life Cycle Assessment, is introduced in chapter 3.2. Finally, the main sources of emissions during the life time of a graving dock and potential sustainable alternatives are treated in chapter 3.3.

Chapter 3.1: Introduction of sustainability

In order to be able to assess the sustainability of a graving dock, it is first important to understand what is meant with the term 'sustainability'. According to the Brundtland Commission, who published their United Nations report 'Our Common Future' in 1987, Sustainable Development can be described as follows:

'Sustainable development ensures that it meets the needs of the present without compromising the ability of future generations to meet their own needs' (Brundtland, 1987)

The term 'needs' here describes both the availability of resources which might otherwise become depleted as well as the presence of a 'clean environment' and 'healthy and prosperous living conditions'. The use of substances which are harmful to the environment and those that cannot be replenished or easily removed from the atmosphere should therefore be prevented. The three main subjects that were addressed by The Brundtland Commission in relation to sustainable development were: 1. Environmental aspects including limited use of finite resources and no release of harmful emissions, 2. Social aspects such as equality and education and 3. Economic growth (Jonkers, 2018).
In this definition, a link can be made to the 17 sustainable development goals which were defined by the United Nations in 2015 as a *'call to action to end poverty, protect the planet and ensure that by 2030 all people enjoy peace and prosperity'* (UNDP, 2022). Similar to the subjects that were defined by the Brundtland Commission, these SDGs are focused on *'social, economic and environmental sustainability'*. Figure 11 shows the 17 defined sustainable development goals (Global Compact Network Netherlands, 2022).

Figure 11: Sustainable development goals, source: (Global Compact Network Netherlands, 2022)

Relating these development goals and the subjects that were identified by the Brundtland Commission, it can be concluded that the realization of a new graving dock would mostly create opportunities for economic growth. In case Damen would decide not to follow the developments in the shipping industries by increasing their capacity, clients will choose for a different shipyard instead, which would not only have consequences for the economic development of Damen and its employees, but also for the economic development of the Harlingen municipality and surroundings. Where opportunities are created for economic growth, the main challenge for a construction project is to follow the sustainable developments goals that are related to environmental aspects. In civil engineering practices, this sustainable development means the transition from a linear to a circular building process, meaning the limited use of finite resources and no release of harmful emissions. Figure 12 shows this building cycle (Jonkers, 2018).

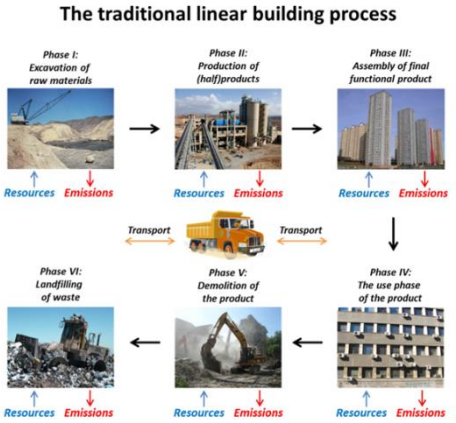

Figure 12: Linear building process, source: (Jonkers, 2018)

In an ideal future scenario, this building cycle is completely closed as the input of new raw materials is barely necessary due to the recycling and reuse of materials and elements of structures which are at the end of their lifetime. No emissions of harmful compounds occur anymore and waste is no longer considered waste but serves as a useful resource for new projects. This scenario can be seen in figure 13 (Jonkers, 2018).

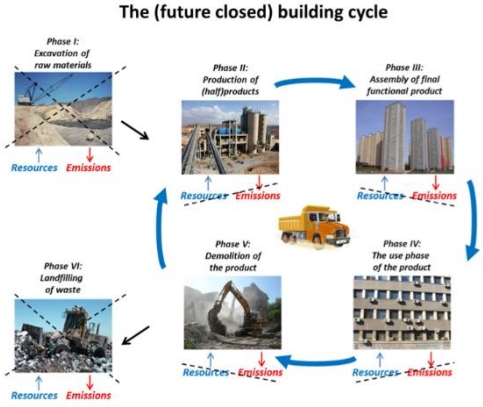

Figure 13: Circular building process, source: (Jonkers, 2018)

In order to contribute to this circular building cycle, the 9R framework has been developed by Potting et al in 2017, which states the possible strategies that can be implemented in a

construction project. Figure 14 shows the 9R framework (Potting, Hekkert, Worrell, & Hanemaaijer, 2017).

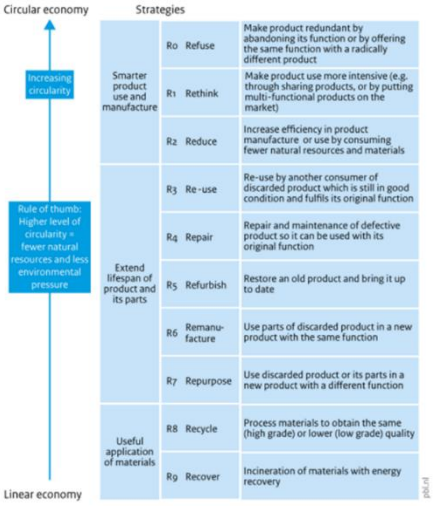

Figure 14: 9R framework, source: (Potting, Hekkert, Worrell, & Hanemaaijer, 2017)

As can also be read from figure 14, the shorter the loop in the R-framework, meaner the lower the 'R' strategy, the bigger the contribution to an increase in circularity is. For a construction project, this often means that the earlier these strategies are taken into account during the decision-making process, the more possibilities there are and the larger the level of impact of these strategies is. With level of impact, the project scale which is influenced by the strategy is meant. Looking at the figure 15, we can say that shorter strategy loops correspond to strategies which influence the structure on a macro level. The complete design of the structure with all its systems is done while keeping the strategy in mind. On the other hand, the largest strategy loops might only influence the structure on micro level, meaning the individual elements of the structure (Geng & Doberstein, 2008).

Figure 15: Scale of impact, source: (Geng & Doberstein, 2008)

The shortest loops in the 9R framework are Refuse (R0), Rethink (R1) and Reduce (R2). These strategies aim to use smart manufacturing, and smarter product use to eliminate the waste at the design stage itself. In Appendix N, it is described how these strategies could be implemented in the design of a graving dock.

The medium loops of the 9R framework (Reuse (R3), Repair (R4), Refurbish (R5), Remanufacture (R6), Repurpose (R7)) aim to extend the lifespan of materials in a structure. These strategies are closely related to the ease of disassembly of the design and depend on the amount of additional energy that is needed to make the element compatible with the current technology and market standards.

Recycle and Recovery (R8 and R9) are the longest loops in the framework and are typically applied to elements which are considered to be 'waste' which would require a large amount of energy input to create a new purpose. In a project, one should aim for the shortest loop

possible. For this project this would mean to not construct a graving dock at all and try to increase Damen's capacity in a different way, for example by purchasing an already existing floating dock which has the same dimensions. However, the decision of constructing a new graving dock has already been made at an earlier stage and at a 'higher level' of decision making. For the purpose of this thesis, the designer therefore has no say in this and this strategy (R0) will therefore not be considered. This can also be said for the Rethink (R1) strategy since structures such as a graving dock simply do not allow for a lot of multi-purpose functions except for perhaps the generation of green energy by placing solar panels.
The focus will instead be on the Reduce (R2) strategy, so to increase the efficiency in product manufacture or use by minimizing the amount of natural resources and materials since this allows for the implementation of more innovative design techniques.

Chapter 3.2: Life Cycle Assessment

It can be concluded that most of the possibilities for integrating one of these strategies in the actual design of the graving dock in an impactful manner lies in shortest loops and specifically in the Reduce (R2) strategy. In order to be able to minimize the use of raw materials and reduce the amount of emissions that are associated with the structural elements of a graving dock, these effects need to quantified. The way in which this is done in practice is by performing a Life Cycle Analysis (LCA) which can describe the environmental impact of the various structural elements during the life time of the product, and describes it in terms of a monetary value, called the Environmental Cost Indicator (ECI). The LCA tool DuboCalc, which is used for civil engineering projects in the Netherlands, uses environmental data of construction materials, construction products and construction-related processes from the National Life Cycle Inventory ('Nationale Milieudatabase') to describe the effects of structural element across several impact categories during every phase of the product's lifetime. In this way, the ECI value for each individual impact category or building phase can be determined or even combined into a ECI value for the complete structure as a whole. For more information regarding the different impact categories and life cycle phases that are typically identified by LCA-software such as DuboCalc, the reader is referred to Appendix N.

Chapter 3.3: Emission sources and sustainable alternatives

Once the 'hotspots' in the environmental impact of the design are known, which are the stages, structural elements or Environmental Impact Categories that contribute most to the total Environmental Cost Indicator of the graving dock, the design can be optimized by applying more sustainable alternatives in a targeted way. Examples of these sustainable design alternatives are treated in Table 1, where they are linked to their corresponding life cycle stage.

Table 1: Sustainable alternative and their corresponding life cycle stage

Life cycle stage	Sustainable alternative
A1 – Raw material supply	- Use sustainable building materials
A2 – Transportation from factory to construction site	
A3 – Manufacturing of the product	- Reducing the amount of concrete necessary in the dock floor by adding fibres to the concrete mixture.
A4 – Transportation from factory to construction site	- Focus on local manufacturers to reduce the amount of transport from production site to construction site.
A5 – Construction installation process	- Use emission-free construction machines/equipment
B1 - Use	
B2 – Maintenance	
B3 – Repair	
B4 – Replacement	
B5 – Refurbishment	
B6 – Energy use	- Generate energy through solar panels on construction hall roof. - Connect the dock to the residual-heat system from the waste incineration plant.
B7 – Water use	- Construct an additional water inlet at the opposite short side to prevent additional sediment cleaning works.
C1 – Demolition process	- Design for disassembly

C2 – Transport from construction site to waste plant	
C3 – Waste processing	
C4 – Disposal	

Some of these methods require some explanation, which is done in the following paragraph.

As far as the A3 stage is concerned, a possible alternative can be to add fibres to the underwater concrete mixture. Most building pits consists of two concrete floor, the first of which is the underwater concrete floor that serves as a watertight barrier to allow the dry pumping of the construction pit and it typically has a temporary function. The second floor is then placed inside the dry building pit and it is a normal reinforced concrete floor which is calculated as if there is no underwater concrete floor underneath. Due to the development of steel fibre reinforced concrete floor, it has become possible to integrate the underwater concrete floor into the structural floor and use this combination for both the water retaining layer as well as the structural floor for the dock. Some example where this Steel Fibre Reinforced Underwater Concrete Floors (SFRUCF) has been applied is the construction of the Albert Cuypgarage in Amsterdam and the 'Royal Van Lent' dry dock. When applying such a integrated SFRUCF, not only is the total volume of concrete needed in the design reduced, the redistribution of forces within the concrete floor is enhanced as well, leading to less leakages and a reduced risk of shrinkage cracks (Apon, 2019). However, the design of such a SFRUCF is not included in the current CUR77 guidelines, but a combination of CUR 77 and CUR 111 is used. Often, the SFRUCF is designed using a linear elastic beam model with a fictive E-modulus of 10.000 MPa (Apon, 2019). Other, more sustainable fibre types could be applicable as well.
One of the main sources of nitrogen dioxide (NO2) and carbon dioxide (CO2) is the combustion of fossil fuels, during the transportation and construction phases of the life cycle. In order to reduce this impact it is possible to use emission-free construction machines and equipment during the installation process (A5).
Considering the energy use of the dock, an interesting opportunity arises. The intended location of the graving dock is next-door to the waste incineration energy plant (Reststoffen Energie Centrale) owned by Omrin. This factory uses combustible non-hazardous residues from households and companies to generate energy which is in turn transformed into electricity. The residual heat that is created during this process gets transported to neighboring industrial companies such as the salt production company Frisia, where part of the residual heat is extracted and the remaining heat-carrying water is transported back to the REC. There are opportunities to expand this pipeline system and connect more places to use the residual heat for varying purposes. Also for a graving dock, this serves as an interesting possibility since some repair works require a constant working environment, for instance when specific types of vessel-coatings and/or paints have to be applied. Connecting the dock to the REC by expanding the existing pipeline infrastructure could serve as a sustainable energy source for the dock.
After the base design is made, the implementation of these a few of these design alternatives will take place.

Chapter 4: Functional Analysis & Programme of Requirements

This chapter aims to describe the basis of the design of the new dock. First of all, the wishes and requirements of the client regarding the facilities, dimensions and general layout of the port is described in section 4.1. Afterwards the various boundary conditions, including the natural, hydraulic and field boundary conditions and in the final section of this chapter, a stake holder analysis is performed.

Chapter 4.1: Wishes and requirements

The client's wishes and requirements are treated in this chapter, where first the functional requirements are treated, based on which a function and object tree is created for the dock. Section 4.1.2 handles the more specific requirements and wishes and Section 4.1.3 summarizes all requirements into a list and gives several visualizations of the dimensional requirements of the dock.

Section 4.1.1: Functional requirements

In any case, the main function of a dock is to enable ship repair and maintenance works to be carried out in a dry environment. Since this is the most import requirement that always needs to be secured, we can distinguish it as the primary function. Based on this, a number of secondary functions can be described that follow from, and support, this primary function. These secondary functions are listed below:

- The dock needs to be provide enough capacity to dock the design vessel, these exact dimensions will be handled later in this chapter.
- The inflow and outflow of water needs to be controlled.
- The dock doors need to be sufficiently watertight, meaning that the amount of water losses and leakage discharge need to be minimized.
- The dock should facilitate sufficient amounts of space for carrying out the maintenance works, meaning that a certain 'extra space' should be added to the dimensions of the design vessel.
- Possibilities for transportation of facilities (equipment, material, personnel) should be provided within the dock.
- The current existing ecological system should be preserved, meaning that the impact of the dock on the environment should be minimized.
- The amount of residual sediment, after emptying of the dock, should be minimized.

From the secondary functions, even some tertiary function can be identified although these serve more as a 'opportunity' than as a strict requirement. Firstly, the dock can ensure possibilities for docking multiple vessels simultaneously by using an intermediate door and secondly the dock (hall) could be used to generate energy by placement of solar panels on the roof of the hall. All of the abovementioned functions can be gathered and displayed in a so-called 'function tree' which can be found in Figure 16 below:

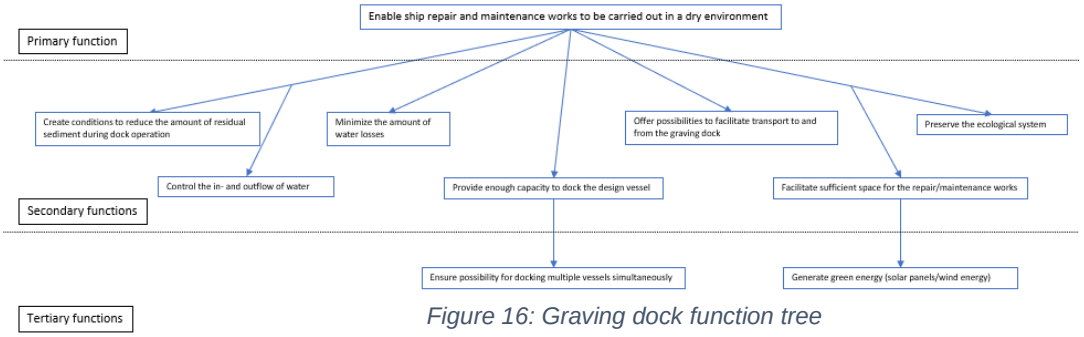

Figure 16: Graving dock function tree

Section 4.1.2: Specific requirements and wishes

Now that the functional requirements of the dock are known, the specific requirements and wishes from the client are treated. Appendix O elaborates on these requirements and can be identified into a so-called object tree, as visible in Figure 17. All of these element make up the total dock and need to be optimized in order to design the dock that meets all the requirements mentioned above.

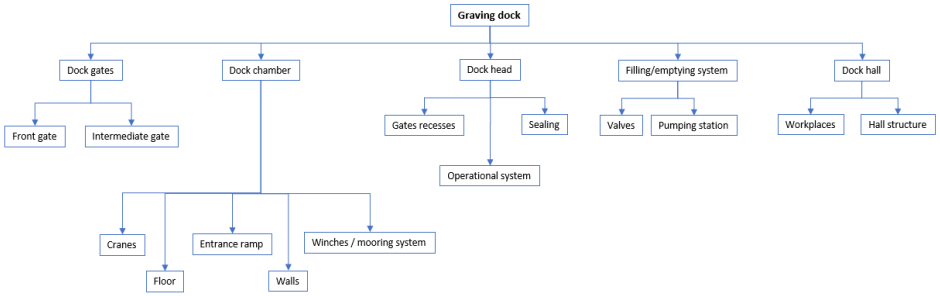

Figure 17: Graving dock object tree

Section 4.1.3: List of Requirements and visualizations

For clarity, the wishes and requirements from Appendix O are repeated in the list below:

Dock chamber requirements:

- Design vessel dimensions: L 134.65 m, B 21.5 m, D 7 m
- Chamber Length 150 m, Width 30 m, Depth 11.8 m
- Ship-carrying block height of 1.80 m
- Fast and effective removal of inflowing sediment

- Entrance ramp must enable entrance of aerial lift, a maximum slope of 20%.
  OR
- 2 overhead rail cranes with 2 trolleys each, capacity of 20 t per trolley

Covering hall requirements:

- Total length of 155 m, width of 50 m, height of 40 m
- Sufficient space for transport of materials and equipment by truck and/or forklift (clear space of 5-10 meters on either side of the dock)
- 6 workspaces must be present with dimensions of 10 x 8 meters and a height of 3.5 meters each, including an office area.

Dock components requirements:

- Dock doors must ensure completely dry environment, minimization of the leakage discharge is a key factor
- Maintenance to the dock door must be able to be performed
- Speed of operation for dock door and emptying/filling system is crucial
- It must be possible to remove the propellor shaft of the vessel within the dock

For reference, the dimensions of the dock and the dock hall are visualized in the following sketches.
Figure 18 shows a front view of the dock, where the design vessel MV Endeavour is drawn as well.

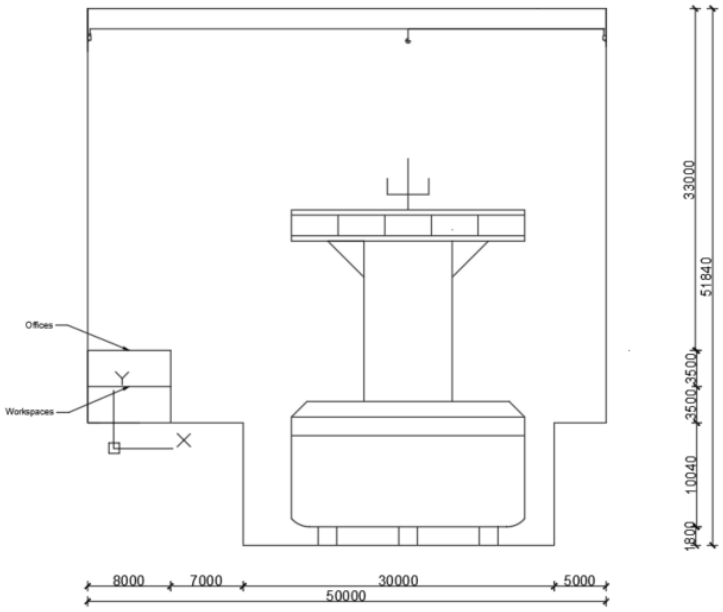

Figure 18: Visualization sketch front view

Figure 19 consequently shows a top view of the dock

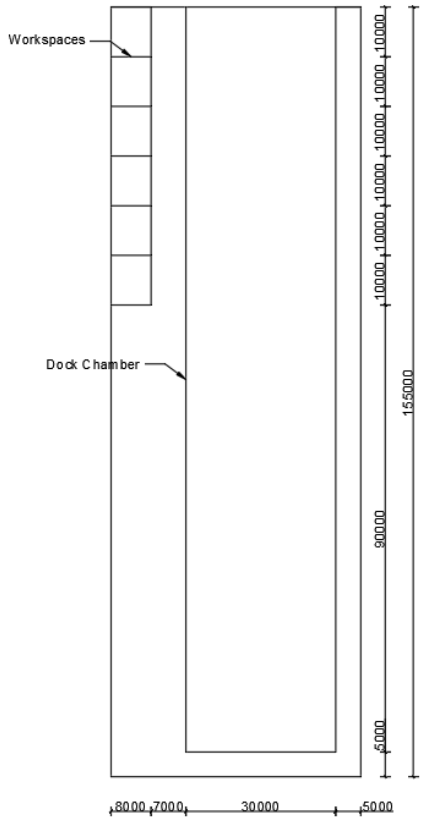

Figure 19: Visualization sketch top view

Chapter 4.2: Boundary conditions

The boundary conditions at the construction site sets the basis for the structural safety of the dock as well as the way in which components such as the foundation and the retaining walls will be constructed. Firstly, the natural boundary conditions are determined and section 4.2.2 handles the field boundary conditions and cable situation.

Section 4.2.1: Natural boundary conditions

Natural boundary conditions consist of soil conditions and various hydraulic boundary conditions such as water levels and groundwater levels and the governing wind directions and forces.

For the soil conditions, three CPT tests in the vicinity of the intended location of the new dock are used from past projects at the LEVVEL factory, which originate from the database of ADONIN B.V. Another CPT test at the location of the current Damen shipyard that stems from 1992 and has been acquired from the Harlingen municipality database. The exact locations and CPT test results can be found in Appendix B. Figure 20 below shows the soil profile which is interpreted from overlapping the three combined CPT test at the intended location of the new graving dock.

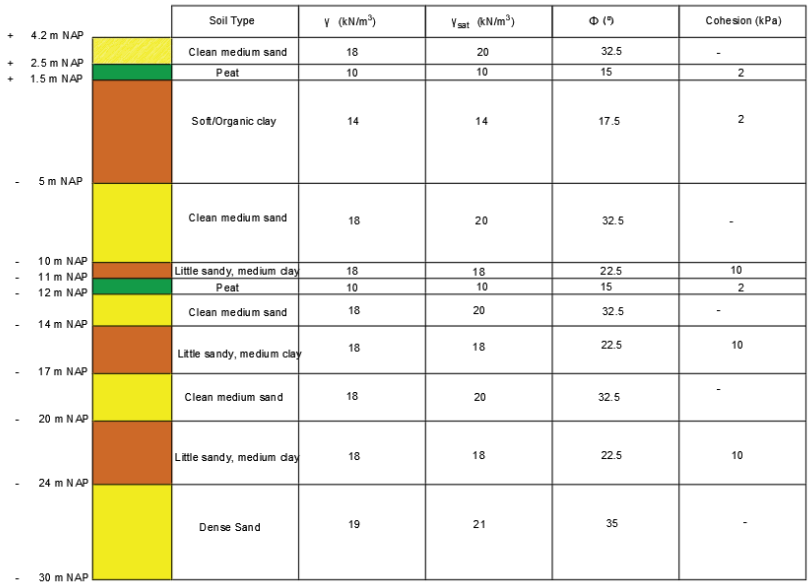

Soil Type	γ (kN/m³)	γsat (kN/m³)	Φ (°)	Cohesion (kPa)
Clean medium sand	18	20	32.5	-
Peat	10	10	15	2
Soft/Organic clay	14	14	17.5	2
Clean medium sand	18	20	32.5	-
Little sandy, medium clay	18	18	22.5	10
Peat	10	10	15	2
Clean medium sand	18	20	32.5	-
Little sandy, medium clay	18	18	22.5	10
Clean medium sand	18	20	32.5	-
Little sandy, medium clay	18	18	22.5	10
Dense Sand	19	21	35	-

Figure 20: Soil profile

The values for the soil parameters where determined using table 2b from NEN9997. In all CPT tests that were performed, the soil profile is characterized by a man-made top layer consisting of clean sand, below which a number of soft layers can be found with a high concentration of organic material, including a 1 meter thick peat layer and consequently a low bearing capacity. Continuing downwards, a number of alternating sand and clay layers are found with a thickness of approximately 3 meters each, with another peat layer at between -11 m NAP and -12 m NAP. A thicker, sandy, clay layer can be found at a depth of -21 m NAP until -25 m NAP. From this point on, the soil consists of dense, strong sand with a large bearing capacity. This strong bottom sand layer serves as a suitable layer to install the retaining walls for the dock as it can transfer the loads from the foundation structure. The deepest clay layer could potentially play a role in preventing the uplift of the dock due to its water retaining properties.
When looking at the lithostratigraphy of the soil composition we can learn more about the properties of the different soil layers. Figure 21 from Dinoloket shows the lithostratigraphic classification of the different soil layers, describing from which historical period the soil originates and consequently what characteristics this soil structure might have (DINOLoket, 2022).

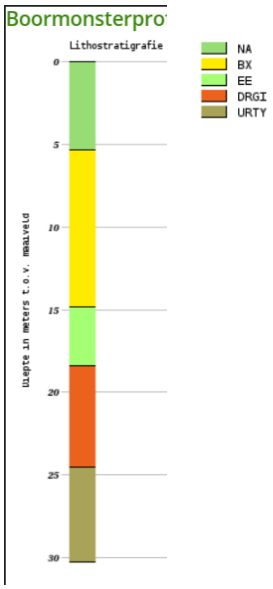

Figure 21: Lithostratigraphic soil profile, source: (DINOLoket, 2022)

The first thing we observe is that the deep sand layer which starts at around -24 m NAP is from the 'Formatie van Urk' which is formed during the Pleistocene-era, the first period of the Quaternary during which several glacial and interglacial period took place. The layer on top of this, the 'Formatie van Drente' originates from this cold period of time as well and has been shaped during the Saalian era (370.000 – 130.000 year ago) during which a thick layer of ice covered the soil. This specific layer package is from the 'Gieten' layer package, consisting of clay and/or loam so it can be concluded that the clay layer that has been found from the CPT tests between -20 and -24 m NAP also originates from the Pleistocene era (Vereniging Ondernemers Technisch Bodemonderzoek, 2006). When looking at the effects of this historical period on the behaviour of the soil, we can conclude that the OCR (over consolidation ratio) of this clay layer from the 'Formatie van Drente' and the sand layer from the 'Formatie van Urk' can be assumed to be high, meaning that the current stress state of the soil layer is low compared to the highest stress that it has been subjected to in the past and so additional settlements due to consolidation of these particular soil layers can be considered to be unlikely. This is different however for the higher laying clay layers, which all originate from the Holocene era, which is a warm, interglacial period that makes up the past 10.000 years until present time. The deepest Holocene formation layer that we can identify from figure 20 is from the 'Eem Formatie' which is characterized by shell-containing sand and clay layers. The sand layer between -17 m NAP and -20 m NAP can be expected to be from this era. The sand layers consist of moderately fine to very coarse grain sizes. Above this, a soil layer package from the 'Formatie van Boxtel', mainly consisting of sand layers which can be interrupted by peat, or organically rich soil layers. This formation makes up the majority of the soil profile from figure 20, approximately from -17 m NAP until -5 m NAP. The sand layers are characterized by well-graded, fine grains which make it suitable to use for different purposes after excavation such as fill sand to be used for construction works. The final formation that can be identified is from the 'Formatie van Naaldwijk', consisting of alternating sand and clay layers, in the soil profile this formation is expected to be found between -5 m NAP and +2.5 m NAP. The OCR of this Holocene soil package is expected to be low, meaning that increased stresses may lead to settlements. Since the top meters of the soil profile consists of artificially placed sand, this layer package may currently still be in the process of consolidation and therefore it is recommended that the foundation of the graving dock reaches the deep sand layer that originates from the Pleistocene era.

The ground water levels are again retrieved from the DINOloket website, and is based on data from a period between 1996 and 2015, where the ground water table was monitored at a location near the Damen Shipyard. The full results can again be found in Appendix B.
The average ground water level can be estimated to be at +3.5 m NAP during these 20 years of monitoring, with a maximum value of +3.66 m NAP. The design ground water level will play a large role in the vertical stability of the graving dock and potential soil settlements.

Design water level
The occurring water levels at the location of the dock are crucial for determining the required draught of the dock, since a sufficient water level is always necessary during docking. The mean water level in the port of Harlingen is found to be at +0.07 meters NAP and the bed level is taken at -7.5 meters below NAP. Locally the port will be deeper but the governing depth for ships to enter the port is at the -7.5 meters NAP and this depth is the minimal guaranteed depth in the port based on the Port of Harlingen port map (Port of Harlingen, 2022). The design height of the dock gate consists of the design water level and a freeboard. The design water level is taken as the same design water level for the local dike ring, which is mentioned to be at +4.9 m NAP (Rijkswaterstaat, 2007). It can be argued that this value is too conservative since the dock gate is not part of the primary flood defense system but for safety considerations, this value is still maintained here. This value is assumed to correspond to the governing storm event in combination with the highest astronomical tide. In order to retrieve the design water level, the following factors will have to be added:

- Long term effects (sea level rise and land subsidence)
- Freeboard to allow a maximum amount of wave overtopping

The wind setup is computed using wave information as described later in this chapter and using equation (4.3) from the Flood Defences reader (Jonkman, Flood Defences, 2021). The governing combination of wind velocity, using a design velocity of 1/100 years at Texel from the Rijkoort-Weibull model of the KNMI of $v_{b,0}$=33.4 m/s and a reduction factor of 0.94 (Smits, 2001), so a design wind speed of v_d=31.4, combining with the fetch from West direction results in a wind setup of 0.5 metres. This wind setup is already included in the chosen water level from the Toetspeil, the governing wind direction and fetch within the port itself that would generate the significant wind waves is from a NNE direction together with a fetch of 370 meters. For determination of the significant wave height and period, the Young & Verhagen equations have been used, leading to H_s=0.2 m and T_s=1.7 s for the governing wind direction and velocity inside the port. A Rayleigh distribution is then assumed for small wave heights. The exceedance probability is taken as 1%, since the scenario of a 1/100 year wave and a 1/100 year storm simultaneously is considered to be sufficiently conservative. The corresponding design wave height is H_d=0.52 m. The governing wave height is the maximum wave height between the significant wind wave height and the significant ship wave height, after consulting multiple employees that work in the port environment, the maximum value for the significant ship wave height is determined to be H_{ship}=0.5 meters. Therefore, required freeboard will be calculated based on the maximum ship wave.
The freeboard depends on the maximum allowable wave overtopping discharge. This value is taken as q_{max}=1 l/s/m, corresponding to the maximum allowable value for building structure elements, as determined in the European Overtopping Manual 2007 (Voorendt & Molenaar, 2020). Using Franco's method for structures with a vertical wall such as the dock door, a freeboard of 0.62 meters is maintained.
For the long term effects a value 0.5 meters is taken, which includes sea level rise, where a relative sea level rise of the North Sea of at least 40 centimeters per century can be expected according to research in 1990 (Voorendt & Molenaar, 2020). An additional 10 centimeters accounts for land subsidence, which is in accordance with a prognosis as made by De Lange & Gunnik from 2011 (Voorendt & Molenaar, 2020). It has to be mentioned that this corresponds to the global, tectonic land subsidence as opposed to a local subsidence which is caused by soil settlements. This value for the long term effects is also in accordance with the RCP4.5 from the IPCC reports, meaning a medium-pessimistic prediction scenario (Church, 2013).

In total, this means that the top of the dock door needs to be placed at +6.10 m NAP.
This is the extreme situation for which the dock door needs to be designed, as both the governing loads for the strength of the door as the required height for the water retaining function of the door are determined by this load case. Furthermore, the average tidal variation changes between -0.99 meters NAP (Mean Low Water (MLW)) and +0.95 meters NAP (Mean High Water (MHW)). After consulting with the client, it is decided to put the bottom level of the dock at the same level as the bottom of the port. In this way, the capacity of the dock with regards to the available depth is maximized while making sure that the amount of inflowing sediment is not enhanced which would be the case if the bottom level of the dock would exceed the bottom level of the port.
At Damen, the required minimal water level for docking is at 0.00 meters NAP, with a rising tidal water level. The same requirement is applied for the new dock which means that the maximum unladen draught of the vessel that can be docked is at 5.7 meters when taking into account the block height of 1.80 meters. In extreme cases, a tidal window can be applied for vessels with a larger draught, but in the current configuration, the design vessel is capable of docking. All in all, this means that the dock gate runs from +6.10 m NAP till -7.5 m NAP, so a total depth of 13.6 meters. These water levels can be found in Figure 22, where the height of the quay, based on the height of the quay at Damen, is shown as well.

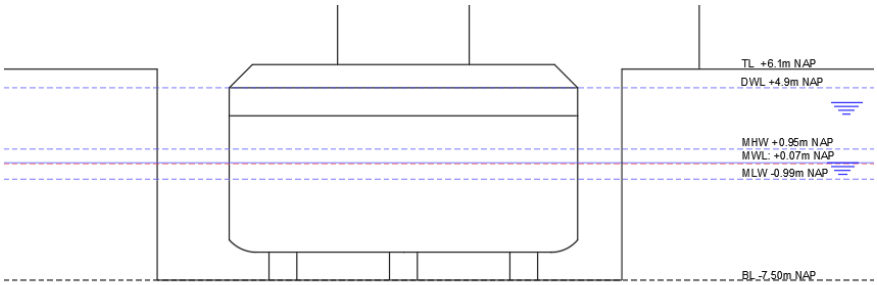

Figure 22: Design water levels

As far as the governing wind direction and forces are concerned, incidents in the past have proven that wind forces play an important role in the design of a sufficiently stable dock hall for this location, due to its coastal orientation and lack of coverage from surrounding buildings, the governing wind forces can take extreme values.
A detailed analysis that has been carried out by Ilja Smits of the Dutch meteorological institute KNMI has developed a 'Rijkoort-Weibull model' that can be used to determine extreme wind values that have not even been measured yet. For this case, the wind velocity with a return period of 100 years for the measuring station at Texel has been chosen, since this is the nearest measuring station that has a coastal situation, being the most similar to Harlingen. The design windspeed, with a corresponding wind direction from the West, is equal to 33.4 m/s (Smits, 2001). According to Eurocode, the value for the velocity pressure q_p depends on the region in the Netherlands where the structure is located, the type of surroundings that the structure experiences (rural, urban or coastal) and the reference height z_e. For our dimensions, this reference height is equal to the minimum value between the design width of the dock in cross wind direction and two time the height of the structure, so z_e=min(b,2h). For the chosen dock orientation, b=155 and 2h=80, so the value of z_e equals to 80 meters. For the wind region and surroundings, it is determined that the dock is located in Area I with a coastal surrounding, which gives a value for q_p of 2.30 kN/m^2.

Figure 23: Wind-area map for the Netherlands with Harlingen highlighted by the red dot

Section 4.2.2: Field boundary conditions and cables and pipelines

The intended location of the dock is expected to partly overlap two different plots, one owned by LEVVEL, which is a consortium between Van Oord, BAM and Rebel, that is responsible for the design, construction, financing and maintenance of the Afsluitdijk reinforcement. The plot is currently used for the production of the blocks that will be placed as the dike revetment on the outer slope of the new dike. The plot boundaries can be seen in figures 24 and 25, which also shows the boundaries for the plot that is currently owned by a waste incineration plant, the REC. For both plots, the part that is intended to be used for the realization of the graving dock is located in the east and is currently not in use by the two owners. The field boundaries in Figure 24 and Figure 25 are retrieved from the Kadasterdata website (Kadasterdata, 2022).

Figure 24: Field boundaries Northern plot, source: (Kadasterdata, 2022)

Figure 24 shows the field boundaries for the Southern plot, owned by REC.

Figure 25: Field boundaries Southern plot, source: (Kadasterdata, 2022)

After investigating the cable and pipeline situation near the intended construction site, it can be concluded that all cables and pipelines are situation along the access road, Lange Lijnbaan, and crosses the Port in line with the road. These include data and electricity cables as well as some major water transport pipelines owned by North Water, which is probably part of the network that supplies industrial water. Altering of these water pipelines would lead to substantial additional costs and should therefore be avoided. Appendix B shows the full pipelines and cable situation, as well as a cross section of the area where these cables and pipelines travel underneath the water. It is visible that one single data cable can potentially intersect the construction site of the dock, this cable would have to be altered or removed.

Chapter 4.3: Stakeholder Analysis

In order to perform a stakeholder analysis, all the various stakeholder are inventoried and their role within the project is shortly described. Each stakeholder is analyzed based on their level of interest and power which is assigned a value between 1 and 10. These values are then displayed on a stakeholder map. Appendix P gives further reasoning behind the results.
The final stakeholder map, displaying the relative importance of each stakeholder, can be seen in Figure 26 below.

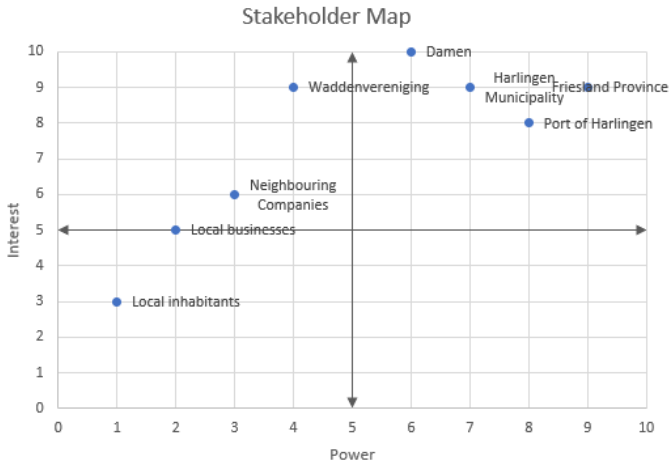

Figure 26: Final stakeholder map

Chapter 5: Development of design alternatives

In this chapter, the first steps in the design of the dock are made by developing a base design in chapter 5.1, where a conceptual design for the basic elements of the dock are made. These consist of the construction pit for the dock chamber and the dock gate. In chapter 5.2, the sustainable design alternatives are implemented in different design alternatives where also other aspects such as the gate operating systems, pumping system and overall layout of the dock can be varied to develop these design alternatives.

Chapter 5.1: Base design

This chapter treats the design of the retaining walls, underwater concrete floor and tension piles and dock gate that forms the core of the base design of the dock. In the design of the floor, the traditional layout is maintained which consists of a layer of water-retaining UCF, followed by a layer of sand-fill above it, followed by a structural floor that carries the ship load.

Section 5.1.1: Retaining walls

The main types of retaining walls that are commonly applied in deep excavation pits are the diaphragm wall and the sheet pile wall. In our case, it would be possible to select one of these wall types for the base design and come up with design alternative that contain different wall types. However, since we aim to minimize the environmental impact of our design it is more time-efficient to select the optimal wall type up front based on available literature. An LCA carried out by ArcelorMittal that compares two alternatives for the execution of a quay wall of a cruise ship terminal concluded that the sheet pile design saved 44% of the amount of CO_2-eq that is emitted compared to the D-wall design (ArcelorMittal Commercial RPS, 2021). Furthermore, a thesis written by L. Van Holst from 2019, which uses a parametric design model for the design of ship locks in the Netherlands, also found that variants which consist of a sheet pile wall shipping chamber had a lower ECI-value and Global Warming Potential than the D-wall alternatives (Van Olst, 2019). The ECI-value for one squared meter of sheet pile is approximately equal to €35 while for a D-wall with a thickness of 1.2 meters without reinforcement this value is €47 (DuboCalc, sd). A combi-wall, consisting of tubular piles that are connected by two Z-profile sheet pile sheets are chosen due to their relatively large section modulus compared to I or H-profiles. In this configuration, the piles are responsible for supplying the required bending stiffness to withstand the earth and water pressures while the sheet piles supply the water-retaining function and support the anchors. The profile of the piles will be 1220x12,5 with a AZ-18 700 sheet pile, both in steel quality S430. Figure 27 shows a schematization of this wall type.

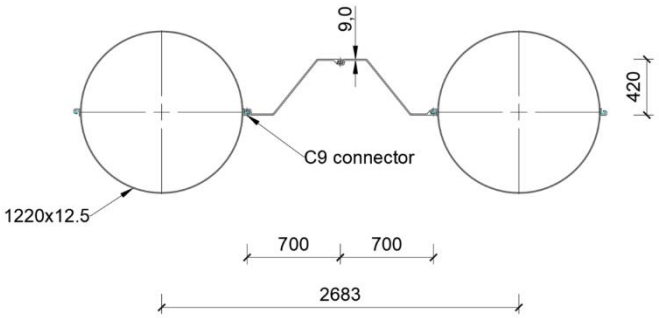

Figure 27: Combi wall section profile

D-sheetpiling is used for the calculation of this combi-wall, the complete calculations can be found in Appendix C. The piles will need to have a minimal length of 18 meters as determined by the D-sheetpiling program. In order to install the bottom of the piles in a sand layer it is chosen to have the bottom of the piles at a level of -18 m NAP. Buckling of the tubular piles can be prevented by making sure that these piles filled with or installed in over consolidated sand. The bottom of the sheet piles are installed at a level of -13 m NAP. GEWI 63.5 anchors are installed at +2 m NAP under an angle of 30 degrees and they have a total length of 23 meters. The grout body is 7 meters long and this configurations ensures that the grout body is placed within a sand layer with a q_c of at least 5 MPa and at a depth of at least 5 meters and at least 1 meter of sand above the toe of the grout body, which is demanded according to the CUR166 (CIE4363 reader, 2018). The centre-to-centre distance of the anchors is equal to the total width of one combi-wall sections, 2.68 meters. Each anchor is pretensioned with a value of 50 kN/m', resulting in a prestressing force of 124 kN per anchor. A waling of 2 UNP260 profiles ties the anchors together. The D-sheetpiling input can be seen in Figure 28, where the water levels and soil properties have been inserted corresponding to the findings in chapter 4. A surcharge load of 20 kPa is applied as is prescribed for RC2 structures according to the Eurocode, while it is reasonable to think that this value might be higher in practice considering the heavy equipment that will be required.

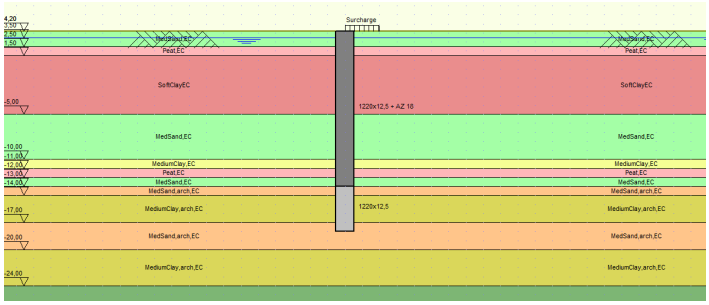

Figure 28: Combi wall schematization

The construction stages of the retaining wall have to be defined next. After installation of the combi wall, an initial excavation is performed to a level of +1.5 m NAP for the installation of the anchors. Next, the building pit is fully excavated to a level of -8.5 m NAP in order to install the tension piles and a 1 meter thick underwater concrete floor. The final stage is the dewatering of the building pit. An overview of these stages can be seen in Figure 29 below.

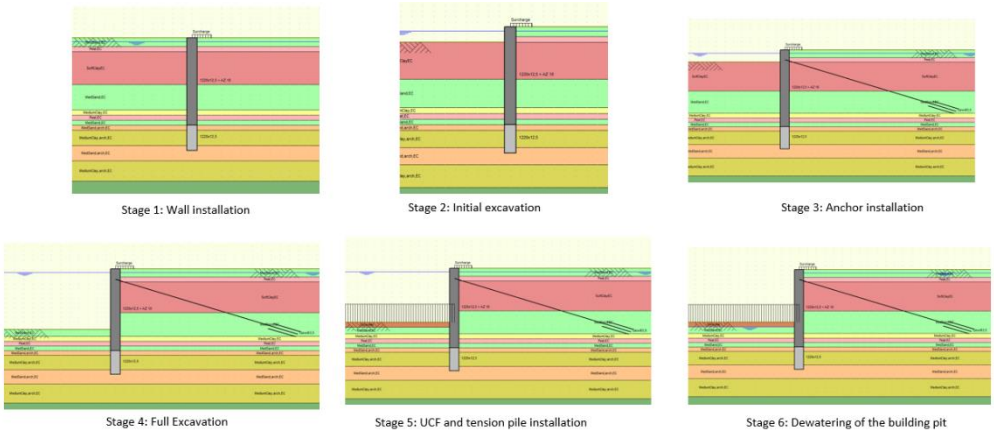

Figure 29: Overview of construction stages

Following the step-by-step plan described in CUR166, the maximum bending moments, shear forces, anchor forces and displacement are determined during each of these stages and for 5 different scenarios which vary in the combination of high or low values for the soil stiffness and ground and water levels. This variation is determined by the safety factors which are already

present in the D-sheet piling software, for a more detailed description of these scenarios Appendix C can be consulted. These maximum values overall can be found in Table 2.

Table 2: Maximum occurring forces and deflection of the retaining wall

	Value	Stage
Bending moment M_{ed} [kNm]	2257	Stage 6 – Step 6.5 * 1.2
Shear Force V_{ed} [kN]	1600	Stage 6 – Step 6.5 * 1.2
Deflection [mm]	42	Stage 6 – Step 6.5
Anchor Force $F_{anchor;d}$ [kN]	947	Stage 6 – Step 6.5 * 1.2

The checks for the strength and stiffness of the combiwall using the design loads from Table 2 are found to be sufficient, as can be seen in Appendix C. For the check of the anchors, the maximum force on the grout body and the maximum force on the anchor rod have to be checked. While in reality anchor tests are supposed to be performed to determine the capacity of the grout body, the CUR166 provides an estimation based on the length of the grout body and the type of sand. This estimation is used to determine the required grout body length of 7 meters. Since the c.t.c. distance of the anchors is 2.68 meters, no mutual influence among anchors is expected. Finally, the critical macro-stability of the system is checked, where the stability factor for Bishop's method is still equal to 2.27, as displayed in Figure 30. It has to be mentioned that the length of the grout body could be increased to a length of 10 meters to use its complete capacity but the current anchor configuration already meets all requirements.

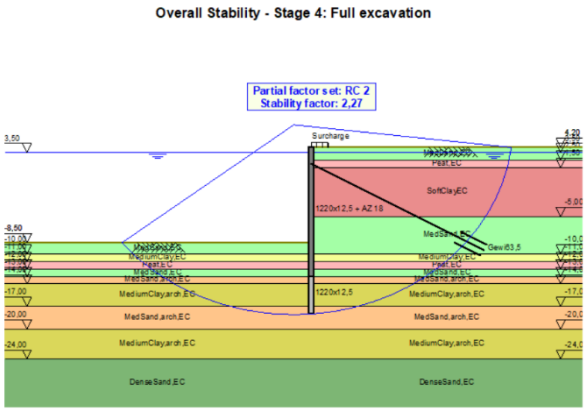

Figure 30: Overall stability combiwall

It can be concluded that the current designed combi wall consisting of tubular piles with a 1220x12.5 profile and AZ-18 700 sheet piles together with the GEWI63.5 anchors meets the design requirements. The total amount of anchors is equal to 124 and the combi wall consists of 125 piles and 248 section of sheet pile. While both the bending moment capacity and shear force capacity of the wall lead to low unity checks that might hint towards an overdesigned retaining wall system, the anchor force and displacement prove to be governing in this case.

Section 5.1.2: UCF and Tension Piles

The design of the underwater concrete floor (UCF) and the tension piles are closely related since they fulfil a combined function to ensure a vertical equilibrium of forces and to prevent water from entering the excavation pit from underneath. The UCF will also function as a strut that locally contributes to the horizontal equilibrium of forces. For the preliminary design of the UCF, an average thickness of 1 meter (1000 millimetres) is assumed with a C20/25 concrete strength class. The center-to-center distance of the tension piles in both the long and short direction influence the strength of the UCF and so the first check is performed in long direction, which is labelled as 'check A' in the CUR77 (CUR-Aanbeveling 77, 2014). These guidelines are for the design unreinforced underwater concrete floors, from which it follows that the maximum c.t.c. distance in long direction is 3 meters, a convenient value of L_y=2.5 meters is chosen since a large c.t.c distance would reduce the amount of tension piles that are needed and consequently reduce the design costs and environmental impact. In short direction the c.t.c. distance should be chosen to be less than L_y to ensure ULS failure is not critical in the long direction, L_x=2.4 meters and $L_{x,edge}$=1.8 meters which is the distance between the sheet pile wall and the first row of tension piles, are chosen. This configuration leads to 60 rows of 12 tension piles, so 720 piles in total. A schematization of the pile plan can be seen in Figure 31 below, where we see a top view of the combi-wall and a more detailed schematization which annotates the chosen c.t.c. distance of the tension piles.

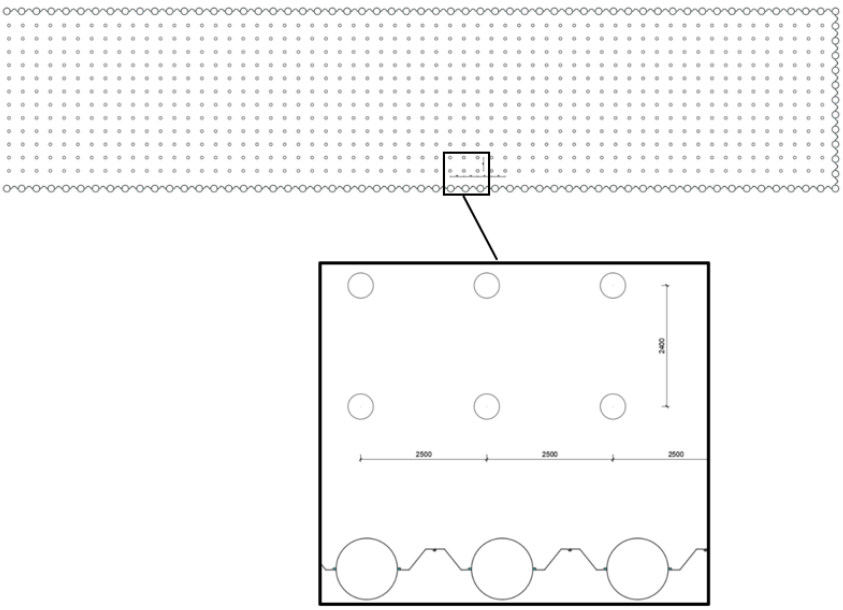

Figure 31: Tension pile plan

For the UCF, checks B2 and G from the CUR77 have been performed which are deemed as the most critical failure mechanisms. By assuming that bending cracks will occur in short direction and the arching phenomenon will be governing, check B2 can be performed without the need for a beam model which simplifies this preliminary design. Check B2 concerns the equilibrium of forces in each arch, using the normal force in the concrete that has been derived from the D-sheetpiling model by modelling the concrete floor as a strut. Check G concerns the punching shear for each tension pile. The full calculation results as well as the strut-schematization of the concrete floor can be found in Appendix C, but it can be concluded that the chosen thickness and concrete strength class together with the chosen c.t.c. distance of the tension piles leads to a sufficiently strong underwater concrete floor.

The chosen tension pile type is a GEWI63.5 anchor with a grouted diameter of 500 mm. As has been determined in chapter 4, the piles need to be installed into the deep dense sand layer which start at a level of approximately -24 m NAP in order to prevent problems due to consolidation. The piles have been checked for the pull-out of a pile group, pull-out of a single pile and the clump criterion. Since the centre-to-centre distance among the piles are

relatively large, the group-effect of the piles is negligible small which can also be concluded from the calculation results in Appendix C. The pull out of a single pile is found to be the governing failure mechanism and a final installation depth of -33 m NAP is necessary to ensure sufficient strength. A cross-section of the final design of the construction pit can be seen in Figure 32, including the anchors, retaining walls, underwater concrete floor and the tension piles.

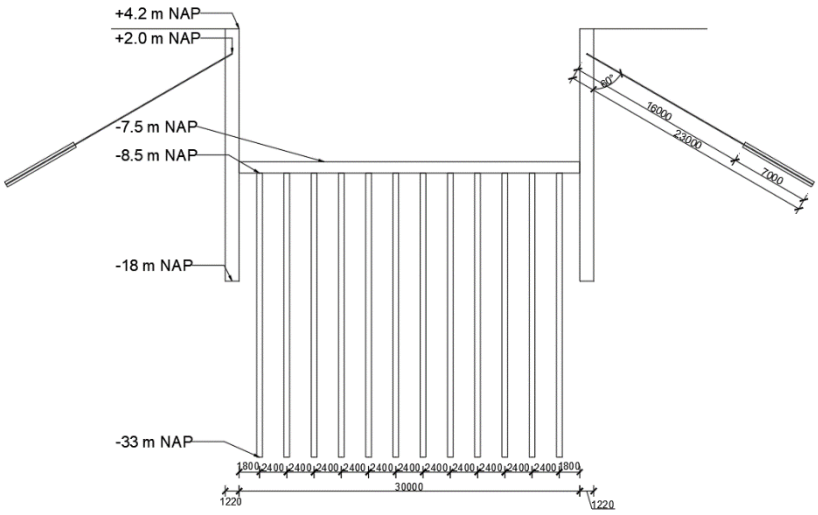

Figure 32: Total construction pit design

Section 5.1.3: Gate design

Regardless of the mode of operation of the dock gate, for which many options are possible that will be later discussed in the design variants, the loads acting on the gate determine the required section modulus of the gate profile. Firstly, the governing loads on the gate need to be determined, which consist of a permanent hydrostatic load and a variable wave load. For the computation of the wave loading, multiple methods exist but for a preliminary design the Sainflou method is widely used due to its simplicity and accuracy. This method is based on Stokes' second order wave theory and applied to non-breaking waves only. The situation that is considered is the design wave which reaches its peak directly in front of the dock gate and is completely reflected. The full calculation of the loads can be found in Appendix C.
The total design loads on the gate is equal to:

$$Q_{design} = \gamma_P * Q_{hydrostatic} + \gamma_Q * Q_{wave,r} = 1.35 * 754.2 + 1.5 * 44.4 = 1085\ kN/m$$

Assuming the gate as a simply supported beam with a width of 13.6 metres and a length of 30 metres, the schematization of the gate in the long direction is displayed in Figure 33.

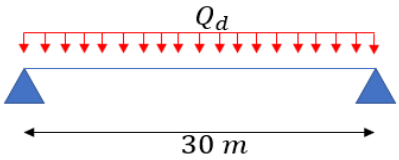

Figure 33: gate schematization long direction

In the short direction, the schematization of the load and the resulting maximum bending moment is less trivial and can be seen in Figure 34 below, consisting of both the hydrostatic and wave loads.

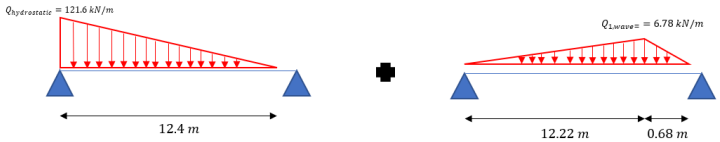

Figure 34: gate schematization short direction

The skin plate of the gate is the first element that has to transfer the loads to the supports and so it also has to be designed to have sufficient strength in the ULS condition and the deformation should be limited during the SLS condition. A thickness of 20 mm is chosen to meet the strength requirements and it is supported by primary load carrying elements in both vertical and horizontal direction in the forms of 7 horizontal girders and 5 vertical posts. In order to meet the SLS requirements with regards to the deformation of the skin plate, 18 additional stiffening elements have been added in vertical direction that are connected to the girders. At the back of the gate, flanges with a thickness of 40 mm with varying widths in both directions are placed to meet the SLS requirements for the total gate in the long direction (with a span of 30 meters). The gate will thus have a total thickness of 1.96 meters, sketches of the side view, top view and total view can be seen in Figure 35 below.

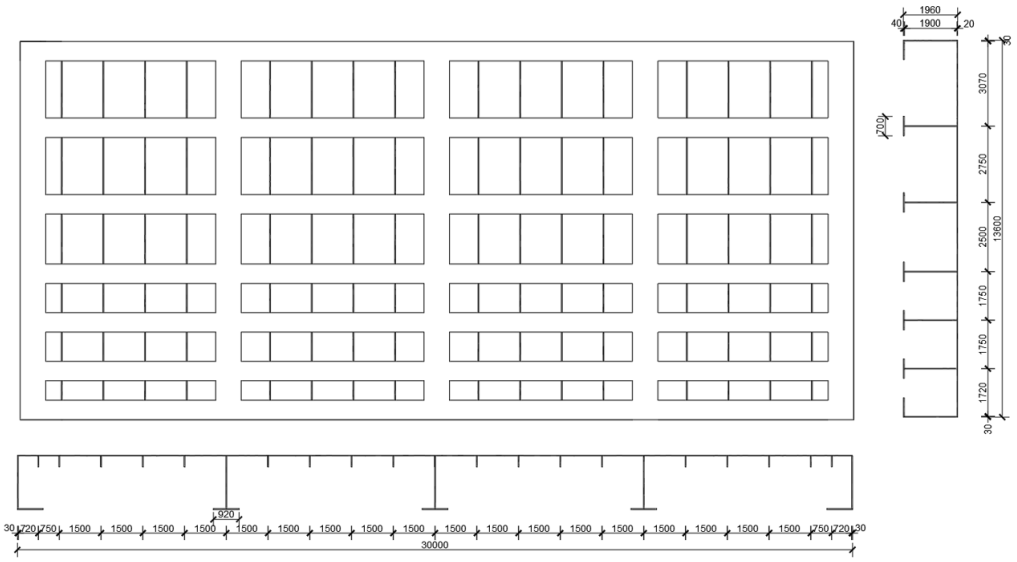

Figure 35: Gate design

The centre-to-centre distance of the girders is reduced near the bottom of the gate in order to follow the shape of the hydrostatic load. In the long direction, the centre-to-centre distance is kept constant at 1.5 meters, except for the final stiffeners that have been added in the centre of the last span in order to meet the requirements for the maximum deflection of the skin plate. It has to be mentioned that the load has be schematized in both direction while in reality the short direction will be governing in carrying the load and so the total weight of the gate can be optimized a bit. However, in reality this margin is considered to be negligible for a preliminary design stage. The results of the design calculations can be found in Appendix C.

Chapter 5.2: Design alternatives

Now that the base design of the dock is made, this section will focus on the implementation of sustainable design alternatives that aim to reduce the environmental footprint of the dock, starting off with the reduction of inflowing sediment.

Section 5.2.1: Dock sedimentation reduction strategies

Possible mitigation measures against the inflow of sediment will be discussed over the next paragraphs, each of which aim to tackle the sedimentation process as described in Chapter 2.2. These options are:

- Creating a **water inlet** at the opposite short side of the chamber that will enable an inflow of water, either through gravity or by installing pumps, when the ships exits the dock chamber, reducing the pressure difference at both sides of the ships and consequently **reducing the inflowing, sediment containing, current.** In case a small amount of sediment is still inside the dock chamber, the inlet can be used to force the sediment towards the gate of the chamber and away from the ship, which would greatly reduce the time and money that is required for cleaning the dock chamber. A number of inlets should be installed that evenly spread the inflowing water over the full width of the dock, to reduce the turbulence of this inflow, leading to the three evenly placed inlets in the figure below. In order to tackle the inflow of sediment during entry of the vessel into the dock, a system of winches can be installed so that tugboats are no longer necessary for this process or at the very most merely to keep the vessel in the correct position for docking. See figure 36 for an illustration of this solution.

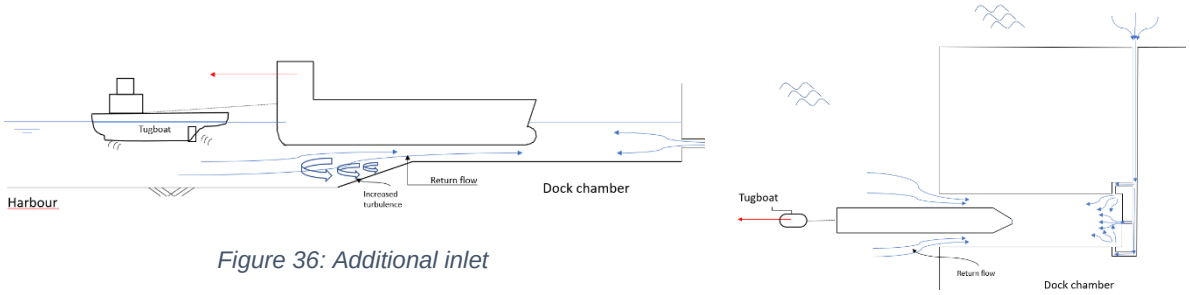

Figure 36: Additional inlet

- As mentioned previously, a system of winches to guide the vessel into the dock makes the use of a tugboat unnecessary, but the addition of a system of winches to pull the vessel back out the dock after the maintenance works have been performed would **make tugboats unnecessary for the complete docking and undocking procedure**. This can be accomplished by constructing a **jetty** that guides a winch system outside of the dock entrance. The main downside of this strategy is the fact that a large jetty with a length equal to the length of the design vessel would stick out into the harbor which would form an obstacle for other marine traffic and operations.

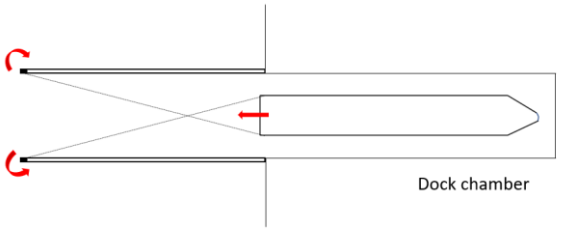

Figure 37: Jetty structure to enable docking using system of winches

- Another option is limiting the spread of sedimentation throughout the dock by **installing obstacles** on the bottom of the dock chamber near the inlet that trap or block the sediment and allow it to be disposed of easily after the (un)docking procedures are finished and the dock chamber is pumped dry. By placing these small obstacles, that shouldn't be too high to avoid contact with the vessel's keel, the flow pattern of the inflowing sediment is altered. Along the sides of the obstacles, the flow velocity is increased but in front of the obstacle the sediment will be deposited as the

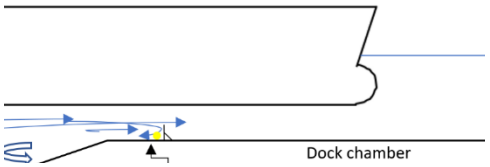

Figure 38: sediment accumulation obstacles

flow velocity will be minimal here. The aim of this mitigation method is to form a barrier for the inflowing sediment which forces it to settle earlier and be collected near the entrance of the dock. The efficiency of this method is questionable however due to the expected turbulence of the inflowing sediment flows, which are likely to not follow laminar flow patterns around the small structures.

- **A bubble screen** can be applied at the entrance of the gate that aims to reduce/prevent the inflow of sediment by forming a barrier for the stirred up sediment. This can potentially be combined with a sliding dock gate that uses hydro jets to move the gate by making these hydro jets multifunctional and supply the required bubble-like barrier. The main downside of this mitigation method is the additional required energy that is necessary.

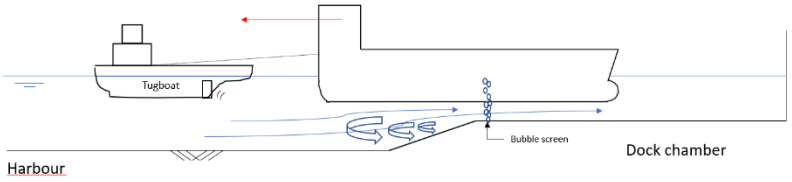

Figure 39: Bubble screen

- Excavation of a sediment retaining barrier in front of the entrance of the dock, where the vertical distance between the bottom of the dock floor and the bottom of the harbor is increased which creates a step that forms a barrier for the sediment near the bottom to enter. This can be elaborated on by placement of a bottom protection. **This method aims to minimize / take away the inflow of sediment into the dock chamber.** Creation of this sediment trap in front of the dock chamber will locally require additional dredging works and over time, this process will have to be repeated due to unavoidable sedimentation of this trap. The effectiveness of this mitigation measure is therefore questionable also due to the role that turbulence plays and the relatively short duration of the docking/undocking procedure which likely will not be long enough for sediments to settle.

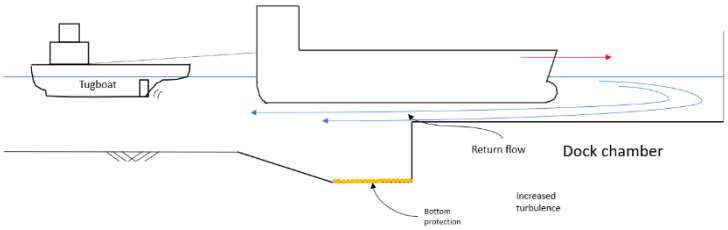

Figure 40: Sedimentation trap

Not all of these mitigation measures are equally appropriate to tackle the sediment issue of the dock chamber and in order to determine which methods are most suitable and should be taken into account when developing the design variants for the dock, a short preliminary multi criteria analysis is performed to be able to discard those solutions which will prove to be either unfeasible or unrealistic. Further details about this MCA can be found in appendix D, which takes the constructability, effectiveness, costs, sustainability and amount of maintenance into account.
From this MCA, two mitigation measures are discarded which are the sediment obstacle and sedimentation trap. Their poor performance on the effectiveness criteria is the main reason for this. The jetty is replaced by a normal system of winches since the construction of a long jetty sticking out into the harbor will be in conflict with harbor regulations.

Section 5.2.2: UCF alternatives

Section 3.3 mentioned the traditional building method in which two separate concrete floors are applied in the design of the dock. An underwater concrete floor with no reinforcement

serves as a watertight barrier to allow the dry pumping of the construction pit and a reinforced structural floor which is designed as if there is no underwater concrete floor underneath. For the design of this graving dock, sustainable alternatives are considered that aim to reduce the total volume of concrete that is necessary in the design of the construction pit. The alternatives that will be assessed are a steel fibre reinforced underwater concrete floor (SFRUCF), a basalt fibre reinforced underwater concrete floor (BFRUCF), a foil construction and a fully reinforced underwater concrete floor.

A steel fibre reinforced UCF is about adding small steel fibres in the concrete mixture to increase the compressive strength, flexural strength, tensile splitting strength and stiffness of the concrete which allows the UCF to also have a structural function or reduce the amount of concrete required. In practice, SFRUCF has been applied in a number of projects such as the Albert Cuyp garage in Amsterdam and the 'Royal Van Lent' dry dock. In these projects, the SFRUCF has been integrated into the structural floor. Not only is the total volume of concrete needed reduced in this way, also the redistribution of forces inside of the floor is improved with regards to a 'traditionally' reinforced floor, leading to less leakages and shrinkage cracks.
The main downside of adding steel fibres is the reduction of the concrete workability and the corrosion of the material. Other fibres such as glass, carbon, polypropylene and basalt have been included in concrete mixes to enhance the mechanical properties of concrete, each of these materials having their own pros and cons, but the use of basalt fibres has risen in recent times due to its high strength and economic efficiency compared to other fibres. Basalt is a volcanic rock that is created by the eruption of igneous rock and typically originates from East Asia. While carbon has similar strength properties as basalt, the main drawback of carbon fibres is its high costs and the production of basalt fibres doesn't need additives and requires less energy than the production of carbon and glass fibres which makes it considerably cheaper. Furthermore, basalt has good mechanical and physical characteristics since it has high corrosion, thermal and freeze-thaw resistance (Bheel, 2020).

When comparing steel and basalt fibres, the influence on the concrete mixture is considered first. The mechanical properties of basalt and steel can be seen in Table 3 below, stemming from a research performed on the characteristics of basalt fibre reinforced concrete (Bheel, 2020).

Table 3: Fibre properties

Types of fibre	Tensile strength [MPa]	Elastic modulus [GPa]	Strain at failure
Basalt fibre	3800-4840	79.3-93.1	3.1-6
Steel fibre	1700-2200	190-210	5-35

As described before, basalt has a higher tensile strength but a lower stiffness than steel. The increased strength properties of basalt and steel fibre reinforced concrete has been subject to research and the results can be compared to further assess the applicability of basalt as an environmentally friendly alternative to steel in the construction industry. Ramesh and Eswari (2021) tested the effects of basalt fibres on the strength properties of concrete by performing failure tests on concrete samples that contained 0%, 0.5%, 1%, 1.5% and 2% basalt fibre volume. The results showed that the highest enhancement in concrete strength occurred at a fibre volume of 1.5% (Ramesh & Eswari, 2021).
Zheng et al (2018) performed the same experiments on steel fibre-reinforced concrete samples that also contained 0%, 0.5%, 1%, 1.5% and 2% fibre volume. These results showed that the strength properties always increased with increased amount of fibre and no 'optimal amount' was found, in contrast to the basalt fibre experiments (Zheng, et al., 2018). The results regarding the increase in strength properties from both experiments for a concrete element that contains 1.5% fibre volume can be found in Table 4 below.

	Basalt fibre reinforced concrete (Ramesh & Eswari, 2021)	Steel fibre reinforced concrete (Zheng, et al., 2018)
Compressive strength increase [%]	4.5	18.2
Tensile splitting strength increase [%]	57	58.5
Flexural strength increase [%]	22.6	25.2

Table 4: Fibre influence on concrete strength comparison

As table 4 shows, the main advantage of applying steel fibres is the significant increase in compressive strength of the concrete compared to the basalt fibres, the other strength increases are of the same order. It has to be mentioned here these conclusions are based on merely one report for each fibre-type and additional research is recommended.
The implementation of these steel and basalt fibres in the base design is performed by altering the material properties of the concrete based on the results portrayed in table above and adding a term to the punching shear capacity of the concrete that is described by the following relation, from CUR111:

$v_{Rfd} = 0.18 * \frac{f_{eqk,3}}{1.4 * \gamma_{ft}}$, where $f_{eqk,3}$ is the flexural stress corresponding to a crack width of 2.5 mm when performing a three-point flexural test and $\gamma_{ft} = 1.25$ according to CUR111 (CUR, 2018).
Since the required information to determine the value of $f_{eqk,3}$ is not present and can only be retrieved by performing the experiments, the increased value for the characteristic flexural strength $f_{ctk,fibre}$ that takes into account the contribution of the fibres is used to compute the value of v_{Rfd}. In reality the value for this strength property will be higher so it is a conservative choice to use the flexural strength of the concrete, it is recommended to perform the test beforehand since this would lead to a better (economic) optimization of the design.
The presence of the fibres increases the strength properties of the concrete as follows:
Table 5: Increased concrete characteristics by implementing fibres

	Basalt fibre reinforced concrete (Ramesh & Eswari, 2021)	Steel fibre reinforced concrete (Zheng, et al., 2018)
f_{ctk}	$f_{ctk,bf} = f_{ctk} * 1.226 = 1.9$ N/mm^2	$f_{ctk,sf} = f_{ctk} * 1.252 = 1.94$ N/mm^2
$f_{ctd,pl}$	$f_{ctd,pl,bf} = f_{ctk} * 1.226 = 1.011$ N/mm^2	$f_{ctd,pl,sf} = f_{ctk} * 1.252 = 1.03$ N/mm^2
f_{ck}	$f_{ck,bf} = f_{ck} * 1.045 = 20.9$ N/mm^2	$f_{ck,sf} = f_{ck} * 1.182 = 23.6$ N/mm^2
$f_{cd,pl}$	$f_{cd,pl,bf} = f_{ck,pl} * 1.045 = 11.18$ N/mm^2	$f_{cd,pl,sf} = f_{ck,pl} * 1.182 = 12.63$ N/mm^2

These altered properties will lead to a reduction of the thickness of the UCF and consequently a large volume of concrete will be saved. The steel fibre reinforced UCF can be reduced to an average thickness of 800 millimeters when maintaining the installation depth p of the anchor head to its minimum allowed value of 175 mm, this would save 900 m^3 of concrete compared to the base design. The thickness of the basalt fibre variant can be reduced to 850 millimeters, saving 675 m^3 of concrete compared to the base design. When maintaining a fibre content of 1.5% by volume which leads to optimal performance of the basalt fibres as determined by (Ramesh & Eswari, 2021), 54 m^3 of steel fibres is required with corresponds to a total weight of roughly 424000 kg of steel fibres. Comparatively, the basalt fibre variant would require roughly 58 m^3 of fibres which correspond to 12300 kg.
The full calculation results of the two altered UCF designs can be seen in Appendix D.

In conclusion, steel-fibre reinforced concrete has higher strength properties that would lead to an increase in concrete savings compared to basalt fibre reinforced concrete, however the environmental impact that is related to the fibres themselves is beneficial for the basalt fibre alternative. Steel fibres are cheaper to produce but comprise of more emissions during the handling and production processes, whereas basalt fibres are lighter and have better endurance towards corrosion and other external factors. Furthermore, three point bending experiments should actually be performed to determine the influence of the fibres on the strength properties of the concrete but due to the lack of resources and the scope of this report this has been omitted.

Foil polder

As mentioned in Section 2.3.4, the use of a foil polder construction could potentially make the need for UCF redundant, as the plastic foil would ensure the water retaining function and the ballast sand on top of the foil ensures the vertical equilibrium. The main downside of this method is the required amount of space since the slopes of the building pit need to be at approximately a 1:3 angle. Since available space is indeed scarce at the desired location of the graving dock due to the presence of the waste incineration plant on the westside and the harbor on the east, it is first established whether the construction of a foil polder is a viable option. For this, an average water level of +0.00 m NAP and a required level of the bottom of the graving dock at -8 m NAP is taken, which a volumetric weight of the ballast sand of γ_{sand}= 16 kN/m^3 and for water γ_{water}=10 kN/m^3. The required thickness for the ballast sand layer can be found to be: $\frac{8*10}{(16-10)} = 13.33\,m$, meaning that the bottom of the foil is to be placed at a depth of -21.33 m NAP and since the ground level is at +4 m NAP, maintaining a slope of 1:3 and a dock hall width of 50 meters, the total width of the construction pit will amount to approximately 200 meters. Figure 41 shows that this amount of space is simply not available at the desired location due to the overlap with the REC.

Figure 41:Required area for foil polder construction

This design alternative is due to its unfeasible amount of required space discarded as a reasonable option and it will not be included in the development of the design variants.

Fully reinforced UCF

The construction of a fully reinforced underwater concrete floor is rare in practice due to the complexity in placing the reinforcement underwater, but in this section, an estimation is made on the amount of concrete that can be saved when applying reinforcement to the base design for the UCF as described in Section 5.1. The amount of reinforcement is determined by the horizontal equilibrium in the concrete cross section, leading to a reinforcement configuration of ⌀20-50 which leads to A_s=6283mm^2/m'. However, this would lead to insufficient space for the pouring of the concrete and so this configuration can be altered to ⌀25-100 and A_s=4909mm^2/m' The reinforcement is included by an increased punching shear strength due to the presence of this reinforcement, so only check G is assumed to be altered, since the tensile strength properties of the concrete are kept the same. The same preliminary calculations are performed as for the fibre reinforced options and the full calculations can again be found in Appendix D. The thickness of the UCF can be reduced to 850 mm. Implementing the reinforcement would save 675 m^3 of concrete, meaning that 26 m^3 of steel is needed corresponding to a weight of 200 tons. Compared to the steel fibre options, it can be concluded that less concrete can be saved and 50% less steel is required. On top of that, it has to be mentioned that this design doesn't perform an SLS check and merely the water-retaining function of the concrete floor is checked with no further structural function. These checks will be performed at a later stage but for now, the option of applying reinforcement to the UCF is included in development of the design alternatives.

Section 5.2.3: Dock gate mode of operation

Section 2.3.2 mentioned the different types of dock gates that exist as well as the pros and cons for each gate type. Using this information, a selection can be made of the most suitable gate types that should be included in the development of the design variants. The main criteria for the dock gate based on which the decision will be made are the ease & speed of operation and removal, water tightness, low maintenance and cost. It has been chosen to include the mitre gate, sliding gate and caisson gate in the development of the design alternative. For a description of these gate types, the reader is referred to Appendix M.

Section 5.2.4: Inlet system

Section 2.3.2 already determined the head filling system to be the better choice over the longitudinal inlet system, mainly due to the low cost and speed of operation. The size of the inlets need to be determined so that the time that is required to fill up the complete dock chamber can be calculated.

Figure 42 shows the relation between the area of the valves and the total filling time of the dock, for which the full calculations can be seen in appendix D

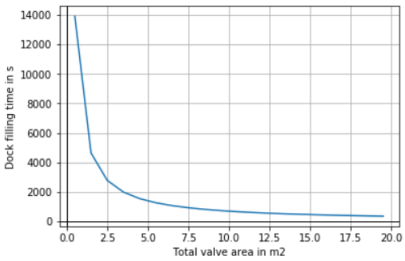

Figure 42: Valve area vs dock filling time

We can conclude from this graph that the minimum valve area should be 5 m^2 as the filling time exponentially increases for smaller values. Taking this minimal valve area, the graphs showing the development of the inflowing discharge Q and the water level difference between the harbor and the dock chamber can be plotted, shown in Figure 43 and Figure 44.

The time required for filling up the dock is around 1400 seconds, which is roughly 25 minutes. The required valve area can be achieved by implementing 2 circular openings with a diameter of 1.8 m^2.

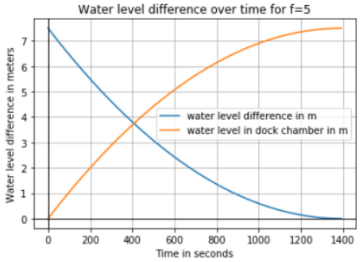

Figure 44: Water level difference over time

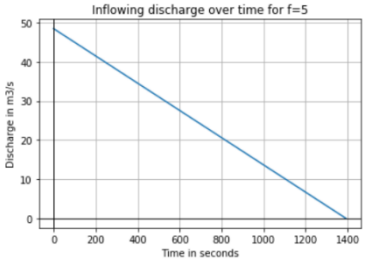

Figure 43: Inflowing discharge over time

Section 5.2.5: Entrance ramp vs overhead cranes

The terms of reference mentioned that either an entrance ramp or a system of overhead cranes must be present in the dock for carrying out the maintenance works by allowing equipment to enter the dock. Both of these options fulfil this function but clear distinctions can be made, the first of which is the high construction costs of the entrance ramp compared to the cranes. On top of that, the design of the retaining wall would have to be altered since a gated opening has to be present in the wall that connects the entrance ramp to the dock and allows the machinery to be placed inside the dock. This brings additional complexities to the design which would be detrimental to the strength and water tightness of the retaining walls. Overhead cranes would simply be installed above the existing dock chamber design without the need for additional excavations or changes to the current design, except for the construction of the cranes

foundation. It can be concluded that the costs and constructability of the cranes is significantly more beneficial than the entrance ramp.
Choosing the overhead cranes would require a vertical clearance above the vessels and consequently the height of the hall would have to be increased. On the other hand, the cranes could also be valuable in the removal of the caisson gate in case the overhead rails are extended beyond the gate of the dock. All in all, the construction of the entrance ramp requires a significant amount of construction costs and together with the negative effects that it would have on the structural integrity of the graving dock chamber leads to the choice of installing overhead cranes that are multifunctional due to their potential role in the removal, placement and maintenance of the gate. The requirements for the cranes as mentioned in the Terms of Reference are a minimum of 2 cranes, each consisting of 2 trolleys with a minimum capacity of 20 t per trolley.

Section 5.2.6: Design variants

The options for the various dock components can be mixed and matched into three different design variants, where for some components one option has already been determined to be the most optimal, namely for the dock filling system and dock mode of operation and therefore these options have been applied to all three design variants. Figure 45 below shows an overview of how these variants have been established.

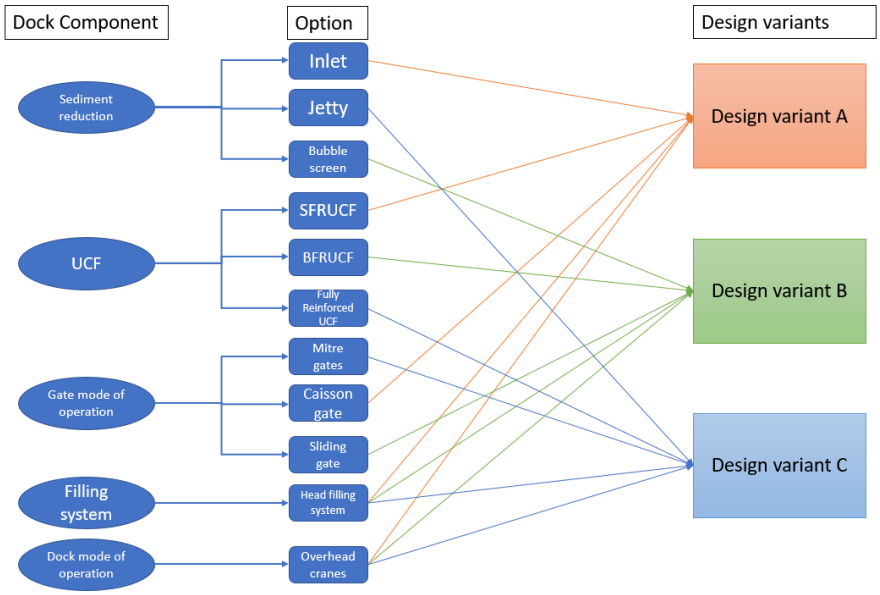

Figure 45: design variant development

Design variant A consists of the additional inlets on the opposite side of the dock chamber in combination with the winch system to reduce sediment inflow into the dock chamber during docking procedures, the traditional UCF is modified by implementing steel fibres into the concrete mix and the structural floor will be integrated into the UCF to reduce the volume of concrete necessary for the design. The mode of operation of the gate is a caisson gate that can be removed with help of the overhead cranes that stick out of the dock hall.
Design variant B uses a bubble screen to filter out the sediment from the inflowing water during docking and a sliding dock is applied here to be able to combine these two objects in the form of hydro jets that create the bubble curtain as well as enable the sliding of the gate. A basalt fibre reinforced underwater concrete floor is applied here, again the structural floor is integrated into the UCF.
Finally, design variant C combines winch system with the fully reinforced UCF to develop a more unorthodox design variant. The mode of operation of the gate is a single leaf miter gate that swings open.
Now that the design variants are developed, the next chapter will elaborate the designs of these design variant.

Chapter 5.3: Design alternatives specification

While the three design variants have been globally introduced in the previous section, a number of design steps need to be performed in order to know the required amount of raw materials, transport and installation works for each variant that can be used in Chapter 6 for the evaluation of the three designs.

Section 5.3.1: UCF design finalization

The design of the UCF needs to be finalized by including the structural function, which will set additional requirements for the thickness of the different floor types. First of all, the various types of loads acting on the floors need to be specified. These are:

- **Upward water pressure:** A permanent load acting on the bottom of the UCF. The magnitude of the nett upward water pressure depends on the ground water table, the thickness of the floor and the installation depth of the floor.
    - Ground water table: two extreme levels for the ground water table will determine the representative load conditions, namely z_{min}=*+0.00 m NAP* and z_{max}=*+3.66 m NAP*
    - The installation depth of the floor stems from the requirement that the top of the floor needs to be at -7.5m NAP. The installation depth $h_{install}$=-7.5 - h_{floor}
    - The thickness of the floor determines the magnitude of the self-weight of the floor, using the volumetric weight of concrete: $\gamma_{concrete}$=23 kN/m^3.

  This leads to an upward water pressure of:

$q_{up} = (h_{installation} + z_{GWT}) * \gamma_{water} - (h_{floor} * \frac{\gamma_{concrete}}{\gamma_m})$, with $\gamma_{water} = 10\ kN/m^3$, $\gamma_m = 1.1$.

In the design, the value of q_{rep} is used for SLS calculations and q_{Ed} is used for ULS calculations. For the bottom fibre check under ship load, the upward water pressure works as a favourable load and so it is corrected by applying a safety factor of 0.9.

$$q_{rep} = q_{up} * \gamma_{G,rep} = q_{up} * 1.0$$

$$q_{Ed} = q_{up} * \gamma_{G,design} = q_{up} * 1.35$$

- **Ship load:** The ship load has been determined for the governing design vessel Kommandor Susan which is a British supply vessel that would lead to the largest concentrated load on the floor of the dock. The vessel's weight is carried by three rows of blocks over the length of the vessel, where the middle row of block is responsible for the majority of the weight. For exact calculations, the reader is referred to appendix E. Figure 46 below show the final weight distribution over a unit width of the floor.

  Again, safety factor γ_{rep} =1.0 is used for SLS calculations and γ_{Ed} =1.5 is used for ULS calculations.

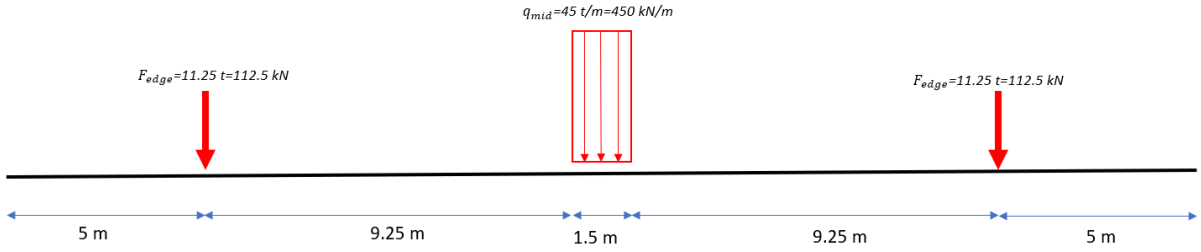

Figure 46: ship load schematization

- **Shrinkage**
  Shrinkage of the concrete can lead to significant strains in the UCF and since the deformations are restrained by the combi walls the resulting tensile stresses can lead to cracks in the floor. Examples of this phenomenon causing cracks which can eventually leads to a loss of water tightness of the floor or a deterioration of the concrete quality are known from neighbouring docks and so it is crucial that sufficient attention is paid to this time dependant effect.
  In order to check the shrinkage of the concrete, the shrinkage strain ε_{cs} must be determined, which is the sum of the autogenous shrinkage ε_{ca} which develops in the first 28 days after the concrete is casted during the hardening of the concrete. The second term is the drying shrinkage strain ε_{cd} which is a slow process of tens of years since it is a function of the migration of water through the hardened concrete. The values of both terms have been determined conform the methods described in NEN-EN1992-1-1, the complete computations can be found in Appendix E and the resulting strains have been found to be:
  $$\varepsilon_{cs} = \varepsilon_{ca} + \varepsilon_{cd} = 0.25 * 10^{-4} + 0.286 * 10^{-3} = 0.311 * 10^{-3}$$
  CUR recommendation 111 prescribes that the loading due to shrinkage is to be applied on the floor through a combination of a tensile force and a bending moment caused by a distribution of the shrinkage strain of 0.9 ε_{cs} at the top of the floor and 0.6ε_{cs} at the bottom of the floor.

- **Thermal load**
  Annual and daily temperature fluctuations will cause additional strains in the floor. The temperature underneath the floor, which is in constant contact with the groundwater, will stay relatively constant. The temperature inside of the dock hall can take extreme values during winter or summer which causes this the concrete to either expand (during summer) or contract (during winter). These strain values have been determined conform NEN-EN 1991-1-5, using the methods that are given for the thermal loads on buildings and a thermal expansion coefficient of 10 $*10^{-6}$ /℃ for reinforced concrete. For the design of the UCF, the winter conditions will lead to an additional tensile load and bending moment leading to tension in the top fibre of the floor. The compression caused by expansion of the floor during summer actually has a beneficial effect on the strength of the floor. This means that being able to control the temperature inside of the dock hall has a beneficial side effect for the bearing capacity of the UCF.

Fatigue
Another point of attention for the UCF is the influence of fatigue since the cyclic behavior of the ship load acting on the floor can lead to fatigue of both the concrete and steel in the floor over time. Fatigue can be described as the weaking of a material by repeated loads and checks need to be performed for the concrete and steel separately (Khatri, 2016). The way in which this is incorporated in the design of the UCF is by performing checks conform Section 6.8 of the NEN-EN1992-1-1 norm (NEN, 2005). The checks can be seen in appendix F, from which it is concluded that the check for the compression of the concrete and shear check can cause problems long-term. It may therefore be advised to increase the concrete strength class to a C30/C37. However, the checks described in the norm are more applicable to short duration cycles such as traffic loads over a bridge deck or railways, the design amount of cycles that is prescribed is in the order of 10^6. For the UCF, with an expected lifetime of 100 years and an average of 20 load cycles per year, this amount of cycles is in the order of 2000, so a factor 500 less. The effect of fatigue can therefore also be expected to be less severe, it is assumed that the current concrete strength class C20/25 is sufficient.

Beam model
A beam model is used to perform more detailed design of the UCF. For this, the floor is regarded as a spring-supported beam with unit width, where the springs in the span of the beam represent the tension piles and at the edges the spring supports represent the

connection between the UCF and the retaining wall. The strut force from the retaining wall acts on the UCF as a normal force and a resulting moment is included at the sides of the beam. The figure below shows an overview of this beam model.

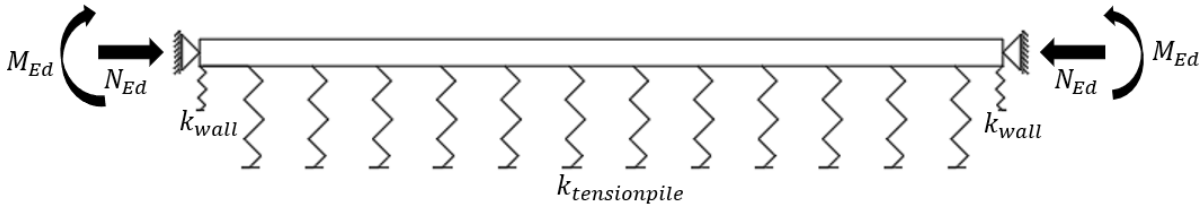

Figure 47: Beam model representation

The representative spring stiffnesses of the tension piles and retaining walls can be determined using geotechnical information, the calculations can be found in Appendix E
CUR77 describes that M_{Ed} due to the eccentricity of the connection between the floor and the wall is equal to:

$$M_{Ed} = N_{Ed} * \frac{h_{floor}}{4}$$

In the design of the integrated dock floor, several load cases can be identified that determine the design of the floor:

- Initial UCF placement
- Placement of (reinforced) structural floor
- Ship load acting on the floor

In the following paragraphs, these load cases are introduced as well as the boundary conditions that form the basis of the design for the 3 UCF design variants.

Phase 1: Initial UCF placement

The first load case is right after the initial UCF layer is casted, which in this case primarily has a water retaining function since the only load acting on the floor is the upward water pressure.

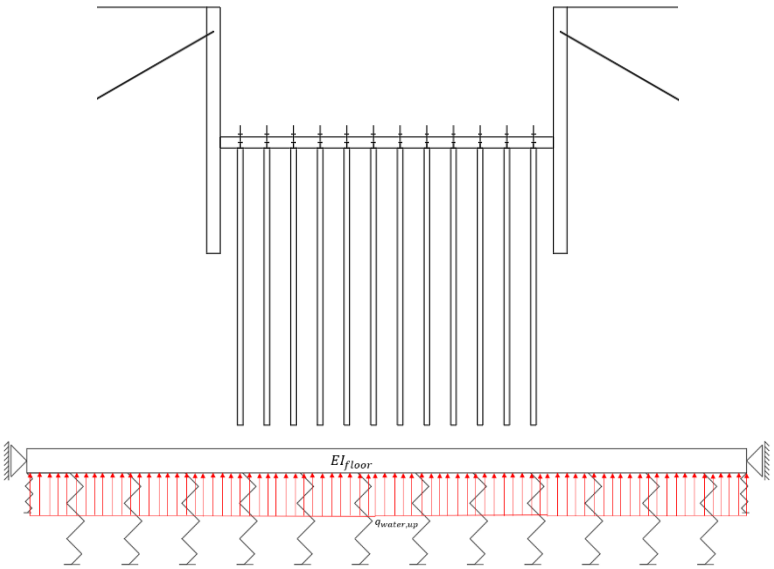

Figure 48: Load phase 1: UCF placement

The load scheme can be seen in figure 48 and this is the similar case for which the base design of the UCF is performed.

The checks that will be performed on this load case are a bending moment check (ULS) in the top fibre of the floor, for which is assumed that cracking of the floor is allowed. A punching shear check at the location of the tension piles and a shear force check (both ULS) complete the design. Finally, shrinkage effects require additional attentional attention during the complete design process of the floor.

Phase 2: Placement of (reinforced) structural floor

After the initial UCF has fully hardened, the rest of the floor is placed. This layer is traditionally reinforced with rebars as opposed to other steel fibre option since this allows for a more efficient placement of the reinforcement and consequently a reduction in the total amount of steel. This top floor layer aims to make the chamber floor completely horizontal, so the even out the tolerances in the initial UCF and it has a structural function to increase the total thickness and bearing capacity of the floor during operation. Figure 49 shows a schematization of this loading phase

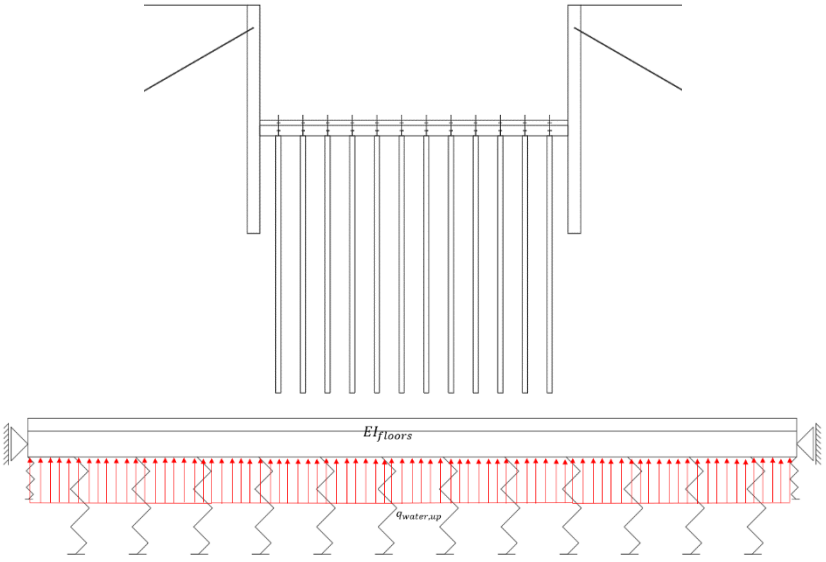

Figure 49: Load phase 2: placement of structural floor

The points of attention of this load scheme are a proper bond between the initial UCF and this top layer, for which two layers of anchor disk plates from the tension piles are necessary and dowels should be installed at a c.t.c. distance of approximately 500 millimetres. Furthermore, the addition of the top layer influences the stress distribution in the UCF through the addition of its self-weight.

Phase 3: Ship load acting on the floor

During operation, the ship load together with the upward water pressure is the governing load case for the complete floor. For the determination of the ship load acting on the floor, it is assumed that this ship is to be placed in the middle of the beam-model (in the short direction

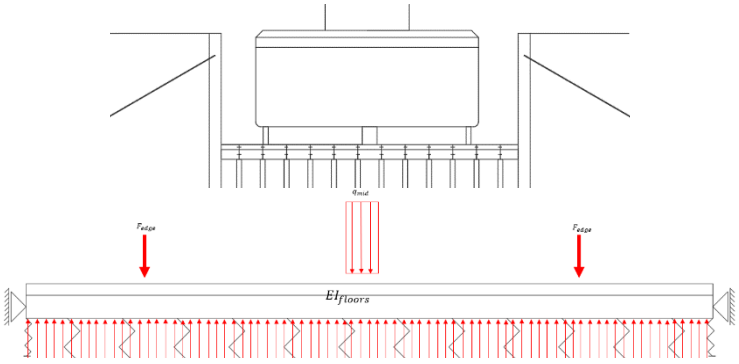

Figure 50: Load phase 3: ship load

of the floor) and no distinction of placement is made for the long direction of the floor is made, meaning that the complete floor is designed to resist the governing ship load. The load case can again be seen in the figure below. The load on the middle block is modelled as a distributed load over a width of 1.5 meters and the load on the two outer blocks are modelled as a point load due to the typically smaller width of these blocks.
The points of attention for this phase of the floor design is the maximum sagging moment at the location of the ship load locally leading to cracks at the bottom fibre of the floor, where the different fibre material can influence the maximum allowed crack width at the bottom since corrosion will not play a factor in case of basalt fibres. Furthermore, the presence of the ship will lead to increased hogging moment near the tension piles and consequently cracks in the top fibres here. As a requirement, the client has determined that the floor should be absolutely water tight due to the fact that oil and other chemicals are common on a dock floor and this might lead to deterioration of the concrete floor if the crack width is too large. According to NEN-EN 1992-3, this means that the UCF is to be allocated to Tightness class 3 (no leakage permitted) and the corresponding requirements for the force distribution inside the floor is that a minimum compressional zone height of 50 mm is required at all times. In other words, taking the shrinkage strains and ship load acting on the floor into account, the resulting cracks in the bottom of the UCF should not pass through the complete floor height (NEN-EN, 2011).
Finally, the foundation piles that are originally designed as tension piles will also serve as compression piles during this loading phase and the capacity of the piles have to be checked accordingly.
The first load phase has already been considered in chapter 5.2, the reader is referred to Appendix F for the calculations behind load phase 2 and load phase 3 and the consequences this has for the three design variants.
The required dimensions of the three floor variants are found to be as follows:

- The initial variant containing the integrated SFRUCF required a 800 mm thick steel-fibre reinforced concrete layer with a 330 mm thick top layer of traditionally reinforced concrete meaning a total floor thickness of 1130 mm.
- The variant containing the integrated BFRUCF required a 850 mm thick steel-fibre reinforced concrete layer with a 280 mm thick top layer of traditionally reinforced concrete meaning a total floor thickness of 1130 mm. While the crack width during the use phase of the floor will also reach a significant magnitude, the favourable characteristics of basalt with regards to its resistance against external conditions means that the exposure of the basalt fibre should not affect the performance of the concrete floor and therefore it can be accepted as long as the requirement regarding the water tightness of the floor is met.
- A UCF with traditional rebars would lead to the smallest thickness, since only a floor with a thickness of 850 mm is sufficient to perform both the water-retaining UCF function and the structural function to carry the ship load. This is due to the fact that the steel can be placed at an effective location, namely near the location of the outer fibre, and the performance of the reinforcement bars is more effective than the randomly spread fibres of the other two variant.

These conclusion may lead to another design alternative, namely a design that combines a layer of basalt fibre reinforced concrete at the bottom for durability considerations in combination with a top layer of steel fibre reinforced concrete for structural reasons topped off by a structural floor with traditional reinforcement since it optimizes the beneficial characteristics of each fibre type. For the current designs, the total volume of concrete for the two fibre-reinforced variants is equal, meaning that the environmental impact score and costs of the fibre material will determine which of these will score better in the evaluation of the design alternatives.

Furthermore, the influence of the thermal load, caused by fluctuations in temperature throughout the year, will lead to significant stresses in the floor and the temperature decrease

during winter can lead to cracks in the top fibre of the concrete floor. Actually when the temperature inside the hall is below -6°C for an extended period of time, the concrete tensile stress in the top fibre will exceed the cracking limits. **This further substantiates the idea of placing a hall on top of the dock where the temperature can be regulated using excess heat from the waste incineration plant since this will increase the durability of the dock floor**.

Section 5.3.2: Sedimentation reduction measures

The variants each require the installation of different sedimentation reduction measures contribution to the environmental impact and required costs for the designs.

Variant A: inlet at the other end of the dock

In order to reduce the inflow of sediment, the flow rate entering the dock through the water inlets needs to equal the displacement of the design vessel. Taking friction losses along the pipe and minor losses from the inlet and bend in the pipe, Appendix G determines that a pipe with a diameter of 2 meters, with a length of 80 meters needs to be installed at a depth of -4 m NAP at the port side and at -6 m NAP at the dock. The installed pumps need to have sufficient capacity to add 2.1 meters of head to a flow rate of 7 m^3/s. Schematization can be seen in Figure 51 and Figure 52 below.

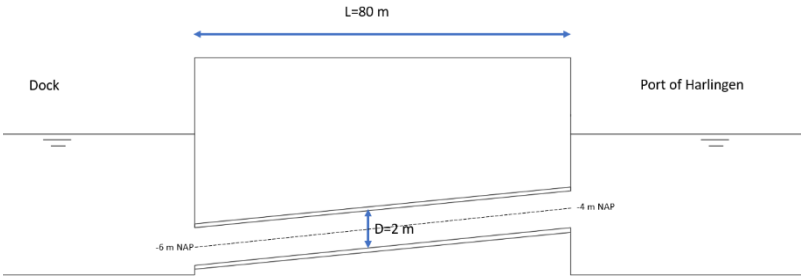

Figure 51: Inlet side view

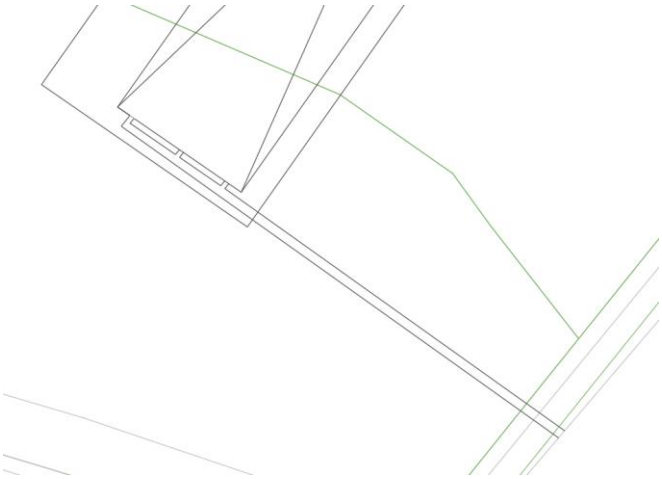

Figure 52: Inlet top view

The manufacturing, transport and placement of the pipe will contribute to the environmental impact as well as the manufacturing, transport, operation and maintenance of the pumping system and gates.

For the other two variants, the manufacturing, transport and placement of respectively the winches and bubble screen as well as the energy consumption during operation and maintenance should be included in the environmental impact analysis which will be conducted in chapter 6.1.

Chapter 6: Evaluation of alternatives and selection

In this chapter, the design alternatives that have been developed in Chapter 5 are evaluated based on their environmental impact and cost of construction, through performing a LCA and Cost and Benefit Analysis respectively. In section 6.3, these results are processed into a Multi Criteria Analysis which also take other aspects into account.

Chapter 6.1: Life Cycle Analysis

By performing a Life Cycle Assessment, the environmental impact of a product or service during its lifetime is determined, including the effects of all required raw materials and occurring emissions in all of the stages of the product's lifetime are estimated (Jonkers, 2018). The procedure to perform such an LCA consists of 4 steps as can be seen in figure 53 below (ISO 14040, 2006).

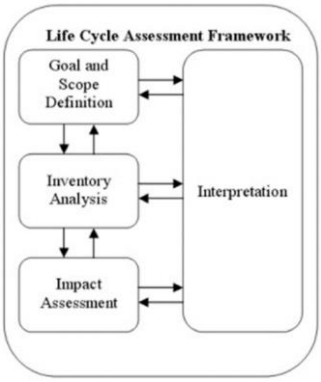

Figure 53: LCA Framework

The first step is to determine the goal and scope of the LCA. In this case, the goal is to identify the hotspots in the base design of the graving dock so that sustainable design alternatives can be developed in an efficient and targeted way. On the other side, the emissions that are involved with the different design variants are compared among each other and to the base design, so that the effects of these sustainable design strategies can be quantified and eventually an optimal design for the graving dock can be made. This optimal design can also be a combination of design elements of the three design variants, which means that the design solutions should also be compared separately. The audience for which the LCA is performed are the clients which in this case are the members of Damen BV.

The functional unit for this LCA can be described as the amount of emissions of the graving dock during a period of 100 years, with an average of 20 ships using the dock per year. The phases that are included are the material production phase (A1-A3), transportation from the production site to the graving dock construction site in Harlingen, installation/construction of the dock, operational phase and maintenance phase of the graving dock. The residual value of the design variants will only be included qualitatively and the transport on-site is neglected due to the limited size of the construction site. Some other aspects that have been left out of this LCA are the following:

- Factors associated with the hall structure, including the hall framework and walls, workspaces, offices and the associated furniture and lightings, etc.
- Fuel used during the transport of the product is assumed to be included in the emission factors given in the databases and are therefore not added
- Equipment used during the maintenance of ships inside of the dock chamber and in the dock hall are not included since they are not part of the dock structure itself. This includes paints, equipment and machinery.

- The contribution from wooden formwork for the construction of concrete elements is considered to be negligibly small.
- The emissions that are associated with the manufacturing of the equipment that is used is neglected due to the lack of available data of this topic and the fact that machinery will be used for numerous building projects which mean the contribution to our total emissions will be minimal nonetheless.
- The assembly and emissions of the concrete production plant. While it is most practical to have a concrete production plant on site, the emissions that are associated with this are neglected due to the lack of available data. It is recommended however to investigate the possibility of using a floating, mobile concrete production plant since this would be beneficial for the transport of the plant itself and the space use on site (Bonton, 2022).
- Other elements that account for less than 5% of the total mass of the structure are neglected.

The LCA aims to determine the Carbon Footprint of each design variant, meaning that only the Global Warming Potential is considered and results are expressed in terms of kg CO_2-equivalents. The reasoning behind this is the larger availability of data for CO_2-emissions for elements that are not present in the DuboCalc database. It is furthermore assumed that, in general, a correlation exists between the GWP and the other environmental impact categories and thus the variant that leads to the least amount of CO_2 emissions can also be expected to have the lowest value for the total Environmental Cost Indicator. For a first estimation of the environmental impact of the design variants, this choice is therefore expected to be sufficiently accurate.
The data has been retrieved from open databases such as DuboCalc, which contains a lot of information for specific civil engineering products, and the Idemat app which has a lot of information regarding the emissions related to raw materials, industrial processes and transport. For some materials, additional research or estimations had to be made to determine the CO_2-emissions associated with that product. The data for the installation phase has been estimated based on indicators for project cost estimations provided by De Boer & De Groot.
It has to be noted that the quality of the LCA largely depends on the quality of the data available in the databases. For DuboCalc, the information is only available for a few elements that may not completely match the profiles in the design and therefore need to be converted which can lead to inaccuracies. Furthermore, information stemming from separate sources may lead to inaccuracies since different producers could use different methods to determine the emissions depending on the type of EPD (Environmental Product Declaration) that is maintained, the standards that are used in different countries and the recency of the data. These factors may cause the need for a critical review of the LCA study.

Section 6.1.1: Life Cycle Inventory

The LCI (Life Cycle Inventory) contains a collection of data regarding the emission factors that are associated with all phases of the dock. Setting up this inventory is a crucial step in performing the LCA, since small variations in emission factors per unit can have big consequences for the total amount of CO_2-equivalent emissions due to the large dimensions of the structure. For the complete Life Cycle Inventory including descriptions, the reader is referred to Appendix H. The on-site transport phase has been neglected due to the short distances covered here compared to the transport of the good from its place of origin to the building site in Harlingen.
For the transport phase, the material's place of origin has been chosen as either the most commonly applied distributor in practice (steel items from the TATA-steel factory in IJmuiden, cement from the ENCI IJmuiden, Gravel from near the Meuse river in Limburg), or by searching for the nearest fabricator of the structural elements. Many of these structural elements such as the combi-wall, anchors and fibres originate from Germany. The LCA data from a EPD from

an Italian distributor is used and so the reinforcement steel is assumed to originate from this factory.
The installation phase also requires some assumptions for equipment running on fuel. Here, the emission factor for diesel is used for simplicity while in practice, some equipment could potentially also run on more sustainable fuel alternatives such as HVO.

For the emissions during the operational phase, a short describing of the mode of operation of the design variants is required. Each operational phase starts with the opening of the gate for which Variant A (caisson gate) uses an external telescopic crane and the emissions stem from its electricity consumption during the 30 minute period that is estimated for the duration of this process, where the crane works at 50% of its maximum capacity. Energy consumption of the sliding gate, which uses the hydro jets and winch system that reels the gate to the side determine the emissions during the 30 minute gate operation for Variant B. Variant C only needs the hydraulic power unit to operate the mitre gate which is expected to take around 30 minutes.
All three variants as well as the base design include the operation of the pumping unit to empty the dock chamber within 3 hours.
The base design does not include any sedimentation mitigation measure and so the dock floor needs to be cleaned by high pressure washers and a sediment removal machine. The sediment then needs to be transported over a distance of 60 km to a special waste plant in Middenmeer. The transport of a 5 centimeter thick sediment layer covering the dock floor by truck is included in the computation of CO_2-emissions of the base design. Furthermore, the fuel consumption of two tugboats running at 50% of their engine capacity is included for the docking duration of 2 hour.
Variant A includes the energy consumption of the pumping unit at the piped inlet during the docking procedure and it is assumed that 1 tugboat is needed for support during docking procedures, where this tugboat runs on 20% of its maximum power.
For Variant B the energy consumption of the hydrojet pumps that create the bubble screen during docking procedures needs to be included as well as the single tugboat guiding the vessel.
Variant C does not include the emissions of tugboats as they are no longer needed with the presence of the winches and the emissions stem from the electricity used by these winches.
The maintenance strategies from which the emissions during the maintenance stage originate are described in Appendix H.

Section 6.1.2: Impact assessment and results

The calculations to obtain the emissions during construction, operation and maintenance phase of the dock base variant can now be determined, for the material phase this requires the total amount of each material element and multiplying this by the emission factor. The emissions for the transport stage also requires these amounts per element. For the installation phase, the productivity of the equipment in combination with the amounts of each element determines the fuel consumption and eventually the total emissions. The emissions during operations are based on 20 ships entering and leaving the dock on average per year and finally the emissions for the maintenance phase can be determine based on the maintenance strategies.
In Appendix H, the calculations behind these phases can be found for each of the 4 design.

The first goal of the LCA was to gain insight into the so-called ‘hotspots’, the aspects that contribute most to the total carbon footprint of the base design, which allows for an effective development of sustainable design alternatives. Figure 54 below illustrates the total emissions of the base design and the relative contribution of each lifetime phase to this total.

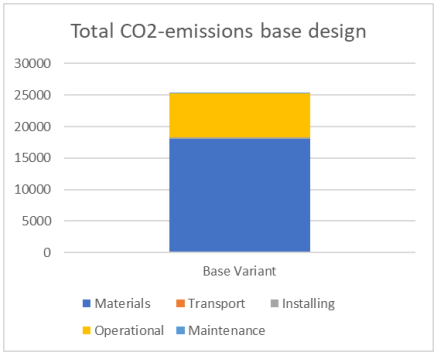

Phase	Emissions [ton CO_2-eq]	Contribution
Material production	17790	71%
Transport to site	74	<1%
Construction	228	1%
Operation	7015	28%
Maintenance	80	<1%
Total	**25385**	**100%**

Figure 54: CO_2-emissions base design

The material production phase is the predominant contributor to the total emissions of the graving dock, which is mainly caused by the reinforced concrete which accounts for nearly 70% of the material production phase. The operational phase, and then mainly the cleaning and disposal of the sediment, is the 2nd largest contributing phase. The contribution of the other phases together is merely 2% of the total. It can be concluded that the sustainable design aspects that have been developed, namely the reduction of the required amount of concrete through an alternative floor package and the sedimentation reduction strategies indeed target the largest contributing factors to the carbon footprint of the dock.
The steel piles that are part of the combi walls is another large contributing factor, as it accounts for 17% of the total material production phase. While no further optimization has been made regarding this aspect, reduction of the floor thickness can also lead to a reduction in pile length since the installation depth of the floor will be less deep. This has not been taken into account here but can potentially serve as another possibility to reduce the carbon footprint of the base design.
The other goal of this LCA was to compare the design variants, initially by looking at the total carbon footprint and then by zooming into the specific design aspects of each variant. Figure 55 illustrates the total emissions of the design variants, for each variant a reduction of emissions can be seen compared to the base design.

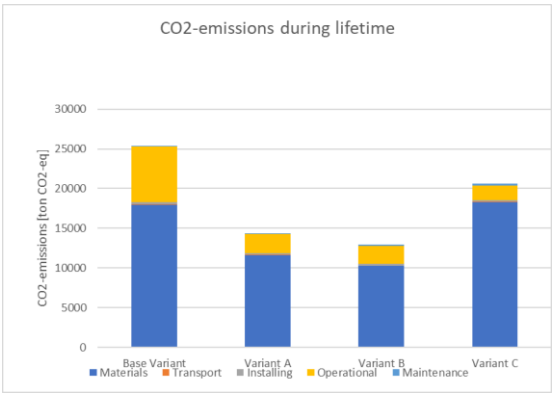

Figure 55: Comparison of CO_2-emissions

The materials production stage and operational phase are still the predominant phases of the lifecycle for the variants and the main reductions are caused by the alternative floor designs. This is also illustrated in Figure 56 which compares the total emissions during the material production, transport and installation phases of the UCF alternatives. The operational and maintenance phases are irrelevant for the dock floor which is why these are omitted here. Variant B shows the greatest reduction in emissions when compared to the base design and the other design variants. The results show a strong correlation with the required amount of reinforced concrete in the design, as this layer for Variant B is 50 mm less thick compared to Variant A. This, together with the lower emissions associated with the basalt fibres compared to steel fibres, results in the difference between Variants A and B. Variant C, which contains

only the concrete floor with traditional rebar reinforcement, actually shows an increase in CO_2-emissions compared to the base design.

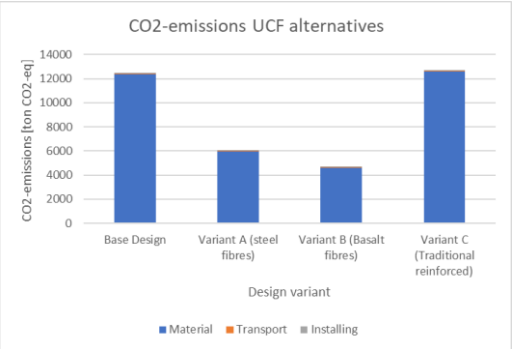

Figure 56: UCF emissions comparison

As far as the sediment reduction strategies are considered, the comparison between the various mitigation measures are depicted in Figure 57. The operational emissions from the table are multiplied by a factor 100 to account for the complete lifetime of the dock.

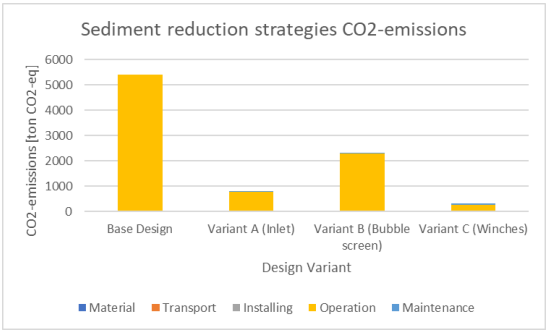

Figure 57: CO_2-emissions sediment reduction strategies

The dominant contributing lifecycle phases differ among the design variants. For the base design, no mitigation measures are installed and extensive cleaning works are necessary which explains why emissions only stem from the operational phase here. For Variant A, the external telescopic crane that removes the gate is the only source of emissions, this process is estimated to be relatively short which explains the limited emissions. The required energy for operation of the bubble screen makes up the majority of the emissions for Variant B and the large amount of moving elements mean that increased maintenance account for the emissions of the winch system for Variant C. All in all, the sediment reduction strategy of Variant C scores best by saving 90% of the emissions that result from removal of the sediment, Variant A saves around 85% of the emissions and Variant B causes 50% less emissions compared to the base design.

Finally, the three dock gate types are compared as depicted in Figure 58

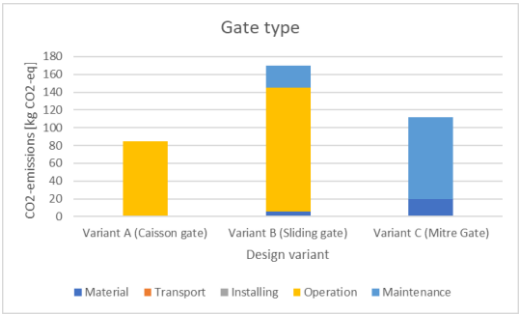

Figure 58: CO_2-emissions gate type alternatives

We can directly conclude that the caisson gate has the smallest carbon footprint compared to the other types, due to the fact that is doesn't require additional driving mechanisms that are installed in the dock head structure that need to be constructed, installed and periodically maintained. It only uses the power from the external crane to remove the gate.

Section 6.1.3: End-of-life phase

The end-of-life phase consists of the demolition of the dock and the residual value that elements of the dock will still have at that point. The design elements that are unique to each design variant will distinguish between the end-of-life value of the design variants, starting off with the UCF variants. It is expected that the demolition of all three floor types will completely crush the (reinforced) concrete and so naturally, no direct reuse of the floors are possible. However, the concrete could be downcycled into other structural materials such as construction rubble and create value in a different purpose.
The elements that set apart the floor types are the fibres inside of the UCF, starting off with the steel fibres present in Variant A. After demolition of the UCF, the steel fibres are also expected to be at the end of their lifetime and so recycling by reheating of the steel in a furnace seems like the only option. This process, as well as separating the steel fibres from the concrete, requires the input of additional energy which contributes to the total lifetime emissions of this design variant A. The same can be said for the floor with rebar reinforcement of Variant C but the process of separating the steel from the concrete should be a lot simpler. Since basalt fibres typically have a longer lifespan than steel, the basalt fibres are expected to have a larger residual strength. However, the basalt fibres cannot be recycled in the way steel can because the production process of the basalt fibre is a one-way process (Slegers, 2022). All in all, the demolition processes of the UCF variant are considered to be similar but the steel variant allow for more possibilities for recycling than the basalt does and so the residual value of variants A and C is considered to be greater than for Variant B.
For the sedimentation reduction strategies, the removal and demolition of the concrete pipe requires additional processes and corresponding emissions compared to Variants B and C. All elements, including the concrete pipe, the hydro jet installation and winches will be at the end of their lifespan and therefore don't offer a lot of residual value, the demolition process of Variant B and C is a lot easier compared to Variant A.
As far as the gate operation systems are concerned, the demolition process of all three variants can be expected to be similar, and where the caisson gate system does not include any additional parts that requires removal or any residual value, some parts of the hydro jet system or mitre gate system could still be recycled and reapplied in other projects. These variants also cause the largest amount of waste products that needs to be treated since there are simply more moving elements for the sliding and mitre gates and so these two variants are both expected to have the least beneficial end-of-life phase.
All in all, the design variants do not offer a great deal of residual value since almost all elements are considered to be at the end of their life span and so they would require additional treatment before being able to serve another purpose. This can be prevented by taking the end-of-life phase into account in the design process at an earlier stage, for example by applying the 'design for disassembly' method which allows for an easier demolition process or by implementing sustainable building materials that have a lifespan that exceeds the lifespan of the dock. This might be at the expense of the costs or structural integrity of the dock though which calls for an accurate assessments of the risks and benefits of applying these sustainable design methods.

Section 6.1.4: Conclusions

All things considered, a few conclusions can be drawn from this LCA:

- The developed design alternatives indeed target the largest contributing factors to the carbon footprint of the base design, namely the amount of reinforced concrete for the dock floor and the emissions during operations associated with the removal and disposal of sediment.

- The amount of reinforced concrete is actually the predominant factor in the complete carbon footprint of a graving dock, since the production of reinforced concrete accounts for 53% of the total emissions during the complete lifecycle of the base design.
- The most sustainable design of the graving dock, purely looking at CO_2-emissions, would be the combination of the UCF-package of Variant B (containing basalt fibre), the winch system of Variant C, and with the installation of a caisson gate.

The LCA is used to determine the most sustainable combination of design alternatives to optimize the carbon footprint of the dock design. However, other criteria such as cost of construction, speed of operation etc. also influence the performance of the design alternative so it cannot directly be concluded that the final design should be the most sustainable combination of design alternatives. A Multi Criteria Analysis should be performed which takes the results from this LCA into account by weighing is against other criteria to eventually come up with the final design.

In the multi criteria analysis, a fourth design variant will be taken into account. This Variant D contains the elements that lead to the lowest carbon footprint with the exception that a piped inlet is chosen due to its speed of operation compared to the winch system and the fact that the carbon footprint of these two sedimentation reduction strategies is similar. So to summarize: **Variant D contains a basalt fibre reinforced UCF, a piped inlet and a caisson gate**, this combination of elements will also be included in the cost benefit-analysis and multi criteria analysis in the next chapters.

Chapter 6.2: Cost-Benefit Analysis

This section aims to identify all costs and benefits present during the lifetime of the dock and give insight into the most cost-effective design options, the estimated required construction costs and the development of the net balance between costs and benefits throughout the lifetime of the dock. The results from this analysis will be applied in the multi criteria analysis since it allows for a ranking of the design alternatives for the cost criteria.
The following costs and benefits can be classified:

Costs	**Benefit**
Construction costs	Yearly docking revenues
Operational costs	
Maintenance costs	

Other potential costs such as the costs of obtaining the required building area, cost of design and other unforeseen costs have been included by adding a factor of 15% over the initial construction costs. It has to be noted that not all construction costs are included in this assessment, for example the hall structure, pump infrastructure, overhead crane structure and foundation, dock head structure, offices and other elements that are excluded in this design will drive up the initial required investment. This is partly accounted for by including the factor of 15% over the calculated construction costs but in practice this margin could prove to be larger.
Other, non-quantifiable benefits such as the increase in rate of employment, increase in docking capacity and reduced waiting times have been omitted from this analysis since it could inclusion can add confusion about the goal of this analysis and steer the analysis in the wrong direction (Molenaar & Voorendt, General lecture notes Hydraulic Structures, 2020).

The structure of this section is similar to that of the LCA in section 6.1; the inventory of costs used per life as well as the actual calculations are placed in Appendix I. Here, a few assumptions that form the base of the analysis are given as well as the interpretation of the results.

Section 6.2.1: Construction costs

The material costs comprise of the costs of the materials, the transport to the construction site and the installation costs. The material cost prices are assumed to include the prices for

extracting the raw material (A1), transport to the production location (A2) and the production process itself (A3). For the transport phase, the costs solely include the fuel costs and these have been determined based on the most recent diesel fuel prices. For barge transport, inland transport has been assumed to be done by use of the Kempenaar vessel, which has been built for Dutch inland navigation with a capacity of approximately 700 tons. Transport coming out of Germany has been assumed to be done by a Dortmunder vessel with a maximum capacity of 1000 tons (Wereld van de Binnenvaart, 2023). Their fuel consumption in €'s per km is then determined by using information from target prices stemming from a 2008 report by NEA which have been adjusted to account for inflation over time. For the Kempenaar Vessel (CEMT II – M2 class) this has been determined to be €5.30 per km and for the Dortmunder (CEMT III – M4 class) this value is €9.30 per km (Van der Meulen, Quispel, & Dasburg, 2009). For transport by truck, the fuel consumption has been determined to be at 40 litres per 100 km, with a diesel litre price of €1.75 per litres results in €0.70 per kilometre (Webfleet, 2020).
The installation phase comprises of the fuel used during installation and the rent of some external cranes that need to be used. For many installation processes of the base design (in the information that has been provided by Adonin), the rent of the equipment is assumed to be processed in the price that is used in the material phase and therefore omitted here. A diesel price of €1.7 per litre is used again together with a kWh price of €0.8/kWh even though this can be considered to be a conservative estimation when taking the developments in energy prices into account.

The total cost of construction of the base variant has been found to be roughly €6.55 million and after adding the 15% to account for design costs and other unforeseen factors, the costs amount €7.55 million. For Variant A, the total construction costs amount to roughly €7.85 million, for Variant B this is roughly €7.99 million, for Variant C roughly €7.1 million and finally for Variant D roughly €7.67 million.
The results for the construction costs can be compared in Figure 59.

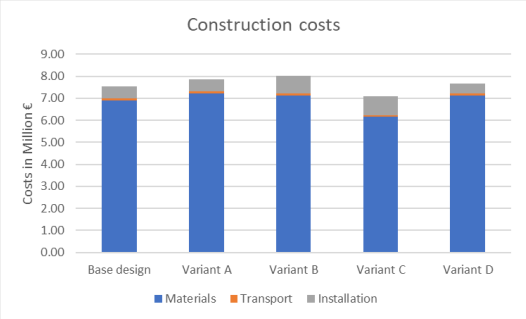

Figure 59: Construction costs comparison

When comparing the construction costs of the design variants, the costs of production of the steel and basalt fibres appear to be larger than the reduction in costs from saving a certain amount of concrete. Additionally, the implementation of the sedimentation reduction strategy and the increased costs that this brings through the purchase of additional elements leads to the result as depicted in figure 59. The design Variants A and B are approximately 5% more expensive than the base design, while design variant C saves around 5% of these costs. Variant D combines the base costs of Variant A with the implementation of the basalt fibres which leads to a beneficial effects with regards to the construction costs. When looking at merely the UCF variants as depicted in Figure 60 below we can conclude that in general, a correlation exists between the reduction in carbon footprint of the dock and the costs of construction. Larger reductions require a larger monetary investment and on the other side the reinforced concrete floor present in variant C leads to a 30% cost reduction compared to the base design but also leads to the largest carbon footprint in the LCA.

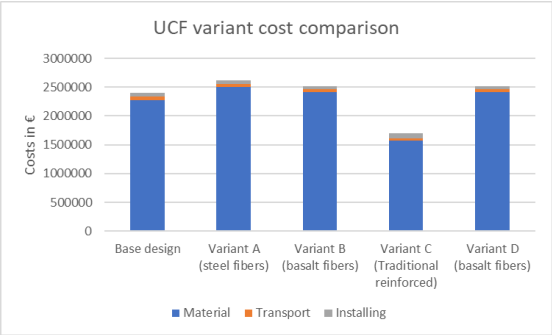

Figure 60: UCF construction costs comparison

The multicriteria analysis in the next chapter should decide which of these floor alternatives should be chosen by weighing the relative importance of the reduction of carbon footprint and minimization of construction costs that the three design variant bring. At first glance, the basalt fibre reinforced UCF appears to score best among those two criteria (carbon footprint reduction and construction costs).
A small note should be made regarding the constructability of the traditional reinforced UCF of Variant C. In practice, placement of this floor type could require additional measures such as the continuous drainage of the building pit before the reinforcement can be accurately placed and the associated costs could drive up the total amount considerably. These additional costs are currently not included in the CBA and therefore the results for Variant C might be inaccurate.

Section 6.2.2: Operational & maintenance costs

The operational costs stem from the energy used during docking procedures and the fuel and rent of tugboats. In following paragraphs, the estimated construction costs are determined per year, where again 20 dockings per year are assumed. All other assumptions regarding the duration of docking procedures maintain from section 6.1.
For the base design, a moderate value is chosen for the disposal fee of the sediment per ton in combination with a conservative amount of sediment that is present in the dock, namely a layer of 5 centimetres on the complete dock floor. The disposal price per ton sediment has been set at €50 per ton after deliberation with supervisors.
For the energy prices, fuel prices of €1.70 per litre of diesel and €0.80 per kWh are maintained and the equipment operates at 50% of their maximum capacity. The rent of the tugboats per hour is set at €400 and for the base design, 2 tugboats are required for a period of 2 hours.
The exact calculations of the operational costs are again placed in Appendix I.

The costs associated with the regulated maintenance strategy as described in chapter 6.1 will be calculated next. Again the costs associated with the inspection of the design elements are estimated to be 5% of the required estimations to construct, transport and install a new element. The reader is referred to Appendix I for the calculations of the maintenance phase per variant, the following paragraph will compare the calculation results.

The yearly operational costs are multiplied by a factor 100 to calculate the total operational costs during the total lifetime of the dock. Figure 61 below shows that the operational costs of the base design are a great deal larger than that of the design variants which proves that prevention of the sedimentation of the dock does not only benefit the carbon footprint of the design but will also drastically lower the total costs.

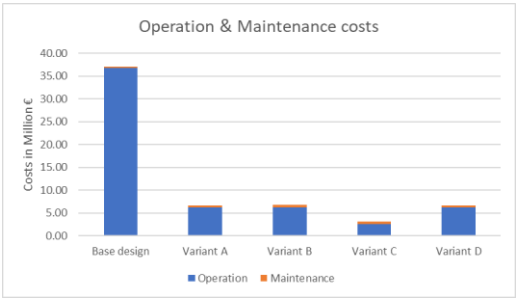

Figure 61: Total operational & maintenance costs

When only taking the costs associated with the sediment reduction strategies into account we can see the same trend, as depicted in Figure 62.

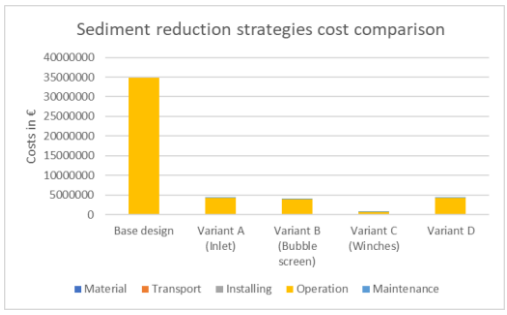

Figure 62: Sedimentation reduction strategies cost comparison

The disposal of the sediment leads to the majority (78%) of the costs associated with the base design and this is no longer needed when sedimentation of the dock is prevented. Variants A and B show similar costs but the system of winches of Variant C is clearly the best-scoring option because tugboats are not needed for this design variant.

As far as the costs involved with the different gate operation modes are concerned it is clear from Figure 63 that the presence of hydro jets and winches for the sliding gate require a lot of additional maintenance which makes the sliding gate variant the most costly.

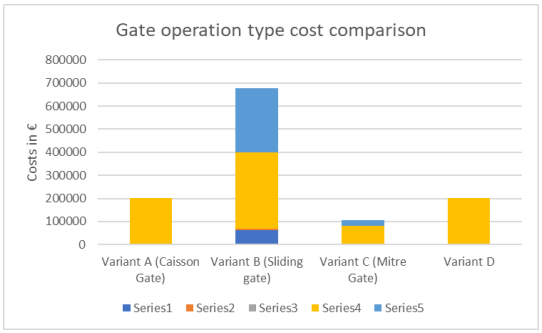

Figure 63: Gate operation type cost comparison

All in all, the total lifetime costs of the design can be combined and plotted to collect all the information into one graphical representation as shown in Figure 64.

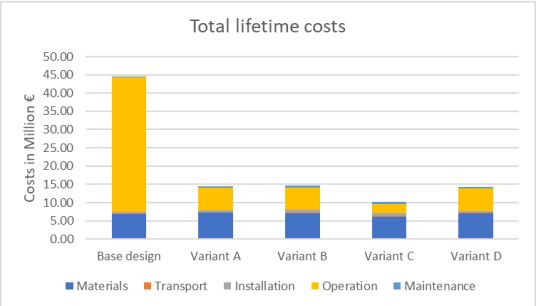

Figure 64: Total lifetime cost comparison

The most cost effective design options would be variant C, but is has to be kept in mind that this variant performed worst in the LCA and so the weighing of these and other criteria during the multi criteria analysis will need to determine the actual optimal design combination. Apart from that, design Variant D would score well on both the financial and sustainability criteria.

Section 6.2.3: Benefits – docking revenues

Throughout the lifetime of the dock, the main quantifiable benefit that will provide a yearly revenue stems from the fee that ship owners have to pay for using the dock when the ship maintenance works are performed. In collaboration with the client, these fees have been set as follows:

	Fee
Docking procedure	€5.000,-
Daily rent	€2.000,-

A fixed amount of €5000,- is paid for docking the ship into the chamber and placing it on the blocks, after that a daily fee €2000,- needs to be paid for each day that the ship is inside of the chamber, a so-called 'sitting-day'. Therefore, the total annual revenues depend on the duration of the maintenance of one vessel and the number of vessels that will use the dock per year. On average, each docking period will last between 10-14 days and 20 dockings per year will take place which means a yearly income between €500.000,- and €660.000,- .

Section 6.2.4: Cost-benefit development over time

All monetary stream flows can now be combined in one overview to determine the development of the net balance between costs and benefits over the lifetime of the structure. In this way, the expected return of investment for the design variants can be made clear and it can be determined whether the construction of the new dock is actually a viable choice over time.

In order to determine whether the investment that is required for the construction of the dock is worth it, the Net Present Value (NPV) is calculated. In this way, the present value of future cash flows is quantified by applying a certain discount rate that describes a required return on an investment. The later the money stream appears, the larger the discount value and so the smaller the value that money stream has in the present year. The NPV accounts for the time value of money and it can be determined using the following equation (Jonkman, Steenbergen, & Morales-Nápoles, Probabilistic Design: Risk and Reliability Analysis in Civil Engineering, 2017):

$$NPV = \sum_{t=0}^{T} \frac{C_t}{(1+r)^t}$$

Where C_t is the nett cash flow (benefits minus costs) in year t and r is the discount rate. In year 0, the construction of the dock takes place and so the investment is made. After this, the yearly flow of money consist of operational and maintenance costs and docking revenues. Applying a discount rate of r=0.025 is common practice and implementing the described maintenance strategies for the design variants, the development of the NPV over time can be seen in Figures 65 and 66 below.

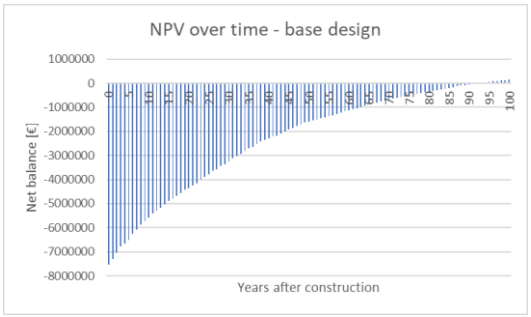

Figure 65: NPV development over time – base design

And for the design variants:

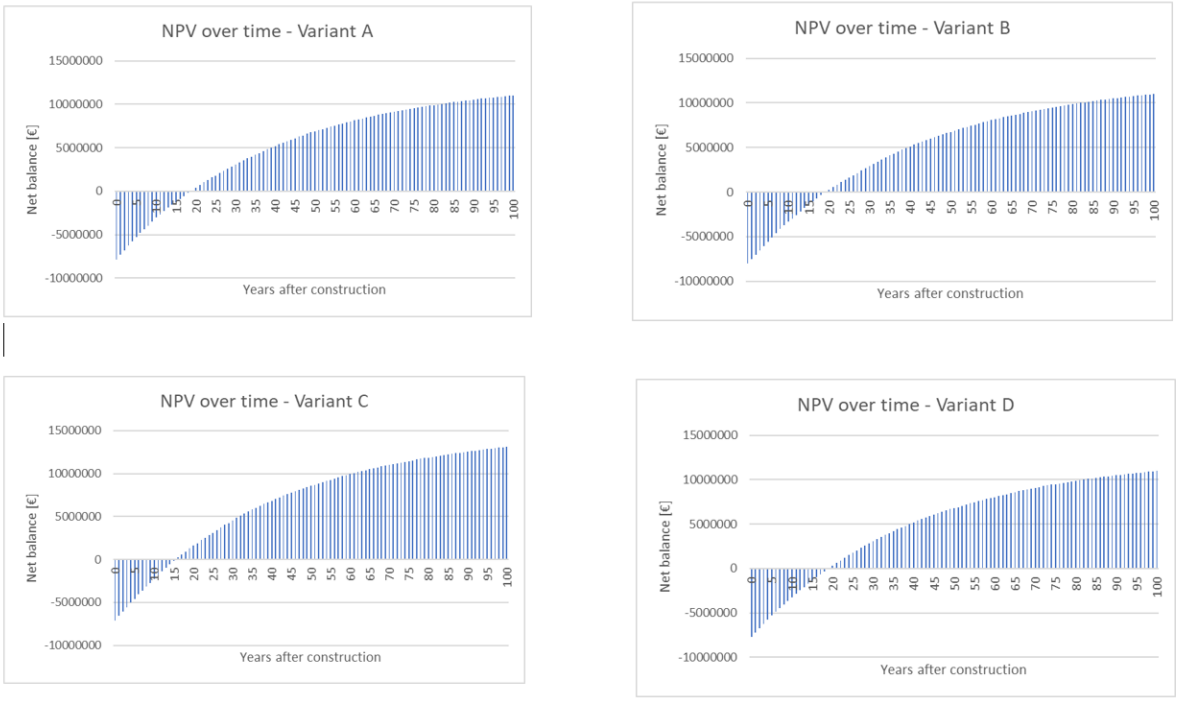

Figure 66: NPV development over time – design variants

The higher yearly operational costs for the base design results in a clearly less viable NPV development over time, with an expected return of investment of approximately 90 years. For all design variants this expected return of investment is shifted to approximately 20 years. The maintenance costs for variants A, B, C and D are in the same order of magnitude and so the main difference maker needs to be found in the difference in annual operational costs among the three design variants, it turns out that the lack of tugboat renting costs saves around €32000 in operational costs per year compared to variants A, B and D and this makes Variant C the most beneficial option over time.

All in all, the main takeaways from this Cost-Benefit Analysis are:

- Comparing the results of the CBA and the LCA it appears that a reduction of carbon footprint requires some additional investments. This is most clearly visible in the

results for the different dock floor packages since variant C clearly is the cheapest option but also leads to an increase in CO_2-emissions compared to the base design.
- Prevention of sedimentation pays off. The disposal of sediment throughout the 100 year lifetime is by far the largest expense and any mitigation method is worth its investment. When comparing the sedimentation reduction measures, the absence of tugboats is the deciding factor that makes the system of winches the most cost-effective option.
- The expected return of investment is approximately 20 years.

Chapter 6.3: Multi Criteria Analysis

The goal of the MCA is to determine the optimal design of the graving dock. A number of criteria need to first be identified, after which a weight (which describes the relative importance of each criteria) is given to these criteria and all design variants are assigned a score between 1 and 10 for each criteria. A weighted average then determines a ranking among the design variants.

First, a brief explanation of the design criteria that are included in this MCA are introduced:

- Reduction of carbon footprint (sustainability): Using information from the LCA, how much CO_2-emissions are saved by each design variant compared to the base design. In general, a correlation exists between the carbon footprint and the other environmental impact categories and thus this criteria also gives an indication of the overall sustainability of the design variants.
- Expected return of investment: While normally MCA's tend to compare criteria that represent a certain value of a design alternative, the costs can still be included by allocating higher scores to variants that require less construction, operational and maintenance costs. In other words, the expected return of investment that represent the break-even point between the costs and revenues gives an overall view of the financial performance of the design variants. The scores will be given based on the results from the cost-benefit analysis.
- Ease of operation: This criteria is a measure for the user-friendliness of the design variant. It includes the required time to perform a docking procedure, the complexity of the operations that need to be performed and how many employees are needed to do so. It also assesses the safety with which the docking procedures are performed and the risk of malfunction of the docking elements.
- Ease of maintenance / accessibility (how easy and fast can the maintenance be performed) This criteria aims to assess the accessibility of the dock elements that need maintenance after a period of time. So how fast can this maintenance be performed and what type of measures need to be taken to do so. This is important since the fast and ease maintenance works mean that the dock is out of service for a minimum amount of time each year which would be beneficial for the yearly revenue of the dock.
- Constructability: This criteria describes the ease of construction of the design variant, including the required construction expertise and knowledge for realization, the duration of the construction of the dock and the type of equipment that is needed.

The next step is assigning a weighting factor to each of these criteria to determine their relative importance in the decision making process and the way that this is done is by comparing the criteria in pairs in a matrix. The procedure is described in Appendix J, but the results are as follows. Ease of operation and sustainability are the most important criteria and are assigned a weight of 35% and 30% respectively, followed by ease of maintenance which is given a weighing factor of 20%, costs is then given a factor of 10% and finally constructability is given a factor of 5%.

The importance of the criteria can change during the lifetime of the dock, during the design and construction phase, the sustainability might be more important but during the operational phase, the ease of operation and ease of maintenance outweigh those other aspects. This could've been accounted for by shifting the weighting factors for the comparison of the design aspects.

The criteria and weighting factors are determined and so the next step is to assign scores to the design variants for each criteria. Table 17 below shows the scores of the variants and underneath the tables, an explanation of the allocated points is given in Appendix J.

Table 6: MCA scores

		Design alternative			
Criteria	**Weight**	**A**	**B**	**C**	**D**
Sustainability	35%	8	9	6	9
Return of Investment	10%	7	6	9	7
Ease of operation	30%	6	7	8	6
Ease of maintenance	20%	9	5	7	9
Constructability	5%	7	6	4	7
	Scores	**7.5**	**7.2**	**7**	**7.8**

The scores for the sustainability criteria result from Figure 55, showing the total carbon footprint of the design variants. The scores for the financial criteria are substantiated by the results from Figure 66 and Figure 64 which shows the total lifetime costs. The remaining criteria require a more subjective assessment, which is explained in Appendix J, which also shows MCA scores for all design elements separately.
It can be concluded that alternative D offers the optimal combination of reduction in carbon footprint, required monetary investments and ease of operation & maintenance. This design variant is therefore chosen to be the recommended build-up for the new graving dock.

Chapter 7: Design Optimization

In this chapter, the results from the Multi Criteria Analysis in chapter 6.2 are used to determine the optimal conceptual design for the dock. The final dock components such as the pumping system, connection to the residual heat network and dock head structure are made.

Chapter 7.1: Remaining dock elements

The multi criteria analysis in Chapter 6.3 has determined Variant D to be the most optimal combination of design alternatives. This means that the dock will have a floor package that contains a 850 millimetre thick underwater concrete floor to which 1.5 volume % basalt fibres are added, integrated a 280 millimetre thick structural floor containing rebars. This configuration saves the largest amount of carbon emissions compared to the base design as it reduces the emissions for the floor by 63%. The sediment reduction emission that is implemented is the piped inlet, that has a diameter of 2 meters, a length of approximately 80 meter and is installed at a depth of -6 m NAP in the dock chamber. This mitigation measure allows for the fastest docking procedure compared to other sedimentation reduction strategies which is it's main benefit. The gate mode of operation that is applied is a caisson gate, meaning that the gate is completely removed from its seat during dockings, either by making the gate float or by lifting it out using cranes. The main benefits of having a caisson gate is in the fact that maintenance can easily be performed and it has a relatively simple constructability compared to the other two automated operation types.

A number of dock elements still need to be considered, starting off with the dock head structure that forms the seat for the dock gate and supplies the water tightness. The design consideration can be found in Appendix Q, Figures 67 and 68 show a side view and front view of the chosen dock head layout and its dimensions.

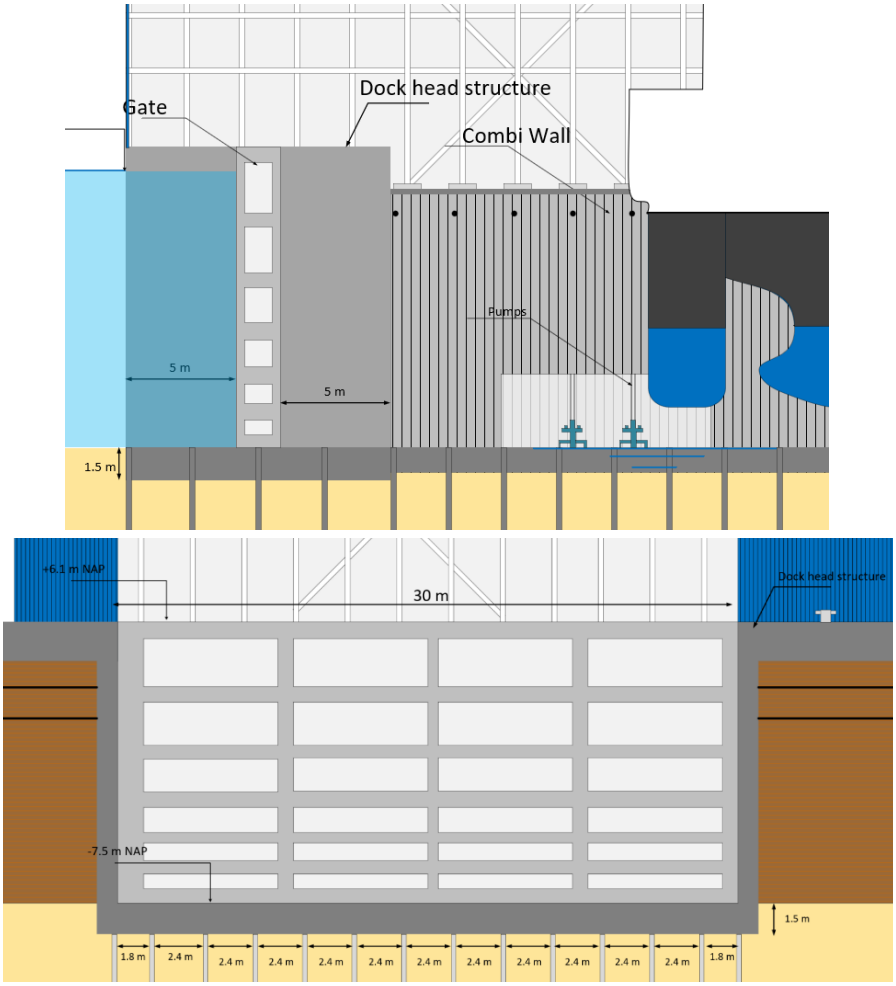

The inclusion of a dock hall is recommended due to the benefits that controlling the environment inside of the hall brings. Not only will the quality of some of the operations within the dock be improved, the elimination of concrete shrinkage due to temperature fluctuations throughout the year will be beneficial for the structural integrity of the dock floor and reduce the probability of cracking. The structural design of the dock hall is not part of this thesis but global requirements for the dimensions are determined and processed in the sketch, these required dimensions are a length of 167 meters, a width of 50 meters and a height of 40 meters.
On top of this, it is highly recommended to include the use of the residual heat from the REC for controlling the hall temperature. This would require the expansion of the infrastructure that would bring the heated water to the dock but since both the equipment (large heat exchangers) and knowhow is present within the Damen company, and it would create a sustainable win-win situation for both Damen as well as the REC, these investments will likely be worth it.
The pumping unit to empty the dock chamber should consist of two centrifugal pumps that have a maximum capacity of 10000 m^3/h such as for example the Amarex KRT K pumps. This pump capacity allow the dock to be pumped dry withing 3 hours which was one of the client's wishes. The pumping unit is installed near the dock gate so that the leakage discharge through the gate can directly be removed from the dock again.
The hall should contain at least 6 workspaces to facilitate the maintenance works and an office area, from which the dock master can operate the dock which is often build above the workspaces. These workspaces should each roughly be 8 by 10 meters and 3.5 meters high.
Two overhead cranes are installed, consisting of 2 trolleys with a capacity of 20 tons per trolley. The choice for overhead cranes over an entrance has been substantiated in section 5.2.5 and the piled foundations of these cranes are not included in the current design.
While all of these elements require additional design steps which have been considered to be outside the scope of this report, they have been included in the sketches below to show indications of their dimensions and locations within the dock. These are by no means the final designs for those elements.

Chapter 7.2: Concluding sketches

The final step is to combine all dock elements into some final sketches. Firstly, Figure 69 shows a sketch with a cross section of the dock.

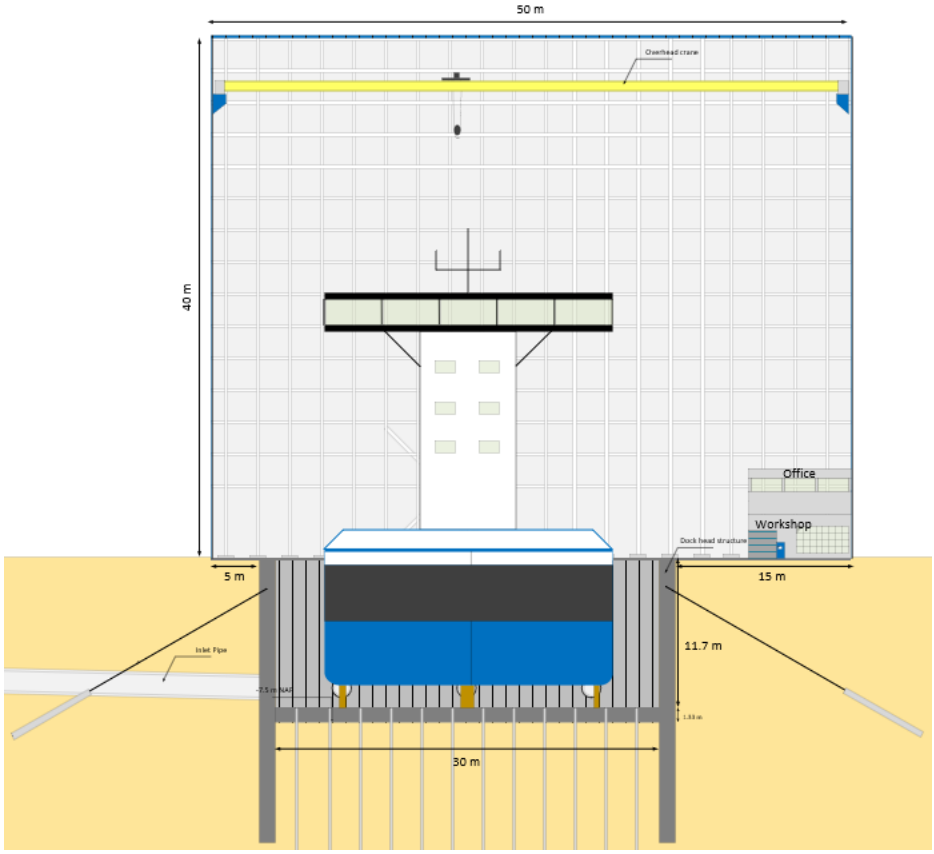

Figure 69: Dock cross section

Figure 70 shows an overall side view of the dock, including pumping units near the gate and the inlet pipe on the far right.

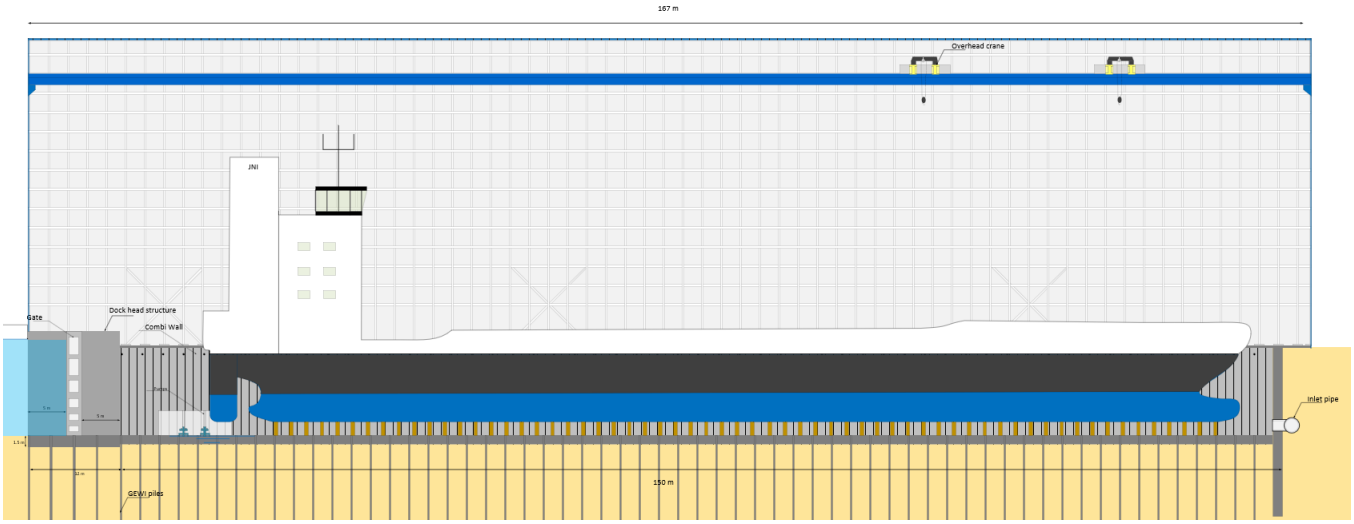

Figure 70: Dock side view

Finally, for completion, Figure 71 shows a top view of the final location of the dock in relation with the current Damen shipyard.

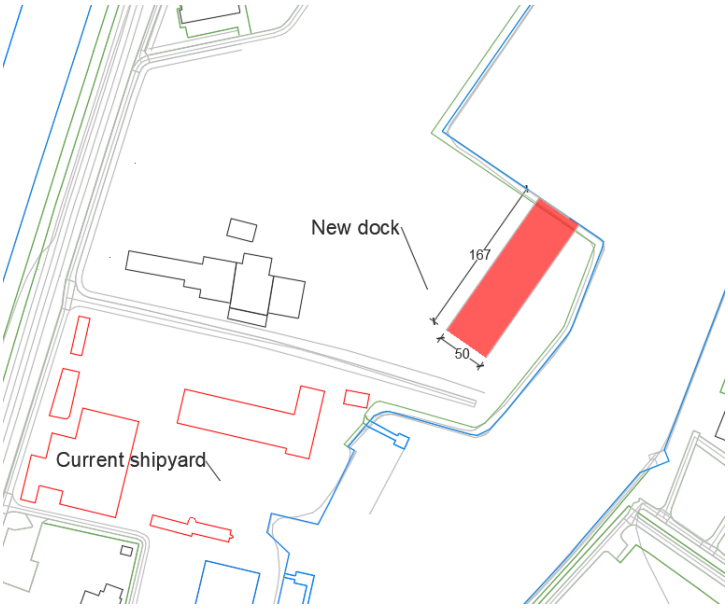

Figure 71: Dock location top view

Chapter 8: Conclusion, discussion and recommendations

This final chapter summarizes the main conclusions, discusses the results and offers recommendations for further research in this field.

Chapter 8.1: Conclusions

This thesis aimed to develop a conceptual design of a graving dock, where the minimization of the environmental impact of the dock was the main focus point. The requirements for this new dock are:

- Sufficient capacity to dock a design vessel with a length of 135 meters, width of 21.5 meters and a draught of 7 meters.
- Total dimensions of the dock chamber including tolerances are a length of 150 meters, width of 30 meters and depth of 11.8 meters.
- A hall on top of the dock where the temperature can be regulated since this allows for better quality of vessel maintenance works and increases the durability of the dock floor.
- A ship-carrying block height of 1.8 meters and dimensions of the covering hall are a length of 155 meters, width of 50 meters and a height of 40 meters.

A base design that takes these requirements into account and serves as a basis for comparison of the sustainable design variants contains the following elements:

- Retaining walls consisting of a combi-wall profile with GEWI63.5 anchors at a centre-to-centre distance of 2.48 meters and tension piles that are installed at a grid of 2.5 by 2.4 meters.
- A floor package consisting of the ‘traditional’ buildup: a 1 meter thick underwater concrete floor (UCF) that solely has a water retaining function, covered by a layer of fill sand and a structural floor of 500 mm thickness containing rebars that carries the loads.
- The design gate has a width of 30 meters, a height of 13.6 meters and weighs 270 tons.
- The foundation of the graving dock should reach the deep sand layer that originates from the Pleistocene era. This sand layer start at -24 meter NAP and has a high bearing capacity in combination with a high over consolidation ratio (OCR), meaning that settlement related damage to the dock can be prevented.

A life cycle analysis (LCA) identifies the following hotspots in the carbon footprint of this base design:

- The amount of reinforced concrete for the dock floor package, accounting for 53% of the total emissions of the base design.
- The removal and disposal of inflowing sediment that enters the dock through a pressure gradient that is created when a vessel enters or leaves the dock.

Alternatives for these two hotspots firstly include the addition of fibers to the concrete mixture of the UCF in order to also give it a structural function that can be integrated into the top floor layer containing rebars, reducing the total concrete volume of the design. The UCF alternatives should meet the watertightness requirements, which means that cracks should not pass through the height of the floor.
Mitigation measures for the inflowing sediment are the construction of a piped inlet on the opposite side of the chamber that aims to take away the pressure gradient during docking, a bubble screen that filters the sediment out of the inflowing water and a system of winches to dock the vessel instead of having to use sediment stirring tugboats. Finally, the mode of operation of the dock gate is varied, which results in three design variant A, B and C:

- Variant A combines a steel fiber reinforced underwater concrete floor (SFRUCF) with a total thickness of 1.13 m with the piped inlet and a caisson gate.
- Variant B has a basalt fiber reinforced underwater concrete floor (BFRUCF) with a total thickness of 1.13 m, a bubble screen and a sliding gate.
- Variant C has a UCF containing rebars with a thickness of 850 mm, a system of winches for docking and a miter gate.

An LCA for each of these design variant found the most sustainable design of the graving dock, purely looking at CO_2-emissions, to be the combination of the UCF-package of Variant B (containing basalt fibers), the gated inlet system of Variant A, and the installation of a caisson gate. These have been combined into a separate design variant D that has been found to reduce the total carbon footprint by nearly 50%. Other takeaways from the evaluation of the design variants by performing the LCA, cost benefit analysis (CBA) and multi criteria analysis (MCA) are:

- Prevention of the sediment inflow should always be part of the design of a dock since it pays off money wise, sustainability wise and the ease of operation is improved. Actually, operational costs due to sediment disposal could make the construction of the dock as a whole not economically viable.
- The use of 'green' construction equipment can reduce the emissions in the installation phase by 25%, but this is only a small fraction of the total carbon footprint and the same can be said for investing in local manufacturers to reduce emissions during the transport phase
- The construction costs amount to roughly 7.6 million euros and the return period of investment is 20 years on average.
- Implementation of an alternative UCF will require some additional investment costs but leads to reduction in emissions, it is therefore up to the client to determine which of these aspects is valued most.

All in all it is concluded that variant D gives the optimal combination of strengths of the different design elements, since the basalt fiber reinforced UCF leads to an optimal combination of construction costs and emission reduction benefits, the use of the gated inlet allows for the most swift and easy operation of the dock and maintenance can easily be performed to the caisson gate.

Chapter 8.2: Discussion

Throughout this report, numerous assumptions have been made that form the basis of the design procedures and evaluation assessments of those designs. First of all, the strength influence of adding steel and basalt fibers to the concrete mixtures are largely based on strength assumptions from external test results, the accuracy of the subsequent conclusions and the increase in compressive, tensile and bending strength of concrete is based on a relatively small number of sources and the accuracy might be debatable. While the resources to perform the necessary three-point bending experiments were lacking, additional research to justify these assumptions is necessary. These results could have big consequences for the results of the thesis, in case the strength properties of the steel- and basalt fibre reinforced concrete mixtures prove to be less in practice than the assumptions made in this report, the required thickness of these floor package would have to be increased as a result of this, which also changes the results of the LCA, CBA and overall performance of the design variants. The same can be said in case the bending tests prove that the strength properties of fibre reinforced concrete are more beneficial than assumed, this would allow for further reduction in the required concrete volume and better scores in the evaluation analyses. While these assumptions are the same for both fibre types, it is more the case that the relative performance of fibre reinforced concrete compared to the floor package of variant C is influenced by this assumption. Depending on the results of the experiments, the preference for variants A and B compared to variant C will either be increased or nullified.

When determining the required height for the gate, it is found that the governing water level is at +4.9m NAP while the ground level in this part of the harbour is at +4.3 m NAP. This means that, under extreme circumstances, floodings can be expected to occur roughly every 100 years. This poses the question whether a heightening of the new dock location is required or that we can accept a periodical flooding of the (area around) the dock. This is a matter of economic optimization taking into account the risk of flooding, the associated economic damages and the costs of the mitigation measures. Perhaps a solution could be to construct a type of 'terp' for protection of equipment and allow the remaining infrastructure to be flooded periodically. While it falls outside of the scope of this thesis to dive into this matter, it can be a cause of concern and requires decision making from (local) authorities.

The watertightness of the floor is crucial for a durable use of the dock and in the design process this is mentioned to be the governing boundary conditions for the UCF. It is mentioned that this means that bending cracks in the bottom of the floor under ship loading conditions must not be able to travel through the complete thickness of the floor and this is ensured by maintaining a certain compression zone height at all times and it is concluded in the design calculations that this is the case at the moment of cracking.

The same can be said for the efficiency of the sedimentation reduction strategies that have not been tested. It is recommended to create physical models to perform scale test to the mentioned strategies. In this report it is assumed that all measures completely take away the inflow of sediment but in practice still some sediment might find its way into the dock chamber. On the other hand the estimation of the sedimentation rate of the new dock might be conservative, the question can be asked whether sedimentation at the location of the new dock will actually pose that large of an issue. Since the sedimentation has been found to be the predominant factor in both the LCA as well as the CBA results, the need for implementation of the mitigation measures resulting from those experiments could have a large impact on the final layout of the dock.

The development of design variants also leaves a lot of room for discussion. Chapter 3 investigated numerous methods to apply more sustainable design alternatives to the base design and eventually the focus is chosen to be on the UCF and sedimentation of the dock. It is not necessary that this choice leads to the best results in practice and so other alternatives that focus on the end-of-life stage of the dock, on sustainable alternatives for other dock elements such as the retaining walls or on alternative construction materials could form the basis for further research in this area and might lead to more beneficial designs. Besides, many combinations of the design elements have not been made. For example the combination of the inlet and the winches could use the benefits of both elements. Fast operation of the winches due to the presence of the inlet combined with the absence of tugboats.

The assessment of the environmental impact of the design variants also requires some assumptions, firstly by setting the boundaries for the LCA and the elements that are and are not included in the assessment. These assumptions are mentioned in Chapter 6.1 but might also alter the accuracy of the results. Similarly, the emission factors used in the LCA stem from multiple different sources that each are based on varying assumptions on their own.

The quality of the LCA largely depends on the quality of the data available in the databases. For DuboCalc, the information is only available for a few elements that may not completely match the profiles in the design and therefore need to be converted which can lead to inaccuracies. Furthermore, information stemming from separate sources may lead to inaccuracies since different producers could use different methods to determine the emissions depending on the type of EPD (Environmental Product Declaration) that is maintained, the standards that are used in different countries and the recency of the data. These factors may cause the need for a critical review of the LCA study. Most accurate emission factors are assumed to stem from the most recent EPDs of every element but again, this might not be available for every element and in practice the distributors that supply the EPDs might not be used. The accuracy of the emission factors used in the LCA has a huge influence on the final design of the dock. The fact that the amount of reinforced concrete is the predominant factor in the carbon footprint of the could potentially be attributed to the fact that this emission factor is manually determined based on data for concrete and steel separately from varying EPD's.

In case this emission factor proves to be significantly less from a more applicable or recent EPD, other elements of the dock might prove to be a bigger contributor and sustainable alternatives will have to focus on these elements, ultimately influencing the final design of the dock as a whole.
All in all, the need for a critical review of the LCA study is large but since the goal of the LCA is mostly about comparison of results among the design variants, it is considered to be sufficient for this report. The LCA is made based on the Global Warming Potential (GWP), in practice other categories such as nitrogen emissions could be more influential and the correlation between amount GWP and amount nitrogen might not be as clear.
The results from the cost benefit analysis do not take into account the costs for the hall structure and its foundations, the workplaces, finalization etc. and the factor of 15% might not cover all of this. In presence, the investment could therefore come out considerably larger and the results might be a lot less optimistic as depicted in chapter 6.2 and additional cost calculations are required. Finally, some comments need to be made about the accuracy of the multi criteria analysis. The weighting factors and assigned scores will always contain a sense of subjectivity and consequently contain a lot of room for discussion. In chapter 6.3, the weighting factors have been determined in collaboration with employees of the client's company and aim to represent the core of the project which is to develop a sustainable dock design that still meets all requirements for structural integrity and smooth operation.

References

Allianz. (n.d.). *Lock & Dock gates.* London: Allianz.

Apon, M. (2019). *Soil-structure interaction of a permanent steel fibre reinforced underwater concrete floor system.* Delft.

Arcadis. (2012). *Structuurvisie gemeente Harlingen 2025.*

ArcelorMittal Commercial RPS. (2021). *Sustainable Ports - Life Cycle Assessment.* Esch zur Alzette: ArcelorMittal Commercial RPS.

Basalt Reinforced Composites. (2022). *Benefits*. Retrieved from BRC website: https://basaltreinforcedcomposites.com/benefits-comparisons/#:~:text=Basalt%20Reinforced%20Rebar%20has%20less,for%20concrete%20reinforcement%20construction%20applications.

Bheel, N. (2020). *Basalt fibre-reinforced concrete: review of fresh and mechanical properties.* Springer Nature Switzerland.

Bij12. (2022). *Stikstof en Natura 2000*. Retrieved from Natura 2000 website: https://www.bij12.nl/onderwerpen/stikstof-en-natura2000/vergunningen-en-toestemmingsbesluiten/vergunning-aanvragen-of-niet/

British Standard. (1988). *Code of Practice for Maritime structures.* BSI.

Brundtland, G. H. (1987). *Our Common Future.* Oslo.

Cheng, Y. (2021). Research on the plume stability of air bubble curtains under low transverse flow velocity environment in dredging engineering. *Ocean Engineering*, 109-133.

Church, J. P. (2013). *2013: Sea Level Change.* Cambridge: Cambridge University Press.

CIE4363 reader. (2018). *Reader Deep Excavations.* Delft.

Confeeder Shipping & Chartering. (2022). *MV Endeavor.* Retrieved from JR shipping website: https://www.jrshipping.com/our-fleet/m-s-endeavor/

CUR. (2018). *CROW-CUR Aanbeveling 111 Staalvezelbetonbedrijsvloeren op palen.*

CUR166. (n.d.). *CUR-Publication 166 - damwandconstructies.* Gouda.

CUR-Aanbeveling 77. (2014). *het onwerpen van ongewapende onderwaterbetonvloeren.*

CUR-rapport 98-9. (2014). *Ontwerpregels voor trekpalen.*

Damen Marine Components. (2022). *Capstans*. Retrieved from Damen Marine Components Web site: https://www.damenmc.com/en/products/deck-equipment/capstans

Damen Marine Components. (2022). *Tugger Winches*. Retrieved from DMC web site: https://www.damenmc.com/en/products/deck-equipment/tugger-winches

Deltares. (2013). *Harbour Sedimentation Harlingen - Delft3D Flexible Mesh pilot*. Retrieved from Deltares website: https://www.deltares.nl/en/projects/harbour-sedimentation-harlingen-pilot-delft3d-flexible-mesh/

Deltares. (2013). *Kenmerkende waarden Kustwateren en Grote Rivieren.*

Dillingh, D. (2013). *Kenmerkende waarden Kustwateren en Grote Rivieren.* Delft: Deltares.

DINOLoket. (2022). *Ondergrondgegevens*. Retrieved from DINOloket website: https://www.dinoloket.nl/ondergrondgegevens

DuboCalc. (n.d.). *Dubocalc webapp*. Retrieved from https://app6.dubocalc.nl/

DYWIDAG-Systems international. (2012). *GEWI - accesoires.*

El Hamdi, A. (2011). *Sedimentation in the Botlek Harbour - A research into driving water exchange mechanisms.*

Feraldi group. (2011, 03 22). *Environdec.* Retrieved from EPD database: https://www.environdec.com/library/epd6689

Fort, J., Koci, J., & Cerny, R. (2021). *Environmental Efficiency Aspects of Basalt Fibers Reinforcement in Concrete Mixtures.* Prague: Czech Technical University.

Fort, J., Koci, J., & Cerny, R. (2021). *Environmental Efficiency Aspects of Basalt Fibers Reinforcement in Concrete Mixtures.* Prague: Czech Technical University.

Franco, L., De Gerloni, M., & Van der Meer, J. (1994). *Wave overtopping on vertical and composite breakwaters.*

Geng, Y., & Doberstein, B. (2008). *Developing the circular economy in China: Challenges and opportunities for achieving 'leapfrog development'.*

Gerkema, T. (2017). Interannual variability of mean sea level and its sensitivity to wind climate in an inter-tidal basin. *Earth Syst. Dynam.*, 1223-1235.

Global Compact Network Netherlands. (2022). *Sustainable Development Goals*. Retrieved from GC Netherlands website: https://gcnetherlands.nl/sdgs/

Google Maps. (2022). Retrieved from https://www.google.nl/maps/@53.1859131,5.43404,14z

IDEMATapp. (2023, February). Idemat app. Delft, Netherlands.

IN2-concrete. (2023, February 22). *IN2-fiber*. Retrieved from https://in2-concrete.com/product/bouwmaterialen/wapening/in2-fiber-basalt/

Jonkers, H. (2018). *Reader 'Sustainability'.* Delft.

Jonkman, S. (2021). *Flood Defences.* Delft: TU Delft.

Jonkman, S., Steenbergen, R., & Morales-Nápoles, O. (2017). *Probabilistic Design: Risk and Reliability Analysis in Civil Engineering.* Delft.

Kadasterdata. (2022). *Kadastrale kaart.* Retrieved from Kadasterdata: https://www.kadasterdata.nl/kadastrale-kaart?q=Lange%20Lijnbaan%2028,%208861NW%20Harlingen&step=1

Khatri, D. (2016). *Fatigue Analysis of Concrete Structures.*

Kim, S.-W., Jang, S.-J., & Kang, D.-H. (2015). *Mechanical Properties and Eco-Efficiency of Steel Fiber Reinforced Alkali-Activiated Slag Concrete.* Daejeon, Korea: Department of Construction Engineering Education.

KLIC. (2022, July 28). *KLIC notification.* Retrieved from Kadaster.

KSB. (2022). *KSB website*. Retrieved from Amarex KRT: https://www.ksb.com/nl-nl/lc/producten/pomp/dompelpomp/amarex-krt/A30B

Maher, A. (2013). *Preparation of a Manual for Management of Processed Dredge material at Upland Sites.*

Marin Teknikk AS. (1999). *Kommandor Susan - Stability Booklet.*

Marine Insight. (2021, January 9). *Dry Dock, Types of Dry Docks & Requirements for Dry Docks*. Retrieved from Marine Insight website: https://www.marineinsight.com/guidelines/dry-dock-types-of-dry-docks-requirements-for-dry-dock/

Molenaar, W. (2020). *Locks.* Delft: TU Delft.

Molenaar, W., & Voorendt, M. (2020). *General lecture notes Hydraulic Structures.* Delft: TU Delft.

Natura2000. (2017). *PAS-gebiedsanalyse Waddenzee (001).*

Natura2000. (2022). *Waddenzee*. Retrieved from Natura2000 website: https://www.natura2000.nl/gebieden/friesland/waddenzee

NEN. (2005). *Eurocode 2: Design of concrete structures.* Delft: Nederlands Normalisatie-instituut.

NEN. (2006). *NEN-EN 1992-3:2006+NB:2011.* NEN.

NEN. (2020). *National Annex to NEN-EN1991-1-4+A1+C2: Wind actions.*

NEN-EN. (2011). *NEN-EN 1992-3:2006 Constructies voor keren en opslaan van stoffen.*

NEN-EN1992-1-1. (1992). *Design of concrete structure.* Eurocode.

Oenema, O. (2019). *Factsheet 'stikstofbronnen'.* Wageningen: Wageningen University & Research.

PB Lifttechnik GmbH. (2022). *Scissor lifts.* Retrieved from PB Lifttechnik GmbH.

PH bouwadvies. (2021). *Stikstofproblemen en gevolgen bouwsector*. Retrieved from PH bouwadvies website: https://ph-bouwadvies.nl/stikstofproblemen-gevolgen-bouwsector/

PH bouwadvies. (2022, May). *Stikstofproblemen en gevolgen bouwsector*. Retrieved from PH bouwadvies web site: https://ph-bouwadvies.nl/stikstofproblemen-gevolgen-bouwsector/

Port of Harlingen. (2022). *Havenkaart.* Retrieved from Port of Harlingen: https://www.portofharlingen.nl/havengebied/havenkaart/

Potting, J., Hekkert, M., Worrell, E., & Hanemaaijer, A. (2017). *Circular economy: measuring innovation in the product chain.* The Hague: PBL Publishers.

Radermacher, M. (2013). The art of screening: effectivesness of silt screens. *Terra et Aqua*, 3-12.

Ramesh, B., & Eswari, S. (2021). *Mechanical behaviour of basalt fibre reinforced concrete: An experimental study.* Pondicherry: Pondicherry Engineering College.

Ravestein Shipyard & Construction Company. (2017, October 12). Animation Caisson Dock Gate D/16 Devonport Bn 474.

Readymix Industries Ltd. (2022, 03 29). *Environdec.* Retrieved from EPD database: https://www.environdec.com/library/epd5720

Rensen, J. (2013). *Staalvezelbeton in de iQwoning.* Eindhoven: Unit Structural Design.

Ricardo-Engine. (2019). *How to Calculate the Fuel Consumption of Diesel Generators*. Retrieved from Ricardo-Engine website: http://www.ricardo-engine.com/new/new-41-765.html

Rijksoverheid. (2020, October 13). *Stikstofaanpak: sterkere natuur, perspectief voor de bouw*. Retrieved from Website van Rijksoverheid: https://www.rijksoverheid.nl/actueel/nieuws/2020/10/13/stikstofaanpak-sterkere-natuur-perspectief-voor-de-bouw

Rijksoverheid. (2021, July 1). *De bouwvrijstelling gaat in op 1 juli 2021*. Retrieved from Rijksoverheid website: https://www.rijksoverheid.nl/actueel/nieuws/2021/07/01/de-bouwvrijstelling-gaat-in-op-1-juli-2021

Rijksoverheid. (2022, May). *Climate policy*. Retrieved from Government of the Netherlands: https://www.government.nl/topics/climate-change/climate-policy/

Rijkswaterstaat. (2007). *Hydraulische Randvoorwaarden primaire waterkeringen.* Rijkswaterstaat, Waterdienst.

Rijkswaterstaat. (2022). *Wet milieubeheer*. Retrieved from Rijkswaterstaat website: https://www.rijkswaterstaat.nl/water/wetten-regels-en-vergunningen/natuur-en-milieuwetten/wet-milieubeheer

RIVM. (2021, September). *Stikstof*. Retrieved from RIVM web site: https://www.rivm.nl/stikstof

Royal Haskoning DHV. (2019). *Dock & Lock Gates.* Royal Haskoning DHV.

Royal Haskoning DHV. (2022). *Dry Docks - key facilities in Smart Shipyards.*

Sagström, J. (2017). *Streamlined LCA model and complete assessment of a hydraulic drive system.* Stockholm: KTH Industrial Engineering and Management.

SEB. (2021). *Routekaart Schoon en Emissieloos Bouwen*. Retrieved from SEB website: https://www.opwegnaarseb.nl/

Slegers, R. (2022). *Basalt to replace steel in concrete quay wall aprons.* Delft: TU Delft.

Smits, I. (2001). *Analysis of the Rijkaart-Weibull model.* KNMI.

Staaltabellen. (n.d.). *balkstaal.*

Teekay Corporation. (2018, April 18). *Step-by-Step: A Glimpse Into The Dry-Docking Process*. Retrieved from Teekay Coorporation Website: https://www.teekay.com/blog/2016/04/18/step-step-glimpse-dry-docking-process/

Tran, N. K. (2015). An empirical study of fleet expansion and growth of ship size in container liner shipping. *International Journal of Production Economics*, 241-253.

UNDP. (2022). *What are the Sustainable Development Goals*. Retrieved from UNDP web site: https://www.undp.org/sustainable-development-goals

Van der Meulen, S., Quispel, M., & Dasburg, N. (2009). *Kostkengetallen binnenvaart 2008.* Zoetermeer: NEA.

Van Leeuwen verankeringen B.V. (2008). *GEWI-paal.*

Van Olst, L. (2019). *Parametric design-tool to optimize preliminary design of navigation lock chambers.* Delft: TU Delft.

van 't Wout, F., Groot, M., Sminia, M., & Haas, M. (2010). *Functionele Specificatie DuboCalc.*

Vanlede, J. (2014). A geometric method to study water and sediment exchange in tidal harbors. *Ocean Dynamics*, 1631-1641.

Vereniging Ondernemers Technisch Bodemonderzoek. (2006). *Ondergrond - Handboek geotechnisch bodemonderzoek.* Purmerend: Rijser Grafische Communicatie.

Voorendt, M., & Molenaar, W. (2020). *Manual Hydraulic Structures.* Delft: Tu Delft.

Waddenvereniging. (2022). *De 10 grootste zorgen van de Waddenvereniging*. Retrieved from Waddenvereniging website: https://waddenvereniging.nl/werelderfgoedmoetbeter

Webfleet. (2020, februari 28). *Hoeveel diesel verbruikt een vrachtwagen per kilometer*. Retrieved from webfleet website: https://www.webfleet.com/nl_nl/webfleet/blog/hoeveel-diesel-verbruikt-een-vrachtwagen-per-kilometer/#:~:text=Gemiddeld%20brandstofverbruik%20vrachtwagen&text=Gemiddeld%20verbruikt%20een%20vrachtwagen%2030,of%20juist%20tussen%20meerdere%20steden.

Wereld van de Binnenvaart. (2023, february 22). *Schepen*. Retrieved from https://wereldvandebinnenvaart.nl/schepen/

Winterwerp, J. (2005). Reducing Harbor Siltation. I: Methodology. *Journal of Waterway, Port, Coastal, and Ocean Engineering*.

Zheng, Y., Wu, X., He, G., Shang, Q., Xu, J., & Sun, Y. (2018). *Mechanical Properties of Steel Fiber-Reinforced Concrete by Vibratory Mixing Technology.* Hindawi.

Appendix A: Design vessels

This appendix gives information on the design vessels that are used for determining the required dimensions of the dock and the hall. All information is retrieved from the JR shipping website (Confeeder Shipping & Chartering, 2022).

MV Endeavour:

CONFEEDER
SHIPPING & CHARTERING

ENFORCER / ENCOUNTER / ENDEAVOR / ENERGIZER/ ENSEMBLE / ENDURANCE

Container vessels with excellent stowage flexibility and a high service speed. Endeavor, Endurance and Ensemble with iceclass E3. Type VH 750. Builder: Volharding Shipyard. Owner: JR Shipping BV.

MAIN PRINCIPALS

L.o.a.	134.65 m	Deadweight	appr. 9450 tdw
L.p.p.	125.60 m	Tonnage	7680 GT
Beam	21.50 m	Service speed	18 knots
Depth	8.80 m		
Draugth	7.00 m		

CLASS REGULATIONS

Germanischer Lloyd ✠ Containership, 100 A5
Solas II-2, reg. 19, MC-AUT
Dutch Shipping Inspectorate (NSI), Dutch flag

MAIN PROPULSION EQUIPMENT

MaK Diesel 8M43, 7200 kW MCR at 500 rpm
Low NOx certificate

CONTAINER CAPACITIES

Capacity	750 TEU, [356 FEU + 22 TEU]
Container Stability	appr. 511, 14 tons homogeneous weight Container stability according to IMO
Reeferpoints	120 pcs. on deck 70 pcs. in hold Reefer monitoring
Block Stowage	all bays, cell-guides in hold
Oversized units deck	high cubes / wide bodies in hold/on 451, 30 ft containers (107 in hold) 313, 45 ft containers (73 in hold) 32, 49 ft containers (on deck)
Dangerous goods	Solas 19, chapter II

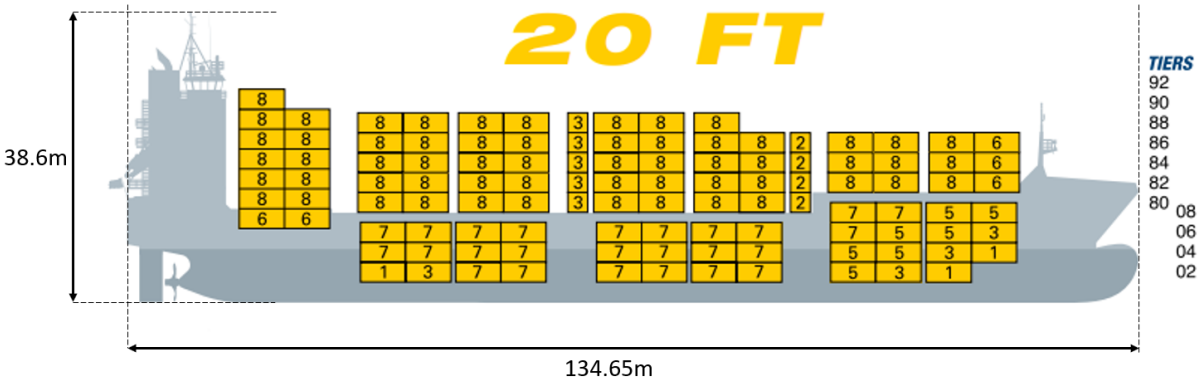

MV Elysee, governing for the required height of the hall:

CONFEEDER
SHIPPING & CHARTERING

ELYSEE

1425 TEU ICE CLASSED CONTAINER VESSEL

Open top container vessel with excellent stowage flexibility and a high service speed.
Builder: Sietas Werft. Type 178. Owner: JR Shipping BV.

MAIN PRINCIPALS

L.o.a.	168.00 m	Deadweight	± 16.950 tdw
L.p.p.	155.40 m	Tonnage	17.600 gt
Beam	26.80 m		8.500 nt
Depth	14.00 m	Service speed	19 kts
Draught	9.60 m		

CLASS REGULATIONS

Germanischer Lloyd ✠ 100 A5 E4, 'Containership', 'Open Top',
Solas II-2, Reg. 19, ✠ MC E4 AUT.
Dutch Shipping Inspectorate (NSI), Dutch flag.

MAIN PROPULSION EQUIPMENT

MAN B&W SL 58/64, 11.200 kW at 121.5 rpm.
IAPP certificate.

CONTAINER CAPACITIES

1425 TEU.
3 Holds, 1 hatch.
Fitted with 40' and 45' cell guides in holds.
Breadths 2,438 m and 2,.500 m in holds
2,438 m 2,500 m and 2.591 m on deck.
Suitable for 20', 30', 40' and 45' containers in holds
20', 30', 40' and 45' containers on deck.

REEFERS

300 pcs on deck and in holds incl. reefer monitoring system.

CONTAINER HEIGHTS

Holds 5 x 8'6" or 1 x 8'6" and 4 x 9'6"

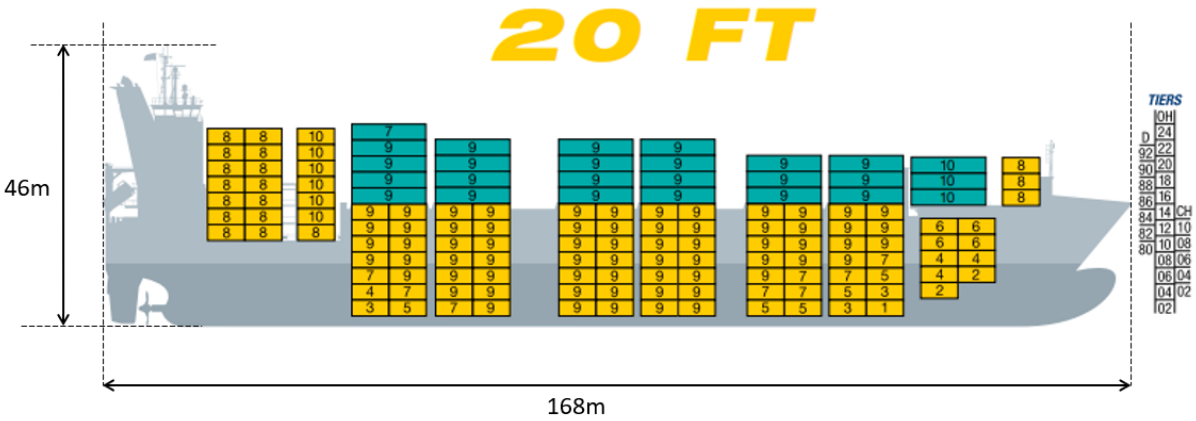
20 FT
46m
168m
TIERS
OH
D
24
22
20
18
16
14
12
10
08
06
04
02
CH

Appendix B: Boundary conditions

Both the 3 locations where the CPT tests were performed and the results can be seen in the following figures. Firstly, the CPT test which is performed at the most west-located spot is shown, from now on labeled as location 1, can be seen in Figure B1.

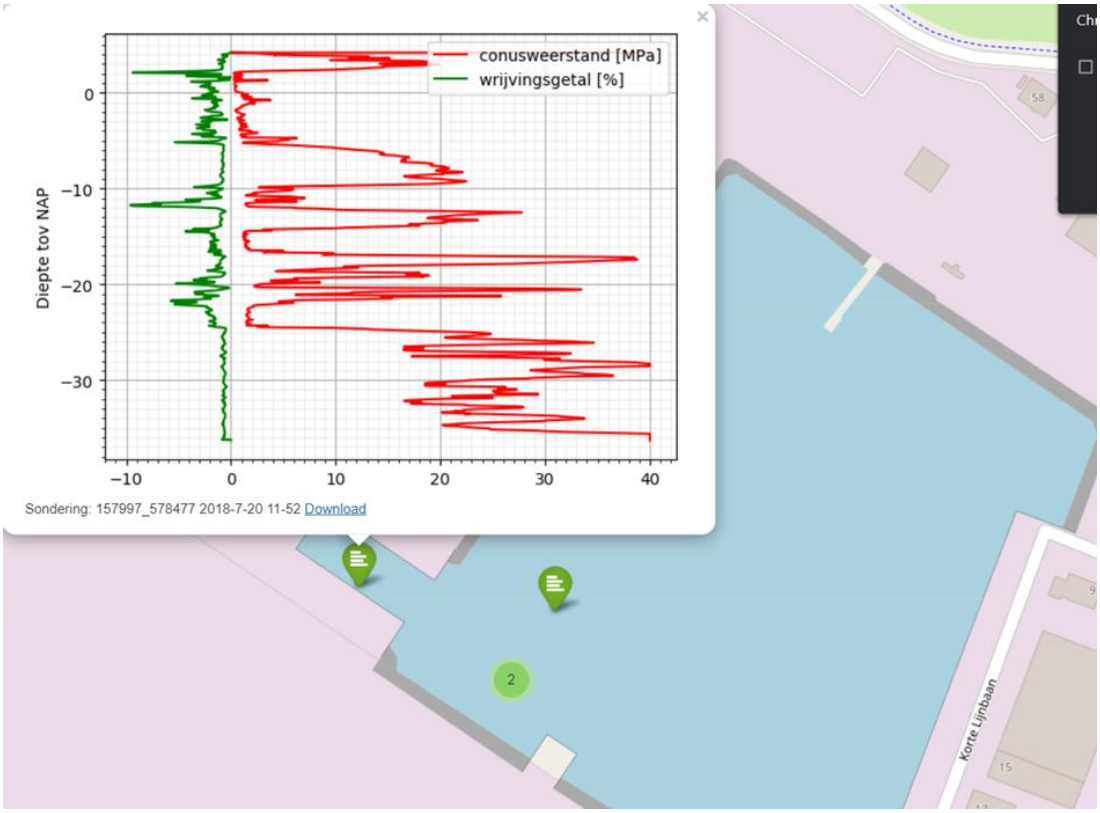

Figure B 1: CPT result location 1

Figure shows the corresponding soil profile, as interpreted from the CPT test, as well as the values for relevant soil parameters which have been determined using table 2b from NEN9997.

Figure B 2: Soil profile location 1

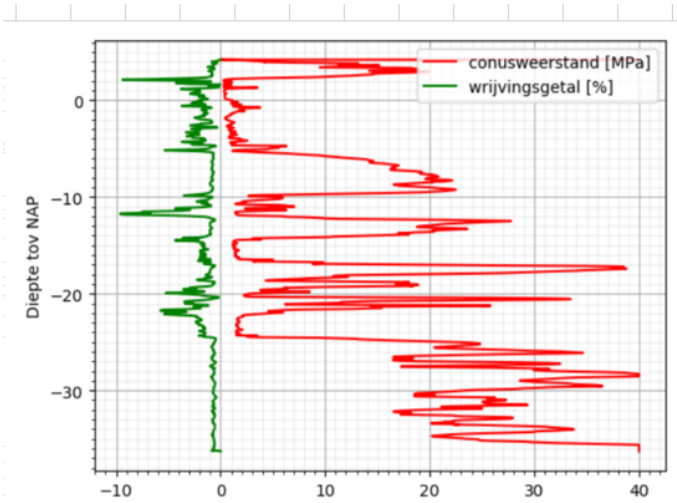

soil type	γ (kN/m3)	γsat (kN/m3)	(degrees	c' (kPa)
clean medium sand	18	20	32.5	-
soft peat	10	10	15	2
soft clay	14	14	17.5	0
little sandy clay medium	18	18	22.5	10
little sandy clay soft	15	15	22.5	0
clean medium sand	18	20	32.5	-
very silty sand	18	20	25	-
peat	11	11	15	2
dense clean sand	19	21	35	-
little sandy clay medium	18	18	22.5	10
dense sand	19	21	35	-
little sandy stiff clay	20	20	22.5	25
Dense sand	19	21	35	-
Dense sand	19	21	35	-
little sandy medium clay	18	18	22.5	10
Dense sand	19	21	35	-

The same is now repeated for the most north-eastern location, from now on labeled as location 2.

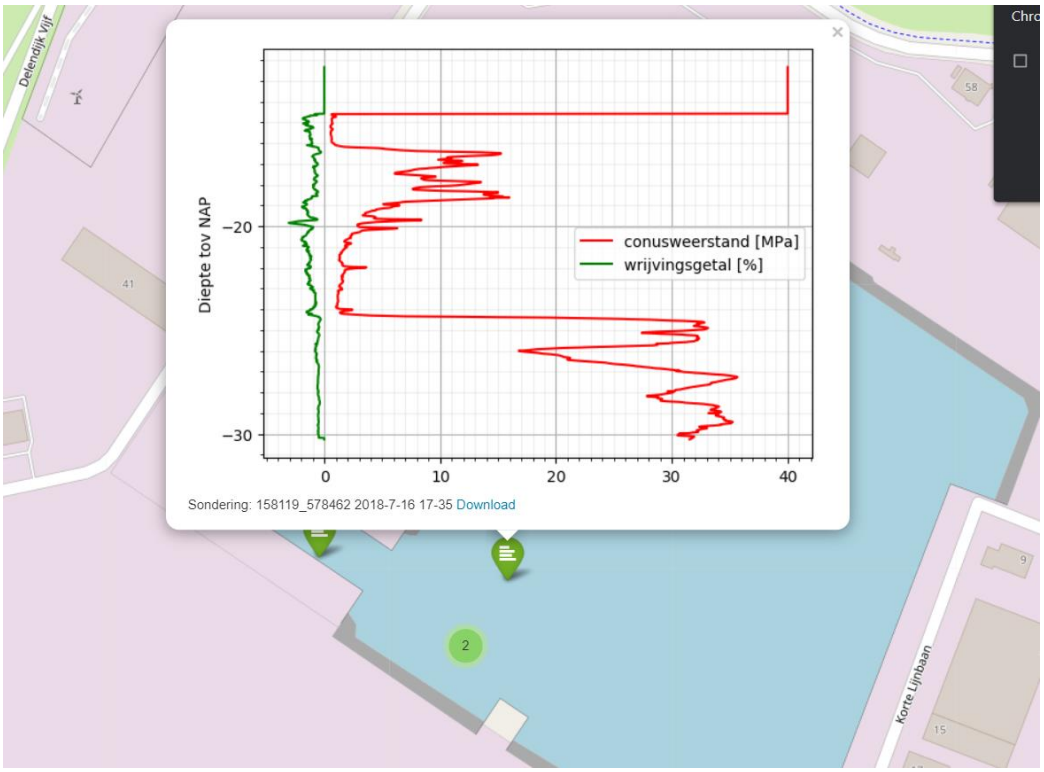

Figure B 3: CPT result location 2

The interpreted soil profile for location 2 is shown in Figure B4.

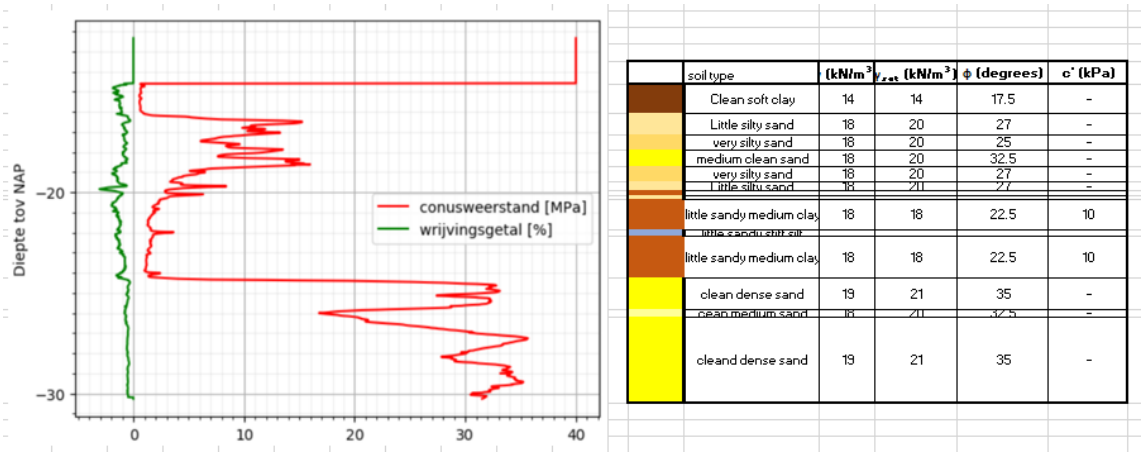

soil type	(kN/m^3)	γ_{sat} (kN/m^3)	ϕ (degrees)	c' (kPa)
Clean soft clay	14	14	17.5	-
Little silty sand	18	20	27	-
very silty sand	18	20	25	-
medium clean sand	18	20	32.5	-
very silty sand	18	20	27	-
Little silty sand	18	20	27	-
little sandy medium clay	18	18	22.5	10
little sandy silt silt				
little sandy medium clay	18	18	22.5	10
clean dense sand	19	21	35	-
cean medium sand	18	20	32.5	-
cleand dense sand	19	21	35	-

Figure B 4: soil profile location 2

Finally for location 3, which is the most south-eastern location, the CPT result is shown in Figure B5.

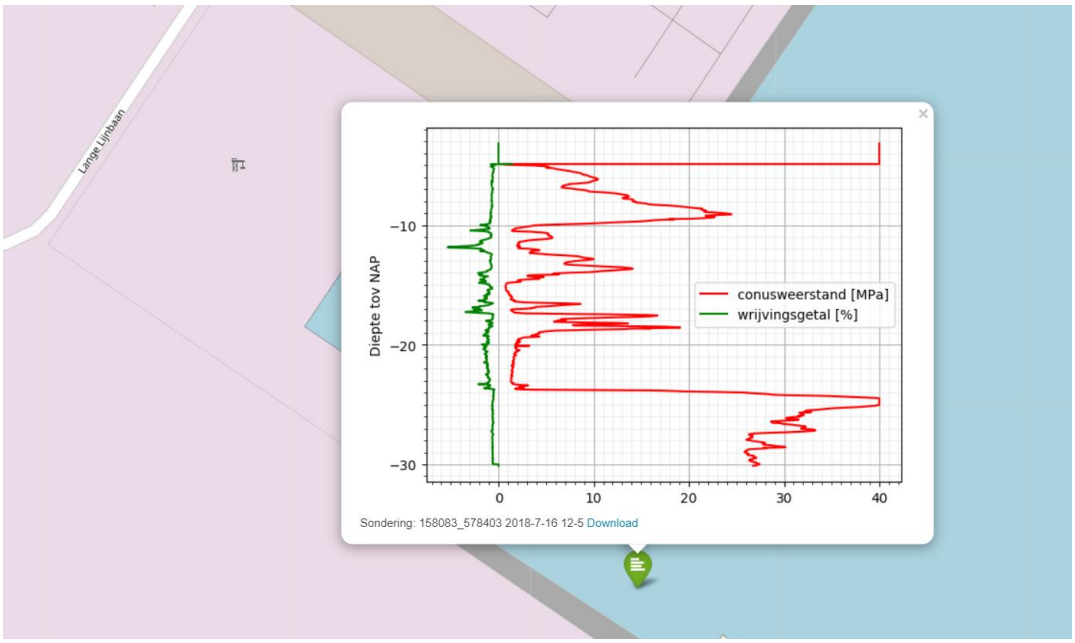

Figure B 5: CPT result location 3

The interpreted soil profile for location 3 is shown in Figure B6.

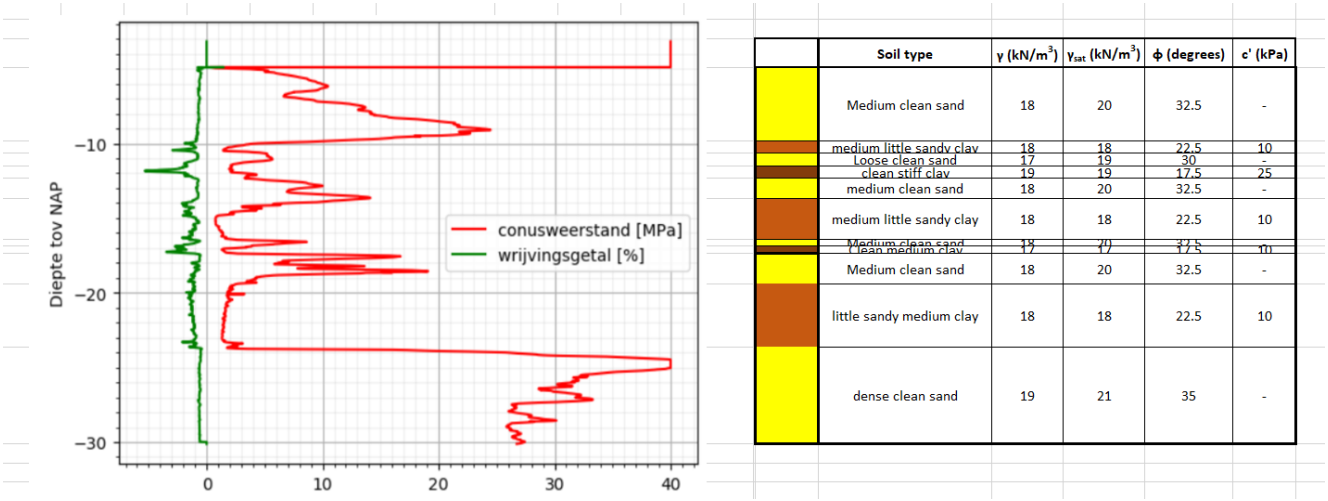

	Soil type	γ (kN/m³)	γsat (kN/m³)	ϕ (degrees)	c' (kPa)
	Medium clean sand	18	20	32.5	-
	medium little sandy clay	18	18	22.5	10
	Loose clean sand	17	19	30	-
	clean stiff clay	19	19	17.5	25
	medium clean sand	18	20	32.5	-
	medium little sandy clay	18	18	22.5	10
	Medium clean sand	19	20	32.5	-
	clean medium clay	17	17	17.5	10
	Medium clean sand	18	20	32.5	-
	little sandy medium clay	18	18	22.5	10
	dense clean sand	19	21	35	-

Figure B 6: Soil profile location 3

When overlapping these CPT tests, a total soil profile can be determined as illustrated in Figure B7, where the fit of the overlap of the CPT tests is not perfect, but still allows for identification of the main soil layer package.

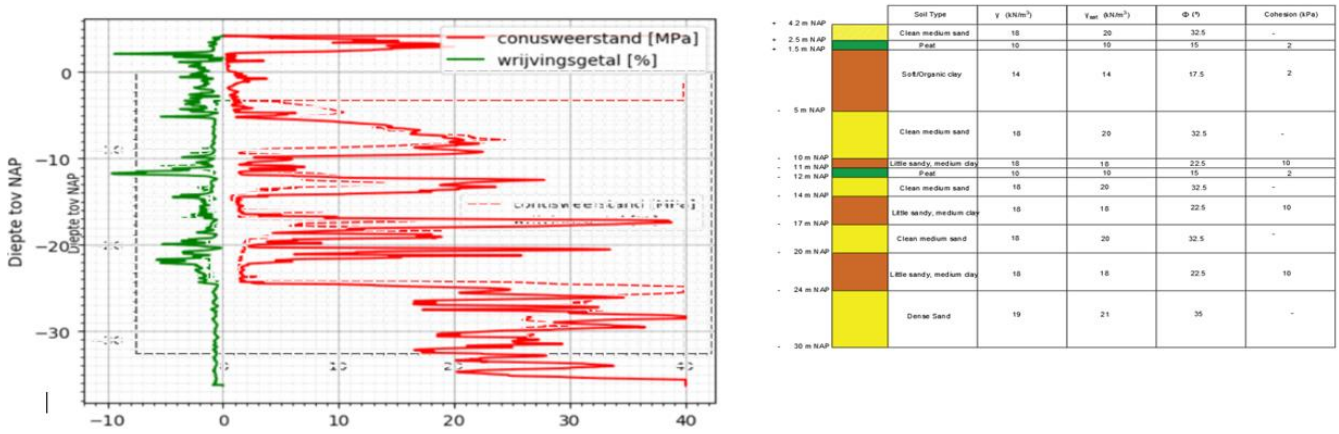

Figure B 7: CPT test overlap leading to identification of the total soil package

Figure B8 shows both the location of the measurements and the results of the groundwater monitoring.

Figure B 8: Location and result of groundwater monitoring, source: (DINOLoket, 2022)

Design water level

The various factors that make up the total design water level are:

- Storm surge level and astronomic tide
- Wind setup
- Wave setup
- Long term effects (sea level rise and land subsidence)
- Freeboard (determined by allowable overtopping discharge)

The storm surge level and astronomic tide are included in the 'Hydraulische randvoorwaarden primaire waterkeringen' by Rijkswaterstaat, which gives a design water level in Harlingen of +4.9 m NAP (Rijkswaterstaat, 2007).

The wind setup has been determined using equation (4.3) from the reader Flood Defences, which reads:

$$\partial h_1 = 0.5\kappa \frac{u^2}{gh} F cos(\varphi)$$

With the following parameters:

- ∂h_1 is the wind setup in meters (m)
- κ is a friction factor
- u is the wind velocity at an altitude of 10 meters (m/s)
- h is the water depth (m)
- F is the fetch (m)
- Φ is the angle between the shore normal and the wind direction (deg)

The wind information as projected in Figure 19 is used to determine the governing wind direction, which is West as this situation gives the largest combination of fetch and wind velocity. Figure B9 below shows a Fetch of 35700 meters, as determined using Google Maps.

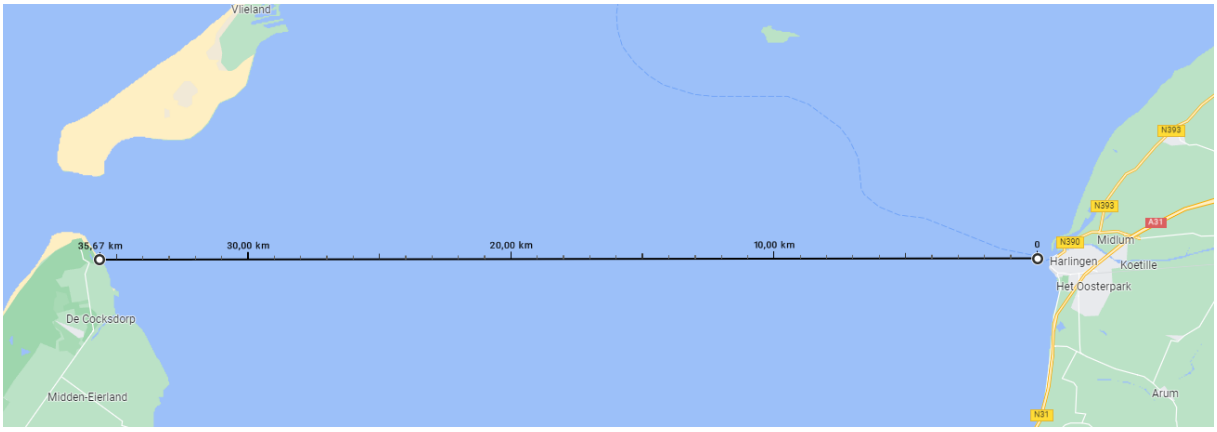

Figure B 9: Longest Fetch across the Wadden sea, source: Google Maps

The corresponding maximum wind velocity is found to 31.4 m/s, the water depth equals 12.4 meters and the value for κ is $3.2*10^{-6}$. Filling in the equation yields:

$$\partial h_1 = 0.5 * 3.2 * 10^{-6} \frac{31.4^2}{9.81 * 12.4} * 35700 * cos(0) = 0.5\, m$$

For determination of the significant wave height, the Young & Verhagen (1996) formulas are used. In this instance, the maximum fetch is taken within the port of Harlingen with regards to the orientation of the dock gate. The corresponding design wind velocity from a NNE,

maintaining a reduction factor of 0.64 (Smits, 2001) is v_{NNE}=33.4 * 0.64=21.38 m/s. The Young & Verhagen equations yield:

$$\tilde{H} = 0.24(\tanh(0.343\tilde{d}^{1.14}) \tanh\left(\frac{0.000441\tilde{F}^{0.79}}{\tanh(0.343\tilde{d}^{1.14})}\right))^{0.572}$$

$$\tilde{T} = 7.69(\tanh(0.1\tilde{d}^{2.01}) \tanh\left(\frac{2.88 * 10^{-7}\tilde{F}^{1.45}}{\tanh(0.1\tilde{d}^{2.01})}\right))^{0.187}$$

With:

$$\tilde{d} = \frac{dg}{u_{10}^2} = \frac{12.4 * 9.81}{21.38^2} = 0.27$$

$$\tilde{F} = \frac{Fg}{u_{10}^2} = \frac{370 * 9.81}{21.38^2} = 7.94$$

This gives:

$$\tilde{H} = 1.19 * 10^{-6}$$

$$\tilde{T} = 1.25$$

Transforming the dimensionless wave height and period to the significant wave height and period gives:

$$H_s = \frac{\tilde{H} * u_{10}^2}{g} = 0.2\ metres$$

$$T_s = \frac{\tilde{T} * u_{10}}{g} = 1.7s$$

In order to retrieve the design wave height from this, a Rayleigh distribution is used. This is accepted for small wave heights. The probability that the design wave height H_d is exceeded during a storm with N waves is:

$$\Pr(H > H_d) = 1 - e^{-Ne^{-2(\frac{H_d}{H_s})^2}}$$

Where N is calculated using the following relation:

$$N = \frac{T_{storm}}{T_s}$$

T_s follows from the earlier Brettschneider equations and T_{storm} for a storm along the coast is around 2 hours (Jonkman, Flood Defences, 2021), leading to:

$$N = \frac{2 * 3600}{1.75} = 4116\ waves$$

The allowed exceedance probability is taken as 0.01 as it is assumed that the combination of a 1/100 wave and the 1/100 water level leads to a sufficiently conservative design. Filling in these parameters yields:

$$0.99 = 1 - e^{-4141e^{-2(\frac{H_d}{0.26})^2}}$$

$$H_d = 0.52\ m$$

For the long term effects a value 0.5 meters is taken, which includes sea level rise, where a relative sea level rise of the North Sea of at least 40 centimeters per century can be expected according to research in 1990 (Voorendt & Molenaar, 2020). An additional 10 centimeters accounts for land subsidence, which is in accordance with a prognosis as made by De Lange & Gunnik from 2011 (Voorendt & Molenaar, 2020).
Finally, the required amount of freeboard is determined by the maximum allowable overtopping discharge during the design scenario. For elements of building structures, the European Overtopping Manual determined a maximum specific discharge of 1 l/s/m, which is equal to 0.001 m^3/s/m. For vertical walls, such as the dock gate, Franco and colleagues proposed the following equation (Franco, De Gerloni, & Van der Meer, 1994):

$$\frac{q}{\sqrt{g * H_s^3}} = ae^{-b\frac{R_c}{\gamma H_s}}$$

Where:

R_c [m] = Overtopping height
q [m^3/m/s] = specific discharge
a,b [-] = empirical coefficients, (a=0.192, b=4.3)
γ [-] = geometrical coefficient (for rectangular shapes, γ=1)
H_s [m] = significant wave height

Filling in all the available parameters:

$$\frac{0.001}{\sqrt{9.81 * 0.5^3}} = 0.192e^{-4.3\frac{R_c}{0.26}}$$

$$R_c = 0.62\ m$$

The long term effects and the freeboard can now be added to the design water level to determine the total required height for the gate with regards to NAP:
$\Delta h_{gate} = 4.9m + 0.5m + 0.62\ m = +6.02\ m\ NAP \approx +6.10\ m\ NAP$
Knowing that the bottom of the dock is at -7.5m NAP, the total height of the gate will be:

$$h_{gate} = 13.6\ m$$

Cable and pipeline situation

Figure B10 shows the complete cable and pipeline situation, as retrieved from the cable and pipeline information center (KLIC). Green cables represent data cable, red represents electricity cable, blue represents water pipelines and purple represents the sewerage system.

Figure B 10: Cable and pipeline situation, source: (KLIC, 2022)

Figure B11 shows the cross sectional location of the industrial water pipeline owned by North Water along the water. A depth of 16 meters below bottom level is reached (KLIC, 2022).

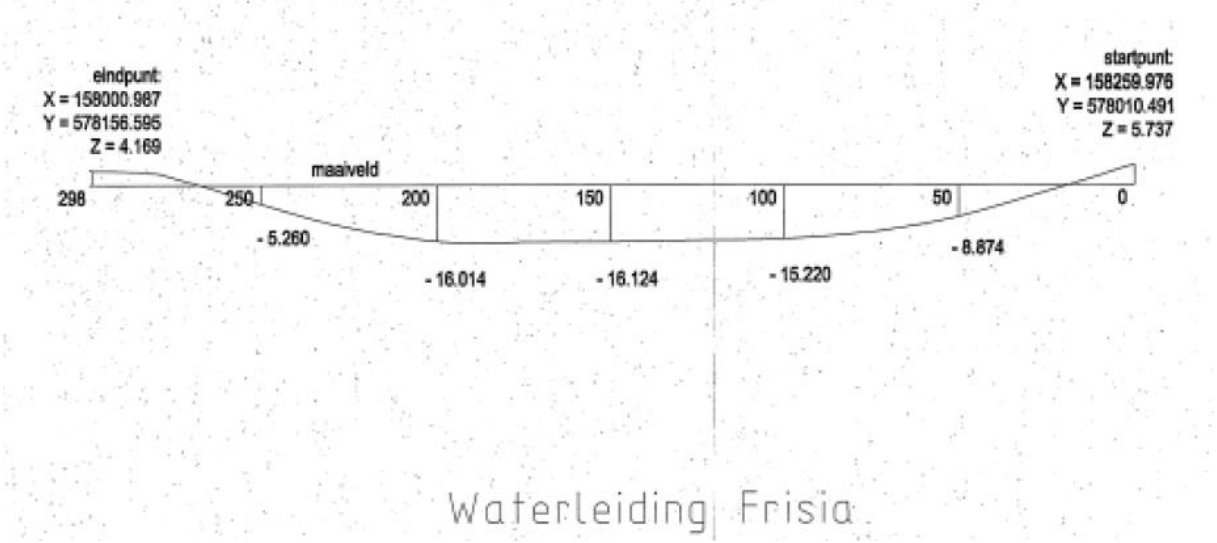

Figure B 11: Water pipeline situation along the water, source: (KLIC, 2022)

Figure B12 shows the same for data and electricity cables, which reaches a depth of 13 meters (KLIC, 2022).

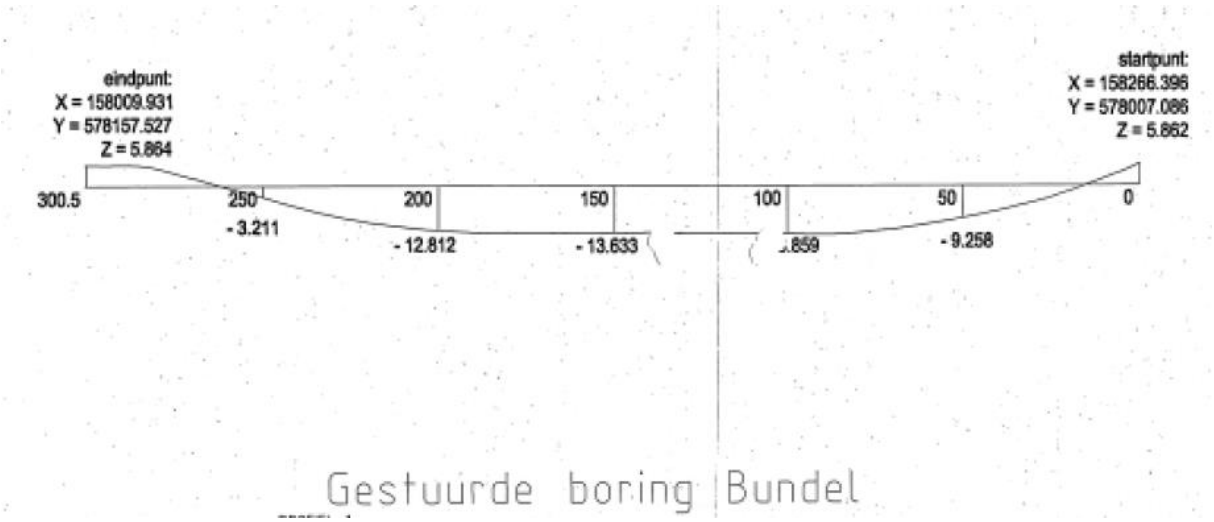

Figure B 12: Data and electricity cable situation along the water, source: (KLIC, 2022)

Appendix C: Base design calculations

This Appendix contains the calculations behind the base design, starting with the retaining wall.

Retaining wall design

For the design of the retaining wall, the step-wise design procedure that is described in the CUR166 is followed, this appendix shows the calculations that have been made.

Step 1: Determine the representative cross section, all relevant external loads and water pressures and the safety class

Figure C 1 shows the representative cross section for the wall, with a water level of +3.5 m NAP as determined in chapter 4. The structure is classified as an RC2 safety class structure and so a surcharge load of 20 kPa is applied.

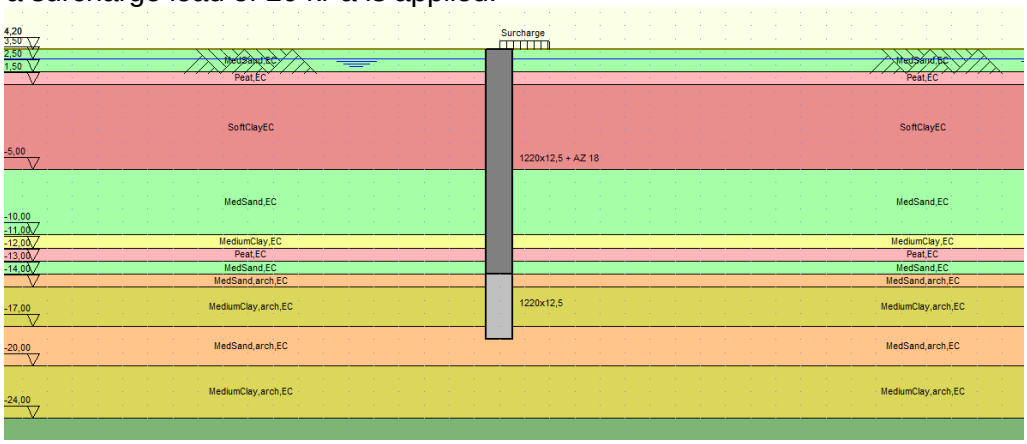

Figure C 1: Retaining wall schematization

Step 2: Determine the characteristic value X_{rep} of the parameters

The values for the soil parameters (c, φ and γ) have been entered as displayed in Figure C2, the delta friction angle δ is equal to 2/3 * φ_d' for clay and sand layers and 0 for the peat layers. The modulus of subgrade reaction for each layer is chosen corresponding to Table 3.3 of CUR166 which is displayed in Figure C 2

	kh;1 [kN/m³]	kh;2 [kN/m³]	kh;3 [kN/m³]
sand			
loose 5	12000	6000	3000
moderate 15	20000	10000	5000
dense 25	40000	20000	10000
clay			
soft 25	2000	800	500
moderate 50	4000	2000	800
dense 200	6000	4000	2000
peat			
soft 10	1000	500	250
moderate 30	2000	800	500

Figure C 2: values for modulus of subgrade reaction source: (CUR166)

Step 3: Determine the design values of the parameters

The safety factors for Class II that are corresponding to the CUR166 are used within D-sheetpiling, as can be found in Figure C 4.

The design values for the properties of the combi wall are presented in Figure C 3, where the material factor for steel is equal to γ_m=1.0. Since the sheet pile wall consists of Z-profiles where the interlocks are not in the neutral bending axis, correction factors to account for oblique bending do not have to be taken into (CUR166).

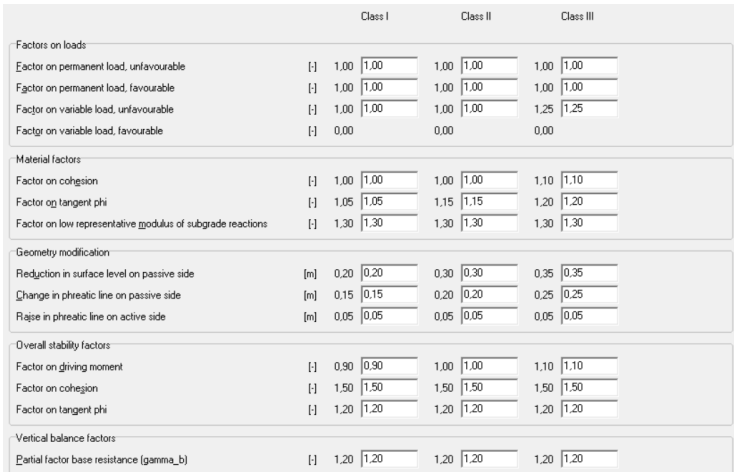

		Class I		Class II		Class III	
Factors on loads							
Factor on permanent load, unfavourable	[-]	1,00	1,00	1,00	1,00	1,00	1,00
Factor on permanent load, favourable	[-]	1,00	1,00	1,00	1,00	1,00	1,00
Factor on variable load, unfavourable	[-]	1,00	1,00	1,00	1,00	1,25	1,25
Factor on variable load, favourable	[-]	0,00		0,00		0,00	
Material factors							
Factor on cohesion	[-]	1,00	1,00	1,00	1,00	1,10	1,10
Factor on tangent phi	[-]	1,05	1,05	1,15	1,15	1,20	1,20
Factor on low representative modulus of subgrade reactions	[-]	1,30	1,30	1,30	1,30	1,30	1,30
Geometry modification							
Reduction in surface level on passive side	[m]	0,20	0,20	0,30	0,30	0,35	0,35
Change in phreatic line on passive side	[m]	0,15	0,15	0,20	0,20	0,25	0,25
Raise in phreatic line on active side	[m]	0,05	0,05	0,05	0,05	0,05	0,05
Overall stability factors							
Factor on driving moment	[-]	0,90	0,90	1,00	1,00	1,10	1,10
Factor on cohesion	[-]	1,50	1,50	1,50	1,50	1,50	1,50
Factor on tangent phi	[-]	1,20	1,20	1,20	1,20	1,20	1,20
Vertical balance factors							
Partial factor base resistance (gamma_b)	[-]	1,20	1,20	1,20	1,20	1,20	1,20

Figure C 4: Safety factor in D-sheetpiling, source: (CUR166)

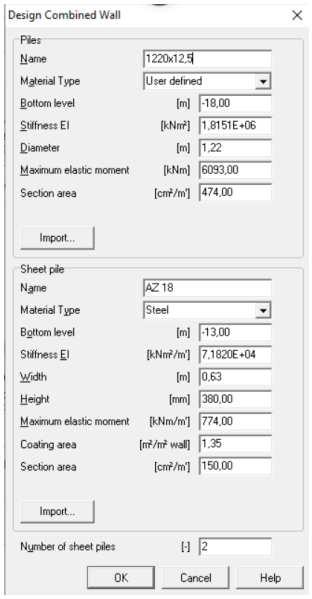

Figure C 3: Combi wall profiles

Step 4: Chose scheme A or B

It is chosen to perform all calculations with the design values for the input parameters which means that scheme A is maintained for this design.

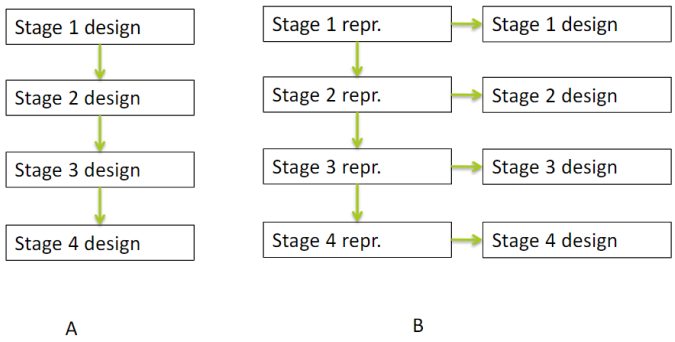

Figure C 5: Design schemes

Step 5: Design the length of the structure

The minimum length of the piles is 17 meters according to the D-sheetpiling calculation in Figure C 6 and to ensure that the pile tip is installed in sand layer, the bottom of the piles will be installed at -18m NAP. The sheet piles can be installed at -13 m NAP since the main function of the sheet pile is to prevent the inflow of water.

Stage 6: Dewatering
Partial factor set: Class II
CUR method: Method A: Partial factors (design values) in all stages

Sheet piling length [m]	Mobilized resistance [%]	Anchor force [kN]	Maximum moment Negative [kNm]	Maximum moment Positive [kNm]	Maximum displacement [mm]
25,00	6,6	-838,78	-1589,9	1779,5	-58,9
24,00	7,0	-752,93	-1454,3	1485,3	-55,2
23,00	7,7	-758,53	-1476,5	1435,8	-55,2
22,00	8,7	-767,37	-1512,6	1357,2	-55,3
21,00	9,6	-785,96	-1588,8	1199,5	-55,5
20,00	9,8	-800,02	-1646,5	1078,0	-55,8
19,00	10,0	-811,66	-1695,6	976,3	-56,2
18,00	10,4	-817,15	-1718,8	931,4	-56,5
17,00	12,5	-804,89	-1667,0	1045,5	-60,7
16,00 Sheet piling unstable ...					

End of Design Calculation

Figure C 6: minimum embedment depth of combiwall

Step 6: Design calculations

The maximum values for the loads on the wall can be found in Figure C 7 as well as in the graphs. Step 6.1 till 6.5 describe the variation in the combination between the soil stiffnesses and water levels from the manual of D-sheetpiling

Table 38.1: *Design values of soil properties according to Step 6 of the CUR 166 procedure*

Step	Limit	k_d (1)	c_d	$\tan\varphi_d$	$\tan\delta_d$
6.1	ULS	$k_{low,rep}/\gamma_k$	$c_{low,rep}/\gamma_c$	$\tan\varphi_{low,rep}/\gamma_{tan\varphi}$	$\tan\delta_{low,rep}/\gamma_{tan\varphi}$
6.2	ULS	$k_{high,rep}$ / 1.0	$c_{low,rep}/\gamma_c$	$\tan\varphi_{low,rep}/\gamma_{tan\varphi}$	$\tan\delta_{low,rep}/\gamma_{tan\varphi}$
6.3	ULS	$k_{low,rep}/\gamma_k$	$c_{low,rep}/\gamma_c$	$\tan\varphi_{low,rep}/\gamma_{tan\varphi}$	$\tan\delta_{low,rep}/\gamma_{tan\varphi}$
6.4	ULS	$k_{high,rep}$ / 1.0	$c_{low,rep}/\gamma_c$	$\tan\varphi_{low,rep}/\gamma_{tan\varphi}$	$\tan\delta_{low,rep}/\gamma_{tan\varphi}$
6.5	SLS	$k_{low,rep}$	$c_{low,rep}$	$\tan\varphi_{low,rep}$	$\tan\delta_{low,rep}$

(1) The high representative value of the modulus of subgrade reaction $k_{high,rep}$ is determined by multiplying the input low representative value $k_{low,rep}$ by 2.25.

Table 38.2: *Design values of ground and water levels according to Step 6 of the CUR 166 procedure*

Step	Limit	Ground (GL)	Water level (WL)	
		Passive side	Passive side	Active side
6.1	ULS	GL_{rep} - ΔGL_{pas}	WL_{rep} + ΔWL_{pas}	WL_{rep} + ΔWL_{act}
6.2	ULS	GL_{rep} - ΔGL_{pas}	WL_{rep} + ΔWL_{pas}	WL_{rep} + ΔWL_{act}
6.3	ULS	GL_{rep} - ΔGL_{pas}	WL_{rep} - ΔWL_{pas}	WL_{rep} + ΔWL_{act}
6.4	ULS	GL_{rep} - ΔGL_{pas}	WL_{rep} - ΔWL_{pas}	WL_{rep} + ΔWL_{act}
6.5	SLS	GL_{rep}	WL_{rep}	WL_{rep}

Figure C 7: Different scenarios for design steps.

Step 6.5 for stage 6 (dewatering) is governing for the maximum bending moment, shear force and deflection of the wall. Note that the values from the graphs in Figure C 8 still need to be multiplied by a factor of 1.2 to reach the design values in Table C 1.

Table C 1: Maximum values of design forces

	Value	Stage
Bending moment M_{ed} [kNm]	2257	Stage 6 – Step 6.5 * 1.2
Shear Force V_{ed} [kN]	1600	Stage 6 – Step 6.5 * 1.2
Deflection [mm]	42	Stage 6 – Step 6.5
Anchor Force $F_{anchor;d}$ [kN]	947	Stage 6 – Step 6.5 * 1.2

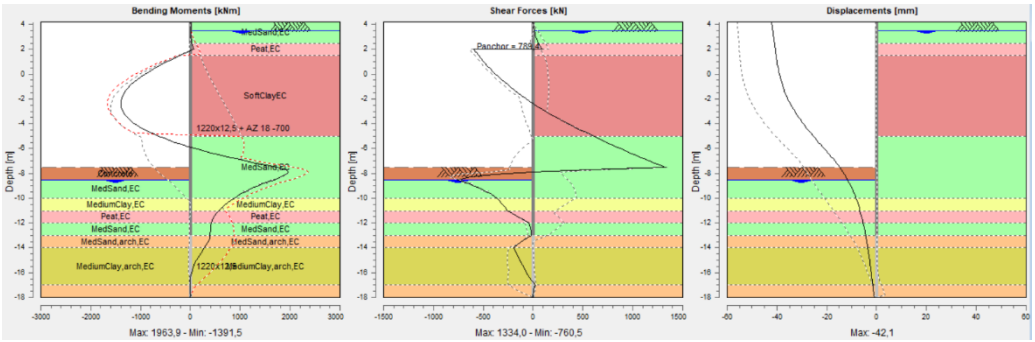

Figure C 8: Graphs showing maximum design values for forces and displacements

Step 7: Checking the design moment.

The maximum allowable bending moment at the location of the maximum acting bending moment on the wall is equal to:

$$M_{r;d;el} = 7069\ kNm.$$
$$M_{e;d;} = 2257 kNm.$$
$$\frac{M_{e;d;}}{M_{r;d;el}} = 0.32$$

The combiwall is sufficiently strong to take up the acting bending moment

Step 8: Checking the shear force

Since D-sheet piling doesn't directly give the maximum allowable shear force of the chosen profile, this will be calculated manually. The following requirement needs to be met:

$$V_{s;d} \leq \frac{V_{r;rep}}{\gamma_{,}}$$

In which γ_m is again equal to 1.0 for steel. The value of Vs;d is equal to 1600 kN, as can be seen in the table from step 6. The value of Vr;rep is computed by assuming the Von Mises yield criterion, which means: $V_{r;rep} = \frac{\tau_y}{\sqrt{3}} * A$, in which τ_y is equal to the yield strength of S430, which is 430 N/mm2. A is the cross-sectional area of the profile, which according to D-sheetpiling is equal to 624 cm^2/m. When looking at 1 meter of the retaining wall this means that: $V_{r;rep} = \frac{430 N/mm^2}{\sqrt{3}} * 62400 mm^2 \approx 1{,}55 * 107N = 15500 kN$, it can therefore be concluded that the requirement regarding the shear strength of the retaining wall is met.

Step 9: Checking the anchor force

The next step is checking the strength of the assumed anchor. Since a grouted anchor is used, there are some requirements regarding the configuration of the anchor that need to be met. First of all, the length of the grout element needs to be at least 5 meters and the complete grout element needs to be in the sandy layer.

Since no creep tests are available, the suitability tests cannot be carried out.

As mentioned at step 6, the maximum anchor force $F_{a;\,max} = 947\ kN$, the design load on the grout element is:

$$F_{a;\,max;\,grout;\,d} = 1{,}1 *\ F_{a,\,max} = 1042\ kN$$

For the resistance of the grout body, figure 5.15 from the Reader Deep Excavation is used to estimate the value of $F_{r,max,gr;rep}$. For a grout body of 7 meters long, this value is approximated to be 1700 kN.

The design value is then derived by dividing the representative value with a safety factor of 1.40:

$$F_{r,\,max,\,gr;\,d} = 1700/1.4 = 1214\ kN$$

Since $F_{r,max,gr;d} > F_{a,max,gr;d}$, the designed grout element is strong enough and needs to be elongated.
Next up, the strength of the anchor rod is tested. The value of the design yield force is equal to 1584 kN, so $F_{r,max,rod,d} = 1584\ kN$
The design value of the force acting on the rod is: $F_{a,max,rod,d} = 1{,}25 * F_{a,max} = 1184 kN$
Since $F_{r,max,rod,d} < F_{a,max,rod,d}$, it can be concluded that the anchor rod is sufficiently strong.
Furthermore, the anchor was prestressed at a value of 124 kN which influences the maximum occurring deflection that will be evaluated in step 10.

Step 10: Checking the deformation

The value of the maximum occurring deformation u_{max} is the displacement in SLS conditions, so only considering step 6.5 of the D-sheetpiling calculation results which is 41,1 millimeters. The deep excavation reader is used to determine the value of the maximum allowable deflection u_{limit}. It is mentioned that Rijkswaterstaat uses 1/200 of the retaining height as u_{limit} with a maximum of 50 mm for final walls and 1/100 and 100 mm for temporary walls (CIE4363 reader, 2018).
Since this is considered to be a permanent wall, the value of u_{limit} is 50 mm. This means that $u_{max} < u_{limit}$ and so the current design meets the requirements regarding deformations.

Step 11: Check other failure mechanisms

The overall stability of the retaining walls are determined in this step, the critical macro-stability of the system is present the full excavation stage where the stability factor for Bishop's method is still equal to 2.27, which is displayed in Figure C 9.

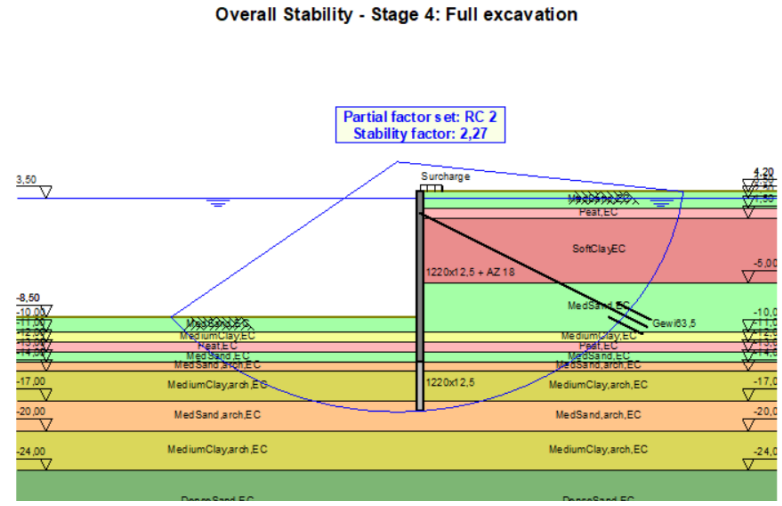

Figure C 9: Overall stability of retaining wall

Since all design steps are performed and all check are successfully performed, we can conclude that the current design fulfils all needs.

Finally, the waling that ties together the anchors needs to be designed, the design moment in the waling is described by:

$$M_{wal;d} = \frac{1}{10} * F_{a;d} * a$$

Where $F_{a;d}$ is the design value of the anchor force, which is equivalent to the maximum force of the grout body, $F_{a;d} = 1042\ kN$ and a is the centre to centre distance of the anchors, $a = 2.48\ m$. Filling this in yield:

$$M_{wal;d} = \frac{1}{10} * 1042 * 2.62 = 273\ kNm$$

The required section modules W_d can now be determined by stating that the maximum allowable moment $M_{rd;wal} = M_{wal;d} = \sigma_{vl;d} * W_d$. Assuming a steel quality S430, the minimal required section modulus is equal to:

$$W_d \geq \frac{M_{wal;d}}{\sigma_{vl;d}} = \frac{2.73 * 10^6 Nmm}{\frac{430N}{mm^2}} = 6.3 * 10^5 mm^3$$

This means that 2 UNP260 profiles are necessary to make up the waling, as they have a $W_{y;el}$ of $3*10^5$ mm^3 each (Staaltabellen).

UCF design

First of all, some decisions have to be made regarding the thickness of the underwater concrete floor and its strength properties. CUR77 requires a minimal average thickness of 800 millimetres and often a thickness of 1 meter is chosen in practice and the same is done for this design. The minimal thickness of the UCF taking placement tolerances into account with tol_{under}=150 mm for a UCF resting on a sand layer and tol_{over}=75 mm for the use of the hop-dobbler method leads to:

$$h_{min} = h_{avg} - \sqrt{(tol_{under}^2 + tol_{over}^2} = 833\ mm$$

A concrete strength class of C20/25 is chosen which has the following relevant properties:

C20/25		
fctk	1.547	N/mm2
fctd,pl	0.825	N/mm2
fck	20	N/mm2
fcd,pl	10.7	N/mm2

The first check that will be performed considers bending cracks in the 'center region' of the UCF in the long direction. This Check A from CUR77 is also used to determine the maximum centre-to-centre distance for the tension piles in long direction L_y by examining the following equation:

$$\sigma_{ct} \leq 1,25 \cdot f_{ctd,pl}$$

where

$$\sigma_{ct} = \frac{6 \cdot M}{h_{min}^{\ 2}}$$

and

$$M = \frac{1}{8} * q * L_y^2$$

Q is the representative value for the loads which is equal to the water pressure at a level of -8.5 m NAP minus the self-weight of the concrete, which is equal to:

$$q = \left((8.5\ m + 3.66\ m) * 10\ \frac{kN}{m^3} \right) - \left(1\ m * \frac{23 \frac{kN}{m^3}}{1.1} \right) = 100\ kN/m^2$$

Where the volumetric weight of the concrete is corrected with a material factor 1.1.
This leads to $L_{y,max}$=3.08 meters, for simplicity, a value of 2.5 meters is chosen.

Next, check G is performed which concerns the punching shear check of the connections between the anchors and the concrete floor. The following must be true (CUR-Aanbeveling 77, 2014):

$V_{Rd} \geq 1.25 * V_{Ed}$

V_{Ed} is equal to the upward pressure q_{Ed} multiplied by the area that is carried by each tension pile. L_x is chosen to be 2.4 metres, this means:

$$V_{Ed} = q_{Ed} * L_x * L_y = (100 * 1.35) * 2.4 * 2.5 = 816kN$$

GEWI63.5 anchors are again chosen as the type of tension pile, for which the CUR77 has prescribed the following checks:

$V_{Rd} = k_r * v_{min} * d_{min} * u_1$

Wherein:

$k_r = 1.0$ if $d_{min} \leq 300mm$

$k_r = 0.6$ if $d_{min} \geq 900mm$

$k_r = 1 - 0.4*(d_{min} - 300)/600$ for other values for d_{min} with d_{min} in mm

v_{min} according to 10.2.2

$d_{min} = h_{avg} - tol_{anchoring} - tol_{under} - p$ with h_{avg}, $tol_{anchoring}$ *and* tol_{under} according to 7.1

$u_1 = \pi*(D + 4*d_{min})$ with D equal to the diameter of the dish

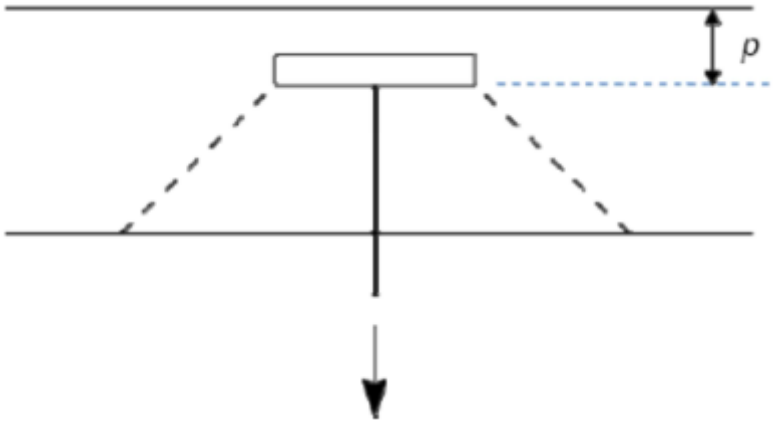

Here, p is the distance between the average level of the top of the floor and the average level of the bottom of the dish. The value of p should be chosen based on:

$p_{min} \leq p \leq p_{max}$

wherein:

$p_{min} = tol_{over} + tol_{anchoring}$

$p_{max} = h_{avg}/2$

Where $tol_{anchoring}$=100 millimeters. This leads to p_{min}=175 mm and p_{max}=500 mm, p=200 mm is chosen here, leading to d_{min}=550 mm and k_r=0.833. For the anchor dish, a cast anchor piece with a diameter of 350 mm is chosen (DYWIDAG-Systems international, 2012).

Anchor piece (cast)

nom-Ø [mm]	article-no.	A/F [mm]	L [mm]	Ø [mm]	t [mm]	weight [kg]
63,5	**63 T 2183 G**	100	125	350	20	23,0

material: iron cast EN GJS-500-7

Coupler

nom-Ø [mm]	article-no.	Ø [mm]	L [mm]	weight [kg]

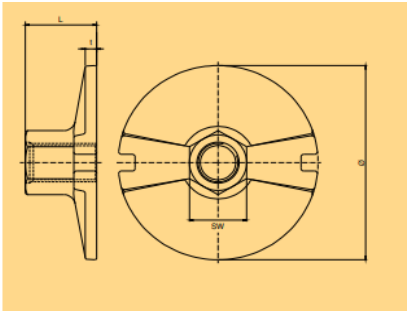

This means a value for u_1=8000 mm and since v_{min}=0.32 N/mm^2, the maximum allowable shear force is equal to:

V_{Rd}=1166 kN, leading to a u.c. of $\frac{1.25*816}{1167} = 0.87$.

Finally, check B2 is performed which checks the bending moment in the short direction without the membrane effect. CUR77 prescribed the following check (CUR-Aanbeveling 77, 2014).

Each field must meet the requirement:

$M_{Ed} \leq M_{Rd}$

wherein:

$M_{Rd} = z * N_{Rd}$

z is the internal level arm for which holds:

$z = z_1$ for smooth tension elements according to 10.2.1

$z = z_2$ for anchors and other tension elements wherein z_2 is not lower than z_1

$z_1 = h_{gem}/2 - tol_{under} - 2/3 * N_{Ed}/f_{cd,pl}$

z_2 shall be determined as follows:

- tension elements with ribs according to 10.2.2 or 10.2.3:

$$z_2 = h_{avg} - tol_{over} - \alpha_r - tol_{under} - (x_{sup} + x_{field})/3$$

- tension elements with the anchoring at a level according to 10.2.4 or 10.2.5:

$$z_2 = h_{avg} - tol_{anchoring} - p - tol_{under} - (x_{sup} + x_{field})/3$$

x_{field} is the height of the concrete compression zone in the center of the field:

$$x_{field} = 2 * N_{Ed}/f_{cd,pl}$$

x_{sup} is the height of the concrete compression zone at the location of the supports:

$$x_{sup} = 2 * N_{Ed}/(f_{cd,pl} * 0.6)$$

The normal force in the concrete floor is determined from D-sheetpiling where the floor is modelled as a strut with E=30000 Mpa, A = 1m^2/m' and L = 15 metres. This leads to a force in the strut of F_{strut}=2460 kN, as can be found in Figure C 10.

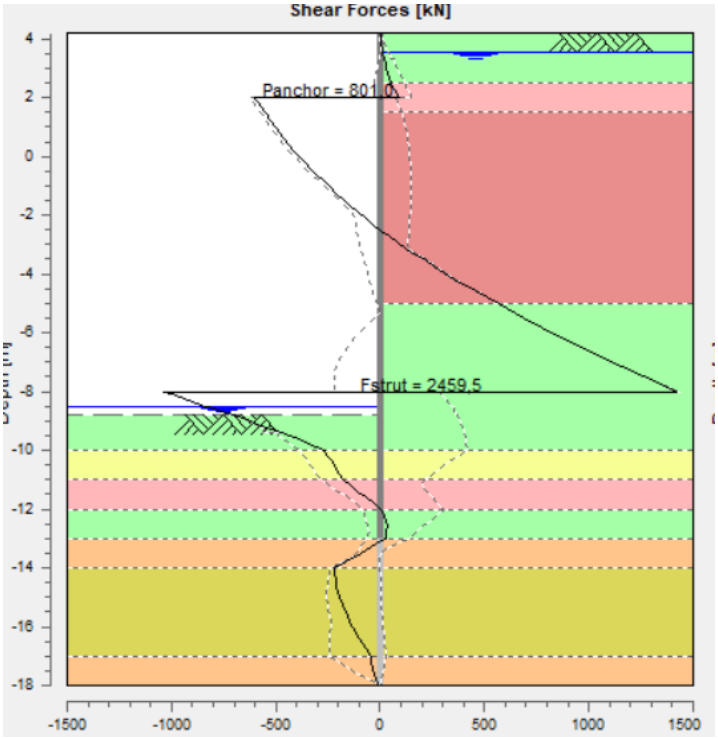

Figure C 10: Force in the concrete strut

N_{ed}=0.9*F_{strut}=2213 kN and M_{Ed}=1/8*q_d*L_x = 98 kNm.

The value of z_1 and z_2 are computed to be 212 mm and 183 mm respectively and so the value for M_{Rd}= N_{ed}* z_2 = 448 kNm, meaning that this check is also verified with a unity check of $\frac{98}{448} = 0.22$.
It can therefore be concluded that the design of the UCF is sufficiently strong.

Tension pile design
Firstly, the strength of the pile group and single pile are determined with regards to the pull-out failure mechanisms. CUR98-9 uses the qc-method to determine the strength, which for a pile group states (CUR-rapport 98-9, 2014):

$$F_{r;tension;d} = \int_0^L q_{c;z;d} \cdot f_1 \cdot f_2 \cdot O_{p;z} \cdot \alpha_{t;z} \, dz$$

in which:

$F_{r;tension;d}$	design value of the tensional capacity in [kN];
f_1	effect of the installation of neighbouring piles ($f_1 \geq 1.0$);
f_2	effect of a tensional load ($f_2 \leq 1.0$);
$\alpha_{t;z}$	coefficient for shaft friction at depth z;
$O_{p;z}$	circumference of the shaft at depth z in [m];
$q_{c;z;d}$	design value for the cone resistance at depth z in [kPa];
L	length of the pile over which shaft friction is taken into account in [m].

The design value of the bearing capacity has to be corrected for using multiple safety factors:

$$q_{c;z;d} = \frac{\xi}{\gamma_{m;b4} \cdot \gamma_{m;var;qc}} \cdot q_{c;z;exc}$$

in which:

$q_{c;z;max}$ cone resistance at a depth of z [m] below ground level in [MPa], where the peaks in the CPT diagram are cut off at values of 15 MPa if these values occur over a distance of at least 1 m, and otherwise for values of 12 MPa;

$q_{c;z;exc}$ cone resistance including the effect of excavation and cut off for respectively 12 and 15 MPa;

ξ factor for the number of CPT's and the redistribution capacity of the structure;

$\gamma_{m;b4}$ material factor for piles loaded in tension according to NEN 9997; $\gamma_{m;b4} = 1.35$;

$\gamma_{m;var;qc}$ factor showing the influence of the fluctuation of loads. For the determination of γ_{var}, the load variations must be quasi-static. This calculation rule does not apply for dynamic fluctuations.

For screwed piles with grout injection or grout mixing, α_t=0.009 and the most conservative value for $\gamma_{m;var;qc}$=1.5 is taken. The value for ξ=1.3 for 3 CPT test in a non-stiff soil (CUR-rapport 98-9, 2014). The effect of excavations on the bearing capacity of the soil have to be taken into account as follows:

$$q_{c;z;exc} = q_{c;z} \cdot \frac{\sigma'_{v;z;exc}}{\sigma'_{v;z;0}} \quad \text{with} \quad q_{c;z;exc} \leq 12 \text{ or } 15 \text{ MPa}$$

in which:

$q_{c;z}$ cone resistance measured before excavation at depth z in [MPa];

$q_{c;z;exc}$ corrected, calculated cone resistance at depth z below the bottom of the excavation in [MPa], where the peaks in the q_c-diagram are cut off at 15 MPa if these values occur over a distance of at least 1 m, and otherwise at 12 MPa;

$\sigma'_{v;z;exc}$ effective vertical stress at depth z below the bottom of the excavation in [kPa];

$\sigma'_{v;z;0}$ initial effective vertical stress at depth z during the execution of the CPT

Next, the value for f_1 is determined from the degree of densification due to the installation of the pile field, described in an increase in the relative density R_e.

The value for r in this case is equal to 5 in the long direction and r=4.8 in the short direction, n=4.
The calculation of f_1 for a varying length of the tension pile can be seen in Table C 2 below.

$f_1 = e^{3 \cdot \Delta R_e}$ (note: e = exponent)

in which ΔR_e is the increase of the relative density due to the installation of the piles. The value ΔR_e of can be determined according to:

$$\Delta R_e = \frac{\sum_1^n \Delta e}{(e_{max} - e_{min})}$$

in which:

Δe	decrease in the void ratio due to the insertion of a soil displacing pile within a distance of $6 \cdot D_{eq}$;
e_0	initial void ratio of the soil;
e_1	void ratio of the soil after the installation;
e_{max} and e_{min}	maximum and minimum void ratio of the soil. The influence of these parameters is limited so a global estimate is sufficient. In most cases for normally consolidated soils in the Netherlands, the values for e_{max} and e_{min} can be taken to be 0.8 and 0.4 respectively;
n	number of piles within a distance of $6 \cdot D_{eq}$.

The value of e_0 can be determined according to:

$$e_0 = -R_e \cdot (e_{max} - e_{min}) + e_{max}$$

in which R_e is the initial value of the relative density of the soil.

$$R_e = 0.34 \cdot \ln \frac{q_{c;z}}{61 \cdot (\sigma'_{v;z;0})^{0.71}}$$

in which:

$q_{c;z}$	value of the cone resistance in [kPa]; not: $q_{c;z}$ not in MPa)
$\sigma'_{v;z}$	initial effective vertical stress at a depth z during the execution of the CPT in [kPa].

$$\sum_1^n \Delta e = \frac{(r-6)}{5.5} \cdot \frac{(1+e_0)}{50}$$

in which:

r	is the distance c.t.c. expressed in D_{eq} of a pile to the pile in question (or another randomly located point) with a maximum of $r = 6$. If $r > 6$ the densification effect is not considered or neglected;
n	is the number of piles within a distance of $6D_{eq}$.

Table C 2: Calculation of f1 for varying pile length

f1								emax	0.8	
								emin	0.4	
	avg									
depth at tc	qc;z	σ'v at top	σ'exc at tc	qc;z;exc						
[m + NAP]	Mpa	kPa	kPa	Mpa	Re	e0	deltae	e1	deltaRe	f1
-24	22	212.6	129	17.13704	0.708132	0.516747	2)	0.492479	0.06067	1.199626
-25	26	223.6	140	20.57318	0.752753	0.498899	0.023982	0.474917	0.059956	1.197059
-26	16	234.6	151	12.83644	0.576087	0.569565	0.025113	0.544452	0.062783	1.207253
-27	25	245.6	162	20.30408	0.716763	0.513295	0.024213	0.489082	0.060532	1.199129
-28	36	256.6	173	29.55951	0.830165	0.467934	0.023487	0.444447	0.058717	1.192619
-29	33	267.6	184	27.36401	0.790449	0.483821	0.023741	0.460079	0.059353	1.194895
-30	19	278.6	195	15.89573	0.593021	0.562792	0.025005	0.537787	0.062512	1.206272
-31	25	289.6	206	21.08504	0.676981	0.529207	0.024467	0.50474	0.061168	1.201421
-32	17	300.6	217	14.44389	0.536857	0.585257	0.025364	0.559893	0.06341	1.209529
-33	24	311.6	228	20.52957	0.645427	0.541829	0.024669	0.51716	0.061673	1.203242
-34	26	322.6	239	22.37897	0.664266	0.534293	0.024549	0.509745	0.061372	1.202154
-35	20	333.6	250	17.31358	0.566968	0.573213	0.025171	0.548041	0.062929	1.207782
-36	40	344.6	261	34.81149	0.794807	0.482077	0.023713	0.458364	0.059283	1.194645
-37	40	355.6	272	34.98352	0.787222	0.485111	0.023762	0.461349	0.059404	1.19508

The next step is to determine the value of the tensional load factor f_2 which takes the decrease in effective stress in the layers from which the pile obtains its tensional bearing capacity into account.

$$f_2 = \frac{q_{c;z;2}}{q_{c;z;1}}$$

in which:

$q_{c;z;1}$ design value of the cone resistance after the installation of the piles in [MPa];
$q_{c;z;2}$ design value of the cone resistance after the tensional load has been exerted on the pile group in [MPa].

The magnitude of f_2 is determined from the design value of the parameters. For the calculation of f_2, over the entire length of the pile, the soil is divided in layers with constant cone resistance $q_{c;z;1}$, each with a thickness of maximally 1 m. The value of f_2 is determined per layer i according to:

$$f_{2;i} = \frac{-M_i + \sqrt{M_i^2 + \left(2\sigma'_{v;d;j;0} + \gamma'_{d;i} \cdot d_i\right)\left(2\sigma'_{v;d;j;0} + \gamma'_{d;i} \cdot d_i - \sum_{n=0}^{i-1} T_{d;n}\right)}}{\left(2\sigma'_{v;d;j;0} + \gamma'_{d;i} \cdot d_i\right)}$$

with:

$$M_i = \frac{f_{1;i} \cdot O_{gr;i} \cdot \alpha_i \cdot q_{c;d;i} \cdot 1000 \cdot d_i}{A}$$

$$T_{d;i} = M_i \cdot f_{2;i}$$

M_i temporary factor for layer i in [kN/m²];
$T_{d;i}$ design value of the contribution of the tensional bearing capacity of layer i in [kN/m²];
$\sigma'_{v;d;j;0}$ design value of the effective vertical stress after excavation (if applicable) in layer boundary j in [kN/m²];
$O_{gr;av;i}$ average circumference of the pile in layer i in [m];
$q_{c;d;i}$ design value of the average cone resistance in layer i in [MPa];
d_i thickness of layer i in [m];
A influence area of the pile in [m²];
$\gamma'_{d;i}$ design value of the effective unit weight of layer i in [kN/m³].

If the values for f_2 are known, we can calculate the bearing capacity of the pile group and also that of a single pile, since for a single pile the equation mentioned earlier is used with f_1=f_2=1.0. These calculations are all performed within Excel, the results can be seen in Table C 3 below, where the last column gives the maximum bearing capacity for a single pile and the second to last column gives the bearing capacity of the pile group. We can conclude that the pull-out of a single pile is the governing failure mechanism and the minimal depth is equal to -33 metres, which is highlighted by the green cells which indicate when $F_{r;tension;d}$ is larger than V_{ed}, with V_{ed} is equal to the upward water pressure, which is equal to: q_{ed}=100 kPa *1.1 = 110 kPa.
V_{ed}=q_{ed}*L_x*L_y=665 kN

Table C 3: Group pile and single pile pullout calculation

	avg													single pile
depth at t	qc;z	σ'v at top	σ'exc at tc	qc;z;exc	qc;z;cor	qc;rep	qc;d	f1	Mi	f2	Td,i	sumTdi	Frtension;	Frtension;d
[m + NAP]	Mpa	kPa	kPa	Mpa	Mpa	Mpa	Mpa	[-]	[kN/m2]	[-]	[kN/m2]	[kN/m2]	[kN]	[kN]
-24	22	212.6	129	17.13704	15	11.53846	5.698006	1.199626	16.10571	0.941708	15.16688	15.16688	91.00126	80.5536578
-25	26	223.6	140	20.57318	12	9.230769	4.558405	1.197059	12.857	0.930174	11.95924	27.12612	362.2624	144.996584
-26	16	234.6	151	12.83644	12	9.230769	4.558405	1.207253	12.96649	0.914884	11.86284	23.82208	600.4833	209.43951
-27	25	245.6	162	20.30408	12	9.230769	4.558405	1.199129	12.87923	0.925889	11.92474	23.78758	838.359	273.882436
-28	36	256.6	173	29.55951	15	11.53846	5.698006	1.192619	16.01164	0.922083	14.76406	26.6888	1105.247	354.436094
-29	33	267.6	184	27.36401	15	11.53846	5.698006	1.194895	16.0422	0.922545	14.79965	29.56371	1400.884	434.989752
-30	19	278.6	195	15.89573	12	9.230769	4.558405	1.206272	12.95595	0.930491	12.0554	26.85505	1669.435	499.432678
-31	25	289.6	206	21.08504	15	11.53846	5.698006	1.201421	16.12981	0.930191	15.00379	27.05919	1940.027	579.986336
-32	17	300.6	217	14.44389	14.4	11.11069	5.486759	1.209529	15.63663	0.934471	14.61198	29.61578	2236.184	657.55357
-33	24	311.6	228	20.52957	12	9.230769	4.558405	1.203242	12.92341	0.940367	12.15274	26.76472	2503.832	721.996497
-34	26	322.6	239	22.37897	15	11.53846	5.698006	1.202154	16.13965	0.93968	15.16611	27.31884	2777.02	802.550154
-35	20	333.6	250	17.31358	15	11.53846	5.698006	1.207782	16.21521	0.941573	15.2678	30.43391	3081.359	883.103812
-36	40	344.6	261	34.81149	12	9.230769	4.558405	1.194645	12.83107	0.947156	12.15303	27.42084	3355.567	947.546738
-37	40	355.6	272	34.98352	12	9.230769	4.558405	1.19508	12.83574	0.952044	12.22019	24.37323	3599.3	1011.98966

Finally, the clump criterion at an installation depth of -33 metres should be checked, which takes the maximum strength of the mobilized soil volume by each pile into account. It can be found that this strength is also sufficient and therefore the governing failure mechanism is indeed pull-out of a single pile, since $F_{clump;max;d}$=1345 kN, the calculations can be seen from Table C 4

$$F_{r;tension;max;d} = \left(V_{cone} + V_{cylinder}\right) \cdot \gamma'_d$$

in which:

V_{cone} volume of the conical shaped soil volume at the bottom of the pile in [m^3];

$V_{cylinder}$ volume of the schematised 'cylindrically shaped' soil volume around the rest of the pile in [m^3];

γ'_d design value of the effective unit weight of the soil in [kN/m^3]. For layered soil stratification, the weight must be taken per layer.

Table C 4: Clump criterion calculation results.

Clump criterion at -33m NAP								
Vcone				**Vcylinder**			**Vpile**	4.704693
angle at tip	23.33333	degrees		Lsand	9	m	gammadc	10.90909
radius	1.25	m		Leff	8.460803	m		
height	0.539197	m		Areatot	7.068583	m2		
Volume	0.88226	m3		Vtot	59.80589	m3		
				Veff	58.14461	m3		
	Frtension,max,d							
	1344.609	kN						

Additional mobilized soil: soil above the dense sand					
	thickness	γ'd	Volume	Vol,eff	
	m	[kN/m3]	m^3	m^3	
medium clay	8	7.3	56.54867	54.97787	399.8391
medium sand	6.5	9.1	45.94579	33.34949	303.1772
peat	1	0	7.068583	7.068583	0
			total		703.0163 kN

Gate design

A schematization of the situation that is used in the Sainflou method to determine the wave loads can be seen in Figure 28, source: (Voorendt & Molenaar, 2020).

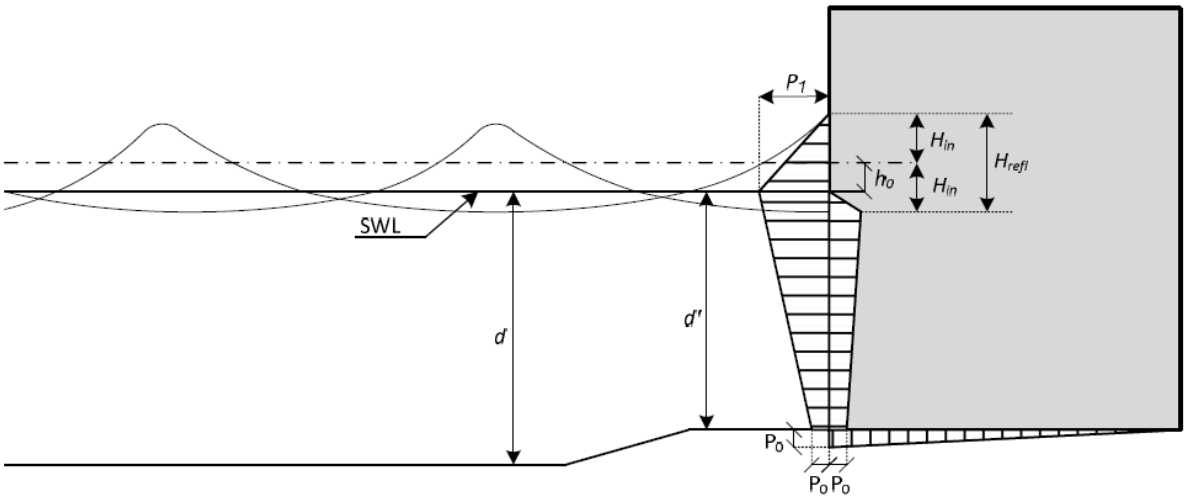

Figure C 11: Sainflou method, source: (Voorendt & Molenaar, 2020)

The still water level in front of the gate will increase with h_0:

$$h_0 = \frac{1}{2} * k * H_{in}^2 * \coth(k * d)$$

Where:

h_0 = increase of mean water level in front of the structure
H_{in}= height of the incoming wave
d = water depth in front of the gate
k = wave number of the incoming wave

For our situation $H_{in}=H_d=0.52$ meters, d = 12.40 meters and the wave number k will be determined assuming deep water, which will have to be checked. The wave length is calculated first using:

$$L = \frac{g * T^2}{2\pi} = \frac{g * 1.75^2}{2\pi} = 4.78\ m$$

Deep water check:

$$\frac{h}{L} > \frac{1}{2} \rightarrow \frac{12.40}{4.78} \approx 2.6 > \frac{1}{2}, deep\ water\ assumption\ is\ valid$$

Wave number k can now be determined:

$$k = \frac{2\pi}{L} = \frac{2\pi}{4.78} = 1.32\ rad/m$$

Which leads to:

$$h_0 = \frac{1}{2} * 1.32 * 0.52^2 * \coth(1.32 * 12.40) = 0.18m$$

The maximum pressure at mean water level p_1 and the pressure near the water bed p_0 are determined as follows:

$$p_1 = \rho * g * (H_{in} + h_0)$$

$$p_0 = \frac{\rho * g * H_{in}}{\cosh(k * d)}$$

We can now compute these values using the parameters we know:

$$p_1 = 1000 * 9.81 * (0.52 + 0.18) = 6.79 kN/m^2$$

$$p_0 = \frac{1000 * 9.81 * 0.52}{\cosh(1.32 * 12.40)} = 0.000000084 = 0\ kN/m^2$$

The characteristic value of the corresponding load per meter width of the gate are now as follows:

$$Q_{wave,r} = \frac{1}{2} * p_1 * (H_{in} + h_0 + d) = \frac{1}{2} * 6.79 * (0.52 + 0.18 + 12.4) = 44.4\ kN/m$$

The Hydrostatic load per meter width of the gate are:

$$Q_{hydrostatic,r} = \frac{1}{2} * \rho_w * d^2 = \frac{1}{2} * 1000 * 12.4^2 = 754.2\ kN/m$$

The total design load on the gate, when applying safety factor γ_P=1.35 for permanent loads and γ_Q=1.5:

$$Q_{design} = \gamma_P * Q_{hydrostatic} + \gamma_Q * Q_{wave,r} = 1.35 * 754.2 + 1.5 * 44.4 = 1085\ kN/m$$

This is the design load that should be used for ULS conditions, for SLS conditions, the representative loads should be used:

$$Q_{rep} = \gamma_P * Q_{hydrostatic} + \gamma_Q * Q_{wave,r} = 1.0 * 754.2 + 1.0 * 44.4 = 799\ kN/m$$

Gate design calculations

Total gate in long direction

For ULS conditions, the bending moment line can be seen in the MatrixFrame screenshot below.

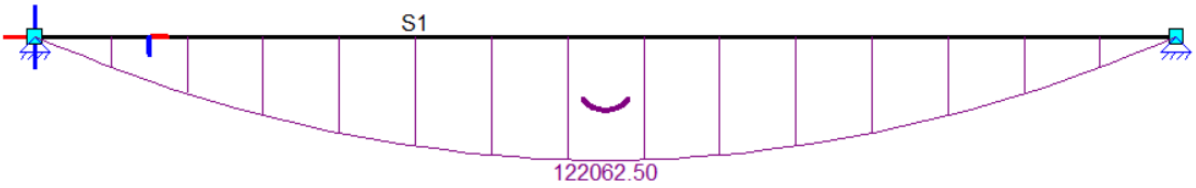

Figure C 12: bending moment total gate, long direction

This leads to a maximum bending moment in the gate of:

$$M_{Ed} = \frac{1}{8} * Q_d * L^2 = \frac{1}{8} * 1085 * 30^2 = 1.22 * 10^5 kNm$$

Consequently, the necessary section modulus for the design of the gate is, assuming a S355 steel quality:

$$W_{Ed} = \frac{M_{Ed}}{\sigma} = \frac{1.22 * 10^{11} Nmm}{355\ N/mm^2} = 3.44 * 10^8 mm^3$$

This is the minimum required section modulus for the ULS, regarding the deflection of the gate a SLS requirement is the following:

$$\delta_{max} = \frac{L}{400} = 75\ mm$$

These requirements form the basis of the design of the support system of the gate, the final design elements and their structural capacity can be found in table C1.

Table C 5: Design elements

Elements	Amount	Thickness	Width per element	Total width	Total area	Distance to top fibre	Distance to NC	I_{own}	$I_{steiner}$	I_{total}
	[-]	[mm]	[mm]	[mm]	[mm^2]	[mm]	[mm]	[mm^4]	[mm^4]	[mm^4]
Skin plate	1	20	13600	13600	272000	10	878	9.07 *10^6	2.1 *10^{11}	2.1 *10^{11}
Girders	7	1900	30	210	399000	970	82	1.2*10^{11}	2.68*10^9	1.2 *10^{11}
Flanges	7	40	700	4900	19600	1940	1052	2.61*10^7	2.2 *10^{11}	2.2 *10^{11}
									Total I_{Rd}=	5.5 *10^{11}

$$W_{Rd} = \frac{I_{Rd}}{h_{down}} = \frac{5.5 * 10^{11} mm^4}{1072\ mm} = 5.1 * 10^8 mm^3$$

Since W_{Rd}>W_{Ed}, the design is sufficiently strong, with a unity check of 0.67. The displacements follow from Matrixframe and it equal to 73 mm, leading to a unity check of 0.97.

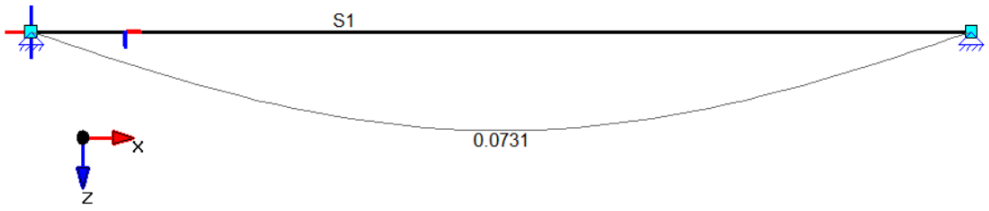

Figure C 13: Deformation total gate long direction

<u>Total gate in short direction:</u>
For ULS conditions, the bending moment line can be seen in the MatrixFrame screenshot

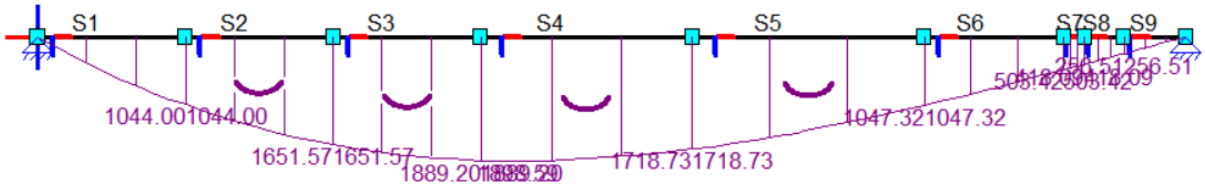

Figure C 14: Bending moment line total gate, short direction

below.

This leads to a maximum bending moment in the gate of:

$$M_{Ed} = 1900kNm$$

Consequently, the necessary section modulus for the design of the gate is, assuming a S355 steel quality:

$$W_{Ed} = \frac{M_{Ed}}{\sigma} = \frac{1.9 * 10^9}{355\ N/mm^2} = 5.35 * 10^6 mm^3$$

This is the minimum required section modulus for the ULS, regarding the deflection of the gate a SLS requirement is the following:

$$\delta_{max} = \frac{L}{400} = \frac{13600}{400} = 33.75\ mm$$

These requirements form the basis of the design of the support system of the gate, the final design elements and their structural capacity can be found in table x.x

Table C 6: Design elements short direction

Elements	Amount	Thickness	Width per element	Total width	Total area	Distance to top fibre	Distance to NC	I_{own}	$I_{steiner}$	I_{total}
	[-]	[mm]	[mm]	[mm]	[mm^2]	[mm]	[mm]	[mm^4]	[mm^4]	[mm^4]
Skin plate	1	20	30000	30000	600000	10	721	2 *10^7	3.1 *10^{11}	3.1 *10^{11}
Posts	5	1900	30	150	285000	970	239	8.6*10^{10}	1.6*10^{10}	1.0 *10^{11}
Stiffeners	18	400	20	360	144000	1720	989	1.9*10^9	1.4*10^{11}	1.4*10^{11}
Flanges	4	40	920	4600	18400	1940	1209	2.5*10^7	2.7 *10^{11}	2.7 *10^{11}
									Total I_{Rd}= 8.3 *10^{11}	

$$W_{Rd} = \frac{I_{Rd}}{h_{down}} = \frac{8.3 * 10^{11} mm^4}{1229\ mm} = 6.7 * 10^8 mm^3$$

Since W_{Rd}>W_{Ed}, the design is sufficiently strong. The displacements follow from Matrixframe and is equal to 0.2 mm. The unity checks might hint towards an overdesigned gate but the strength and deformation of the skin plate would prove to be governing and requires all these elements to be present.

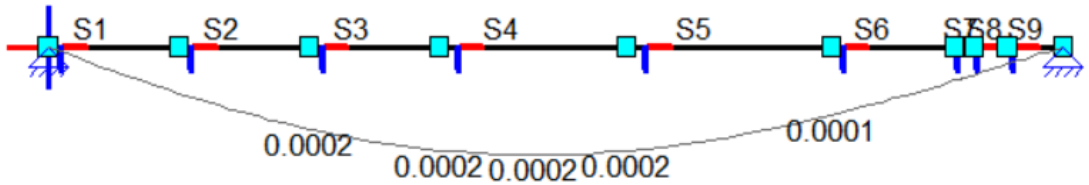

Figure C 15: deformations total gate short direction

<u>Skin plate long direction</u>
The bending moment line as a result of the loading can be seen in the figure below.

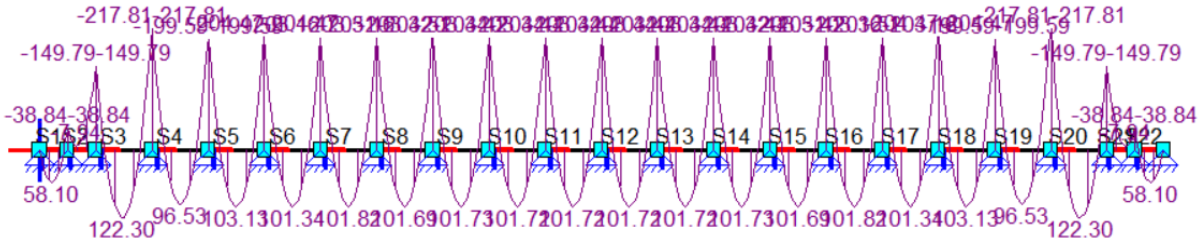

Figure C 16: Bending moment line skin plate long direction

The maximum bending moment can be found from this figure:

$$M_{Ed} = 217.8 kNm$$

For a steel quality S355, this leads to a required section modulus for the skin plate of:

$$W_{Ed} = \frac{M_{Ed}}{\sigma} = \frac{2.18 * 10^8}{355\ N/mm^2} = 6.14 * 10^5 mm^3$$

From table 2, we know that the moment of Inertia of the skin plate is equal to I=2*10^7 mm^4 and since h_{up} =h_{down}=10 mm, the actual section modulus of the skinplate equals to:

$$W_{Rd} = \frac{I_{Rd}}{h_{down}} = \frac{2 * 10^7 mm^4}{10\ mm} = 2 * 10^6 mm^3$$

Since W_{Rd}>W_{Ed}, the design is sufficiently strong with a unity check of 0.31, the maximum deflection each span is equal to:

$$\delta_{max} = \frac{L}{400} = \frac{1500}{400} = 3.75\ mm$$

Matrixframe gives the following deflection, with a maximum value of 3.5 millimetres, meaning a sufficiently stiff design, the unity check is 0.93.

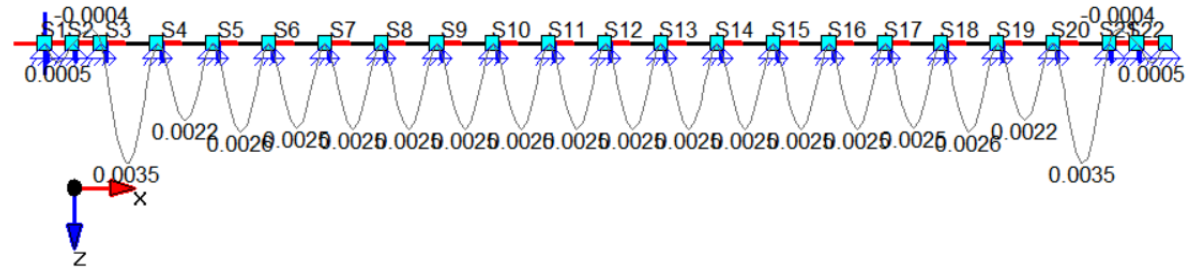

Figure C 17: Deflection skin plate long direction.

Skin plate short direction

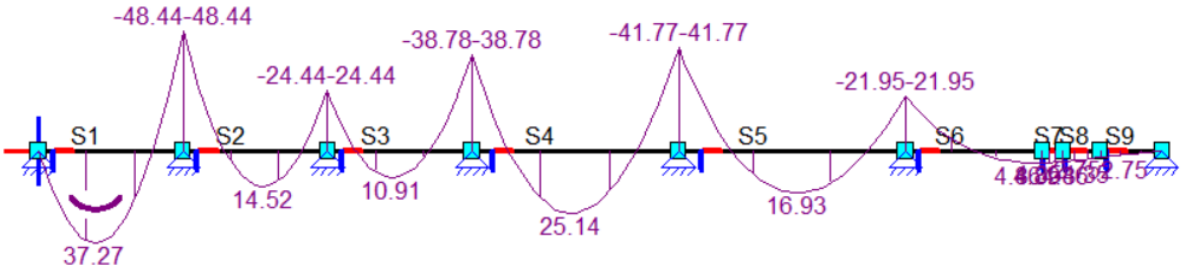

Figure C 18: Bending moment line skinplate short direction.

The bending moment line as a result of the loading can be seen in the figure below.
The maximum bending moment can be found from this figure:

$$M_{Ed} = 48.44kNm$$

For a steel quality S355, this leads to a required section modulus for the skin plate of:

$$W_{Ed} = \frac{M_{Ed}}{\sigma} = \frac{4.84 * 10^7}{355\ N/mm^2} = 1.36 * 10^5 mm^3$$

From table 2, we know that the moment of Inertia of the skin plate is equal to I=9*10^6 mm^4 and since h_{up} =h_{down}=10 mm, the actual section modulus of the skinplate equals to:

$$W_{Rd} = \frac{I_{Rd}}{h_{down}} = \frac{9 * 10^6 mm^4}{10\ mm} = 9 * 10^5 mm^3$$

Since W_{Rd}>W_{Ed}, the design is sufficiently strong with a unity check of 0.15, the maximum deflection each span is equal to:

$$\delta_{max} = \frac{L}{400} = \frac{1750}{400} = 4.375\ mm$$

Matrixframe gives the following deflection, with a maximum value of 3.8 millimetres, meaning a sufficiently stiff design, the unity check is 0.87.

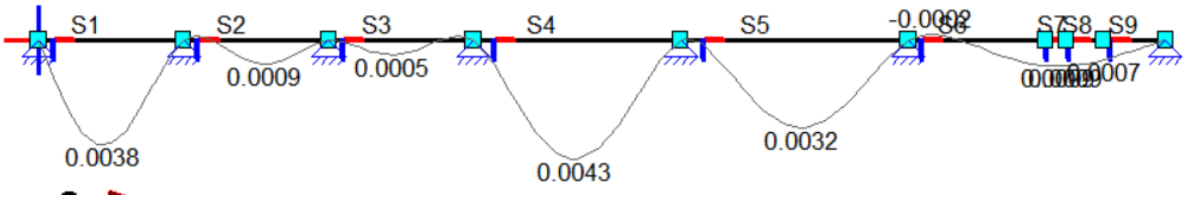

Figure C 19: deflection skin plate short direction.

Appendix D: Development of design alternatives

This appendix collects all background information and design calculations for the development of the design alternatives, starting off with the MCA for the sedimentation reduction strategies as described in chapter 5.2.1.

The criteria that are included in the MCA for the sedimentation reduction strategies are:

- Constructability: the ease of construction of the mitigation measure, including the required construction expertise and knowledge for realization.
- Effectiveness: how well does each alternative manage to prevent the inflow of sediment or enable for an easy disposal of the inflowing sediment. Since this is not accurately known for each measure, an qualitative estimation will be made.
- Costs: Including the cost of construction and the costs of operation and maintenance.
- Sustainability: The environmental impact that is involved with this mitigation measure which includes the required amount of energy, emissions during construction and maintenance and total lifetime of the solution.
- Maintenance: Frequency of maintenance and maintenance accessibility.

Each of these criteria is then given a weight based on their relative importance, effectiveness is chosen to be the most important criteria and is given a weight of 40, with feasibility and sustainability being assigned a weight of 20 and costs and maintenance a weight of 10. This distribution of the weights is a subjective decision and is based on the time and money that can be saved when the sediment clean up works are effectively prevented and considering the additional environmental impact that is involved with the disposal of the sediment after it has been cleaned up, since the sediment is typically heavily contaminated and cannot be disposed back into the harbor.
Each mitigation measure will be scored on a scale of 1-5 for each of the 5 criteria and a weighted average is then taken to determine a ranking among the alternatives. Table 5 below shows the scores given and the results of the MCA.

Table D 1: Comparison of sedimentation options

		Alternative				
Criteria	**Weight**	Water inlet	Jetty	Sediment obstacle	Bubble screen	Sediment trap
Constructability	20	3	2	3	4	5
Effectiveness	40	5	4	1	4	2
Costs	10	2	2	4	2	3
Sustainability	20	3	3	3	1	1
Maintenance	10	4	5	3	2	2
	Total score	**3.8**	**3.3**	**2.3**	**3**	**2.5**

The sediment trap option is given the highest score for the constructability criteria since it does not include the design of a structure of some sort, merely the excavation of the trap in front of the gate is sufficient. The other options are not extremely complex engineering projects but the constructability of the jetty is considered to be worse due to the possible conflicts with port regulations. The effectiveness of the water inlet is assumed to be best but should be tested, for example by setting up a physical model. The sediment obstacle option scores worst on the effectiveness criteria due to the turbulence of the flow, but is the cheapest option construction

wise and the same can be said for the siltation trap. The water inlet and jetty would require a significant amount of construction costs, the bubble screen is costly during operation procedures and the sediment trap requires additional costs during maintenance when the sediment trap has to be excavated again after a period of time. As far as the sustainability of the alternatives are considered, the water inlet, jetty and sediment obstacles would mainly cause emissions during construction but no additional energy is necessary and the lifetime of these concepts is the longest. The bubble screen requires continuous energy and is expected to have a shorter lifetime, the sediment trap requires excavations works every few years and a lot of contaminated sediment will need to be disposed of, these two alternatives therefore score worst for this criteria. Finally, the least amount of maintenance is required for the jetty and water inlet, the latter might only require the disposal of residue sand near the inlet and outlet of the pipeline. The bubble screen has a risk of clogging and maintenance works will have to be performed to the power unit of the installation. As mentioned before, the sediment trap would require continuous periodical maintenance and therefore also scores low on this criteria.

Steel fibres

For the steel fibre reinforced UCF, the average floor thickness is taken as 800 millimetres and so:

$h_{min} = h_{avg} - \sqrt{(tol_{under}^2 + tol_{over}^2} = 633\ mm$ and as mentioned before, the concrete strength

C20/25		
fctk,sf	1.93375	N/mm2
fctd,pl,sf	1.03125	N/mm2
fck,sf	23.6	N/mm2
fcd,pl,sf	12.626	N/mm2

properties are increased by the presence of the steel fibre:

The first check that will be performed considers bending cracks in the 'center region' of the UCF in the long direction. This Check A from CUR77 should be performed to check whether the c.t.c distance L_y=2.5 meters as determine in the base design is still allowed. The following equation is again used:

where

$$\sigma_{ct} = \frac{6 \cdot M}{h_{min}^{\ 2}}$$

and

$$M = \frac{1}{8} * q * L_y^2$$

$$\sigma_{ct} \leq 1{,}25 \cdot f_{ctd,pl}$$

q is the representative value for the loads which is equal to the water pressure at a level of -8.5 m NAP minus the self-weight of the concrete, which is equal to, which due to the decrease of the thickness of the floor increases to:

$$q = \left((8.5\ m + 3.66\ m) * 10\ \frac{kN}{m^3}\right) - \left(0.8\ m * \frac{23\frac{kN}{m^3}}{1.1}\right) = 104.8\ kN/m^2$$

Where the volumetric weight of the concrete is corrected with a material factor 1.1.

This leads to $L_{y,max}$=2.56 meters, so a value of 2.5 meters is still sufficient.

Next, check G is performed which concerns the punching shear check of the connections between the anchors and the concrete floor. The following must be true (CUR-Aanbeveling 77, 2014):

$V_{Rd} \geq 1.25 * V_{Ed}$

V_{Ed} is equal to the upward pressure q_{Ed} multiplied by the area that is carried by each tension pile. L_x is chosen to be 2.4 metres, this means:

$$V_{Ed} = q_{Ed} * L_x * L_y = (104.8 * 1.35) * 2.4 * 2.5 = 849kN$$

Again, the value of V_{Rd} is given as follows:

$V_{Rd} = k_r * v_{min} * d_{min} * u_1$

Wherein:
$k_r = 1.0$ if $d_{min} \leq 300mm$
$k_r = 0.6$ if $d_{min} \geq 900mm$
$k_r = 1 - 0.4*(d_{min} - 300)/600$ for other values for d_{min} with d_{min} in mm
v_{min} according to 10.2.2
$d_{min} = h_{avg} - tol_{anchoring} - tol_{under} - p$ with h_{avg}, $tol_{anchoring}$ *and* tol_{under} according to 7.1
$u_1 = \pi*(D + 4*d_{min})$ with D equal to the diameter of the dish

But here, an additional component v_{Rfd} that accounts for the presence of the steel fibre can be added, this components can be calculated as follows:

$$v_{Rfd} = 0.18 * \frac{f_{eqk,3}}{1.4 * \gamma_{ft}} = 0.18 * \frac{f_{ctk,sf}}{1.4 * 1.25} = 0.2\ N/mm^2$$

So the total $v_{new}=v_{min}+v_{Rfd}$.
The value of p is changed from 200 mm in the base design to p_{min}=175 mm, which results in u_1=5812 mm and since v_{min}=0.39 N/mm^2, v_{new}=0.59 N/mm^2 and the maximum allowable shear force is equal to:
V_{Rd}=1213 kN, leading to a u.c. of $\frac{1.25*849}{1213} = 0.88$.

Finally check B2 is performed again, where the strut force in the concrete remains the same, but the value of z changes to 63 mm, resulting in a value for $M_{Rd}= N_{ed}* z_2$ = 156 kNm.
$M_{Ed}=1/8*q_d*L_x$ = 102 kNm meaning that this check is also verified with a unity check of $\frac{102}{156} = 0.66$.
It can therefore be concluded that the design of the UCF including the steel fibres is still sufficiently strong.

Basalt fibres
The procedure can again be done for the basalt fibre reinforced UCF, this time an average floor thickness of 850 millimetres is taken and so:

$$h_{min} = h_{avg} - \sqrt{(tol_{under}^2 + tol_{over}^2)} = 683\ mm$$

And the increased concrete strength properties are:

C20/25		
fctk	1.90	N/mm2
fctd,pl	1.01	N/mm2
fck	20.9	N/mm2
fcd,pl	11.18	N/mm2

Check A leads to a maximum value for L_y of 2.75 so the chosen c.t.c. distance of 2.5 meters can be maintained. The representative value for the water pressure is equal to:

$$q = \left((8.5\ m + 3.66\ m) * 10\ \frac{kN}{m^3}\right) - \left(0.85\ m * \frac{23\frac{kN}{m^3}}{1.1}\right) = 103.8\ kN/m^2$$

Next, check G is performed again but here, the additional component v_{Rfd} that accounts for the presence of the basalt fibre can be added, this components can be calculated as follows:

$$v_{Rfd} = 0.18 * \frac{f_{eqk,3}}{1.4 * \gamma_{ft}} = 0.18 * \frac{f_{ctk,bf}}{1.4 * 1.25} = 0.2\ N/mm^2$$

So the total $v_{new}=v_{min}+v_{Rfd}$.
The value of p is changed from 200 mm in the base design to p_{min}=175 mm, which results in u_1=6440 mm and since v_{min}=0.35 N/mm^2, v_{new}=0.55 N/mm^2 and the maximum allowable shear force is equal to:
V_{Rd}=1368 kN, V_{Rd}= (q_{rep} *1.35)*L_x *L_y=841 kN leading to a u.c. of $\frac{1.25*841}{1368} = 0.77$.

For check B2, value of z changes to 73 mm, resulting in a value for M_{Rd}= N_{ed}* z_2 = 180 kNm.
M_{Ed}=1/8*q_d*L_x = 101 kNm meaning that this check is also verified with a unity check of $\frac{101}{180} = 0.56$.
It can therefore be concluded that the design of the UCF including the basalt fibres is still sufficiently strong.

Fully reinforced UCF
Designing the amount of reinforcement in the UCF is done by assuming horizontal equilibrium in the concrete cross section. This means that the force in the steel has to be equal to the force in the concrete compression zone. In other words:

$$N_s = N_c = A_s * f_{yd}$$

The force in the concrete zone is equal to N_{Ed} as applied in the UCF design and follows from the strut force acting on the concrete from the retaining wall. From this we can find that N_c=2213 kN and since f_{yd}=435 N/mm^2 we find that the minimum amount of reinforcement is equal to $A_{s,min}$=5088 mm^2/m'.
Eventually a reinforcement layout of ⌀20-50 is chosen with leads to A_s=6283mm^2/m' and, when maintaining a cover of 50 mm, the reinforcement ratio is equal to ρ=0.0067, which is higher than the minimal reinforcement ratio for C20/25 so the chosen configuration is sufficient.
The check including the reinforcement bars with a reinforcement ratio of 0.67% is included by altering the puncher shear strength of the concrete and decreasing h_{avg} to 850 millimeters as is done for the basalt fibre option.
The new value for v_{rdc}, taking into account the reinforcement is given by the following relation:

$$v_{Rd,c} = 0.12 * k * (100\rho * f_{ck})^{1/3}$$

With k and f_{ck} remaining unchanged and ρ=0.0067 this leads to $v_{rd,c}$=0.48 N/mm^2, V_{Rd}=1206 kN and the u.c. of 0.87. All other checks remains sufficient.

Head filling system
For determining the filling time of the dock, a number of assumptions have to be made initially such as the fact that the gate can be considered as a case of 'submerged flow' and that the valves in the gates are completely opened straight away. The inertia of the water mass flowing into the dock chamber is neglected as well as the friction of the water flow. This leads to the following equation that can be used for the discharge through the valves:

$$Q = m_s * f * \sqrt{2 * g * \Delta h} \qquad (1)$$

Where m_s is the discharge coefficient for submerged flow (m_s=0.8), f is the total area of the valves and Δh is the water level difference between the dock chamber and the port. In reality, both Q and Δh are time-dependent variables and the principle of mass conservation can be used to describe the following relation:

$$Q(t) = -A * \frac{d\Delta h}{dt} \qquad (2)$$

Where A is the horizontal area of the dock chamber.

Combining (1) and (2) yields the following:
$\frac{d\Delta h}{\sqrt{\Delta h(t)}} = -\frac{m_s * f}{A}\sqrt{2g}\,dt$, which after integration becomes: $\sqrt{\Delta \mathrm{h}(t)} = -\frac{m_s f}{2A} * \sqrt{2g} * t + C$ (3)
Initially, at t=0, the dock chamber is empty and the water level difference Δh is equal to h_0, which is the water level in the port, so the integration constant can be determined to be equal to $\sqrt{h_0}$.
Filling this into (3) and evaluating the square root yields an expression for Δh(t):
$\Delta \mathrm{h}(\mathrm{t}) = \frac{2g}{4}\left(\frac{m_s f}{A}\right)^2 * t^2 - \frac{m_s f}{A} * \sqrt{2g * h_0} * t + h_0$ (4)
Combining (4) and (2) yields:
$Q(t) = -\frac{m_s{}^2 f^2 g}{A} * t + m_s * f * \sqrt{2 * g * \Delta h_0}$ (5)

By setting (5) equal to zero, the total filling time of the dock chamber can be found to be:

$$T_{total} = \frac{2 * A * \sqrt{h_0}}{m_s * f * \sqrt{2g}}$$

The total filling time can be plotted against the total area of the valves, using A = 30*150 = 4500 m^2, m_s=0.8, g = 9.81 m^2/s and h_0=7.5 m. . The value for h_0 is equal to the average water level in the harbour which is at +0.00 m NAP, this is the minimum water level to start the docking procedure.
This plot can be seen in Figure D1 below.

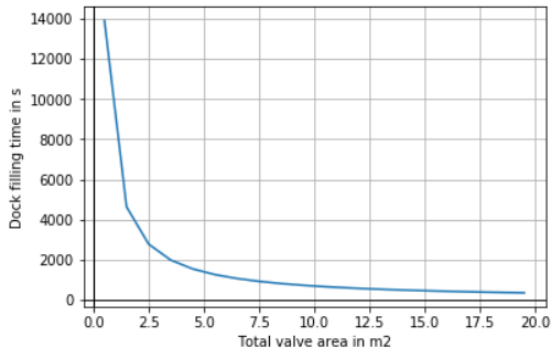

Figure D 1: Total valve area vs dock filling time

We can conclude from this graph that the minimum valve area should be 5 m^2 as the filling time exponentially increases for smaller values. Taking this minimal valve area, the graphs showing the development of the inflowing discharge Q and the water level difference between the harbor and the dock chamber can be plotted, shown in Figure D2 and Figure D3.
The time required for filling up the dock is around 1400 seconds, which is roughly 25 minutes.

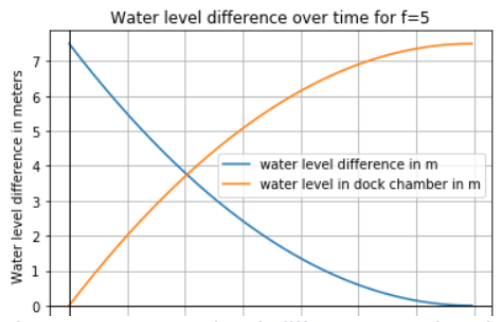

Figure D 3: water level difference vs time in seconds

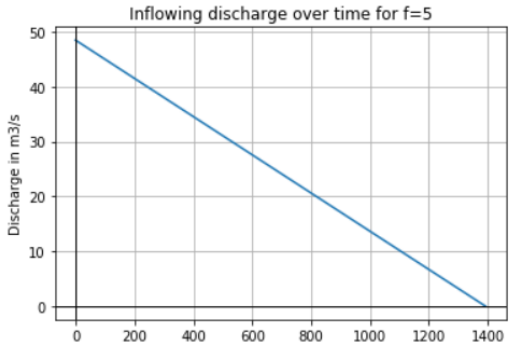

Figure D 2: Inflowing discharge over time

Appendix E: UCF loads

This appendix collects the information behind determining the design loads on the UCF.

Ship load

The ship load has been determined for the governing design vessel Kommandor Susan which is a British supply vessel that would lead to the largest concentrated load on the floor of the dock. The loading condition that is taken is the ballast arrival loading condition which means a total ship displacement of 3534 tons according to the Stability Booklet that is provided by Damen Harlingen (Marin Teknikk AS, 1999). The corresponding shear force diagram can be seen in the figure E1 below, from this it is possible to estimated the distributed loads caused by the weight of the vessel including the upward water pressure, since the shear force diagram shows the nett shear force acting on the outmost fibre of the vessel hull itself in a submerged condition which means that the water pressure must be subtracted to reach the total distributed weight of the ship.

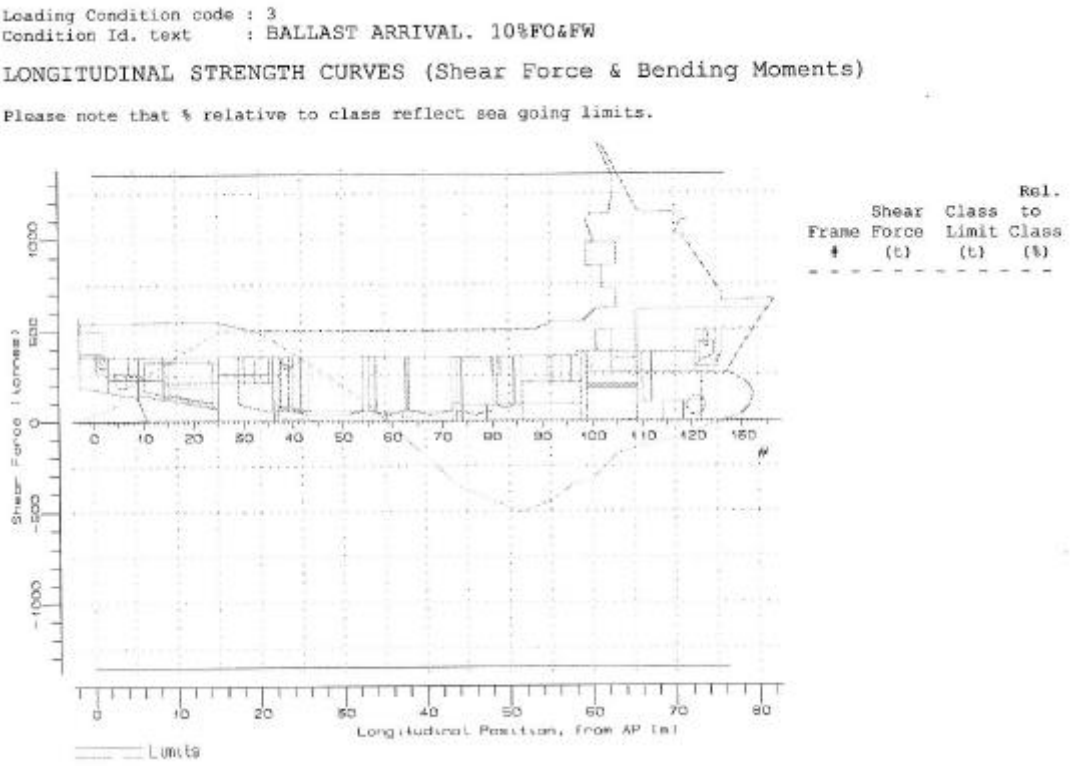

Figure E 1: Ship shear force distribution, (Marin Teknikk AS, 1999)

The nett distributed can now be retrieved by investigated the slope in the shear force diagram, which yield:

$$q_1 = 500\ t\ /\ 28\ meter\ \approx 18\ t\ /\ m$$

$$q_2 = 1000\ t\ /\ 46\ meter\ \approx 22\ t\ /\ m$$

$$q_3 = 500t/35\ meter\ \approx 14\ \ t\ /\ m$$

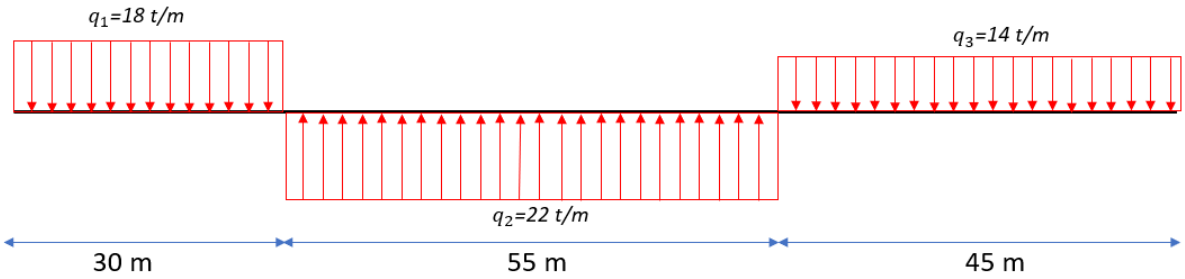

Figure E 2

To estimate the upward directed water pressure due to the displacement of the vessel, it is assumed that this is distributed equally over the length of the vessel, which is equal to roughly 130 meter resulting in a distributed load of 3534/130 ≈27 t/m. This will lead to an overestimation of the governing peak load since the displacement of the vessel is not equally distributed over the length as well. The vessel is widest in the middle section and becomes slimmer near the bow and the stern and so the estimation in this appendix will lead to an overly dimensioned but structurally safe floor. The final weight distribution can therefore be retrieved by subtracting the upward directed pressure from the diagram in figure E2, to reach the final pressure distribution as can be seen in figure E3 below.

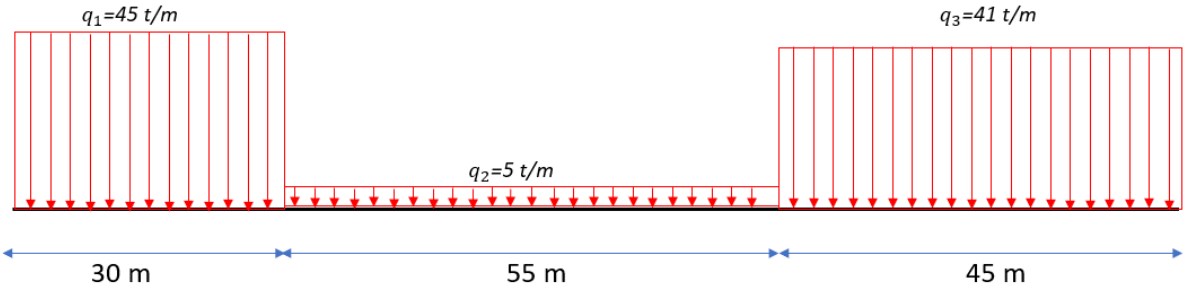

Figure E 3: Ship weight distribution

Blocks are typically placed at a centre to centre distance of 2 meters or less, meaning that the governing load on one 'row' of blocks, consisting of a wider centre block and two edge blocks, is equal 90 tons.

The middle block carries roughly 75% of the total load and the other 25 % of the load is distributed over the two outer blocks, which means that q_{mid}=45 t/m=450 kN/m and F_{edge}=11.25 t = 112.5 kN. The result can be seen in the diagram below.

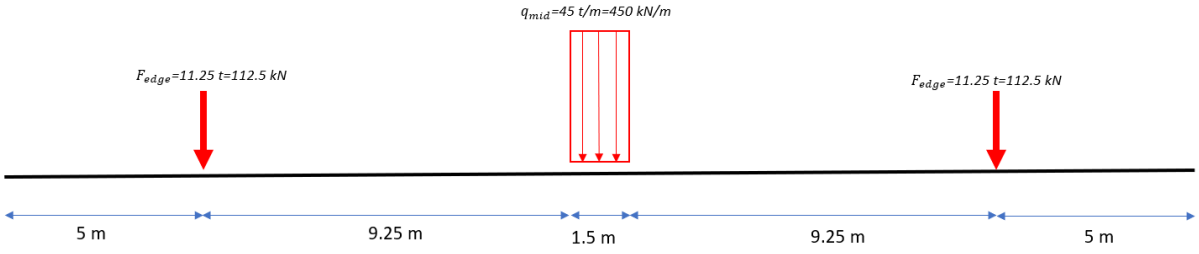

Shrinkage

The total shrinkage of the floor consists of the autogenous and drying shrinkage, meaning that the following equation needs to be determined:

$$\varepsilon_{cs} = \varepsilon_{ca} + \varepsilon_{cd}$$

Firstly, the autogenous shrinkage strain ε_{ca} is determined using the relations in NEN-EN 1992-1-1:

$$\varepsilon_{ca}(\infty) = 2.5(f_{ck} - 10) * 10^{-6} = 0.025 * 10^{-3}$$

The drying shrinkage strain is harder to determine:

$$\varepsilon_{cd} = \beta_{ds} * k_h * \varepsilon_{cd,0}$$

Where:

$$\varepsilon_{cd,0} = 0.85 * \left((220 + 110 * \alpha_{ds1}) * \exp\left(-\alpha_{ds2} * \frac{f_{cm}}{f_{cm0}}\right)\right) * 10^{-6} * \beta_{RH}$$

$$\beta_{RH} = 1.55 * (1 - (\frac{RH}{RH_0})^3)$$

With:

- F_{cm} = 28 N/mm^2
- F_{cm0} = 10 N/mm^2
- α_{ds1} = 4
- α_{ds2} =0.12
- RH=70 %
- $RH0$=100 %

Which leads to: $\beta_{RH} = 1.018$ and $\varepsilon_{cd,0} = 0.41 * 10^{-3}$

Factor k_h and β_{ds} both depend on the value of h_0, for which CUR recommendation states that for a steelfibre reinforced concrete floor, the relation h_0=2h can be used, so h_0=1600 mm.

Table 3.3 of EN 1992-1-1 states that k_h=0.7.

$$\beta_{ds} = \frac{(t - t_s)}{(t - t_s) + 0.04\sqrt{h_0^3}}$$

Where t is taken as 100 years (365000 days) and t_s = 28 days, leading to $\beta_{ds} = 0.999956$.

And so $\varepsilon_{cd} = 0.286 * 10^{-3}$ and $\varepsilon_{cs} = 0.31 * 10^{-3}$.

The effect of this concrete shrinkage on floor can be taken into account in two ways, according to CUR 111:

- Load case 1: an equally spread tensile stress resulting from $1.0\varepsilon_{cs}$ leading to a tensile load of $F_{shrinkage}=E_c * k_\varphi * h_{floor} * \varepsilon_{cs}$
- Load case 2: a combination of a tensile force and a bending moment caused by a distribution of the shrinkage strain of 0.9 ε_{cs} at the top of the floor and $0.6\varepsilon_{cs}$ at the bottom of the floor, leading to a tensile force of $F_{shrinkage}=E_c * k_\varphi * h_{floor} * 0.75\varepsilon_{cs}$ and $M_{shrinkage} = E_c * k_\varphi * h_{floor}^2/12 * (0.15\varepsilon_{cs}/h)$.

k_φ is determined to be 0.43 according to the relations in NEN-1992-1-1 which leads to:

Load case 1: $F_{shrinkage}$=964 kN

Load case 2: $F_{shrinkage}$=723 kN and $M_{shrinkage}$=12 kNm.

Thermal load

The temperature in the dock hall can increase to a maximum of temperature of $T_{out,max}$=30 ℃ in summer and a minimum temperature $T_{out,max}$=-25 ℃ in winter according to Table 5.2 of NEN-EN 1991-1-1-5. The temperature at the bottom side of the floor stays constant around T_{in}=10

℃ conform table 5.3. The uniform temperature component of a constructive element follow from equation (5.1) in chapter 5.2 as follows:

$$\Delta T = T - T_0$$

Where T_0 is the initial temperature of the structural element, conform Appendix A, T_0=10 ℃. The change in temperature at either side of the floor during summer and winter is:

$$\Delta T_{top,summer} = T_{out,max} - T_0 = 30 - 10 = 20℃$$

$$\Delta T_{top,winter} = T_{out,min} - T_0 = -25 - 10 = 35℃$$

$$\Delta T_{bottom} = T_{in} - T_0 = 10 - 10 = 0℃$$

Leading to the following profiles over the height of the floor, which is linear according to Appendix D.

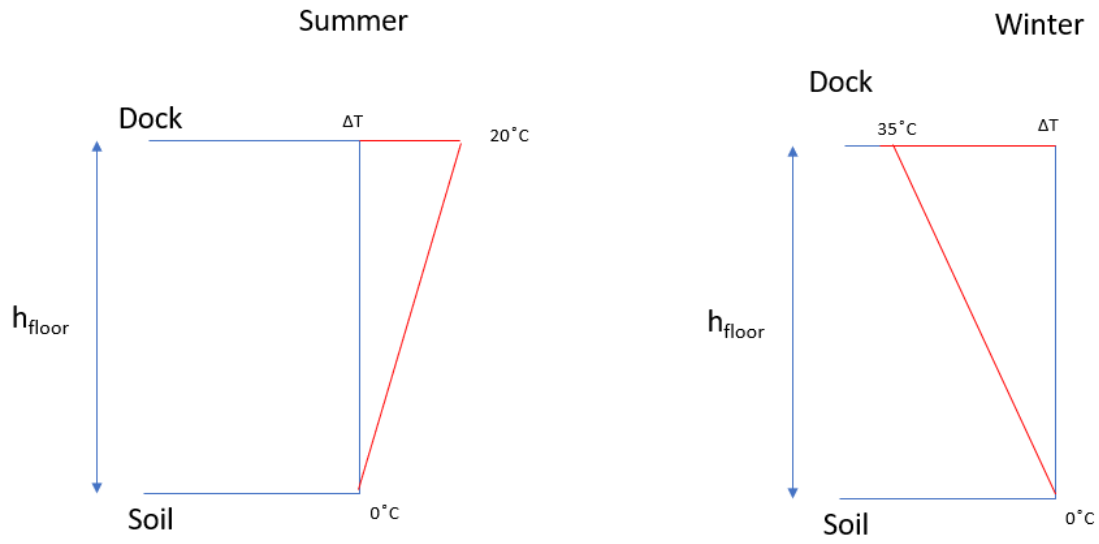

With a thermal expansion coefficient of 10 *10^{-6} / ℃ for reinforced concrete according to Appendix B, the strain in the floor due to the thermal contraction or expansion of the concrete is as follows:

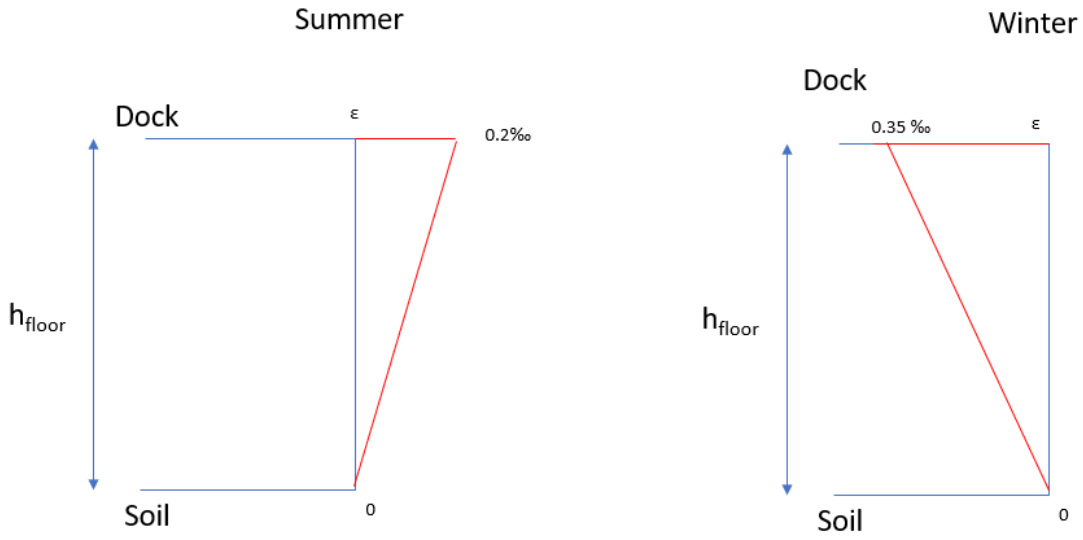

This strain distribution lead to compressive forces in the concrete in summer and a bending moment leading to compression in the top fibre. In winter however, the thermal effects lead to a Tensile force acting on the concrete cross section with the magnitude:

$$F_{thermal} = \frac{1}{2} * b * (\varepsilon * E) * h_{floor}$$

And a bending moment leading to tensile stresses in the top fibre with a magnitude of:

$$M_{thermal} = F_{thermal} * (\frac{h_{floor}}{2} - \frac{h_{floor}}{3})$$

Taking this into account during the design of the floor has lead to significant stresses in the concrete and the requirement regarding no cracks in the top fibre of the concrete can no longer be met. In conclusion: temperature decrease during winter can lead to cracks in the top fibre of the concrete. Actually when the temperature inside the hall is below -6 ℃ for an extended period of time, the concrete tensile stress in the top fibre will exceed the cracking limits. This further substantiates the idea of placing a hall on top of the floor where the temperature can be regulated.

Appendix F: UCF Design calculations

This Appendix contains the calculations behind the design of the UCF variants.

Fatigue

The first check is performed for the reinforcement steel in the UCF, where section 6.8.6 of NEN-EN1992-1-1 norm (NEN, 2005) mentions the following requirement:

(1) Adequate fatigue resistance may be assumed for unwelded reinforcing bars under tension, if the stress range under frequent cyclic load combined with the basic combination is $\Delta\sigma_S \leq k_1$.

Note: The value of k_1 for use in a Country may be found in its National Annex. The recommended value is 70MPa.

This value for $\Delta\sigma_s$ for the UCF can be found to be $\Delta\sigma_s$=42 MPa under an assumed E-modulus for cracked concrete of E=10000 N/mm^2. For the verification of concrete under compression, the following check is performed:

With $\sigma_{c,min}$=0 N/mm^2 and $\sigma_{c,max}$=7.28 N/mm^2, the value for $f_{cd,fat}$ is computed to be:

$$\frac{\sigma_{c,max}}{f_{cd,fat}} \leq 0{,}5 + 0{,}45\frac{\sigma_{c,min}}{f_{cd,fat}} \qquad (6.77)$$

$\leq 0{,}9$ for $f_{ck} \leq 50$ MPa

$\leq 0{,}8$ for $f_{ck} > 50$ MPa

where:

$\sigma_{c,max}$ is the maximum compressive stress at a fibre under the frequent load combination (compression measured positive)

$\sigma_{c,min}$ is the minimum compressive stress at the same fibre where $\sigma_{c,max}$ occurs. If $\sigma_{c,min}$ is a tensile stress, then $\sigma_{c,min}$ should be taken as 0.

$$f_{cd,fat} = 0.85 * f_{cd}\left(1 - \frac{f_{ck}}{250}\right) = 10.4\ N/mm^2$$

Filling this in yields:

$$\frac{\sigma_{c,max}}{f_{cd,fat}} = 0.7 > 0.5$$

And so this requirement is not met and the concrete strength class should be increased to a C30/37. However, the checks described in the norm are more applicable to short duration cycles such as traffic loads over a bridge deck or railways, the design amount of cycles that is prescribed is in the order of 10^6. For the UCF, with an expected lifetime of 100 years and an average of 20 load cycles per year, this amount of cycles is in the order of 2000, so a factor 500 less. The effect of fatigue can therefore also be expected to be less severe, it is assumed that the current concrete strength class C20/25 is sufficient.

Finally, the shear checks that should be performed are as follows (NEN, 2005):

- for $\frac{V_{Ed,min}}{V_{Ed,max}} \geq 0$:

$$\frac{|V_{Ed,max}|}{|V_{Rd,c}|} \leq 0{,}5 + 0{,}45\frac{|V_{Ed,min}|}{|V_{Rd,c}|}\begin{cases} \leq 0{,}9 \text{ up to C50/60} \\ \leq 0{,}8 \text{ greater than C55/67} \end{cases}$$

where:

$V_{Ed,max}$ is the design value of the maximum applied shear force under frequent load combination

$V_{Ed,min}$ is the design value of the minimum applied shear force under frequent load combination in the cross-section where $V_{Ed,max}$ occurs

$V_{Rd,c}$ is the design value for shear-resistance according to Expression (6.2.a).

In our case, these values are:

- $V_{Ed,min}$=188 kN (see figure F1)
- $V_{Ed,max}$=475 kN (see figure F1)

- $V_{Rd,c}$=777 kN (see appendix C)

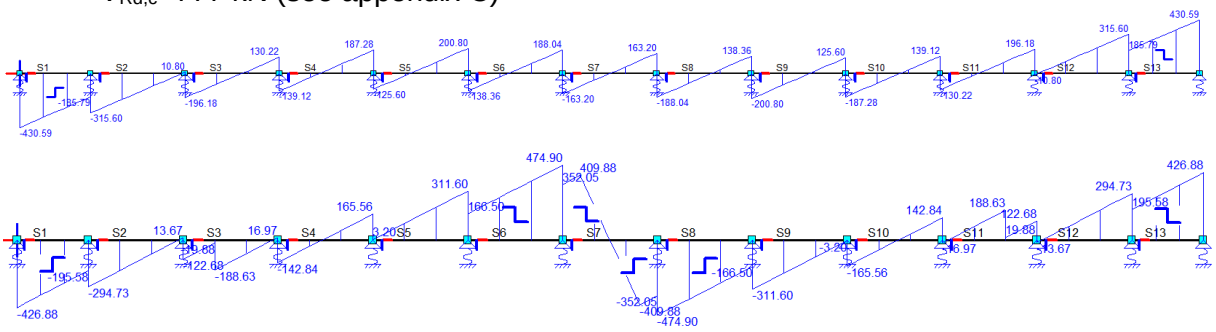

Figure F 1: Shear force diagrams

Filling in the values yields:

$$\frac{V_{Ed,max}}{V_{Rd,c}} = 0.61 \leq 0.5 + \frac{V_{Ed,min}}{V_{Rd,c}}$$

$$0.61 \leq 0.61$$

So this required is (just about) met. Referring back to the conclusion made earlier, since the amount of cycles in the lifetime of the UCF is significantly smaller than those used to perform the checks and so the effect of fatigue for the UCF can be expected to be less severe, the current UCF is concluded to be sufficient resistant against fatigue effects.

The change of direction of the acting load also has influence on the tension piles, as the piles mainly need to be able to absorb compressional forces in case a ship load is present. The maximum tensional force that a pile has to take as been determined to be around 700 kN but under ship loads, this same piles has to take roughly 450 kN of compressional forces. This has been accounted for in the design of the tension piles by inclusion of the factor $\gamma_{m;var;qc}$ which, according to the reader Deep Excavations, accounts for the influence of the variation of the loads. A conservative value of $\gamma_{m;var;qc}$=1.5 is applied while a factor of 1.4 would've been sufficient following the equations in the reader (CIE4363 reader, 2018). All in all it is concluded that the variation of the load direction acting on the tension piles has been sufficiently included in the design of the piles.

UCF Beam model

The spring stiffnesses for the tension piles consist of a few different terms which can be combined using the following equation (CUR-Aanbeveling 77, 2014):

$$\frac{1}{k_{tensionpile}} = \frac{1}{k_{shaft}} + \frac{1}{k_{elastic}} + \frac{1}{k_{undersoil}}$$

Where:

K_{shaft} is the spring stiffness of the shaft friction

$K_{elastic}$ is the elastic extension of the pile

$K_{undersoil}$ is the rise of the soil under the pile tip due to the relief

For anchor piles, the representative value for the spring stiffness of the shaft friction equals:

$$k_{shaft;rep} = 120 * R_{s;cal;max}$$

Where the value for $R_{s;cal;max}$, which is the shaft resistance of the pile calculated in the design of the tension piles, is equal to 721 kN. This means that:

$$k_{shaft;rep} = 120 * 721 = 86520\ kN/m$$

For the determination of the elastic spring stiffness of the pile it is assumed that the grout body as a length of 10 meters so that the part of the pile that is installed in the strong sand layer is fully grouted. The value for $k_{elastic}$ can be calculated as follows:

$$k_{elast} = \frac{EA}{L_1 + \frac{1}{2}(L - L_1)}$$

The modulus of elasticity of the pile is equal to 200 * 10^6 kN/m^2 and with a pile area of 0.00317 m^2, EA amounts to 634*10^3 kN. L_1 is the ungrouted length of the pile, so L_1=14.5 m and L=24.5 m. Filling this in yields:

$$k_{elast} = \frac{634 * 10^6}{14.5 + \frac{1}{2}(10)} = 32500\ kN/m$$

For the determination of $k_{undersoil}$, CUR77 recommends that it of secondary importance compared to the shaft friction resistance and that is can therefore be neglected, meaning that $k_{undersoil}=\infty$

This means that $k_{tensionpile}$=23625 kN/m and after including a factor of variation of $\sqrt{2}$ results in:

$$k_{tensionpile} = 16706 kN/m$$

A similar procedure is followed for the combi-wall, where the shaft friction resistance has been retrieved from the D-sheetpiling calculation and amount to $R_{s,cal,max}$=601 kN. This means that:

$$k_{shaft,wall} = 120 * 601 = 72120 kN/m$$

For the elastic spring stiffness of the combi wall, the coating area of the piles and the sheet pile section combined is found from the D-sheetpiling database and amounts to 1.33 m^2/m. This has to be transformed into a coating area per unit meter width of the wall section and so it is divided by the length of the wall section which is equal 2.68 meters. The area of wall per meter width and per meter height is therefore 0.5 m^2/m/m. The combined section runs from -8 m NAP till -18 m NAP and so L=10 meters. L_1=1 meter, which gives:

$$k_{elast} = \frac{0.5 * 200 * 10^6}{1 + \frac{1}{2} * (9)} = 18181 * 10^3\ kN/m$$

So:

$$\frac{1}{k_{sheetpile}} = \frac{1}{72120} + \frac{1}{18181 * 10^3}$$

Which amounts to $k_{sheetpile}$=71835 kN/m, and including the factor of variation again yields:

$$k_{sheetpile} = 101590\ kN/m$$

SFRUCF – loading phase 2

For determining the cracking moment of the UCF it is assumed that the tensile stress in the top fibre of the concrete is equal to f_{ctm}=2.21 N/mm^2 and the resulting compressive strain in the bottom fibre of the concrete $\varepsilon_{c,bottom}$<1.75 ‰. The corresponding stress and strain diagrams can be seen in Figure F2 below.

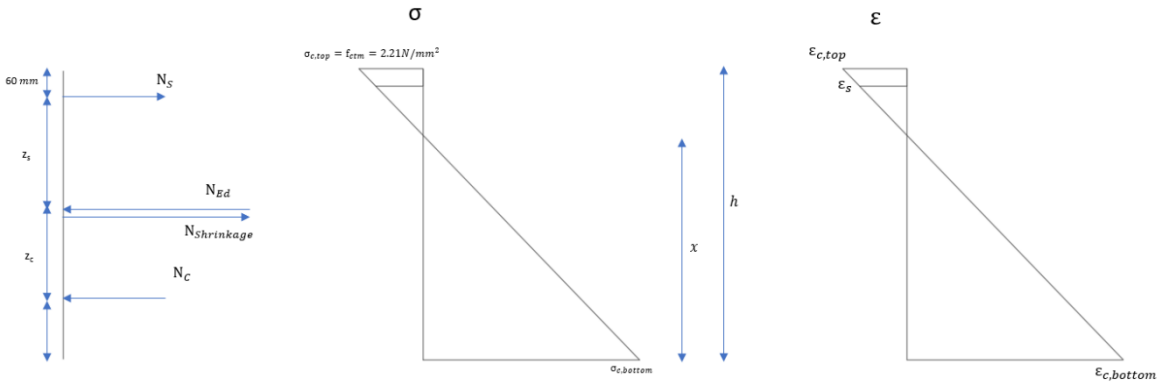

Figure F 2

The E-modulus of the concrete, required for determining the strain distribution of the concrete is:

$$E = \frac{f_{cd}}{\varepsilon_c} = \frac{15.7}{1.75 * 10^{-3}} = 8968\ N/mm^2$$

The height of the compression zone x is determined by an horizontal equilibrium of forces, so:

$$N_s - N_c - N_{Ed} - N_{c,trek} + N_{shrinkage} = 0$$

The separate terms of this equation are:

$$N_c = \frac{\frac{1}{2} b x^2 * \varepsilon_{c,top} * E_c}{h - x}$$

$$N_{c,trek} = \frac{1}{2} * f_{ctm} * (h - x) * b$$

Where b is the unit width of 1000 mm and h is the total height of the cross section, $h=h_{avg}-tol_{under}+ 330$ mm = 980 mm.

$$N_s = A_s \sigma_s = A_s * \frac{h - x - c}{h - x} * \varepsilon_{c,top} * E_s$$

Where c is the concrete cover of 60 mm and E_s=200000 N/mm^2.

$$N_{shrinkage} = \left(0.75 * \varepsilon_{cs} * k_\varphi\right) * E_c * h * b = 814\ kN$$

N_{Ed} = 2213 kN and so the value for x can be found to be 590 mm. Filling this into the equations for N_c and N_s gives:

$N_c = 986\ kN$ and $N_s = 215\ kN$ and the $\varepsilon_{c,bottom}$= 0.4‰ < 1.75 ‰.

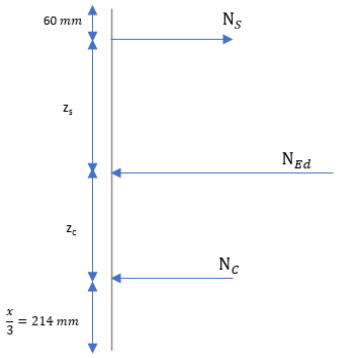

Figure F 3

M_{cr} follows from figure F3, where

$$z_c = \frac{h}{2} - c = 430\ mm$$

$$z_s = \frac{h}{2} - \frac{x}{3} = 293\ mm$$

$$z_{c,trek} = \frac{h}{2} - \frac{h - x}{3} = 360\ mm$$

$$M_{shrinkage} = \frac{(E_c * k_\varphi * h^2)}{12} * \frac{0.15 \varepsilon_{cs}}{h} = 14.18\ kNm$$

$$M_{cr} = N_c * z_c + N_s * z_s + N_{c,trek} * z_{c,trek} - M_{shrinkage} = 522\ kNm$$

The acting bending moments from the upward water pressure q_{rep}=101 kN/m/m' and the moments at the supports can be seen in the M-line below from matrixframe.

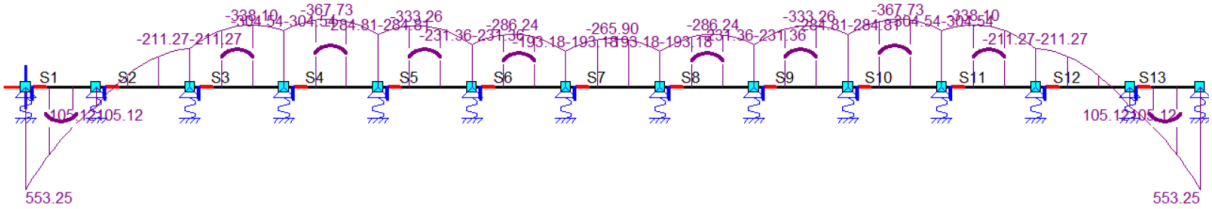

The maximum bending moment is M_{Ed}=368 kNm and since this is smaller than M_{cr}, no cracks are expected to occur, with a u.c. of 0.70.

For the bearing capacity of the concrete, it is assumed that the reinforcement steel yields, meaning that $\varepsilon_s > \varepsilon_{yd}$=2.175‰, on the concrete side, the concrete compression zone has a bi-linear shapes and $\varepsilon_c = \varepsilon_{cu}$=3.5‰, resulting in the following stress and strain diagrams:

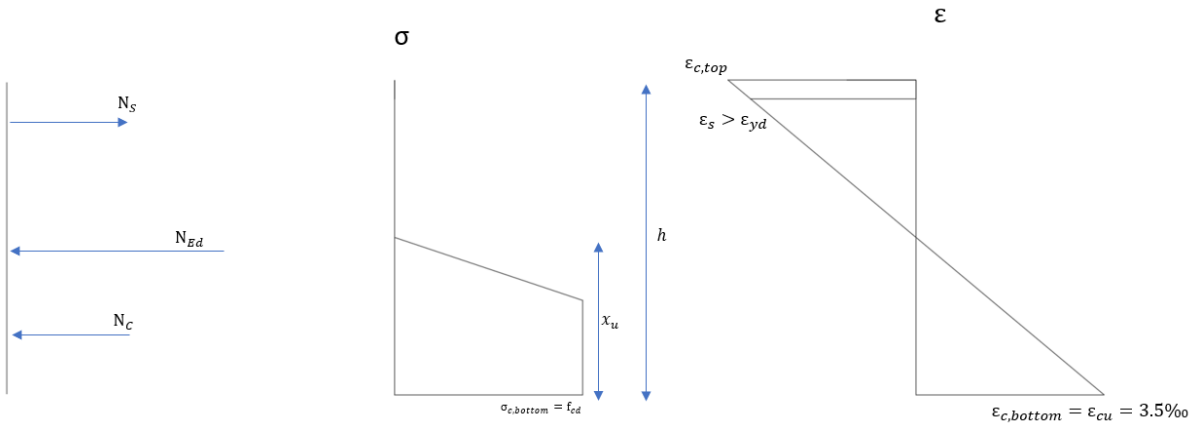

Figure F 4

Again, a horizontal equilibrium of forces leads to the height of the compression zone x_u:

$$N_s - N_c - N_{Ed} + N_{shrinkage} = 0$$

The separate terms of this equation are:

$$N_c = 0.75 * b * {x_u}^2 * f_{cd}$$

Where b is the unit width of 1000 mm and h is the total height of the cross section is 930 mm. The force in the reinforcement steel amounts to:

$$N_s = A_s f_{yd} = A_s * 435 \frac{N}{mm^2} = 2135\ kN$$

N_{Ed} = 2213 kN and so the value for x can be found to be:

$$x_u = \frac{N_s + N_{Ed} - N_{shrinkage}}{0.75 * b * f_{cd}} = 300\ mm$$

Filling this into the equations for N_c:

$N_c = 3533\ kN$, the resulting strain diagram can be used to check the first assumption of the yielding reinforcement steel.

$$\varepsilon_s = \frac{\varepsilon_{cu}}{x_u} * (h - x_u - c) = 7.22\ ‰ > \varepsilon_{yd}$$

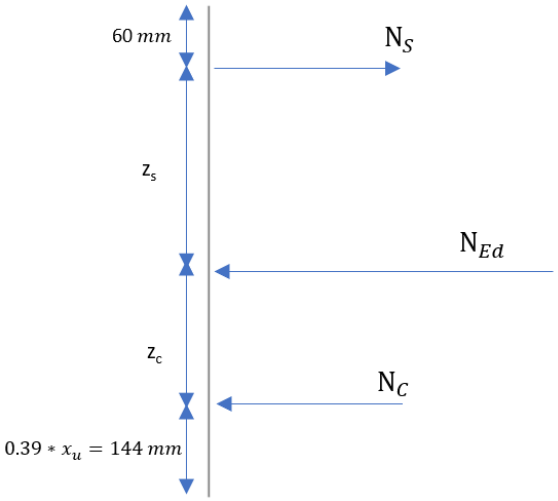

Figure F 5

M_{Rd} follows from figure F5, where

$$z_s = \frac{h}{2} - c = 430\ mm$$

$$z_c = \frac{h}{2} - 0.39x_u = 373\ mm$$

$$M_{Rd} = N_c * z_c + N_s * z_s - M_{shrinkage} = 2222\ kNm$$

The acting bending moments from the upward water pressure q_{Ed}=1.35*101=136 kN/m/m' and the moments at the supports can be seen in the M-line below from matrixframe.

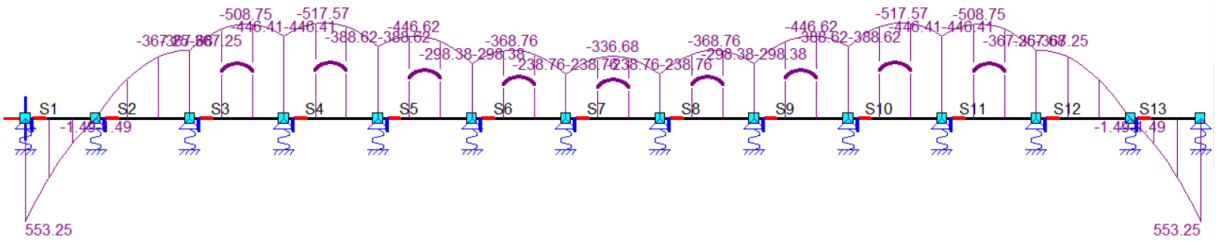

The maximum bending moment is M_{Ed}=518 kNm and since this is smaller than M_{Rd}, the cross section is sufficiently strong with a u.c. of 0.23.

SFRUCF – loading phase 3

SLS checks: The governing bending moment inside the UCF in this loading phase is equal to M_{Ed}=654 kNm as can be seen in the bending moment line below corresponding to a combination of the shipload and the ground water level of +0.00 m NAP since this would lead to the largest bending moment in the bottom fibre of UCF.

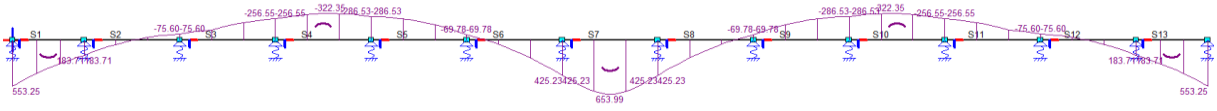

The cracking moment M_{cr} is again found from an equilibrium of forces between the strut force N_{Ed} from the combi-wall and the compressional and tensile forces in the concrete cross section. For determining the cracking moment of the UCF it is assumed that the tensile stress in the bottom fibre of the concrete is equal to f_{ctm}=2.21 N/mm^2 and the resulting compressive strain in the bottom fibre of the concrete $\varepsilon_{c,bottom}$<1.75 ‰. The corresponding stress and strain diagrams can be seen below.

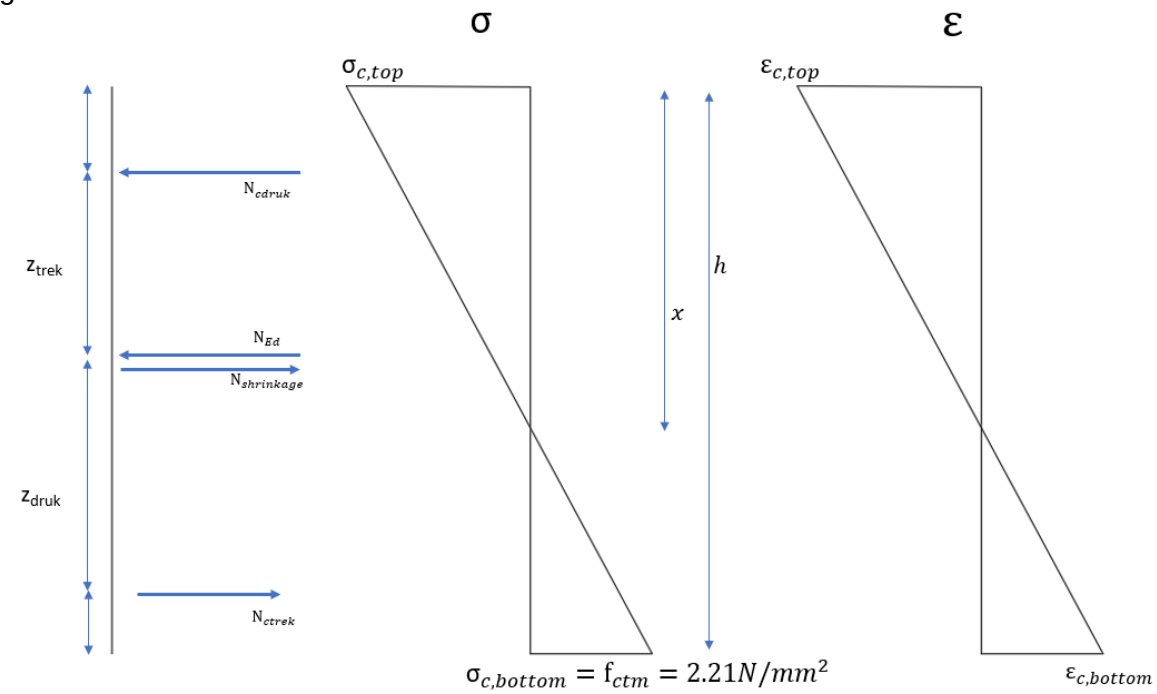

Figure F 6

The E-modulus of the concrete, required for determining the strain distribution of the concrete is:

$$E = \frac{f_{cd}}{\varepsilon_c} = \frac{15.7}{1.75 * 10^{-3}} = 8968\ N/mm^2$$

The height of the compression zone x is determined by an horizontal equilibrium of forces, so:

$$N_{c,t} - N_{c,c} - N_{Ed} + N_{shrinkage} = 0$$

The separate terms of this equation are:

$$N_{c,c} = \frac{\frac{1}{2} b x^2 * \varepsilon_{c,bottom} * E_c}{h - x}$$

Where b is the unit width of 1000 mm and h is the total height of the cross section, h=h_{avg}-tol_{under}+ 330 mm = 980 mm.

$$N_{c,t} = \frac{1}{2} b (h - x) * \varepsilon_{c,bottom} * E_c$$

Where c is the concrete cover of 60 mm and E_s=200000 N/mm^2.

N_{Ed} = 2213 kN, $N_{shrinkage}$=814 kN and so the value for x can be found to be 683 mm. Filling this into the equations for $N_{c,c}$ and Nc,t gives:

$N_{c,c} = 1736\ kN$ and $N_{c,t} = 328\ kN$ and the $\varepsilon_{c,bottom}$= 0.57 < 1.75 ‰.

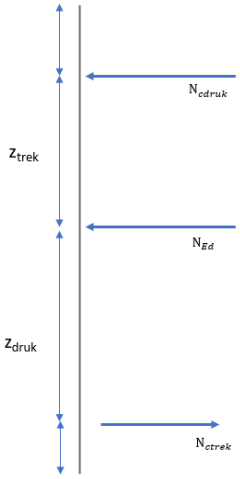

Figure F 7

M_{cr} follows from figure F7, where

$$z_{c,c} = \frac{h}{2} - \frac{x}{3} = 262\ mm$$

$$z_{c,t} = \frac{h}{2} - \frac{h-x}{3} = 391\ mm$$

$$M_{cr} = N_{c,c} * z_{c,c} + N_{c,t} * z_{c,t} + M_{shrinkage} = 597\ kNm$$

M_{Ed}>M_{cr} and so cracks can be expected in the bottom of the floor. After the concrete is cracked, the tensile strength of the steel fibres is activated, the stress distribution in the cross section will include a term of these steel fibre according to CUR 111:

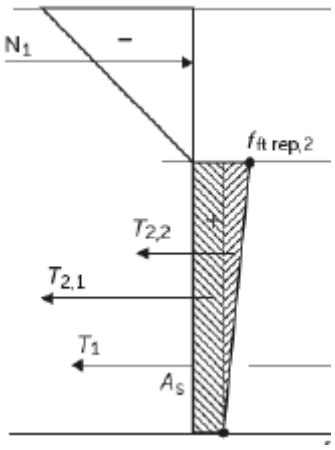

Figure F 8

The magnitude of the contribution of the steel fibre is therefore determined by the value of $f_{ft,rep,2}$ which is determined by performing a 3 point bending test corresponding to the residual strength of the test member at an occurring crack width of 2.5 mm. Test results from a report that reported such 3 point bending tests with a fibre ratio in the test element of 40 kg/m^3, corresponding to roughly 1.5 volume %, is used. Using the results, a ratio between the flexural strength of an uncracked member and f_{R2}, which is the flexural strength of the test member at a 2.5 mm crack width, is determined. Afterwards, a conversion factor is used from the same report to transform f_{R2} into $f_{ft,rep2}$ which will be used in the design of the floor. The first ratio to

determine f_{R2} is done to account for the different concrete strength class between the tests in the report and the C20/25 in the design of the concrete.

The ratio between f_{ctm} and $f_{R,2}$ is found to be roughly 1.6, stemming from a summary of the test results from the report (Rensen, 2013):

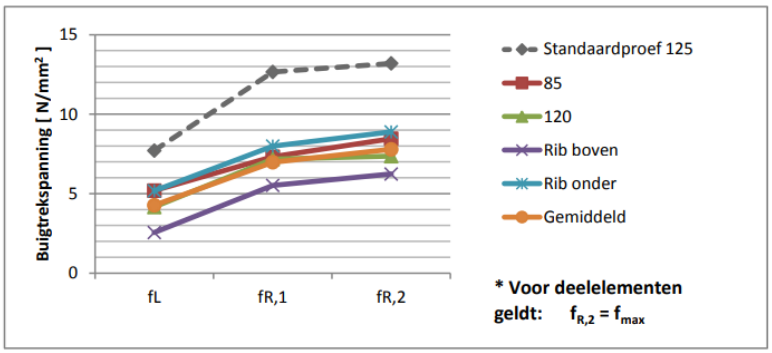

Figuur 6.8: Buigtreksterkte elementen uit casco - Geometrie is van invloed op sterkte

Element	fL	fR,1	fR,2
	[N/mm2]	[N/mm2]	[N/mm2]
85	5,19	7,32	8,46
120	4,16	7,18	7,36
Rib boven	2,56	5,52	6,24
Rib onder	5,18	7,99	8,89
Gemiddeld	4,27	6,98	7,79
Standaardbalkjes	7,71	12,66	13,2

Tabel 6.1: Waarden buigtreksterkte elementen - Gebruikt in verdere berekening

Figure F 9: three point bending test results, source: (Rensen, 2013)

This leads, in our case, to $f_{R,2}$=1.6*2.21 N/mm^2 = 3.61 N/mm^2.

The conversion factor is taken as the conversion factor for CMOD3 which is equal to 0.37.

bepalen treksterktes uiterste vezel:

$$f^{f}_{ct,j} = f_{Rj} * \text{omrekenfactor}$$

	factor
LOP	1,00
$CMOD_1$:	0,45
$CMOD_2$:	-
$CMOD_3$:	0,37
$CMOD_4$:	0,25

Formules (3)

And so the value for $f_{ft,rep}$ that is used in the design of the SFRUCF is equal to $f_{ft,rep}$=0.37 * f_R = 1.34 N/mm^2

The maximum allowable crack width is 0.2 mm and the occurring crack width in the steel-fibre reinforced concrete can be determined by the following equation from CUR 111 (CUR, 2018):

$$w_{max} = 2(h - h_x) * \varepsilon_{ft,max}$$

Where h_x is the height of the compression zone and $\varepsilon_{ft,max}$ is the maximum tensile strain in the SFRUCF.

As previously determined, the acting bending moment is larger than the cracking moment. The height of the compression zone and consequently the tensile strain in the bottom will be altered

by inclusion of the additional bending moment term M_{Ed}-M_{cr} that increases the strain in the top fibre, assuming a cracked E-modulus of 10 GPa, as follows:

$$\varepsilon_{top,cracked} = \varepsilon_{top,uncracked} + \frac{M_{additional}}{W} * \frac{1}{E_{cracked}} = 0.29‰$$

After performing another equilibrium calculation with the use of Maple, the height of the compression zone is found to be 666 mm and so the resulting crack width amounts to:

$$w_{max} = 2(980 - 655) * 0.29‰ = 0.1992 \text{ mm}$$

```
> Ned := 2213000; Nc := 0.5·x·1000·sigmatop; Ns1 := 1.34·1000·(980 − x); Nshrinkage := 814360; Mshrinkage := 14.175·10^6;
                                  Ned := 2213000
                                  Nc := 500.0 x sigmatop
                                  Ns1 := 1.31320000 × 10^6 − 1340.00 x
                                  Nshrinkage := 814360
                                  Mshrinkage := 1.417500000 × 10^7
> hc := (980/2) − (x/3); hs1 := (980/2) − ((980 − x)/2); hs2 := (980/2) − (2·(980 − x)/3)
                                  hc := 490 − x/3
                                  hs1 := x/2
                                  hs2 := −490/3 + 2x/3
> somH := Nc − Ns1 + Nshrinkage − Ned;
                                  somH := 500.0 x sigmatop − 2.71184000 × 10^6 + 1340.00 x
> Mrd := Nc·hc + Ns1·hs1 + Mshrinkage;
                                  Mrd := 500.0 x sigmatop (490 − x/3) + ((1.31320000 × 10^6 − 1340.00 x) x)/2 + 1.417500000 × 10^7
> eq1 := somH = 0;
                                  eq1 := 500.0 x sigmatop − 2.71184000 × 10^6 + 1340.00 x = 0
> eq2 := Mrd = 654·10^6;
                                  eq2 := 500.0 x sigmatop (490 − x/3) + ((1.31320000 × 10^6 − 1340.00 x) x)/2 + 1.417500000 × 10^7 = 654000000
> solve({eq1, eq2}, [x, sigmatop]);
                                  [[x = 655.8990869, sigmatop = 5.589076918], [x = −4703.421475, sigmatop = −3.833135016]]
>
```

Figure F 10

This is an acceptable crack width, since w_{max}<0.2 mm. As far as the watertightness of the floor is concerned, it must be ensured that the crack doesn't pass through the complete height of the floor, in other words, a compressional zone must still be present under these circumstances. Figure F10 proves that this is indeed the case, equilibrium is reached even under cracked conditions, and so the floor is indeed sufficiently watertight for this loading condition.

For the ultimate bearing capacity under ULS conditions, the acting bending moment is retrieved by applying a safety factor of 1.5 on the ship load and 0.9 on the upward water pressure, leading to a governing bending moment of 1111 kNm, as visible on the M-line below:

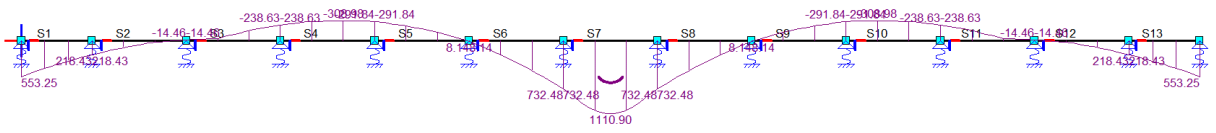

The resisting bending moment results from an equilibrium of forces inside the the concrete floor, including the effect of the steel fibres, as can be seen in the figure below from CUR 111.

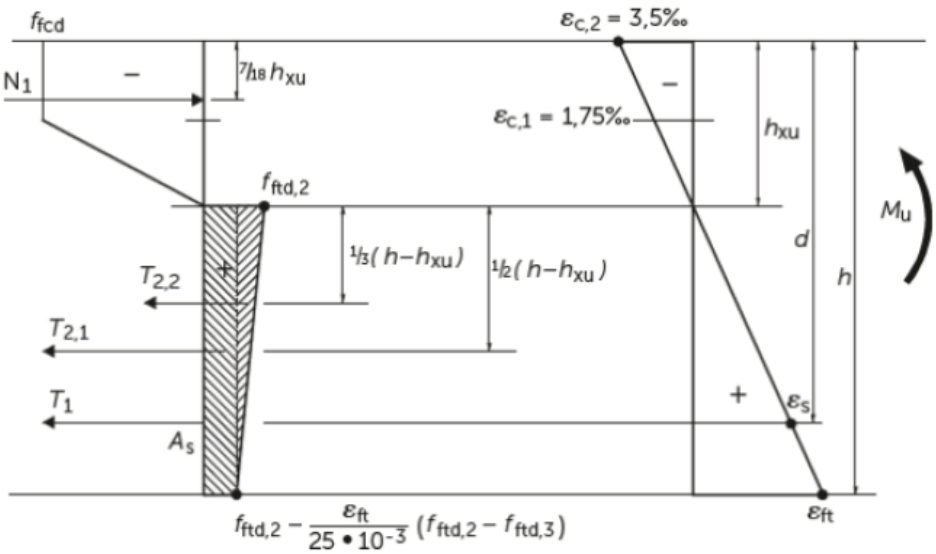

Figure F 11

In our case, the strut force from the combiwalls has to be included and the terms T_1 is not present since there is no traditional reinforcement in the bottom of the floor. The total cross sectional forces and stress and strain diagrams can be seen below: σ ε

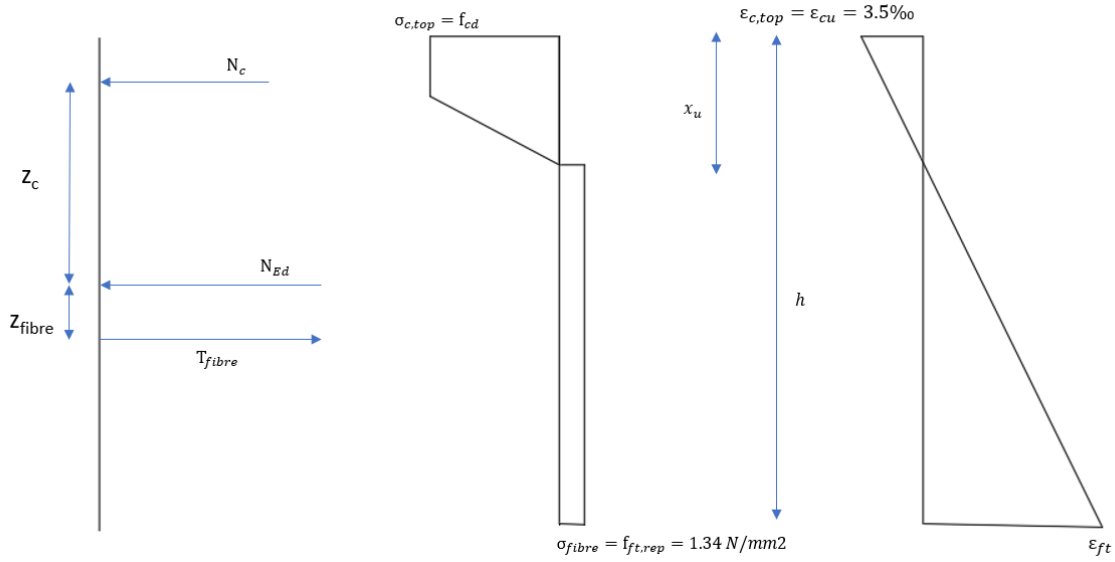

Figure F 12

The height of the compression zone x is determined by an horizontal equilibrium of forces, so:

$$N_c - T_{fibre} - N_{Ed} + N_{Shrinkage} = 0$$

The separate terms of this equation are:

$$N_c = 0.75 * b * {x_u}^2 * f_{cd}$$

Where b is the unit width of 1000 mm and h is the total height of the cross section is 980 mm. The force in the tensile zone amounts to:

$$T_{fibre} = (h - x) * b * 1.34 \frac{N}{mm^2}$$

N_{Ed} = 2213 kN, $N_{shrinkage}$=814 kN and so the value for x can be found to be:

$$x_u = 207\ mm$$

Filling this into the equations for N_c:

$N_c = 2436\ kN$ and $T_{fibre} = 1033\ kN$

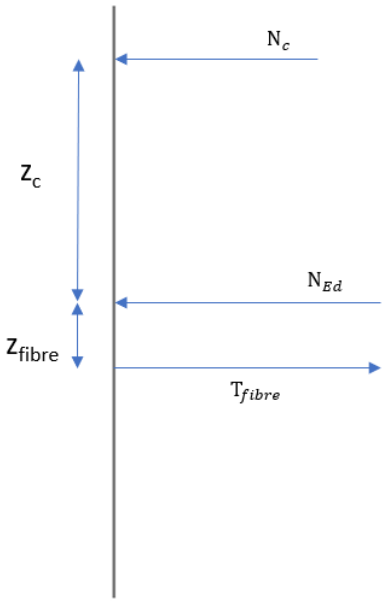

Figure F 13

M_{Rd} follows from figure F13, where

$$z_c = \frac{h}{2} - 0.39x = 409\ mm$$

$$z_{fibre} = \frac{h}{2} - \frac{h - x}{2} = 103.5\ mm$$

$$M_{Rd} = N_c * z_c + T_{fibre} * z_{fibre} + M_{shrinkage} = 1118\ kNm$$

With a narrow unity check of 0.99, this ULS check is found to be governing in the design of the floor.

The shear force V_{Ed} acting on the floor amounts to 475, from the V-line below:

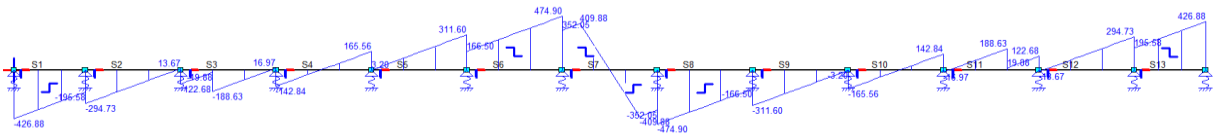

The resisting shear force amounts to 797 kN so this checks is sufficient.

For the deflection, Matrixframe is used which gives an occurring deflection of 5.5 mm. The maximum allowable deflection is L/250, with a c.t.c. distance of 2.4 meters results in u_{max}=9.6 mm, so the deflection check is also sufficient.

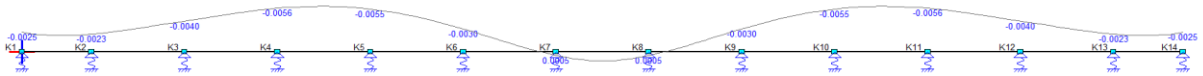

BFRUCF – loading phase 2

For determining the cracking moment of the UCF it is assumed that the tensile stress in the top fibre of the concrete is equal to f_{ctm}=2.21 N/mm^2 and the resulting compressive strain in the bottom fibre of the concrete $\varepsilon_{c,bottom}$<1.75 ‰. The corresponding stress and strain diagrams can be seen below.

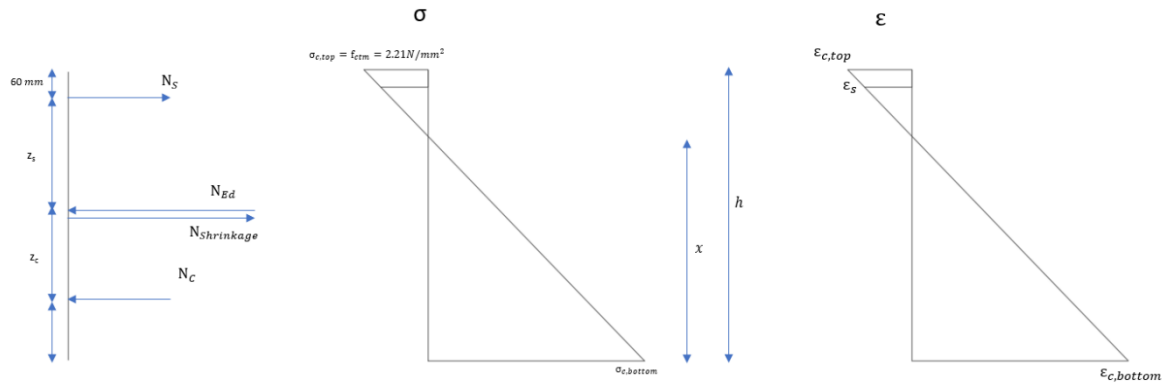

Figure F 14

The E-modulus of the concrete, required for determining the strain distribution of the concrete is:

$$E = \frac{f_{cd}}{\varepsilon_c} = \frac{13.9}{1.75 * 10^{-3}} = 7942\ N/mm^2$$

The height of the compression zone x is determined by an horizontal equilibrium of forces, so:

$$N_s - N_c - N_{Ed} - N_{c,trek} + N_{shrinkage} = 0$$

The separate terms of this equation are:

$$N_c = \frac{\frac{1}{2} b x^2 * \varepsilon_{c,top} * E_c}{h - x}$$

$$N_{c,trek} = \frac{1}{2} * f_{ctm} * (h - x) * b$$

Where b is the unit width of 1000 mm and h is the total height of the cross section, h=h_{avg}-tol_{under}+ 280 mm = 980 mm.

$$N_s = A_s \sigma_s = A_s * \frac{h - x - c}{h - x} * \varepsilon_{c,top} * E_s$$

Where c is the concrete cover of 60 mm and E_s=200000 N/mm^2.

$$N_{shrinkage} = \left(0.75 * \varepsilon_{cs} * k_\varphi\right) * E_c * h * b = 721\ kN$$

N_{Ed} = 2213 kN and so the value for x can be found to be 707 mm. Filling this into the equations for N_c and N_s gives:

$N_c = 2023\ kN$ and $N_s = 224\ kN$ and the $\varepsilon_{c,bottom}$= 0.72‰ < 1.75 ‰.

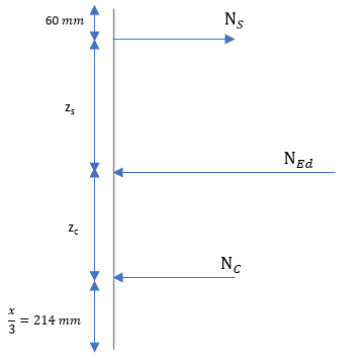

Figure F 15

M_{cr} follows from figure F15, where

$$z_c = \frac{h}{2} - c = 430\ mm$$

$$z_s = \frac{h}{2} - \frac{x}{3} = 254\ mm$$

$$z_{c,trek} = \frac{h}{2} - \frac{h-x}{3} = 399\ mm$$

$$M_{shrinkage} = \frac{(E_c * k_\varphi * h^2)}{12} * \frac{0.15\varepsilon_{cs}}{h} = 12.55$$

$$M_{cr} = N_c * z_c + N_s * z_s + N_{c,trek} * z_{c,trek} - M_{shrinkage} = 719\ kNm$$

The acting bending moments from the upward water pressure q_{rep}=101 kN/m/m' is M_{Ed}=368 kNm and since this is smaller than M_{cr}, no cracks are expected to occur, with a u.c. of 0.51.

For the bearing capacity of the concrete, it is assumed that the reinforcement steel yields, meaning that $\varepsilon_s > \varepsilon_{yd}$=2.175‰, on the concrete side, the concrete compression zone has a bi-linear shapes and $\varepsilon_c = \varepsilon_{cu}$=3.5‰, resulting in the following stress and strain diagrams:

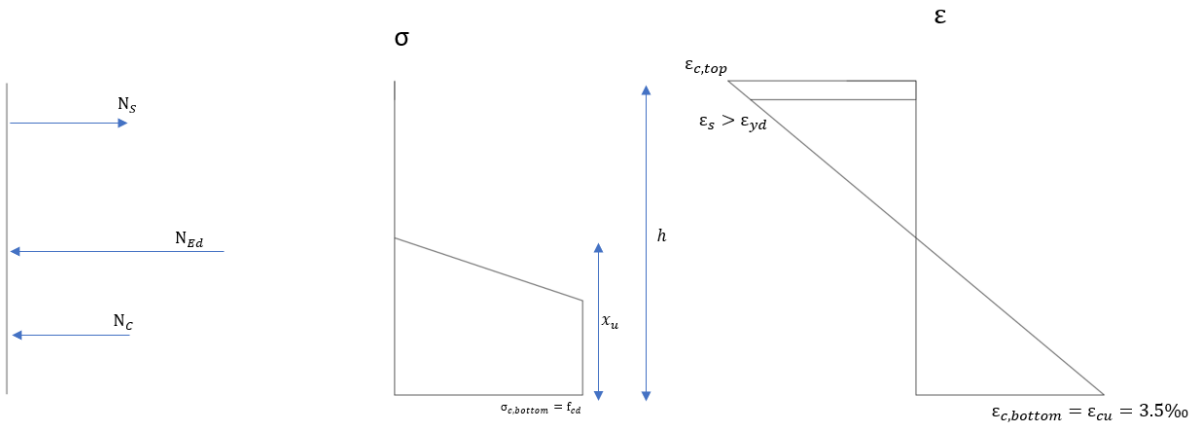

Figure F 16

Again, a horizontal equilibrium of forces leads to the height of the compression zone x_u:

$$N_s - N_c - N_{Ed} + N_{shrinkage} = 0$$

The separate terms of this equation are:

$$N_c = 0.75 * b * {x_u}^2 * f_{cd}$$

Where b is the unit width of 1000 mm and h is the total height of the cross section is 930 mm. The force in the reinforcement steel amounts to:

$$N_s = A_s f_{yd} = A_s * 435 \frac{N}{mm^2} = 2135\ kN$$

N_{Ed} = 2213 kN and so the value for x can be found to be:

$$x_u = \frac{N_s + N_{Ed} - N_{shrinkage}}{0.75 * b * f_{cd}} = 348\ mm$$

Filling this into the equations for N_c:

$$N_c = 3627\ kN$$

The resulting strain diagram can be used to check the first assumption of the yielding reinforcement steel, as is required according to Eurocode norm 1992-1-1 (NEN-EN1992-1-1, 1992):

$$\varepsilon_s = \frac{\varepsilon_{cu}}{x_u} * (h - x_u - c) = 5.75\ ‰ > \varepsilon_{yd}$$

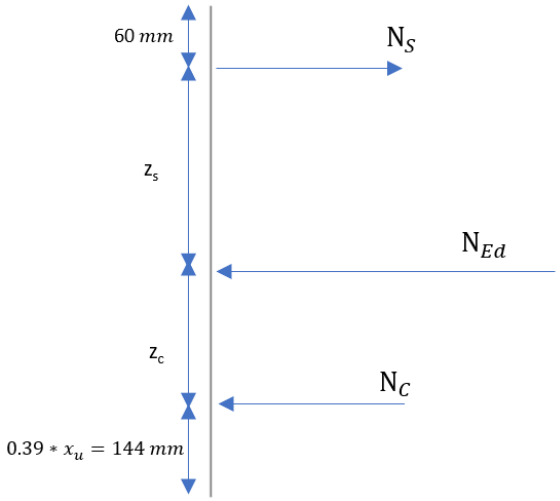

Figure F 17

M_{Rd} follows from figure F17, where

$$z_s = \frac{h}{2} - c = 430\ mm$$

$$z_s = \frac{h}{2} - 0.39 x_u = 3547\ mm$$

$$M_{Rd} = N_c * z_c + N_s * z_s - M_{shrinkage} = 2191\ kNm$$

The acting bending moments from the upward water pressure q_{Ed}=1.35*101=136 kN/m/m' is M_{Ed}=518 kNm and since this is smaller than M_{Rd}, the cross section is sufficiently strong with a u.c. of 0.23 .

BFRUCF – loading phase 3

SLS checks: The governing bending moment inside the UCF in this loading phase is equal to M_{Ed}=654 kNm. The cracking moment M_{cr} is again found from an equilibrium of forces between the strut force N_{Ed} from the combi-wall and the compressional and tensile forces in the concrete cross section. For determining the cracking moment of the UCF it is assumed that the tensile stress in the bottom fibre of the concrete is equal to f_{ctm}=2.21 N/mm^2 and the resulting compressive strain in the bottom fibre of the concrete $\varepsilon_{c,bottom}$<1.75 ‰. The corresponding stress and strain diagrams can be seen below.

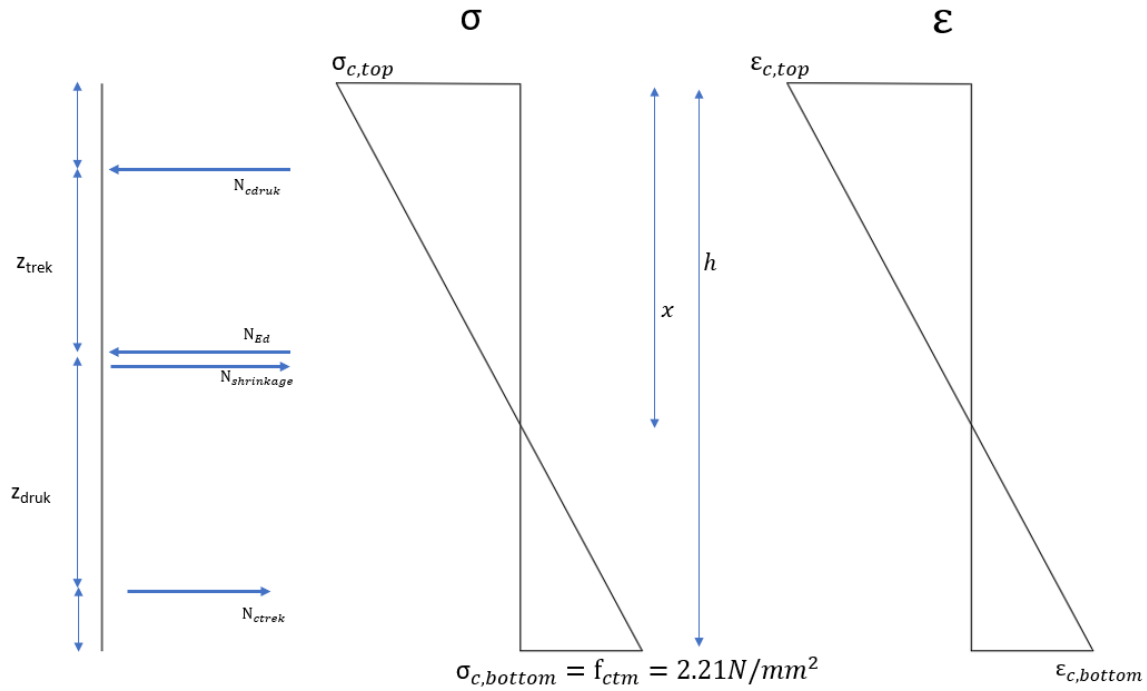

Figure F 18

The height of the compression zone x is determined by an horizontal equilibrium of forces, so:

$$N_{c,t} - N_{c,c} - N_{Ed} + N_{shrinkage} = 0$$

The separate terms of this equation are:

$$N_{c,c} = \frac{\frac{1}{2} b x^2 * \varepsilon_{c,bottom} * E_c}{h - x}$$

Where b is the unit width of 1000 mm and h is the total height of the cross section, h=h_{avg}-tol_{under}+ 280 mm = 980 mm.

$$N_{c,t} = \frac{1}{2} b(h - x) * \varepsilon_{c,bottom} * E_c$$

Where c is the concrete cover of 60 mm and E_s=200000 N/mm^2.

N_{Ed} = 2213 kN, $N_{shrinkage}$=721 kN and so the value for x can be found to be 690 mm. Filling this into the equations for $N_{c,c}$ and Nc,t gives:

$N_{c,c} = 1814\ kN$ and $N_{c,t} = 321\ kN$ and the $\varepsilon_{c,bottom}$= 0.66‰ < 1.75 ‰.

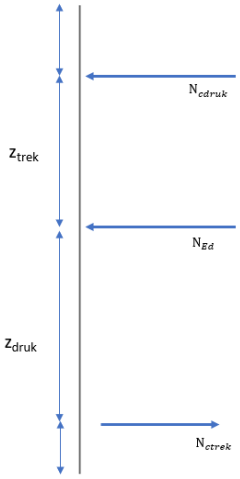

Figure F 19

M_{cr} follows from figure F19, where

$$z_{c,c} = \frac{h}{2} - \frac{x}{3} = 260\ mm$$

$$z_{c,t} = \frac{h}{2} - \frac{h-x}{3} = 393\ mm$$

$$M_{cr} = N_{c,c} * z_{c,c} + N_{c,t} * z_{c,t} + M_{shrinkage} = 610\ kNm$$

M_{Ed}>M_{cr} and so cracks can be expected in the bottom of the floor. After the concrete is cracked, the tensile strength of the steel fibres is activated, the stress distribution in the cross section will include a term of these steel fibre according to CUR 111:

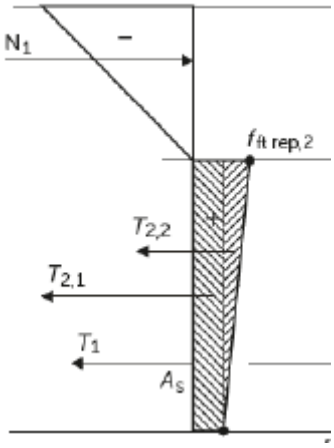

Figure F 20

The magnitude of the contribution of the steel fibre is therefore determined by the value of $f_{ft,rep,2}$ which is determined in the same way as described for the steel fibre variant but now applying the ratios to the strength properties of the basalt fibre reinforced concrete leading to to $f_{R,2}$=1.6*2.21 * (1.226/1.5) = 3.54 N/mm^2. And so the value for $f_{ft,rep}$ that is used in the design of the BFRUCF is equal to $f_{ft,rep}$=0.37 * f_R = 1.31 N/mm^2

The occurring crack width in the steel-fibre reinforced concrete can be determined by the following equation from CUR 111 (CUR, 2018):

$$w_{max} = 2(h - h_x) * \varepsilon_{ft,max}$$

Where h_x is the height of the compression zone and $\varepsilon_{ft,max}$ is the maximum tensile strain in the BFRUCF.

As previously determined, the acting bending moment is larger than the cracking moment. The height of the compression zone and consequently the tensile strain in the bottom will be altered by inclusion of the additional bending moment term M_{Ed}-M_{cr} that increases the strain in the fibre, assuming a cracked E-modulus of 10 GP, as follows:

$$\varepsilon_{bottom,cracked} = \varepsilon_{bottom,uncracked} + \frac{M_{additional}}{W} * \frac{1}{E_{cracked}} = 0.33‰$$

After performing another equilibrium calculation with the use of Maple, the height of the compression zone is found to be 689 mm and so the resulting crack width amounts to:

$w_{max} = 2(980 - 671) * 0.33$=0.204 mm

```
> Ned := 2213000; Nc := 0.5·x·1000·sigmatop; Ns1 := 1.31·1000·(920 − x); Ns2 := (1.31 − 1.31)·0.5·1000·(920 − x);
                                   Ned := 2213000
                                   Nc := 500.0 x sigmatop
                                   Ns1 := 1.20520000 × 10^6 − 1310.00 x
                                   Ns2 := 0.
> hc := (920/2) − (x/3); hs1 := (920/2) − ((920 − x)/2); hs2 := (920/2) − (2·(920 − x)/3);
                                   hc := 460 − x/3
                                   hs1 := x/2
                                   hs2 := −460/3 + 2x/3
> somH := Nc − Ns1 − Ns2 − Ned;
                                   somH := 500.0 x sigmatop − 3.41820000 × 10^6 + 1310.00 x
> Mrd := Nc·hc + Ns1·hs1 + Ns2·hs2;
                                   Mrd := 500.0 x sigmatop (460 − x/3) + (1.20520000 × 10^6 − 1310.00 x) x/2
> eq1 := somH = 0;
                                   eq1 := 500.0 x sigmatop − 3.41820000 × 10^6 + 1310.00 x = 0
> eq2 := Mrd = 683·10^6;
                                   eq2 := 500.0 x sigmatop (460 − x/3) + (1.20520000 × 10^6 − 1310.00 x) x/2 = 683000000
> solve({eq1, eq2}, [x, sigmatop])
                                   [[x = 689.4707009, sigmatop = 7.295432216], [x = −5908.096655, sigmatop = −3.777123927]]
```

Figure F 21

For the ultimate bearing capacity under ULS conditions, the acting bending moment 1111 kNm. The resisting bending moment results from an equilibrium of forces inside the the concrete floor, including the effect of the steel fibres, as can be seen in the figure below from CUR 111.

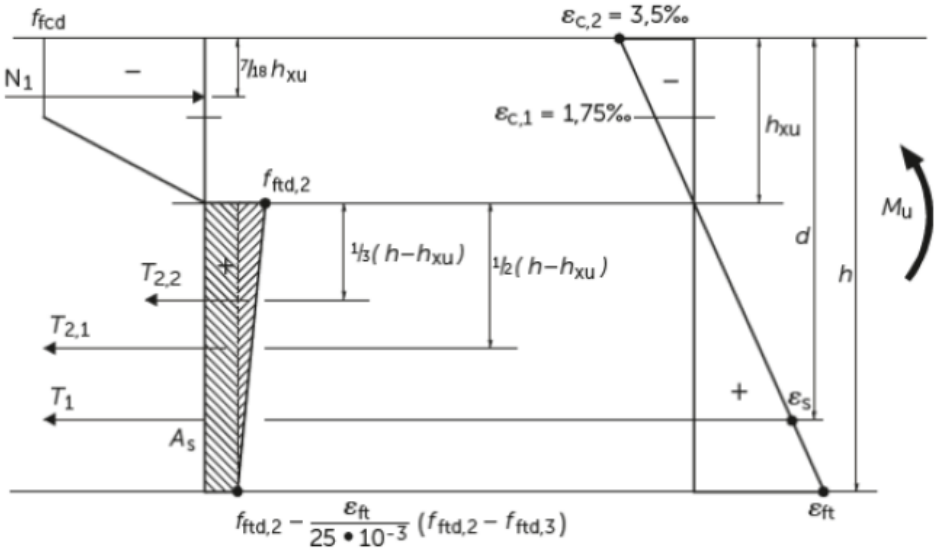

Figure F 22

In our case, the strut force from the combiwalls has to be included and the term T_1 is not present since there is no traditional reinforcement in the bottom of the floor. The total cross sectional forces and stress and strain diagrams can be seen below:

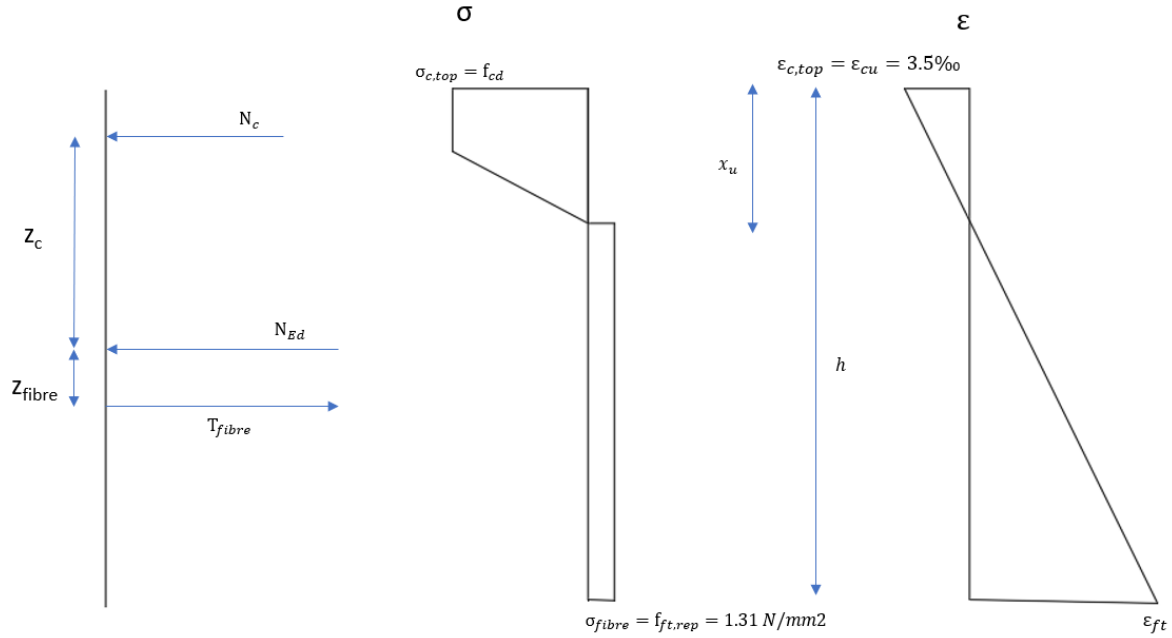

Figure F 23

The height of the compression zone x is determined by an horizontal equilibrium of forces, so:

$$N_c - T_{fibre} - N_{Ed} + N_{Shrinkage} = 0$$

The separate terms of this equation are:

$$N_c = 0.75 * b * {x_u}^2 * f_{cd}$$

Where b is the unit width of 1000 mm and h is the total height of the cross section is 980 mm. The force in the tensile zone amounts to:

$$T_{fibre} = (h - x) * b * 1.31 \frac{N}{mm^2}$$

N_{Ed} = 2213 kN and so the value for x can be found to be:

$$x_u = 238\, mm$$

Filling this into the equations for N_c:

$N_c = 2048\, kN$ and $T_{fibre} = 973\, kN$

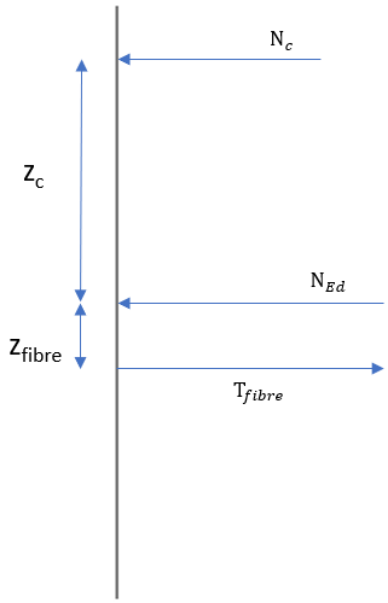

Figure F 24

M_{Rd} follows from figure F24, where

$$z_c = \frac{h}{2} - 0.39x = 397\, mm$$

$$z_{fibre} = \frac{h}{2} - \frac{h - x}{2} = 119\, mm$$

$$M_{Rd} = N_c * z_c + T_{fibre} * z_{fibre} + M_{shrinkage} = 1114\, kNm$$

With a narrow unity check of 0.99, this ULS check is found to be governing in the design of the floor.

The shear force V_{Ed} acting on the floor amounts to 475, from the V-line below:

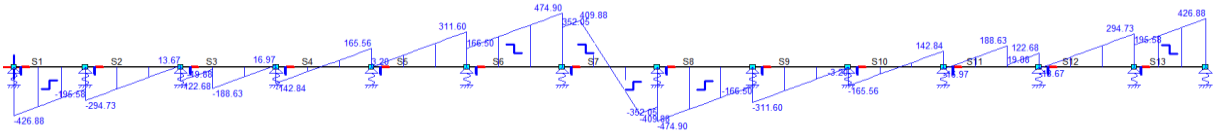

The resisting shear force amounts to 735 kN so this checks is sufficient.

For the deflection, Matrixframe is used which gives an occurring deflection of 5.5 mm. The maximum allowable deflection is L/250, with a c.t.c. distance of 2.4 meters results in u_{max}=9.6 mm, so the deflection check is also sufficient.

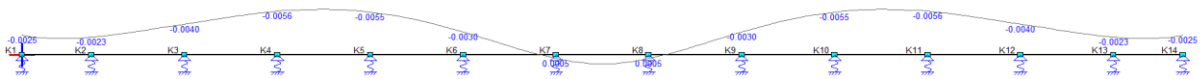

Rebar reinforced – loading phase 2

For determining the cracking moment of the UCF it is assumed that the tensile stress in the top fibre of the concrete is equal to f_{ctm}=2.21 N/mm^2 and the resulting compressive strain in the bottom fibre of the concrete $\varepsilon_{c,bottom}$<1.75 ‰. The corresponding stress and strain diagrams can be seen below.

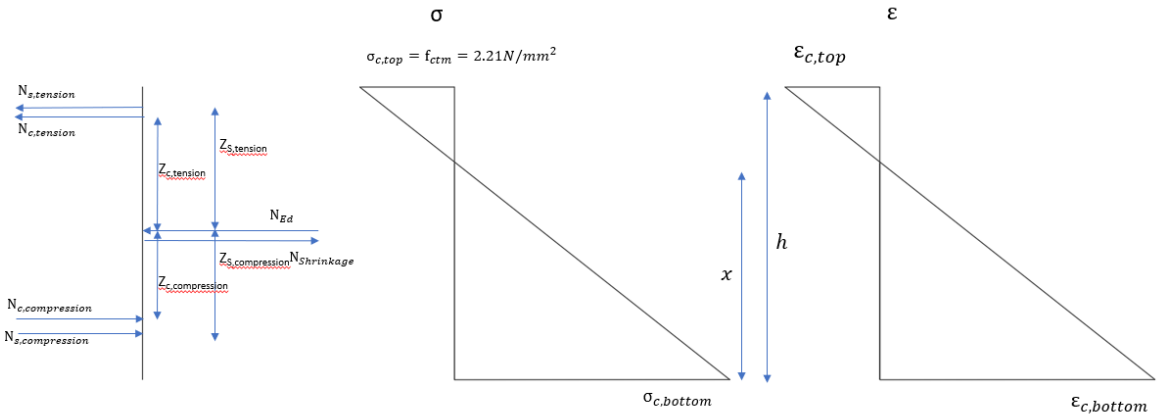

Figure F 25

The E-modulus of the concrete, required for determining the strain distribution of the concrete is:

$$E = \frac{f_{cd}}{\varepsilon_c} = \frac{13.3}{1.75 * 10^{-3}} = 7600\ N/mm^2$$

The height of the compression zone x is determined by an horizontal equilibrium of forces, so:

$$N_{c,compression} + N_{S,compression} - N_{c,tension} - N_{S,tension} - N_{Ed} + N_{Shrinkage} = 0$$

The separate terms of this equation are:

$$N_{c,compression} = \frac{\frac{1}{2} b x^2 * \varepsilon_{c,top} * E_c}{h - x}$$

$$N_{c,tension} = \frac{1}{2} b (h - x) * f_{ctm}$$

Where b is the unit width of 1000 mm and h is the total height of the cross section, h=h_{avg}-tol_{under} = 700 mm.

$$N_{S,compression} = A_{s,bottom} * \frac{x - c}{h - x} * \varepsilon_{c,top} * E_s$$

$$N_{S,tension} = A_{s,top} * \frac{h - x - c}{h - x} * \varepsilon_{c,top} * E_s$$

Where c is the concrete cover of 60 mm and E_s=200000 N/mm^2.

$$N_{Shrinkage} = \left(0.75 * \varepsilon_{cs} * k_{\varphi}\right) * E_c * h * b = 480\ kN$$

N_{Ed} = 2213 kN and so the value for x can be found to be 493 mm. Filling this into the equations the other force terms gives.

$N_{c,compr} = 1419\ kN$ and $N_{s,compression} = 731\ kN$ and the $\varepsilon_{c,bottom}$= 0.75‰ < 1.75 ‰.

$N_{c,tension} = 209\ kN$ and $N_{s,tension} = 204\ kN$

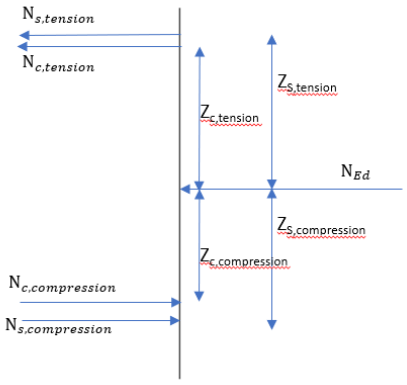

Figure F 26

M_{cr} follows from figure F26, where

$$z_{c,compression} = \frac{h}{2} - \frac{x}{3} = 279\ mm$$

$$z_{s,compression} = \frac{h}{2} - c = 281\ mm$$

$$z_{c,tension} = \frac{h}{2} - \frac{h-x}{3} = 175\ mm$$

$$z_{S,tension} = \frac{h}{2} - c = 281\ mm$$

$$M_{shrinkage} = \frac{(E_c * k_{\varphi} * h^2)}{12} * \frac{0.15\varepsilon_{cs}}{h} = 4.05$$

$$M_{cr} = N_{c,comp} * z_{c,comp} + N_{s,comp} * z_{s,comp} + N_{c,tension} * z_{c,tension} + N_{s,tension} * z_{s,tension} - M_{shrinkage} = 568\ kNm$$

The acting bending moments from the upward water pressure q_{rep}=102.3kN/m/m' and the moments at the supports can be seen in the M-line below from matrixframe.

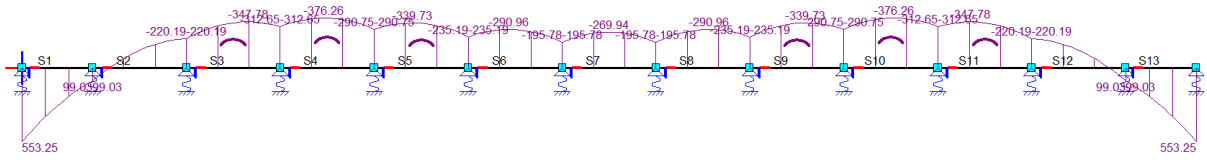

The maximum bending moment is M_{Ed}=377 kNm and since this is smaller than M_{cr}, no cracks are expected to occur, with a u.c. of 0.66.

For the bearing capacity of the concrete, it is assumed that the reinforcement steel yields, meaning that $\varepsilon_{s,top}>\varepsilon_{yd}$=2.175‰, on the concrete side, the concrete compression zone has a bi-linear shapes and $\varepsilon_c=\varepsilon_{cu}$=3.5‰, resulting in the following stress and strain diagrams:

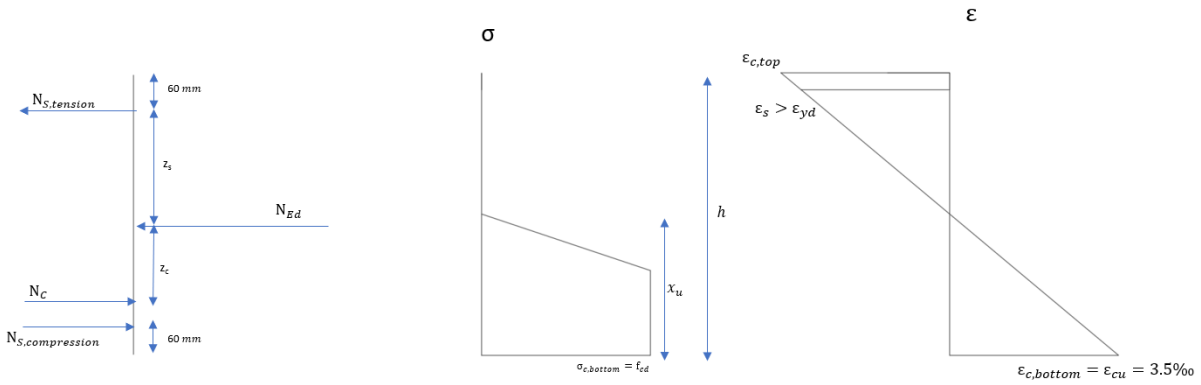

Figure F 27

Again, a horizontal equilibrium of forces leads to the height of the compression zone x_u:

$$N_c + N_{s,compression} - N_{tension} - N_{Ed} + N_{shrinkage} = 0$$

The separate terms of this equation are:

$$N_c = 0.75 * b * {x_u}^2 * f_{cd}$$

Where b is the unit width of 1000 mm and h is the total height of the cross section is 682 mm. The force in the reinforcement steel amounts to:

$$N_{s,tension} = A_{s,top} f_{yd} = A_{s,top} * 435 \frac{N}{mm^2} = 2135\ kN$$

$$N_{s,compr} = A_{s,bottom} f_{yd} = A_{s,compr} * 435 \frac{N}{mm^2} = 2278\ kN$$

N_{Ed} = 2213 kN, $N_{shrinkage}$=481 kN and so the value for x can be found to be:

$$x_u = \frac{N_{s,tension} + N_{Ed} - N_{s,compr} - N_{shrinkage}}{0.75 * b * f_{cd}} = 159\ mm$$

Filling this into the equations for N_c:

$$N_c = 1590\ kN$$

The resulting strain diagram can be used to check the first assumption of the yielding reinforcement steel as is required according to Eurocode norm 1992-1-1 (NEN-EN1992-1-1, 1992):

$$\varepsilon_s = \frac{\varepsilon_{cu}}{x_u} * (h - x_u - c) = 10.16\ ‰ > \varepsilon_{yd}$$

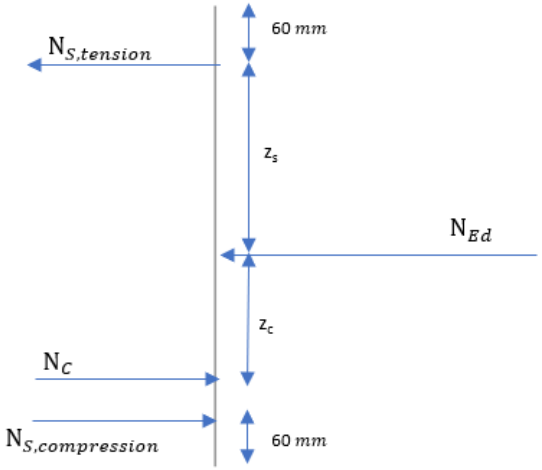

Figure F 28

M_{Rd} follows from figure F28, where

$$z_c = \frac{h}{2} - 0.39x_u = 279\ mm$$

$$z_{s,tension} = z_{s,compr} = \frac{h}{2} - c = 281\ mm$$

$$M_{Rd} = N_c * z_c + N_{s,tension} * z_{s,tension} + N_{s,comp} * z_{s,comp} + M_{shrinkage} = 1680\ kNm$$

The acting bending moments from the upward water pressure q_{Ed}=138 kN/m/m' and the moments at the supports can be seen in the M-line below from matrixframe.

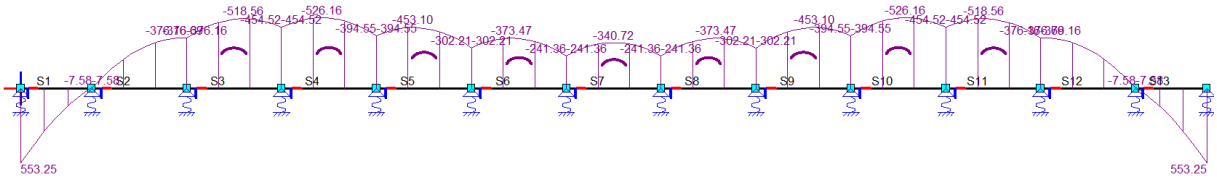

The maximum bending moment is M_{Ed}=527 kNm and since this is smaller than M_{Rd}, the cross section is sufficiently strong with a u.c. of 0.31.

Rebar reinforced – loading phase 3

SLS checks: The governing bending moment inside the UCF in this loading phase is equal to M_{Ed}=660 kNm as can be seen in the bending moment line below corresponding to a combination of the shipload and the ground water level of +0.00 m NAP since this would lead to the largest bending moment in the bottom fibre of UCF.

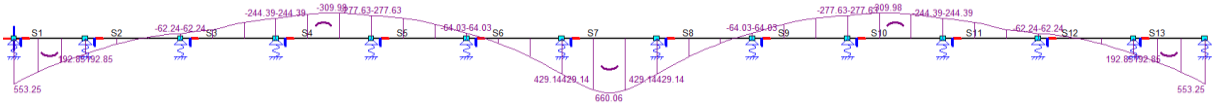

The cracking moment M_{cr} is again found from an equilibrium of forces between the strut force N_{Ed} from the combi-wall and the compressional and tensile forces in the concrete cross section. For determining the cracking moment of the UCF it is assumed that the tensile stress in the bottom fibre of the concrete is equal to f_{ctm}=2.21 N/mm^2 and the resulting compressive strain in the bottom fibre of the concrete $\varepsilon_{c,bottom}$<1.75 ‰. The corresponding stress and strain diagrams can be seen below.

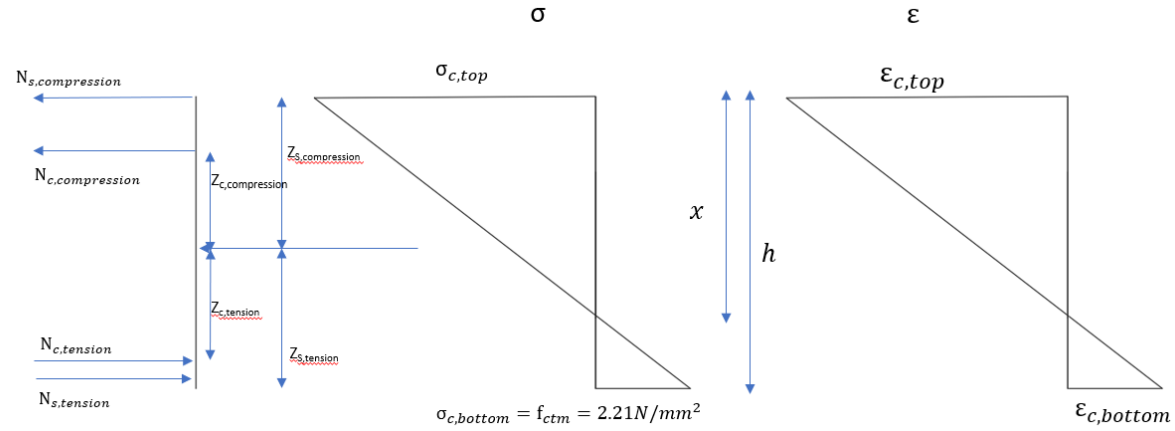

Figure F 29

The horizontal equilibrium of forces:

$$N_{c,compression} + N_{S,compression} - N_{c,tension} - N_{S,tension} - N_{Ed} + N_{shrinkage} = 0$$

The separate terms of this equation are:

$$N_{c,compression} = \frac{\frac{1}{2} b x^2 * \varepsilon_{c,top} * E_c}{h - x}$$

$$N_{c,tension} = \frac{1}{2} b(h - x) * f_{ctm}$$

Where b is the unit width of 1000 mm and h is the total height of the cross section, h=h_{avg}-tol_{under} = 700 mm.

$$N_{S,compression} = A_{s,bottom} * \frac{x - c}{h - x} * \varepsilon_{c,top} * E_s$$

$$N_{S,tension} = A_{s,top} * \frac{h - x - c}{h - x} * \varepsilon_{c,top} * E_s$$

Where c is the concrete cover of 60 mm and E_s=200000 N/mm^2.

N_{Ed} = 2213 kN and so the value for x can be found to be 497 mm. Filling this into the equations the other force terms gives.

$N_{c,compr} = 1473\ kN$ and $N_{s,compression} = 673kN$ and the $\varepsilon_{c,top}$= 0.78‰ < 1.75 ‰.

$N_{c,tension} = 205\ kN$ and $N_{s,tension} = 206kN$

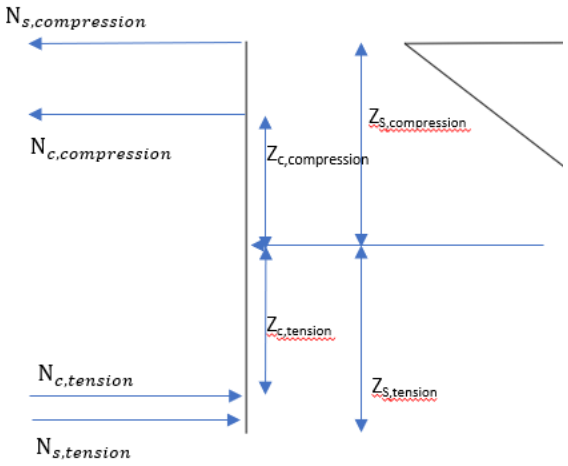

Figure F 30

M_{cr} follows from figure F30, where

$$z_{c,compression} = \frac{h}{2} - \frac{x}{3} = 279\ mm$$

$$z_{s,compression} = \frac{h}{2} - c = 281\ mm$$

$$z_{c,tension} = \frac{h}{2} - \frac{h-x}{3} = 176\ mm$$

$$z_{S,tension} = \frac{h}{2} - c = 281\ mm$$

$$M_{cr} = N_{c,comp} * z_{c,comp} + N_{s,comp} * z_{s,comp} + N_{c,tension} * z_{c,tension} + N_{s,tension} * z_{s,tension} - M_{shrinkage} = 643\ kNm$$

M_{Ed}>M_{cr} and so cracks can be expected in the bottom of the floor.

The maximum allowable crack width is 0.2 mm, following a frequent load combination for XS3 according to Table 7.1N in the NEN-EN 1992-1-1 and the occurring crack width in the reinforced concrete can be determined by the following equation from the same norm (NEN-EN1992-1-1, 1992):

$$w_{\max} = \frac{1}{2}\frac{f_{ctm}}{\tau_{bm}}\frac{\phi}{\rho}\frac{1}{E_s}\left(\sigma_s - \alpha\sigma_{sr} + \beta\varepsilon_{cs}E_s\right)$$

	crack formation stage	stabilized cracking stage
Short term loading	$\alpha = 0{,}5\ (0{,}6)$ $\beta = 0$ $\tau_{bm} = 2{,}0\ f_{ctm}$	$\alpha = 0{,}5(0{,}6)$ $\beta = 0$ $\tau_{bm} = 2{,}0\ f_{ctm}$
long term or dynamic loading	$\alpha = 0{,}5\ (0{,}6)$ $\beta = 0$ $\tau_{bm} = 1{,}6\ f_{ctm}$	$\alpha = 0{,}3\ (0{,}4)$ $\beta = 1$ $\tau_{bm} = 2{,}0\ f_{ctm}$

In our case, we have long term loading under the stabilized cracking stage, meaning that α=0.3 and β=1, $\tau_{bm}=2f_{ctm}$. The effective reinforcement ratio has to be used in this equation, which takes into account the effective tensile zone under bending:

$$h_{c,eff} = \min\left(2{,}5(h-d); \left(\frac{h-x}{3}\right)\right) = 117\ mm$$

$$A_{c,eff} = h_{c,eff} * 1000\ mm = 1.17 * 10^5\ mm^2$$

$$\rho_{eff} = \frac{A_{s,bottom}}{A_{c,eff}} = 0.044$$

Furthermore σ_s is the total steel stress and σ_{sr} is the steel stress at the moment of cracking. In our case,

$$\sigma_s = \frac{M_{Ed}}{A_s * z} = \frac{660 * 10^6 Nmm}{5236\ mm^2 * 456\ mm} = 276\ N/mm^2$$

$$\sigma_{sr} = \frac{M_{cr}}{A_s * z} = \frac{634 * 10^6 Nmm}{5236\ mm^2 * 456\ mm} = 237\ N/mm^2$$

Filling it all in yields:

$$wmax = \frac{1}{4} * \frac{20}{0.045} * \frac{1}{200000} * (276 - 0.3 * 237 - 0.00031 * 200000) = 0.12mm$$

This is an acceptable crack width, since w_{max}<0.2 mm. As far as the watertightness of the floor is concerned, it must me ensured that the crack doesn't pass through the complete height of the floor, in other words, a compressional zone must still be present under these circumstances.

For the ultimate bearing capacity under ULS conditions, the acting bending moment is retrieved by applying a safety factor of 1.5 on the ship load and 0.9 on the upward water pressure, leading to a governing bending moment of 1117 kNm, as visible on the M-line below:

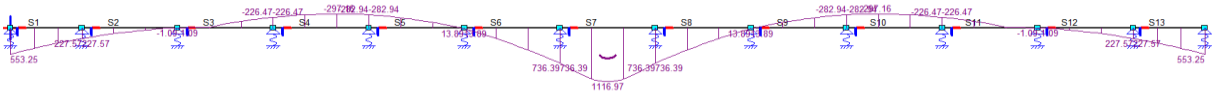

The resisting bending moment results from an equilibrium of forces inside the the concrete floor, including the effect of the steel fibres, as can be seen in the figure below:

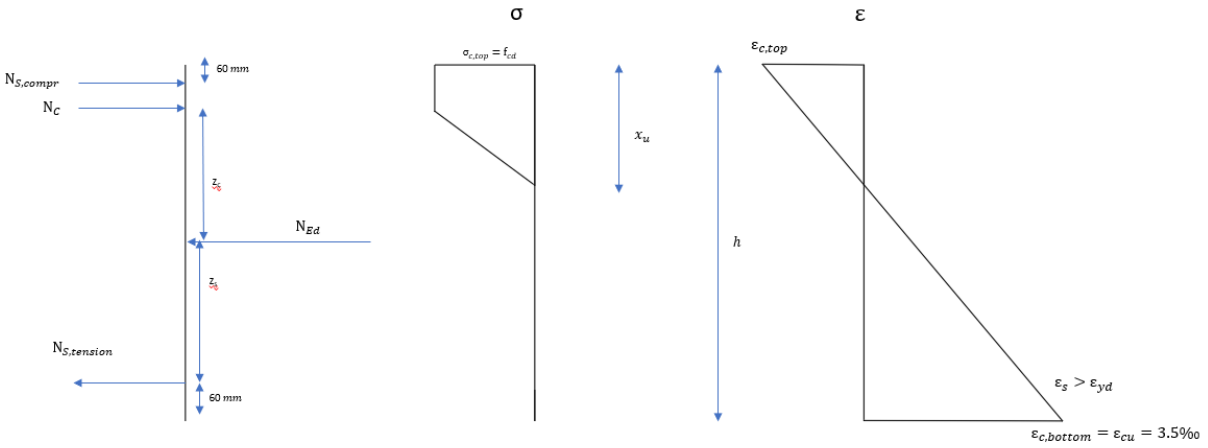

Figure F 31

The height of the compression zone x is determined by an horizontal equilibrium of forces, so:

$$N_c + N_{S,compr} - N_{Ed} - N_{S,tension} + N_{shrinkage} = 0$$

The separate terms of this equation are:

$$N_c = 0.75 * b * {x_u}^2 * f_{cd}$$

Where b is the unit width of 1000 mm and h is the total height of the cross section is 880 mm. The force in the reinforcement steel amounts to:

$$N_{s,compression} = A_{s,top} f_{yd} = A_{s,top} * 435 \frac{N}{mm^2} = 2135\ kN$$

$$N_{s,tension} = A_{s,bottom} f_{yd} = A_{s,compr} * 435 \frac{N}{mm^2} = 2278\ kN$$

N_{Ed} = 2213 kN and so the value for x can be found to be:

$$x_u = \frac{N_{s,tension} + N_{Ed} - N_{s,compr} - N_{shrinkage}}{0.75 * b * f_{cd}} = 188\ mm$$

Filling this into the equations for N_c:

$$N_c = 1875\ kN$$

The resulting strain diagram can be used to check the first assumption of the yielding reinforcement steel, as is required according to Eurocode norm 1992-1-1 (NEN-EN1992-1-1, 1992):

$$\varepsilon_s = \frac{\varepsilon_{cu}}{x_u} * (h - x_u - c) = 8.08\ ‰ > \varepsilon_{yd}$$

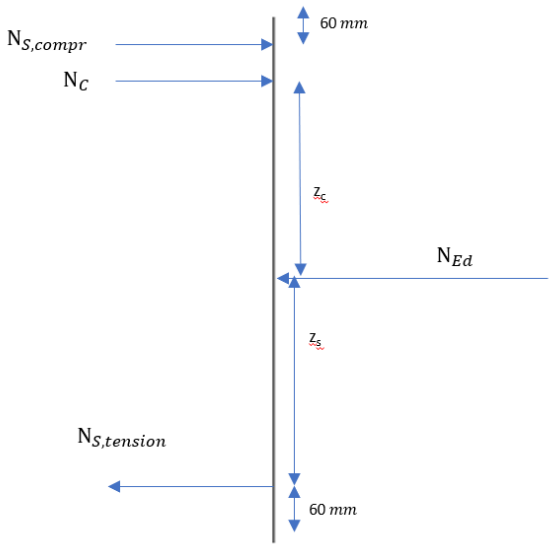

Figure F 32

M_{Rd} follows from figure F32, where

$$z_c = \frac{h}{2} - 0.39x_u = 268\ mm$$

$$z_{s,tension} = z_{s,compr} = \frac{h}{2} - c = 281\ mm$$

$$M_{Rd} = N_c * z_c + N_{s,tension} * z_{s,tension} + N_{s,comp} * z_{s,comp} + M_{shrinkage} = 1747\ kNm$$

The maximum bending moment is M_{Ed}=1117 kNm and since this is smaller than M_{Rd}, the cross section is sufficiently strong with a u.c. of 0.64.

The shear force V_{Ed} acting on the floor amounts to 478kN, from the V-line below:

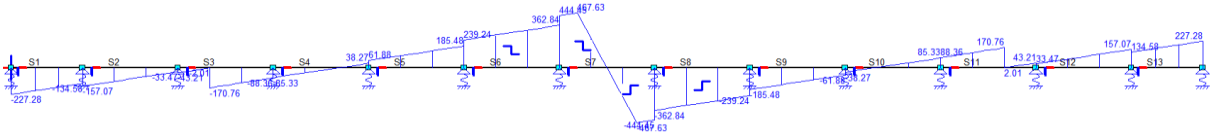

The resisting shear force amounts to 582 kN so this checks is sufficient.

For the deflection, Matrixframe is used which gives an occurring deflection of 5.8 mm. The maximum allowable deflection is L/250, with a c.t.c. distance of 2.4 meters results in u_{max}=9.6 mm, so the deflection check is also sufficient.

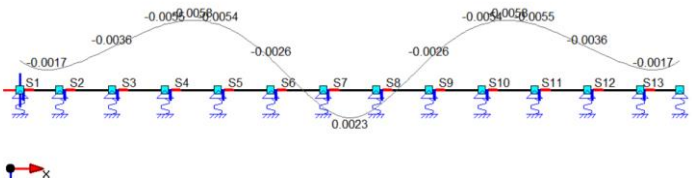

Appendix G: Sediment reduction strategies

This Appendix contains additional information regarding the sediment reduction strategies. n

Inlet short side

The dimensions of the pipeline running from the port into the dock are determined by the required discharge that has to flow through the pipe to prevent the inflow of sediment into the dock chamber. This Q_{req} is determined by the displacement of the vessel and the velocity of the vessel when it leaves the dock. The nett cross sectional area of the design vessel is determined by the following equation:

$$A_{ship} = Draught * Width * C_M$$

Where the draught of the ship is determined for a Ballast-Departure loading condition of 3.5 meters and the C_M is the midship coefficient, retrieved from the Hydrostatical Calculations chapter of the Ship's Stability booklet, for a trim of +0.00 m and a draught of 3.5 meters, C_m=0.997 and Width = 20 meters. While this is the cross sectional area for the midship section and the hull shape becomes slimmer near the fore and the aft of vessel, the results will give the extreme value of the displacement for which the inlet system will be designed. Filling in these values yields:

$$A_{ship} = 3.5 * 20 * .997 = 69.3m^2$$

In order to determine the flow rate entering the dock as the vessel leaves, this nett cross section needs to be multiplied with the velocity of the vessel during undocking. Based on conversation with Damen employees, this velocity is estimated at 0.1 m/s, resulting in a Q_{req}=69.3*0.1=6.93 m^3/s.

The mean velocity of the return current u_r flowing into the dock can now be determined as well, under average docking conditions (water level at +0.00 m NAP):

$$Q_{req} = Q_{in} = A_{dock,nett} * u_r$$

With:

$$A_{dock,nett} = A_{dock} - A_{ship} = (7.5 * 30) - 69.3 = 225\ m^2$$

$$u_r = 0.045\ m/s$$

The flow rate entering the dock through the inlet pipes must at least be equal to Q_{req}. The pipe transferring this flow from the port into the dock consists of coarse concrete pipe with a diameter of 2 meters, that bifurcates into 3 smaller pipes to spread the inflow of water along the short side of the chamber.

With a diameter of D=2 m and thus a cross sectional area of the pipe of A_{pipe}=3.14 m^2, the required flow velocity near the outlet of the pipe is:

$$V_{req} = \frac{Q_{req}}{A_{pipe}} = 2.21\ m/s$$

In terms of velocity head:

$$H_{req} = \frac{V_{req}^2}{2 * g} = 0.25\ m$$

Along the pipelines, a number of head losses will cause the loss of velocity. In order to meet the required head at the entrance, the following equation for the velocity head at the inlet of the pipeline H_{in} needs to be met:

$$H_{req} + \Delta H = H_{in}$$

Where the head loss is a some of all minor and friction losses:

$$\Delta H = \left(\sum K_L\right) * \frac{v_{in}^2}{2 * g}$$

Where $\sum K_L$ consists of losses at the inlet, friction losses over the length of the pipe and a 90 degree bend.

The loss coefficient for a slightly rounded entrance is K_L 0.2 (source hydraulic manual). For a 90 degree bend with a factor R/D=2, where R is the radius of the bend and D is the diameter of the pipe, and a factor ε=0.25 mm for coarse concrete, the loss coefficient is found to be K_L=0.2, source: vano engineering.

The major loss in terms of friction will be determined by using the Darcy-Weisbach equation:

$$\Delta H_f = f \frac{L}{D} \frac{u^2}{2g}$$

Where f is a friction factor, L is the length of the pipe section and D is the diameter of the pipe. The length of the pipe section has an estimated length of 80 meters, as can be seen in Figure G1 below.

Figure G 1

For determining the friction factor *f*, the Moody diagram is used, which also requires the Reynolds number that in turn depends on the flow velocity in the pipe. Iterations have been performed based on a first estimated flow velocity of 10 m/s, which eventually leads to a friction factor of 0.012, for a Re=1.27*10^7 and ε/D = 1.25*10^{-5}.

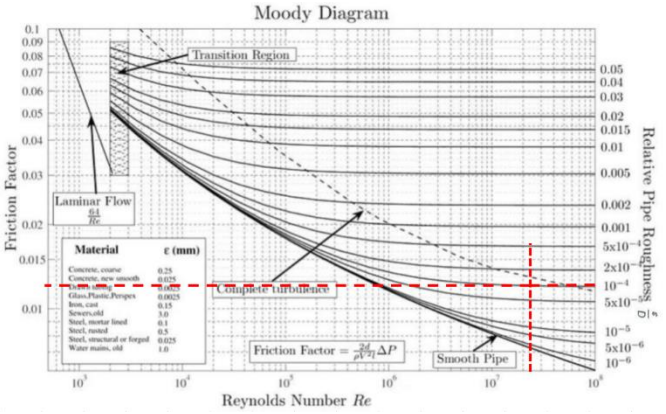

Figure G 2: Moody diagram, source: (Voorendt & Molenaar, 2020)

Resulting in a friction loss coefficient of:

$$K_f = f\frac{L}{D} = 0.012\frac{80}{2} = 0.48$$

The total loss coefficient is a sum of all aforementioned terms:

$$\sum K_L = 0.2 + 0.2 + 0.48 = 0.88$$

Filling this into the Bernoulli equation:

$$H_{req} + \Delta H = H_{in}$$

$$H_{req} + 0.88\frac{u_{in}^2}{2g} = \frac{u_{in}^2}{2g}$$

$$H_{req} = (1 - 0.88)\frac{u_{in}^2}{2g}$$

$$u_{in} = \sqrt{\frac{2gH_{req}}{0.12}} = 6.37\frac{m}{s}\ and\ H_{in} = 2.1\ m$$

Meaning that the chosen pump system needs to have sufficient capacity to add 2.1 m of head to a flow rate of 7 m^3/s. The centreline of the pipe should be installed at a depth of -4 m NAP at the port side and while the calculations have be made for a pipeline that is assumed to be horizontal along its trajectory, it is also possible to apply a certain slope as the pipeline head towards the dock and install the outlet of the pipe at -6 m NAP for example, as this would also decrease the required pump head. A number of gates should be installed near the outlets, for example by applying a 'knife gate valve'.

Appendix H: LCA details

Firstly, the source of information for the Life Cycle Inventory (LCI) is further explained in the following paragraphs.

In the following sub-sections, the emissions factors per relevant lifetime phase are listed in tables.

Material production stage

In Table H1, an overview of all materials extracted, emission factors and data sources are mentioned. Also, the design variant in which the specific material is applied is mentioned.

Table H 1: Material inventory

Materials	Unit	Emission factor	Unit	Source	Design variant
Reinforced concrete	[dm^3]	0.33	kg CO_2-eq / dm^3	EPD	All
Steel piles	[m']	1196	kg CO_2-eq / m'	DuboCalc	All
Sheet pile wall	[m']	554	kg CO_2-eq / m'	DuboCalc	All
Steel	[kg]	0.65	kg CO_2-eq / kg	Idematapp	All
Steel coating	[m^2]	4	kg CO_2-eq / m^2	Idematapp	All
UCF	[m^3]	105	kg CO_2-eq / m^3	DuboCalc	All
Anchors	[# of anchors]	2393	kg CO_2-eq / anchor	DuboCalc	All
Tension piles	[# of piles]	2393	kg CO_2-eq / pile	DuboCalc	All
Sand	[100 kg]	0.24	kg CO_2-eq / 100 kg	Idematapp	Base
Pumps	[# of pumps]	724	kg CO_2-eq / pump	Estimation	All
Concrete pipe	[m']	238	kg CO_2-eq / m'	DuboCalc	A
Steel fibres	[kg]	1.6	kg CO_2-eq / kg	(Kim, Jang, & Kang, 2015)	A
Basalt fibres	[ton]	398	kg CO_2-eq / ton	(Fort, Koci, & Cerny, Environmental Efficiency Aspects of Basalt Fibers Reinforcement in Concrete Mixtures, 2021)	B
Hydro jet	[# of hydrojet]	362	kg CO_2-eq / hydrojet	Estimation	B
Winch	[# of winches]	2111	kg CO_2-eq / winch	Estimation	B , C
Hydraulic motor	[# of motors]	9670	kg CO_2-eq / motor	(Sagström, 2017)	B, C

Since only limited information is available in the DuboCalc database, the emission factors for the steel piles, sheet piles and anchors have been adjusted to better represent the profiles applied in the dock design. For example, DuboCalc has data for the use of steel pile with a diameter of 700 mm and a wall thickness of 12 mm, a factor of 2 is added to this emission factor to represent the larger profile used in our design since more steel is required. The same is done for all other elements for which the data in the DuboCalc library are not exactly matching the design.

For the reinforced concrete the information from an Environmental Product Declaration (EPD), which contains all LCA information for one specific product of one specific distributor, for reinforcement steel is combined with information from the EPD from a ready-mix concrete distributor. While the question arises whether the reinforcement steel will actually be used from this Italian distributor, the information does give an indication. The EPD for the reinforcement steel mentions a total GWP of 587 kg CO_2-eq/ton steel, which equal to 4579 kg CO_2-eq/m^3 steel (Feraldi group, 2011), and for C25/30 ready mix concrete containing CEMII cement the GWP value is 261 kg CO_2-eq/m^3 (Readymix Industries Ltd., 2022). Again, the strength class and cement type might not complete represent the one used in the design and so the accuracy of this data is debatable. However, for this conceptual design it is assumed to be sufficient. Combining this data, together with a 1.5% reinforcement ratio leads to a value of 0.33 kg CO_2-eq/dm^3

The steel coating will be applied to the inner side of the combiwall that is exposed inside the dock chamber, the complete inner side of the dock gate and on the outer side of the dock gate from -2 m NAP till the top of the dock gate. This is because the coating will only be applied to

steel components that are susceptible to corrosion by being in alternating contact with water and air. Steel elements that are continuously in contact with water (the bottom part of the outer side of the dock gate) or in continuous contact with the soil (the outside of the combi wall) will be protected by applying a cathodic protection.
For the pumping unit, the total emissions per pump is determined by taking the emission factor per kg of crude iron steel (2.35 kg CO_2-eq per kg, (IDEMATapp, 2023)) and the process of rolling steel (2.35 kg CO_2-eq per kg, (IDEMATapp, 2023)) multiplied by the weight of a single pump which is estimated to be 225 kg (KSB, 2022) . In this estimation, processes such as painting the steel, manufacturing of the power unit and other aspects are disregarded. The pump of choice is a Amarex KRT K pump which is a centrifugal pump with a maximum capacity of 10000 m^3/h, 2 pumps are chosen for emptying the dock chamber.
The same emission factors for the dock pump are also applied for the inlet pumps (variant A) and the hydro jets (variant B) for simplicity even though the capacity of these pumps can be chosen to be less than the inlet pumps, the weight of these pumps are expected to be of a similar order of magnitude.
For the winches (the dock winches in Variant C and the gate-operating winches in Variant B) the emissions are determined in a similar way as the pumps. The chosen winches are so-called tugger winches with a weight of 650 kg each (Damen Marine Components, 2022). Variant C requires 6 of these in total and Variant B require 2.
The emissions of the hydraulic motor are taken from an LCA that has been performed by Johan Sagström for a hydraulic motor with a capacity of 45 kW and a weight of 1200 kg (Sagström, 2017).

Material transport stage
Table H2 gives a summary of the materials that are required in the design, their place of origin, transport mode, distance and emission factor for the transport mode. The location of the construction site allows for transport over river directly to the site and this has been applied where possible.
Table H 2: Transport inventory

Materials		Place of origin	Transport mode	Distance [km]	Emission Factor	Unit	Design variant
Concrete	Cement	IJmuiden	Barge (river)	120	0.203	kg CO_2-eq/t.10km	All
	Sand	Harlingen	Barge (river)	2	0.203	kg CO_2-eq/t.10km	All
	Gravel	Limburg	Barge (river)	350	0.203	kg CO_2-eq/t.10km	All
	Pipe	Burgum	Barge (river)	45	0.203	kg CO_2-eq/t.10km	A
Steel	Reinforcement steel	Brescia (Italy)	Barge (river)	1200	0.203	kg CO_2-eq/t.10km	All
	Steel piles	Essen (Germany)	Barge (river)	283	0.203	kg CO_2-eq/t.10km	All
	Sheet piles	Essen (Germany)	Barge (river)	283	0.203	kg CO_2-eq/t.10km	All
	Gate	IJmuiden to Heeg	Truck	127	0.078	kg CO_2-eq/t.km	All
		Heeg to Harlingen	Barge (river)	45	0.203	kg CO_2-eq/t.10km	All
	Anchors	Langefeld (Germany)	Barge (river)	319	0.203	kg CO_2-eq/t.10km	All
	Fibre	Neidenstein (Germany)	Barge (river)	623	0.203	kg CO_2-eq/t.10km	A
Basalt Fibre		Sangerhausen (Germany)	Barge (river)	566	0.203	kg CO_2-eq/t.10km	B
Pumps		Winterswijk	Truck	290	0.078	kg CO_2-eq/t.km	All
Hydrojet		Winterswijk	Truck	290	0.078	kg CO_2-eq/t.km	B
Winch		Hardinxveld-Giessendam	Barge (river)	200	0.203	kg CO_2-eq/t.10km	B,C
Hydraulic motor		Hengelo	Barge (river)	180	0.203	kg CO_2-eq/t.10km	B,C

For the materials, their place of origin has been chosen as either the most commonly applied distributor in practice (steel items from the TATA-steel factory in IJmuiden, cement from the ENCI IJmuiden, Gravel from near the Meuse river in Limburg), or by searching for the nearest fabricator of the structural elements. Many of these structural elements such as the combi-wall, anchors and fibres originate from Germany. The LCA data from a EPD from an Italian distributor is used and so the reinforcement steel is assumed to originate from this factory.
The steel that is used for the construction of the gate is first transported from IJmuiden to Heeg, where the gate is made at Nauta Heeg and then transported from Heeg to Harlingen.
The pumps and hydro jets are produced at Pentair Nijhuis Pompen BV in Winterswijk, the winches at Damen Marine Components in Hardinxveld-Giessendam and the hydraulic motor at Holland Hydraulics BV in Hengelo. Finally, the concrete pipe is constructed at LB Betonproducten in Burgum.

Installation stage

Table H3 shows the different installation activities, the equipment required and the fuel/energy consumption of the machinery. In every case, the more climate friendly electrical option is chosen if available.

Table H 3: Installation phase inventory

Activity		**Equipment**	**Productivity**	**Diesel consumption [Litres/hour]**	**Energy consumption [kWh/h]**	**Design variant**
Pile installation	Installation	Hydraulic crane	2 piles per day	-	141	All
		Vibratory Hammer	2 piles per day	48	-	All
	Welding	Welding aggregate	2 piles per day	9		All
Sheet pile wall installation	Installation	Hydraulic crane	7 meters per day		141	All
		Vibratory hammer	7 meters per day	48		All
	Welding	Welding aggregate	2 sections per hour	9		All
Finishing locks	Cleaning	Pressure washer	64 locks per day	0.8		All
		Aerial work platform	64 locks per day		12	All
	Welding	Welding aggregate	2 sections per hour	9		All
		Aerial work platform	2 sections per hour		12	All
Excavation		Cutter suction dredger	7000 m^3/hour	594		All
Anchor/tension pile installation		Installation rig	1 anchor per hour	49		All
		Grout pump	1 anchor per hour	0.8		All
UCF pouring		Concrete pump	100 m^3/hour	15		All
Dewatering	Pumping	Drainage pump	6000 m^3/day	10		All
		Crane vessel		24		All
	Cleaning	High pressure washer	200 m^2/day	0.8		All
		Sediment removal machine	85 m^2/day	24		All
Land filling		Hydraulic crane	1300 m^3/day		141	Base

Placement of structural floor	Placement of reinforcement	Telescopic crane	1500 kg/h		400	All
	Pouring concrete	Concrete pump	100 m^3/hour	15		All
Gate placement		Floating crane	1 unit per day		132	All
Pump placement		Mobile crane	1 unit per day		101	All
Inlet construction	Excavation	Hydraulic crane	1300 m^3/day		141	A
	Pipe placement	Mobile crane	1 unit per day		101	A
	Pump placement	Mobile crane	1 unit per day		101	A
Sliding gate installation	Hydrojet installation	Mobile crane	4 units per day		101	B
	Gate operating system	Mobile crane	2 units per day		101	B
Mitre gate driving system installation		Mobile crane	1 unit per day		101	C
Winch installation		Mobile crane	6 units per day		101	C

The value for the productivity is needed for calculating the total amount of energy consumption for the construction of the dock. For equipment running on fuel, the emission factor for diesel is used for simplicity. In practise, some equipment could potentially also run on more sustainable fuel alternatives such as HVO, but this has been neglected. To estimate the diesel consumption per hour, it is assumed that diesel generators consume around 0.2 litres/kW/hour (Ricardo-Engine, 2019).

Operational phase

Per Variant, an overview of what the operational phase comprises can be found in the tables below.

Table H 4: Operational phase – Base design

Activity		**Equipment**	**Productivity**	**Diesel consumption [Litres/hour]**	**Energy consumption [kWh/h]**	**Note**
Dock emptying		Pumps	3 hours per docking		800	
Sediment removal	Cleaning	High pressure washer	10000 m^2/day	0.8		
		Sediment removal machine	85 m^3/h	24		
	Sediment transport	Truck	270 tons			Transport Harlingen to Middenmeer (60 km)
Tugboats support during docking		Tugboat	2 h/docking activity	94		2 tugboats running at 50% of max capacity

Table H 5: Operational phase – Variant A

Activity	**Equipment**	**Productivity**	**Diesel consumption [Litres/hour]**	**Energy consumption [kWh/h]**	**Note**

Gate operation	Telescopic crane	0.5 hours per docking activity		505	Electric telescopic crane with 450 t capacity
Dock emptying	Pumps	3 hours per docking		800	
Inlet operation	Inlet pumps	1 hour per docking activity		400	
Tugboats support during docking	Tugboat	2 h/docking activity	94		1 tugboat running at 20% of max capacity

Table H 6: Operational phase – Variant B

Activity	**Equipment**	**Productivity**	**Diesel consumption [Litres/hour]**	**Energy consumption [kWh/h]**	**Note**
Gate operation	Hydro jets	0.5 hours per docking activity		27	
	Winches	0.5 hours per docking activity		180	
Dock emptying	Pumps	3 hours per docking		800	
Bubble screen operation	Hydro jets	1 hour per docking activity		27	
Tugboats support during docking	Tugboat	2 h/docking activity	94		1 tugboat running at 20% of max capacity

Table H 7: Operational phase – Variant C

Activity	**Equipment**	**Productivity**	**Diesel consumption [Litres/hour]**	**Energy consumption [kWh/h]**	**Note**
Gate operation	Hydraulic power unit	5 minutes per docking activity	-	50	
Dock emptying	Pumps	3 hours per docking	-	800	
Docking/undocking vessel	Winches	1 hour per docking activity	-	180	

Maintenance stage

Each of the design variants require a regulated maintenance strategy for the pumping unit. It is chosen to perform dock pump inspections every 5 years, where the emissions associated with this are estimated to be 5% of the required estimations to construct, transport and install a new pump unit. The dock pumps unit has an expected lifetime of 25 years and so new pumps need to be installed three times through the lifetime of the dock. Other 'moving' parts of the design variant will need to be regularly inspected and replaced as well, this maintenance strategy can be seen below. The steel elements that need to be coated will be recoated every 20 years.

Table H 8: Maintenance strategy

Activity	**Frequency**	**Variant**
Dock pump inspection	Every 5 years	All
Dock pump replacement	Every 25 years	All
Gate & Combi-wall coating	Every 20 years	All
Inlet pump inspection	Every 5 years	A
Inlet pump replacement	Every 25 years	A
Hydrojet inspection	Every 5 years	B
Hydrojet replacement	Every 25 years	B
Gate driving system inspection	Every 5 years	B
Gate driving system replacement	Every 25 years	B
Hydraulic motor inspection	Every 5 years	C

Hydraulic motor replacement	Every 25 years	C
Winches inspection	Every 5 years	C
Winches replacement	Every 25 years	C

Impact assessments – base design

The calculations to obtain the emissions during construction, operation and maintenance of the dock base variant can now be determined, for the material phase this requires the total amount of each material element and multiplying this by the emission factor. The table below shows an overview, where the final column shows the relative contribution of each design element to the total emissions.

Table H 9:Material phase – Base design

Materials	**Total amount**	**Unit**	**Emission factor**	**Unit**	**Total emissions [ton CO_2-eq]**	**Contribution**
Reinforced concrete	36000000	[dm^3]	0.33	kg CO_2-eq / dm^3	11880	68%
Steel piles	2775	[m']	1196	kg CO_2-eq / m'	33181	18%
Sheet pile wall	174	[m']	554	kg CO_2-eq / m'	96	<1%
Steel	269622	[kg]	0.65	kg CO_2-eq / kg	175	1%
Steel coating	4509	[m^2]	4	kg CO_2-eq / m^2	18	<1%
UCF	4500	[m^3]	105	kg CO_2-eq / m^3	472	3%
Anchors	124	[# of anchors]	2393	kg CO_2-eq / anchor	297	2%
Tension piles	720	[# of piles]	2393	kg CO_2-eq / pile	1723	10%
Sand	36000	[100 kg]	0.24	kg CO_2-eq / 100 kg	8.64	<1%
Pumps	2	[# of pumps]	724	kg CO_2-eq / pump	1.449	<1%
				Total	**17789**	**100%**

The material that contributes most to the total emissions is the reinforced concrete, which is mainly due to the contribution of cement and the fact that a significant amount of this material is required in all of the designs. It makes sense to target this main contributor when trying to decrease the emissions of the design, which is done in the design variants by opting for a different dock floor build-up.

The following step is calculating the amount of emissions associated with transportation of the products from the place of manufacturing to the construction site. The table below shows the total transport emissions for the base design.

Table H 10: Transport phase – Base design

Activity		Equipment	Productivity	Diesel consumption [Litres/hour]	Energy consumption [kWh/h]	Hours	Total diesel consumption [litres]	Total Electricity consumption [kWh]	Total emissions [ton CO_2-eq]	Contribution
Pile installation	Installation	Hydraulic crane	2 piles per day	-	141	500		70500	11.8	6%
		Vibratory Hammer	2 piles per day	48	-	500	24214		39.4	20%
	Welding	Welding aggregate	2 piles per day	9		62.5	561		0.9	<1%
Sheet pile wall installation	Installation	Hydraulic crane	7 meters per day		141	411		58011	9.8	5%
		Vibratory hammer	7 meters per day	48		411	19925		32.4	17%
	Welding	Welding aggregate	2 sections per hour	9		62	557		0.9	<1%
Finishing locks	Cleaning	Pressure washer	64 locks per day	0.8		31	25		0.04	<1%
		Aerial work platform	64 locks per day		12	31		372	0.06	<1%
	Welding	Welding aggregate	2 sections per hour	9		62	557		0.9	<1%
		Aerial work platform	2 sections per hour		12	62		744	0.1	<1%
Excavation		Cutter suction dredger	7000 m^3/hour	594		9	5159		8.4	4%
Anchor/tension pile installation		Installation rig	1 anchor per hour	49		844	41356		67.3	35%
		Grout pump	1 anchor per hour	0.8		844	675		1.1	<1%
UCF pouring		Concrete pump	100 m^3/hour	15		45	662		1.1	1%
Dewatering	Pumping	Drainage pump	6000 m^3/day	10		90	900		1.465	1%
		Crane vessel		24		90	2120		3.50	2%
	Cleaning	High pressure washer	200 m^2/day	0.8		180	144		0.2	<1%
		Sediment removal machine	85 m^2/day	24		53	1249		2	1%
Land filling		Hydraulic crane	1300 m^3/day		141	14		1952	0.3	<1%
Placement of structural floor	Placement of reinforcement	Telescopic crane	1500 kg/h		400	177		70650	11.9	6%
	Pouring concrete	Concrete pump	100 m^3/hour	15		22.5	331		<1%	0%
Gate placement		Floating crane	1 unit per day		132	8		1056	0.2	<1%
Pump placement		Mobile crane	1 unit per day		101	8		807	0.1	<1%
								Total	**194.6**	**100%**

The combination of large volumetric weight and distance make the transport of Gravel from Limburg to Harlingen the predominant factor in the emissions during transportations. In absolute terms, the total emissions during this phase are only a fraction of the material construction phase but when aiming to decrease the transport emissions, reduction in the amount of concrete needed will again be the most effective.

Table H 11: Installation phase – Base design

Materials		Total amount [ton]	Place of origin	Transport mode	Distance [km]	Emission Factor	Unit	Total emissions [ton CO_2-eq]	Contribution
Concrete	Cement	972	IJmuiden	Barge (river)	120	0.203	kg CO_2-eq/t.10km	2.4	3%
	Sand	6300	Harlingen	Barge (river)	2	0.203	kg CO_2-eq/t.10km	0.5	<1%
	Gravel	7155	Limburg	Barge (river)	350	0.203	kg CO_2-eq/t.10km	50.8	69%
Steel	Reinforcement steel	265	Brescia (Italy)	Barge (river)	1200	0.203	kg CO_2-eq/t.10km	6.4	9%
	Steel piles	1026	Essen (Germany)	Barge (river)	283	0.203	kg CO_2-eq/t.10km	5.9	8%
	Sheet piles	323	Essen (Germany)	Barge (river)	283	0.203	kg CO_2-eq/t.10km	1.9	3%
	Gate	270	IJmuiden to Heeg	Truck	127	0.078	kg CO_2-eq/t.km	2.7	4%
		270	Heeg to Harlingen	Barge (river)	45	0.203	kg CO_2-eq/t.10km	0.2	<1%
	Anchors & tension piles	506	Langefeld (Germany)	Barge (river)	319	0.203	kg CO_2-eq/t.10km	3.3	4%
Pumps		0.466	Winterswijk	Truck	290	0.078	kg CO_2-eq/t.km	0.007	<1%
							Total	**74**	**100%**

The main contributors in the installation phase are the installing of the anchors and tension piles and the combi-wall. These elements form the basis of the design of the dock for which optimizations will not be done.

By choosing electrical equipment where possible, 15% of installation emissions can be saved compared to traditional equipment running on diesel.

Table H 12: operational phase – base design

Activity	Frequency	Emissions per activity [ton CO2-eq]	Emissions during lifetime [ton CO2-eq]	Contribution
Dock pump inspection	Every 5 years	0.086	1.6	2%
Dock pump replacement	Every 25 years	1.7	5.2	7%
Gate & Combi-wall coating	Every 20 years	18	72	91%
		Total	**79**	**100%**

The emissions during operations are based on 20 ships entering and leaving the dock on average per year, where emptying the dock requires 3 hours and docking procedures itself require around 1 hour per activity. The table shows the emissions per year, so during a lifetime of 100 years, 5800 tons of CO2-eq are expected, where transport and disposal of the sediment is the main contributing factor. Mitigation measures that aim to prevent the need for cleaning procedures could therefore prove to be effective.

The emissions associated with the maintenance phase can be seen in table H13.

Table H 13: Maintenance phase base design

Activity		Equipment	Productivity	Diesel consumption [Litres/hour]	Energy consumption [kWh/h]	Hours per year	Emissions per year [ton CO_2-eq/year]	Contribution
Dock emptying		Pumps	3 hours per docking		800	60	16.2	23%
Sediment removal	Cleaning	High pressure washer	10000 m^2/day	0.8		72	0.2	<1%
		Sediment removal machine	85 m^3/h	24		53	4.1	6%
	Sediment transport	Truck	270 tons			-	25.2	36%
Tugboats support during docking		Tugboat	2 h/docking activity	94		40	24.4	35%
						Total	**70**	**100%**

The limited amount of mechanical structures and moving parts lead to a small contribution of the maintenance phase of the base design.

Impact assessments – Variant A

The same calculation procedures are now performed for the different design variants, starting with Variant A.

Compared to the base design, this variant consists of less reinforced concrete, UCF concrete but adds the contribution of steel fibres and the construction of the inlet.

Table H 14: Material phase – variant A

Materials	Total amount	Unit	Emission factor	Unit	Total emissions [ton CO_2-eq]	Contribution
Reinforced concrete	14850000	[dm^3]	0.33	kg CO_2-eq / dm^3	4900	42%
Steel piles	2775	[m']	1196	kg CO_2-eq / m'	33181	29%
Sheet pile wall	174	[m']	554	kg CO_2-eq / m'	96	1%
Steel	269622	[kg]	0.65	kg CO_2-eq / kg	175	1%
Steel coating	4509	[m^2]	4	kg CO_2-eq / m^2	18	<1%
UCF	3600	[m^3]	105	kg CO_2-eq / m^3	378	3%
Anchors	124	[# of anchors]	2393	kg CO_2-eq / anchor	297	3%
Tension piles	720	[# of piles]	2393	kg CO_2-eq / pile	1723	15%
Pumps	2	[# of pumps]	724	kg CO_2-eq / pump	1.5	<1%
Steel fibre	423900	[kg]	1.6	kg CO_2-eq / kg	678.2	6%
Concrete pipe	80	[m']	238.2	kg CO_2-eq / m'	19	<1%
Inlet pumps	2	[# of pumps]	724	kg CO_2-eq / pump	1.5	<1%
				Total	**11605**	**100%**

The total amount of emissions is significantly lower than the base design, stemming from the fact that less reinforced concrete is needed which is the predominant factor in this lifecycle phase. The inclusion of the steel fibres and inlet construction are significantly less than the effects from concrete saving floor design.
The emissions during the transport phase of Variant A can be seen in Table H15

Table H 15: Transport phase – variant A

Materials		Total amount [ton]	Place of origin	Transport mode	Distance [km]	Emission Factor	Unit	Total emissions [ton CO_2-eq]	Contribution
Concrete	Cement	732	IJmuiden	Barge (river)	120	0.203	kg CO_2-eq/t.10km	2.4	3%
	Sand	2034	Harlingen	Barge (river)	2	0.203	kg CO_2-eq/t.10km	0.5	<1%
	Gravel	5390	Limburg	Barge (river)	350	0.203	kg CO_2-eq/t.10km	50.8	60%
	Pipe	137	Burgum	Barge (river)	45	0.203	kg CO_2-eq/t.10km	0.1	<1%
Steel	Reinforcement steel	175	Brescia (Italy)	Barge (river)	113	0.203	kg CO_2-eq/t.10km	4.2	7%
	Steel piles	1026	Essen (Germany)	Barge (river)	283	0.203	kg CO_2-eq/t.10km	5.9	9%
	Sheet piles	323	Essen (Germany)	Barge (river)	283	0.203	kg CO_2-eq/t.10km	1.9	3%
	Gate	270	IJmuiden to Heeg	Truck	127	0.078	kg CO_2-eq/t.km	2.7	4%
		270	Heeg to Harlingen	Barge (river)	45	0.203	kg CO_2-eq/t.10km	0.2	<1%
	Anchors & tension piles	506	Langefeld (Germany)	Barge (river)	319	0.203	kg CO_2-eq/t.10km	3.3	5%
	Fibres	424	Neidenstein (Germany)	Barge (river)	623	0.203	kg CO_2-eq/t.10km	5.3	8%
Pumps		0.9	Winterswijk	Truck	290	0.078	kg CO_2-eq/t.km	0.015	<1%
							Total	**64**	**100%**

As expected, the reduction in required amount of gravel leads to a reduction in CO_2-emissions during the transportation phase.
The emissions during the installation phase of Variant A can be seen in table H16.

Table H 16: Installation phase – variant A

Activity		Equipment	Productivity	Diesel consumption [Litres/hour]	Energy consumption [kWh/h]	Hours	Total diesel consumption [litres]	Total Electricity consumption [kWh]	Total emissions [ton CO_2-eq]	Contribution
Pile installation	Installation	Hydraulic crane	2 piles per day	-	141	500	-	70500	11.8	6%
		Vibratory Hammer	2 piles per day	48	-	500	24214	-	39.4	21%
	Welding	Welding aggregate	2 piles per day	9	-	62.5	561	-	0.9	<1%
Sheet pile wall installation	Installation	Hydraulic crane	7 meters per day	-	141	411	-	58011	9.8	5%
		Vibratory hammer	7 meters per day	48	-	411	19925	-	32.4	17%
	Welding	Welding aggregate	2 sections per hour	9	-	62	557	-	0.9	<1%

Finishing locks	Cleaning	Pressure washer	64 locks per day	0.8	-	31	25	-	0.04	<1%
		Aerial work platform	64 locks per day	-	12	31	-	372	0.06	<1%
	Welding	Welding aggregate	2 sections per hour	9	-	62	557	-	0.9	<1%
		Aerial work platform	2 sections per hour	-	12	62	-	744	0.1	<1%
Excavation		Cutter suction dredger	7000 m^3/hour	594	-	9	5159	-	8.4	4%
Anchor/tension pile installation		Installation rig	1 anchor per hour	49	-	844	41356	-	67.3	35%
		Grout pump	1 anchor per hour	0.8	-	844	675	-	1.1	<1%
UCF pouring		Concrete pump	100 m^3/hour	15	-	36	662	-	0.8	1%
Dewatering	Pumping	Drainage pump	6000 m^3/day	10	-	90	900	-	1.465	<1%
		Crane vessel		24	-	90	2120	-	3.50	<1%
	Cleaning	High pressure washer	200 m^2/day	0.8	-	180	144	-	0.2	1%
		Sediment removal machine	85 m^2/day	24	-	53	1249	-	2	2%
Placement of structural floor	Placement of reinforcement	Telescopic crane	1500 kg/h	-	400	117	-	70650	7.9	<1%
	Pouring concrete	Concrete pump	100 m^3/hour	15	-	14.9	331	-	0.3	1%
Gate placement		Floating crane	1 unit per day	-	132	8	-	1056	0.2	0%
Pump placement		Mobile crane	1 unit per day	-	101	8	-	807	0.1	0%
	Excavation	Hydraulic crane	1300 m^3/day	-	141	6	-	833	0.1	<1%
	Pipe placement	Mobile crane		-	101	40	-	4040	0.7	<1%
	Pump placement	Mobile crane	1 unit per day	-	101	8	-	808	0.1	<1%
								Total	**191**	**100%**

No major reductions can be found in this phase, the quantities of elements that make up the base of the dock chamber structure are unchanged.

The emissions during the operational phase of Variant A can be seen in Table H17.

Table H 17: Operational phase – variant A

Activity	Equipment	Productivity	Diesel consumption [Litres/hour]	Energy consumption [kWh/h]	Hours per year	Emissions per year [ton CO_2-eq/year]	Contribution
Gate operation	Telescopic crane	0.25 hours per docking	-	505	20	0.85	3%
Dock emptying	Pumps	3 hours per docking	-	800	60	16.2	66%
Inlet operation	Pumps/gate	1 hour per docking	-	400	72	2.7	11%
Tugboats support during docking	Tugboat	2 h/docking activity	94	-	40	4.8	20%
					Total	**25**	**100%**

As expected, the emissions during operational phase are significantly reduced by the prevention of sediment cleaning and disposal activities.

The emissions during the maintenance phase of Variant A can be seen in Table H18

Table H 18: Maintenance phase – variant A

Activity	Frequency	Emissions per activity [ton CO2-eq]	Emissions during lifetime [ton CO2-eq]	Contribution
Dock pump inspection	Every 5 years	0.086	1.6	2%
Dock pump replacement	Every 25 years	1.7	5.1	6%
Inlet pump inspection	Every 5 years	0.086	1.6	2%
Inlet pump replacement	Every 25 years	1.7	5.1	6%
Gate & Combi-wall coating	Every 20 years	18	72	84%
		Total	**86**	**100%**

Presence of more pumps will naturally ask for more maintenance of the design, but the total increase in emissions is relatively small.

Impact assessments – Variant B

Compared to the base design, this variant consists of less reinforced concrete and underwater concrete but adds the contribution of basalt fibres and the construction of bubble screen and gate operating system. The calculations for the materials phase can be seen in Table H19.

Table H 19: Materials phase – variant B

Materials	Total amount	Unit	Emission factor	Unit	Total emissions [ton CO_2-eq]	Contribution

Reinforced concrete	12600000	[dm^3]	0.33	kg CO_2-eq / dm^3	4158	41%
Steel piles	2775	[m']	1196	kg CO_2-eq / m'	33181	32%
Sheet pile wall	174	[m']	554	kg CO_2-eq / m'	96	1%
Steel	269622	[kg]	0.65	kg CO_2-eq / kg	175	2%
Steel coating	4509	[m^2]	4	kg CO_2-eq / m^2	18	<1%
UCF	3825	[m^3]	105	kg CO_2-eq / m^3	401	4%
Anchors	124	[# of anchors]	2393	kg CO_2-eq / anchor	297	3%
Tension piles	720	[# of piles]	2393	kg CO_2-eq / pile	1723	17%
Pumps	2	[# of pumps]	724	kg CO_2-eq / pump	1.5	<1%
Basalt fibre	123	[ton]	398	kg CO_2-eq / ton	49	<1%
Hydrojet	4	[# of hydrojets]	724	kg CO_2-eq / 2 hydrojet	1.5	<1%
Gate operating system	2	[# of winches]	2111	kg CO_2-eq / winch	4.2	<1%
	2	[# of hydromotor]	9670	kg CO_2-eq / motor	19	<1%
				Total	**10262**	**100%**

The total amount of emissions is significantly lower than the base design, stemming from the fact that less reinforced concrete is needed which is the predominant factor in this lifecycle phase. The inclusion of the basalt fibres and hydro jet construction are significantly less than the effects from the concrete saving floor design. Compared to Variant A, the presence of basalt fibres as opposed to steel fibre leads to a reduction in total emissions.

The emissions during the transport phase of Variant B can be seen in Table H20.

Table H 20: Transport phase – Variant B

Materials		**Total amount [ton]**	**Place of origin**	**Transport mode**	**Distance [km]**	**Emission Factor**	**Unit**	**Total emissions [ton CO_2-eq]**	**Contribution**
Concrete	Cement	732	IJmuiden	Barge (river)	120	0.203	kg CO_2-eq/t.10km	1.8	3%
	Sand	2034	Harlingen	Barge (river)	2	0.203	kg CO_2-eq/t.10km	0.08	<1%
	Gravel	5390	Limburg	Barge (river)	350	0.203	kg CO_2-eq/t.10km	38.3	65%
Steel	Reinforcement steel	148	Brescia (Italy)	Barge (river)	1200	0.203	kg CO_2-eq/t.10km	3.6	6%
	Steel piles	1026	Essen (Germany)	Barge (river)	283	0.203	kg CO_2-eq/t.10km	5.9	10%
	Sheet piles	323	Essen (Germany)	Barge (river)	283	0.203	kg CO_2-eq/t.10km	1.9	3%
	Gate	270	IJmuiden to Heeg	Truck	127	0.078	kg CO_2-eq/t.km	2.7	5%
		270	Heeg to Harlingen	Barge (river)	45	0.203	kg CO_2-eq/t.10km	0.2	<1%
	Anchors & tension piles	506	Langefeld (Germany)	Barge (river)	319	0.203	kg CO_2-eq/t.10km	3.3	6%
Basalt	Fibres	123	Sangerhausen (Germany)	Barge (river)	566			1.4	3%
Pumps		0.5	Winterswijk	Truck	200	0.078	kg CO_2-eq/t.km	0.007	<1%
Hydrojet		0.5	Winterswijk	Truck	200	0.078	kg CO_2-eq/t.km	0.007	<1%
Gate operation system	Hydraulic motor	2.5	Hengelo	Barge (river)	180	0.203	kg CO_2-eq/t.10km	0.046	<1%
	Winches	1.3	Hardinxveld-Giessendam	Barge (river)	200	0.203	kg CO_2-eq/t.10km	0.005	<1%
							Total	**59**	**100%**

Again, the reduction in emissions can be allocated to the reduction of gravel transport.

The emissions during the installing phase of Variant B can be seen in Table H21

Table H 21: Installation phase – variant B

Activity		**Equipment**	**Productivity**	**Diesel consumption [Litres/hour]**	**Energy consumption [kWh/h]**	**Hours**	**Total diesel consumption [litres]**	**Total Electricity consumption [kWh]**	**Total emissions [ton CO_2-eq]**	**Contribution**
Pile installation	Installation	Hydraulic crane	2 piles per day	-	141	500	-	70500	11.8	6%
		Vibratory Hammer	2 piles per day	48	-	500	24214	-	39.4	21%
	Welding	Welding aggregate	2 piles per day	9	-	62.5	561	-	0.9	<1%
	Installation	Hydraulic crane	7 meters per day	-	141	411	-	58011	9.8	5%

Sheet pile wall installation		Vibratory hammer	7 meters per day	48	-	411	19925	-	32.4	17%
	Welding	Welding aggregate	2 sections per hour	9	-	62	557	-	0.9	<1%
Finishing locks	Cleaning	Pressure washer	64 locks per day	0.8	-	31	25	-	0.04	<1%
		Aerial work platform	64 locks per day	-	12	31	-	372	0.06	<1%
	Welding	Welding aggregate	2 sections per hour	9	-	62	557	-	0.9	<1%
		Aerial work platform	2 sections per hour	-	12	62	-	744	0.1	<1%
Excavation		Cutter suction dredger	7000 m^3/hour	594	-	9	5227	-	8.5	5%
Anchor/tension pile installation		Installation rig	1 anchor per hour	49	-	844	41356	-	67.3	35%
		Grout pump	1 anchor per hour	0.8	-	844	675	-	1.1	<1%
UCF pouring		Concrete pump	100 m^3/hour	15	-	38.25	563	-	0.9	<1%
Dewatering	Pumping	Drainage pump	6000 m^3/day	10	-	90	900	-	1.465	1%
		Crane vessel		24	-	90	2120	-	3.5	2%
	Cleaning	High pressure washer	200 m^2/day	0.8	-	180	144	-	0.2	<1%
		Sediment removal machine	85 m^2/day	24	-	53	1249	-	2	1%
Placement of structural floor	Placement of reinforcement	Telescopic crane	1500 kg/h	-	400	99	-	39564	6.7	4%
	Pouring concrete	Concrete pump	100 m^3/hour	15	-	12.6	185	-	0.3	<1%
Gate placement	Hydrojet placement	Mobile crane	4 unit per day	-	101	8	-	808	0.1	<1%
	Gate operation system	Mobile crane	2 unit per day	-	101	8	-	404	0.1	<1%
	Gate installation	Floating crane	1 unit per day	-	132	8	-	1056	0.2	<1%
Pump placement		Mobile crane	1 unit per day	-	101	8	-	808	0.1	<1%
								Total	**189**	**100%**

No major reductions can be found in this phase.
The emissions during the operational phase of Variant B can be seen in Table H22

Table H 22: Operational phase – variant B

Activity	**Equipment**	**Productivity**	**Diesel consumption [Litres/hour]**	**Energy consumption [kWh/h]**	**Hours per year**	**Emissions per year [ton CO_2-eq/year]**	**Contribution**
Gate operation	Hydrojets	0.5 hours per docking	-	27	20	0.2	1%
	Winches	0.5 hours per docking		180		1.2	5%
Dock emptying	Pumps	3 hours per docking	-	800	60	16.2	71%
Bubble screen	Hydrojets	1 hour per docking	-	27	40	0.4	2%
Tugboats support during docking	Tugboat	2 h/docking activity	94	-	40	4.8	21%
					Total	**23**	**100%**

The fact that that the hydro jets seem to have an efficient energy consumption compared to the inlet pumps in Variant A leads to a reduction in emissions compared to the other variants.
Maintenance
The emissions during the maintenance phase of Variant B can be seen in Table H23

Table H 23: Maintenance phase – variant B

Activity	**Frequency**	**Emissions per activity [ton CO2-eq]**	**Emissions during lifetime [ton CO2-eq]**	**Contribution**
Dock pump inspection	Every 5 years	0.072	1.4	1%
Dock pump replacement	Every 25 years	1.7	5.1	3%
Hydrojet inspection	Every 5 years	0.086	1.7	1%
Hydrojet replacement	Every 25 years	1.7	5.2	3%
Hydraulic motor inspection	Every 5 years	1	18.5	10%
Hydraulic motor replacement	Every 25 years	19.5	59	33%
Gate driving system inspection	Every 5 years	0.2	4.1	2%
Gate driving system replacement	Every 25 years	4.4	13.1	7%
Gate & Combi-wall coating	Every 20 years	18	72.1	40%
		Total	**180**	**100%**

Maintenance emissions of this Variant are significantly larger than Variant A, due to the presence of more electrical/mechanical elements that require maintenance throughout the lifetime of the dock.

Impact assessments – Variant C

Compared to the base design, this variant consists of a little less reinforced concrete and no underwater concrete but it adds the contribution of the 6 winches and the gate operation system. The total emissions for this phase can be found in table H24

Table H 24: Material phase – Variant C

Materials	Total amount	Unit	Emission factor	Unit	Total emissions [ton CO_2-eq]	Contribution
Reinforced concrete	38250000	[dm^3]	0.33	kg CO_2-eq / dm^3	12622	69%
Steel piles	2775	[m']	1196	kg CO_2-eq / m'	33181	18%
Sheet pile wall	174	[m']	554	kg CO_2-eq / m'	96	<1%
Steel	269622	[kg]	0.65	kg CO_2-eq / kg	175	1%
Steel coating	4509	[m^2]	4	kg CO_2-eq / m^2	18	<1%
Anchors	124	[# of anchors]	2393	kg CO_2-eq / anchor	297	2%
Tension piles	720	[# of piles]	2393	kg CO_2-eq / pile	1723	9%
Pumps	2	[# of pumps]	724	kg CO_2-eq / pump	1.5	<1%
WInches	6	[# of winches]	2111	kg CO_2-eq / winch	12.7	<1%
Hydraulic motor	2	[# of units]	9670	kg CO_2-eq / motor	19.4	<1%
				Total	**18283**	**100%**

The emissions for this phase are less than the base designs, since the required amount of reinforced concrete is less. However, the design requires a thicker layer of reinforced concrete due to the absence of the UCF layer and therefore the total amount of CO_2 emissions are significantly larger for Variant C than for the other two design Variants.

The emissions during the transport phase of Variant C can be seen in Table H25

Table H 25: Transport phase – Variant C

Materials		Total amount [ton]	Place of origin	Transport mode	Distance [km]	Emission Factor	Unit	Total emissions [ton CO_2-eq]	Contribution
Concrete	Cement	551	IJmuiden	Barge (river)	120	0.203	kg CO_2-eq/t.10km	1.3	2%
	Sand	1530	Harlingen	Barge (river)	2	0.203	kg CO_2-eq/t.10km	0.06	<1%
	Gravel	4055	Limburg	Barge (river)	350	0.203	kg CO_2-eq/t.10km	28.8	52%
Steel	Reinforcement steel	450	Brescia (Italy)	Barge (river)	1200	0.203	kg CO_2-eq/t.10km	11	20%
	Steel piles	1026	Essen (Germany)	Barge (river)	283	0.203	kg CO_2-eq/t.10km	5.9	11%
	Sheet piles	323	Essen (Germany)	Barge (river)	283	0.203	kg CO_2-eq/t.10km	1.9	3%
	Gate	270	IJmuiden to Heeg	Truck	127	0.078	kg CO_2-eq/t.km	2.7	5%
		270	Heeg to Harlingen	Barge (river)	45	0.203	kg CO_2-eq/t.10km	0.2	1%
	Anchors & tension piles	506	Langefeld (Germany)	Barge (river)	319	0.203	kg CO_2-eq/t.10km	3.3	6%
Pumps		0.5	Winterswijk	Truck	200	0.078	kg CO_2-eq/t.km	0.007	<1%
Gate operation system	Hydraulic motor	2.5	Hengelo	Barge (river)	180	0.203	kg CO_2-eq/t.10km	0.046	<1%
Winches		3.9	Hardinxveld-Giessendam	Barge (river)	200	0.203	kg CO_2-eq/t.10km	0.015	<1%
							Total	**55**	**100%**

The emissions during the installation phase of Variant C can be seen in Table H26

Table H 26: Installation phase – Variant C

Activity		Equipment	Productivity	Diesel consumption [Litres/hour]	Energy consumption [kWh/h]	Hours required	Total diesel consumption [litres]	Total Electricity consumption [kWh]	Total emissions [ton CO_2-eq]	Contribution
Pile installation	Installation	Hydraulic crane	2 piles per day	-	141	500	-	70500	11.8	6%
		Vibratory Hammer	2 piles per day	48	-	500	24214	-	39.4	20%
	Welding	Welding aggregate	2 piles per day	9	-	62.5	561	-	0.9	<1%
Sheet pile wall installation	Installation	Hydraulic crane	7 meters per day	-	141	411	-	58011	9.8	5%
		Vibratory hammer	7 meters per day	48	-	411	19925	-	32.4	16%
	Welding	Welding aggregate	2 sections per hour	9	-	62	557	-	0.9	<1%
Finishing locks	Cleaning	Pressure washer	64 locks per day	0.8	-	31	25	-	0.04	<1%
		Aerial work platform	64 locks per day	-	12	31	-	372	0.06	<1%
	Welding	Welding aggregate	2 sections per hour	9	-	62	557	-	0.9	<1%
		Aerial work platform	2 sections per hour	-	12	62	-	744	0.1	<1%
Excavation		Cutter suction dredger	7000 m^3/hour	594	-	9	5159	-	8.4	4%
Anchor/tension pile installation		Installation rig	1 anchor per hour	49	-	844	41356	-	67.3	33%
		Grout pump	1 anchor per hour	0.8	-	844	675	-	1.1	<1%
Placement of structural floor	Placement of reinforcement	Telescopic crane	1500 kg/h	-	400	300	-	120105	20.2	10%
	Pouring concrete	Concrete pump	100 m^3/hour	15	-	38.25	563	-	0.9	<1%
Dewatering	Pumping	Drainage pump	6000 m^3/day	10	-	90	900	-	1.465	1%
		Crane vessel		24	-	90	2120	-	3.5	2%
	Cleaning	High pressure washer	200 m^2/day	0.8	-	180	144	-	0.2	<1%
		Sediment removal machine	85 m^2/day	24	-	53	1249	-	2	1%
Gate placement	Gate installation	Floating crane	1 unit per day	-	132	8	-	1056	0.2	<1%
Pump placement		Mobile crane	1 unit per day	-	101	8	-	808	0.1	<1%
Winch installation		Mobile crane	1 unit per day	-	101	8	-	808	0.1	<1%
								Total	**202**	**100%**

No major reductions can be found in this phase.

The emissions during the operational phase of Variant C can be seen in Table H27

Table H 27: Operational phase – Variant C

Activity	Equipment	Productivity	Diesel consumption [Litres/hour]	Energy consumption [kWh/h]	Hours per year	Emissions per year [ton CO_2-eq/year]	Contribution
Gate operation	Hydraulic power unit	30 minutes per docking	-	50	3	0.007	<1%
Dock emptying	Pumps	3 hours per docking	-	800	60	16.2	87%
Docking/undocking vessels	Winches	1 h/docking activity	-	180	40	2.4	13%
					Total	**18.6**	**100%**

Due to the short duration of gate operation and absence of tugboats for this variant, the emissions during operation of the dock throughout its lifetime is relatively low.

The emissions during the maintenance phase of Variant C can be seen in Table H28.

Table H 28: Maintenance phase – Variant C

Activity	Frequency	Emissions per activity [ton CO2-eq]	Emissions during lifetime [ton CO2-eq]	Contribution
Dock pump inspection	Every 5 years	0.072	1.4	1%
Dock pump replacement	Every 25 years	1.7	5.1	2%
Hydraulic motor inspection	Every 5 years	1.7	32.8	15%
Hydraulic motor replacement	Every 25 years	19.5	58.5	26%
Winch inspection	Every 10 years	0.6	12.3	6%
Winch replacement	Every 50 years	13	39	18%
Gate & Combi-wall coating	Every 20 years	18	72	33%
		Total	**222**	**100%**

More mechanical components mean more maintenance and 6 winches also means that 6 new winches are needed after 50 years.

Appendix I: Cost-Benefit analysis details

This appendix gives the details behind the cost benefit analysis, starting off with the cost inventory per life cycle stage.

Table I 1: Material costs inventory

Materials	Unit	Price per unit [€]	Source	Design variant
Reinforced concrete	[m^3]	410	ADONIN reference project	All
Combi wall	[m^2]	90	ADONIN reference project	All
Steel gate	[ton]	2000	Estimation	All
Steel coating	[m^2]	10	Estimation	All
UCF	[m^3]	172	ADONIN reference project	All
Anchors	[# of anchors]	2920	ADONIN reference project	All
Tension piles	[# of piles]	2920	ADONIN reference project	All
Sand	[m^3]	13	ADONIN reference project	Base
Pumps	[# of pumps]	15000	Estimation	All
Concrete pipe	[m']	475	LBN Betonproducten B.V.	A, D
Steel fibres	[kg]	3	Estimation	A
Basalt fibres	[kg]	10	Estimation	B, D
Hydrojet	[# of hydrojet]	10000	Estimation	B
Winch	[# of winches]	10000	Estimation	B , C
Hydraulic motor	[# of motors]	2000	Estimation	B, C

The prices for the elements that make up the base design, such as the combi walls, UCF, reinforced concrete, anchors, tension piles and sand have been retrieved from a reference project provided by ADONIN where the prices have been adjusted to 2023 by accounting for price changes due to inflation over time.

The gate price per ton has been estimated at 2000 euros per ton which includes the price of steel and the construction costs for the gate.

The price for steel coating of the gate and combi wall has been estimated with help of experience from DAMEN.

LBN Betonproducten B.V. provided the costs for the concrete pipe per running meter for the pipe with the largest available diameter in their product range.

The prices for the steel and basalt fibres originate from online research (IN2-concrete, 2023) and the prices for the hydro jets, winches and hydraulic driving unit are estimated based on the estimated price per pump unit and online research.

Table I2 shows the transport prices.

Table I 2: Transport cost inventory

Materials		Place of origin	Transport mode	Distance [km]	Costs [€/km]	Design variant
Concrete	Cement	IJmuiden	Kempenaar	120	5.3	All
	Sand	Harlingen	Kempenaar	2	5.3	All
	Gravel	Limburg	Kempenaar	350	5.3	All
	Pipe	Burgum	Kempenaar	45	5.3	A
Steel	Reinforcement steel	Brescia (Italy)	Kempenaar	1200	5.3	All
	Steel piles	Essen (Germany)	Dortmunder	283	9.3	All
	Sheet piles	Essen (Germany)	Dortmunder	283	9.3	All
	Gate	IJmuiden to Heeg	Truck	127	0.7	All
		Heeg to Harlingen	Kempenaar	45	5.3	All
	Anchors	Langefeld (Germany)	Dortmunder	319	9.3	All
	Fibre	Neidenstein (Germany)	Dortmunder	623	9.3	A
Basalt Fibre		Sangerhausen (Germany)	Dortmunder	566	9.3	B

Pumps	Winterswijk	Truck	290	0.7	All
Hydrojet	Winterswijk	Truck	290	0.7	B
Winch	Hardinxveld-Giessendam	Kempenaar	200	5.3	B,C
Hydraulic motor	Hengelo	Kempenaar	180	5.3	B,C

Table H3 shows an overview of the fuel consumptions for the installation phase from the fuel costs for the installation phase is determined. For the rent of equipment, the following estimated prices are maintained based on estimations and online research as shown in Table I3:

Table I 3: Equipment rent prices

Equipment	Rent price [€/day]
Hydraulic crane	200
Telescopic crane	290
Mobile crane	200
Aerial work platform	140

The calculations of the construction costs are performed for each of the design variants, starting with the base design.

For the materials phase of the base design, the costs per element can be determined as follows:

Table I 4: Material costs – base design

Materials	Unit	Price per unit [€]	Amount	Total costs [€]	Contribution
Reinforced concrete	[m^3]	410	3600	1476000	25%
Combi wall	[m^2]	90	7092	638280	11%
Steel gate	[ton]	2000	270	540000	9%
Steel coating	[m^2]	10	4500	45000	1%
UCF	[m^3]	172	4500	774000	13%
Anchors/Tension piles	[# of anchors]	2920	844	2464480	41%
Sand	[m^3]	13	2250	29250	<1%
Pumps	[# of pumps]	15000	2	30000	1%
			Total	**€5.997.010**	**100%**

The largest contributing factor to the total construction costs are found to be the anchors and tension piles and the floor package.

Transport costs for the base design are given in the table below

Table I 5: Transport costs – base design

Materials		Place of origin	Transport mode	Distance [km]	Amount [ton]	Amount of trips	Total [km]	Costs [€/km]	Total costs [€]	Contribution
Concrete	Cement	IJmuiden	Kempenaar	120	972	2	480	5.3	2544	3%
	Sand	Harlingen	Kempenaar	2	6300	10	40	5.3	312	<1%
	Gravel	Limburg	Kempenaar	350	7155	11	7700	5.3	40810	51%
Steel	Reinforcement steel	Brescia (Italy)	Kempenaar	1200	265	1	2400	5.3	12720	16%
	Steel piles	Essen (Germany)	Dortmunder	283	1026	2	1132	9.3	10528	13%
	Sheet piles	Essen (Germany)	Dortmunder	283	323	1	566	9.3	5264	7%
	Gate	IJmuiden to Heeg	Truck	127	270	10	2540	0.7	1778	2%
		Heeg to Harlingen	Kempenaar	45	270	1	90	5.3	477	1%
	Anchors	Langefeld (Germany)	Dortmunder	319	506	1	638	9.3	5933	7%
Pumps		Winterswijk	Truck	290	0.47	1	400	0.7	280	<1%
								Total	**€80.546**	**100%**

Similar to the life cycle analysis, the transport of the gravel that is used to produce concrete is the predominant factor in the total costs of the transport phase. Furthermore, the contribution of the transport phase to the total is minimal compared to the material phase.

The costs of the installation phase consist of fuel and rent prices where the number of hours that equipment is required depends on the productivity of that equipment. An overview of the costs can be seen in the table below.

Table I 6: Installation costs – base design

Activity		Equipment	Hours required	Total diesel consumption [litres]	Total Electricity consumption [kWh]	Total costs [€]	Contribution
Pile installation	Installation	Hydraulic crane	500		70500	56400	12%
		Vibratory Hammer	500	24214		41164	9%
	Welding	Welding aggregate	62.5	561		954	<1%
Sheet pile wall installation	Installation	Hydraulic crane	411		58011	46409	10%
		Vibratory hammer	411	19925		33872	7%
	Welding	Welding aggregate	62	557		946	<1%
Finishing locks	Cleaning	Pressure washer	31	25		42	<1%
		Aerial work platform	31		372	298	<1%
	Welding	Welding aggregate	62	557		946	<1%
		Aerial work platform	62		744	595	<1%
Excavation		Cutter suction dredger	9	5159		8770	2%
		Excavation, dry	-	-	-	18000	4%
		Excavation, wet	-	-	-	85500	18%
Anchor/tension pile installation		Installation rig	844	41356		70305	15%
		Grout pump	844	675		1148	<1%
UCF pouring		Concrete pump	45	662		1126	<1%
Dewatering	Pumping	Drainage pump	90	900		1530	<1%
		Crane vessel	90	2120		3603	1%
	Cleaning	High pressure washer	180	144		245	<1%
		Sediment removal machine	53	1249		2124	<1%
Land filling		Hydraulic crane	14		1952	1562	<1%
Placement of structural floor	Placement of reinforcement	Telescopic crane	177		70650	56520	12%
	Pouring concrete	Concrete pump	22.5	331		563	<1%
Gate placement		Floating crane	8		1056	845	<1%
Pump placement		Mobile crane	8		807	645	<1%
Machinery rent		Hydraulic crane	925	-	-	23132	5%
		Telescopic crane	177	-	-	6403	1%
		Mobile crane	8	-	-	200	<1%
		Aerial work platform	93	-	-	1628	0%
					Total	**€465.476**	**100%**

The costs for performing the excavations result from the beforementioned reference project and is divided into the removal of dry and wet soil.
The total cost of construction of the base variant has been found to be roughly €6.55 million and after adding the 15% to account for design costs and other unforeseen factors, the costs amount €7.55 million. Comparison between the costs of construction of the design variant can be done after the construction costs of the other design variant have been calculated.

For Variant A, the material costs are shown in table I7.

Table I 7: Material costs – Variant A

Materials	Unit	Price per unit [€]	Amount	Total costs [€]	Contribution
Reinforced concrete	[m^3]	410	1485	608850	10%
Combi wall	[m^2]	90	7092	638280	10%
Steel gate	[ton]	2000	270	540000	9%
Steel coating	[m^2]	10	4500	45000	1%
UCF	[m^3]	172	3600	619200	10%
Anchors/Tension piles	[# of anchors]	2920	844	2464480	39%
Pumps	[# of pumps]	15000	4	60000	1%
Steel fibres	[kg]	3	423900	1271700	20%
Concrete pipe	[m']	475	80	38000	1%
			Total	**€6.285.510**	**100%**

The reduction in costs that result from the reduced volume of concrete is negated by the increased costs of the steel fibres. This has resulted in a price increase compared to the base design.
Transport costs for this variant are given in table I8.

Table I 8: Transport costs – Variant A

Materials	Place of origin	Transport mode	Distance [km]	Amount [ton]	Amount of trips	Total [km]	Costs [€/km]	Total costs [€]	Contribution

Concrete	Cement	IJmuiden	Kempenaar	120	732	2	480	5.3	2544	3%
	Sand	Harlingen	Kempenaar	2	2034	3	12	5.3	64	<1%
	Gravel	Limburg	Kempenaar	350	5390	8	5600	5.3	29680	36%
	Pipe	Burgum	Kempenaar	45	137	1	90	5.3	477	1%
Steel	Reinforcement steel	Brescia (Italy)	Kempenaar	1200	175	1	2400	5.3	12720	16%
	Steel piles	Essen (Germany)	Dortmunder	283	1026	2	1132	9.3	10528	13%
	Sheet piles	Essen (Germany)	Dortmunder	283	323	1	566	9.3	5264	6%
	Gate	IJmuiden to Heeg	Truck	127	270	10	2540	0.7	1778	2%
		Heeg to Harlingen	Kempenaar	45	270	1	90	5.3	477	1%
	Anchors	Langefeld (Germany)	Dortmunder	319	424	1	638	9.3	5933	7%
	Fibres	Neidenstein (Germany)	Dortmunder	623	506	1	1246	9.3	11588	14%
Pumps		Winterswijk	Truck	290	.47	1	400	0.7	280	<1%
								Total	**€81.332**	**100%**

The costs of the installation phase consist of fuel and rent prices where the number of hours that equipment is required depends on the productivity of that equipment. An overview of the costs can be seen in table I9.

Table I 9: Installation costs – Variant A

Activity		**Equipment**	**Hours required**	**Total diesel consumption [litres]**	**Total Electricity consumption [kWh]**	**Total costs [€]**	**Contribution**
Pile installation	Installation	Hydraulic crane	500		70500	56400	12%
		Vibratory Hammer	500	24214		41164	9%
	Welding	Welding aggregate	62.5	561		954	<1%
Sheet pile wall installation	Installation	Hydraulic crane	411		58011	46409	10%
		Vibratory hammer	411	19925		33872	7%
	Welding	Welding aggregate	62	557		946	<1%
Finishing locks	Cleaning	Pressure washer	31	25		42	<1%
		Aerial work platform	31		372	298	<1%
	Welding	Welding aggregate	62	557		946	<1%
		Aerial work platform	62		744	595	<1%
Excavation		Cutter suction dredger	9	5159		8770	2%
		Excavation, dry	-	-	-	18000	4%
		Excavation, wet	-	-	-	85500	18%
Anchor/tension pile installation		Installation rig	844	41356		70305	15%
		Grout pump	844	675		1148	<1%
UCF pouring		Concrete pump	45	662		1126	<1%
Dewatering	Pumping	Drainage pump	90	900		1530	<1%
		Crane vessel	90	2120		3603	1%
	Cleaning	High pressure washer	180	144		245	<1%
		Sediment removal machine	53	1249		2124	<1%
Placement of structural floor	Placement of reinforcement	Telescopic crane	177		70650	56520	12%
	Pouring concrete	Concrete pump	22.5	331		563	<1%
Gate placement		Floating crane	8		1056	845	<1%
Pump placement		Mobile crane	8		807	645	<1%
Inlet construction	Excavation	Hydraulic crane	6		833	666	
	Pipe placement	Mobile crane	40		4040	3232	
	Pump placement	Mobile crane	8		808	646	
Machinery rent		Hydraulic crane	917	-	-	22936	5%
		Telescopic crane	177	-	-	6403	1%
		Mobile crane	56	-	-	1400	<1%
		Aerial work platform	93	-	-	1628	<1%
					Total	**€469.463**	**100%**

The total cost of construction of this variant, including the 15% for unforeseen costs has been found to be roughly €7.85 million.

Now for Variant B, starting off with the material costs in table I10.

Table I 10: Material costs – Variant B

Materials	**Unit**	**Price per unit [€]**	**Amount**	**Total costs [€]**	**Contribution**
Reinforced concrete	[m^3]	410	1260	516600	8%
Combi wall	[m^2]	90	7092	638280	10%
Steel gate	[ton]	2000	270	540000	9%
Steel coating	[m^2]	10	4500	45000	1%
UCF	[m^3]	172	3825	657900	11%
Anchors/Tension piles	[# of anchors]	2920	844	2464480	40%
Pumps	[# of pumps]	15000	2	30000	<1%

Basalt fibres	[kg]	10	123356	1233560	20%
Hydro jet	[#]	10000	4	40000	1%
Winches	[#]	10000	2	20000	<1%
Hydraulic motor	[#]	2000	2	4000	<1%
			Total	**€6.189.820**	**100%**

Transport costs for Variant B are given in table I11.

Table I 11: Transport costs – Variant B

Materials		**Place of origin**	**Transport mode**	**Distance [km]**	**Amount [ton]**	**Amount of trips**	**Total [km]**	**Costs [€/km]**	**Total costs [€]**	**Contribution**
Concrete	Cement	IJmuiden	Kempenaar	120	732	2	480	5.3	2544	3%
	Sand	Harlingen	Kempenaar	2	2034	3	12	5.3	64	<1%
	Gravel	Limburg	Kempenaar	350	5390	8	5600	5.3	29680	35%
Steel	Reinforcement steel	Brescia (Italy)	Kempenaar	1200	175	1	2400	5.3	12720	15%
	Steel piles	Essen (Germany)	Dortmunder	283	1026	2	1132	9.3	10528	13%
	Sheet piles	Essen (Germany)	Dortmunder	283	323	1	566	9.3	5264	6%
	Gate	IJmuiden to Heeg	Truck	127	270	10	2540	0.7	1778	2%
		Heeg to Harlingen	Kempenaar	45	270	1	90	5.3	477	1%
	Anchors	Langefeld (Germany)	Dortmunder	319	123	1	638	9.3	5933	7%
Basalt	Fibres	Neidenstein (Germany)	Dortmunder	623	506	1	1246	9.3	10528	13%
Pumps		Winterswijk	Truck	200	.47	1	400	0.7	280	<1%
Hydro jet		Winterswijk	Truck	200	.47	1	400	0.7	280	<1%
Gate operating system	Hydraulic motor	Hengelo	Kempenaar	180	2.5	1	360	5.3	1908	2%
	Winches	Hardinxveld-Giessendam	Kempenaar	200	1.3	1	400	5.3	2120	3%
								Total	**€84.103**	**100%**

An overview of the installation costs is given in table I12.

Table I 12: Installation costs – Variant B

Activity		**Equipment**	**Hours required**	**Total diesel consumption [litres]**	**Total Electricity consumption [kWh]**	**Total costs [€]**	**Contribution**
Pile installation	Installation	Hydraulic crane	500		70500	56400	8%
		Vibratory Hammer	500	24214		41164	6%
	Welding	Welding aggregate	62.5	561		954	<1%
Sheet pile wall installation	Installation	Hydraulic crane	411		58011	46409	7%
		Vibratory hammer	411	19925		33872	5%
	Welding	Welding aggregate	62	557		946	<1%
Finishing locks	Cleaning	Pressure washer	31	25		42	<1%
		Aerial work platform	31		372	298	<1%
	Welding	Welding aggregate	62	557		946	<1%
		Aerial work platform	62		744	595	<1%
Excavation		Cutter suction dredger	9	5159		8770	1%
		Excavation, dry	-	-	-	18000	3%
		Excavation, wet	-	-	-	85500	12%
Anchor/tension pile installation		Installation rig	844	41356		70305	10%
		Grout pump	844	675		1148	<1%
UCF pouring		Concrete pump	45	662		1126	<1%
Dewatering	Pumping	Drainage pump	90	900		1530	<1%
		Crane vessel	90	2120		3603	1%
	Cleaning	High pressure washer	180	144		245	<1%
		Sediment removal machine	53	1249		2124	<1%
Placement of structural floor	Placement of reinforcement	Telescopic crane	177		70650	56520	8%
	Pouring concrete	Concrete pump	22.5	331		563	<1%
Gate placement	Hydro jet installation	Mobile crane	8		808	646	<1%
	Gate operation system	Mobile crane	4		404	323	<1%
	Gate installation	Floating crane	8		1056	845	<1%
Pump placement		Mobile crane	8		807	645	<1%
Machinery rent		Hydraulic crane	911	-	-	182286	27%
		Telescopic crane	177	-	-	51221	7%
		Mobile crane	20	-	-	4000	1%
		Aerial work platform	93	-	-	13020	2%
					Total	**€684.049**	**100%**

The total cost of construction of this variant has been found to be roughly €7.99 million including the factor of 15% for unforeseen costs. Next, the construction costs for Variant C is calculated, starting with the material costs in table I13.

Table I 13: Material costs – Variant C

Materials	Unit	Price per unit [€]	Amount	Total costs [€]	Contribution
Reinforced concrete	[m^3]	410	3825	1568250	29%
Combi wall	[m^2]	90	7092	638280	12%
Steel gate	[ton]	2000	270	540000	10%
Steel coating	[m^2]	10	4500	45000	1%
Anchors/Tension piles	[# of anchors]	2920	844	2464480	46%
Pumps	[# of pumps]	15000	2	30000	1%
Winches	[#]	10000	6	60000	1%
Hydraulic motor	[#]	2000	2	4000	<1%
			Total	**€5.350.010**	**100%**

Transport costs are given in table I14.

Table I 14: Transport costs – Variant C

Materials		Place of origin	Transport mode	Distance [km]	Amount [ton]	Amount of trips	Total [km]	Costs [€/km]	Total costs [€]	Contribution
Concrete	Cement	IJmuiden	Kempenaar	120	551	1	240	5.3	1272	2%
	Sand	Harlingen	Kempenaar	2	1530	3	12	5.3	64	<1%
	Gravel	Limburg	Kempenaar	350	4055	6	4200	5.3	22260	34%
Steel	Reinforcement steel	Brescia (Italy)	Kempenaar	1200	450	1	2400	5.3	12720	20%
	Steel piles	Essen (Germany)	Dortmunder	283	1026	2	1132	9.3	10528	16%
	Sheet piles	Essen (Germany)	Dortmunder	283	323	1	566	9.3	5264	8%
	Gate	IJmuiden to Heeg	Truck	127	270	10	2540	0.7	1778	3%
		Heeg to Harlingen	Kempenaar	45	270	1	90	5.3	477	1%
	Anchors	Langefeld (Germany)	Dortmunder	319	506	1	638	9.3	5933	9%
Pumps		Winterswijk	Truck	200	.47	1	400	0.7	280	1%
Gate operating system	Hydraulic motor	Hengelo	Kempenaar	180	2.5	1	360	5.3	1908	3%
	Winches	Hardinxveld-Giessendam	Kempenaar	200	3.9	1	400	5.3	2120	3%
								Total	**€64.603**	**100%**

And the installation costs in table I15.

Table I 15: Installation costs – Variant C

Activity		Equipment	Hours required	Total diesel consumption [litres]	Total Electricity consumption [kWh]	Total costs [€]	Contribution
Pile installation	Installation	Hydraulic crane	500		70500	56400	7%
		Vibratory Hammer	500	24214		41164	5%
	Welding	Welding aggregate	62.5	561		954	<1%
Sheet pile wall installation	Installation	Hydraulic crane	411		58011	46409	6%
		Vibratory hammer	411	19925		33872	4%
	Welding	Welding aggregate	62	557		946	<1%
Finishing locks	Cleaning	Pressure washer	31	25		42	<1%
		Aerial work platform	31		372	298	<1%
	Welding	Welding aggregate	62	557		946	<1%
		Aerial work platform	62		744	595	<1%
Excavation		Cutter suction dredger	9	5159		8770	1%
		Excavation, dry	-	-	-	18000	2%
		Excavation, wet	-	-	-	85500	11%
Anchor/tension pile installation		Installation rig	844	41356		70305	9%
		Grout pump	844	675		1148	<1%
Placement of structural floor	Placement of reinforcement	Telescopic crane	300		120105	96084	13%
	Pouring concrete	Concrete pump	38	563		957	<1%
Dewatering	Pumping	Drainage pump	90	900		1530	<1%
		Crane vessel	90	2120		3603	1%
	Cleaning	High pressure washer	180	144		245	<1%
		Sediment removal machine	53	1249		2124	<1%
Gate installation		Floating crane	8		1056	845	<1%
Pump& gate driving unit placement		Mobile crane	8		808	646	<1%
Winch installation		Mobile crane	8		807	645	<1%
Machinery rent		Hydraulic crane	911	-	-	182286	24%
		Telescopic crane	300	-	-	87000	11%
		Mobile crane	16	-	-	32000	0%
		Aerial work platform	93	-	-	13020	2%
					Total	**€757.536**	**100%**

The total cost of construction including the uncertainty range of 15%, has been found to be roughly €7.1 million.

Finally, the construction costs for Variant D are calculated starting off with the material costs in table I16. This is a combination of Variant A and Variant B.

Table I 16: Material costs – Variant D

Materials	Unit	Price per unit [€]	Amount	Total costs [€]	Contribution
Reinforced concrete	[m^3]	410	1260	516600	8%
Combi wall	[m^2]	90	7092	638280	10%
Steel gate	[ton]	2000	270	540000	9%
Steel coating	[m^2]	10	4500	45000	1%
UCF	[m^3]	172	3825	657900	11%
Anchors/Tension piles	[# of anchors]	2920	844	2464480	40%
Pumps	[# of pumps]	15000	4	60000	1%
Basalt fibres	[kg]	10	123356	1233560	20%
Concrete pipe	[m']	475	80	38000	1%
			Total	**€6.193.820**	**100%**

Transport costs are given in table I17

Table I 17: Transport costs – Variant D

Materials		Place of origin	Transport mode	Distance [km]	Amount [ton]	Amount of trips	Total [km]	Costs [€/km]	Total costs [€]	Contribution
Concrete	Cement	IJmuiden	Kempenaar	120	732	2	480	5.3	2544	3%
	Sand	Harlingen	Kempenaar	2	2034	3	12	5.3	64	<1%
	Gravel	Limburg	Kempenaar	350	5390	8	5600	5.3	29680	37%
	Pipe	Burgum	Kempenaar	45	137	1	90	5.3	477	1%
Steel	Reinforcement steel	Brescia (Italy)	Kempenaar	1200	175	1	2400	5.3	12720	16%
	Steel piles	Essen (Germany)	Dortmunder	283	1026	2	1132	9.3	10528	13%
	Sheet piles	Essen (Germany)	Dortmunder	283	323	1	566	9.3	5264	7%
	Gate	IJmuiden to Heeg	Truck	127	270	10	2540	0.7	1778	2%
		Heeg to Harlingen	Kempenaar	45	270	1	90	5.3	477	1%
	Anchors	Langefeld (Germany)	Dortmunder	319	424	1	638	9.3	5933	7%
Basalt	Fibres	Sangerhausen (Germany)	Dortmunder	566	123	1	1132	9.3	10528	13%
Pumps		Winterswijk	Truck	290	.47	1	400	0.7	280	<1%
								Total	**€80.272**	**100%**

The costs of installation for Variant D are displayed in table I18.

Table I 18: Installation costs – Variant D

Activity		Equipment	Hours required	Total diesel consumption [litres]	Total Electricity consumption [kWh]	Total costs [€]	Contribution
Pile installation	Installation	Hydraulic crane	500		70500	56400	12%
		Vibratory Hammer	500	24214		41164	9%
	Welding	Welding aggregate	62.5	561		954	<1%
Sheet pile wall installation	Installation	Hydraulic crane	411		58011	46409	10%
		Vibratory hammer	411	19925		33872	7%
	Welding	Welding aggregate	62	557		946	<1%
Finishing locks	Cleaning	Pressure washer	31	25		42	<1%
		Aerial work platform	31		372	298	<1%
	Welding	Welding aggregate	62	557		946	<1%
		Aerial work platform	62		744	595	<1%
Excavation		Cutter suction dredger	9	5159		8770	2%
		Excavation, dry	-	-	-	18000	4%
		Excavation, wet	-	-	-	85500	18%
Anchor/tension pile installation		Installation rig	844	41356		70305	15%
		Grout pump	844	675		1148	<1%
UCF pouring		Concrete pump	45	662		1126	<1%
Dewatering	Pumping	Drainage pump	90	900		1530	<1%
		Crane vessel	90	2120		3603	1%
	Cleaning	High pressure washer	180	144		245	<1%
		Sediment removal machine	53	1249		2124	<1%
Placement of structural floor	Placement of reinforcement	Telescopic crane	177		70650	56520	12%
	Pouring concrete	Concrete pump	22.5	331		563	<1%
Gate placement		Floating crane	8		1056	845	<1%
Pump placement		Mobile crane	8		807	645	<1%
Inlet construction	Excavation	Hydraulic crane	6		833	666	
	Pipe placement	Mobile crane	40		4040	3232	
	Pump placement	Mobile crane	8		808	646	
Machinery rent		Hydraulic crane	917	-	-	22936	5%
		Telescopic crane	177	-	-	6403	1%
		Mobile crane	56	-	-	1400	<1%
		Aerial work platform	93	-	-	1628	<1%
					Total	**€469.463**	**100%**

The total cost of construction of this variant, including the 15% for unforeseen costs has been found to be roughly €7.67 million.

Discussion and comparison of the result can be seen in section 6.2, the following section here show the calculations for the operational costs of each variant.

Firstly for the base design, the operation costs are displayed in Table I 19

Table I 19: Operational costs – base design

Activity		Equipment	Productivity	Diesel consumption [Litres/hour]	Energy consumption [kWh/h]	Hours per year	Costs per year [€]	Contribution
Dock emptying		Pumps	3 hours per docking		800	60	19200	6%
Sediment removal	Cleaning	High pressure washer	10000 m^2/day	0.8		72	49	<1%
		Sediment removal machine	85 m^3/h	24		53	1062	<1%
	Sediment transport	Truck	270 tons			-	840	<1%
	Sediment disposal	-	270 tons				270000	89%
Tugboats support during docking		Tugboat fuel	2 h/docking activity	94		80	12762	4%
		Tugboat rent	2 h/docking activity	-	-	80	64000	21%
						Total	**€367.913**	**100%**

For design variants A, and D the costs per year are identical and stem from energy use of the pumps and the rent of a single tugboat to balance the ship during docking. Table I20 below shows an overview.

Table I 20: Operational costs – Variant A&D

Activity	Equipment	Productivity	Diesel consumption [Litres/hour]	Energy consumption [kWh/h]	Hours per year	Costs per year [€]	Contribution
Gate operation	Telescopic crane	0.25 hours per docking	-	505	10	2020	3%
Dock emptying	Pumps	3 hours per docking	-	800	60	19200	31%
Inlet operation	Pumps/gate	1 hour per docking	-	400	20	3200	5%
Tugboat support during docking	Tugboat fuel	2 h/docking activity	94	-	80	6381	10%
	Tugboat rent	2 h/docking activity	-	-	80	32000	51%
					Total	**€62.801**	**100%**

The fact that no sediment needs to be disposed here leads to a large reduction in operational costs, this can also be seen in the operational costs for Variant B in table I21.

Table I 21: Operational costs – Variant B

Activity	Equipment	Productivity	Diesel consumption [Litres/hour]	Energy consumption [kWh/h]	Hours per year	Costs per year [€]	Contribution
Gate operation	Hydrojets	0.5 hours per docking	-	27	20	432	1%
	Winches	0.5 hours per docking		180	20	2880	5%
Dock emptying	Pumps	3 hours per docking	-	800	60	19200	31%
Bubble screen	Hydrojets	1 hour per docking	-	27	40	864	1%
Tugboats support during docking	Tugboat fuel	2 h/docking activity	94	-	80	6381	10%
	Tugboat rent	2 h/docking activity			80	32000	52%
					Total	**€61.757**	**100%**

The operational costs per year for this variant is in the same order of magnitude of variant A, meaning a considerable saving compared to the base design.
Finally, the operational costs per year for Variant C are calculated below in table I22.

Table I 22: Operational costs – Variant C

Activity	Equipment	Productivity	Diesel consumption [Litres/hour]	Energy consumption [kWh/h]	Hours per year	Costs per year [€]	Contribution
Gate operation	Hydraulic power unit	30 minutes per docking	-	50	20	800	3%
Dock emptying	Pumps	3 hours per docking	-	800	60	19200	87%
Docking/undocking vessels	Winches	1 h/docking activity	-	180	40	5760	13%
					Total	**€25.760**	**100%**

Using the winches docking procedure saves the tugboat rent costs which makes this variant the cheapest during operation.

The maintenance costs for the base design is calculated in table I23 below.

Table I 23: Maintenance costs – base design

Activity	Frequency	Costs per activity [€]	Costs during lifetime [€]	Contribution
Dock pump inspection	Every 5 years	1556	29569	10%
Dock pump replacement	Every 25 years	31125	93374	31%
Gate & Combi-wall coating	Every 20 years	45000	180000	59%
		Total	**€302.943**	**100%**

The design variants will have larger maintenance costs since there are simply more maintenance-requiring elements. For variants A and D this results in the following costs:

Table I 24: Maintenance costs – Variant A&D

Activity	Frequency	Costs per activity [€]	Costs during lifetime [€]	Contribution
Dock pump inspection	Every 5 years	1556	29569	7%
Dock pump replacement	Every 25 years	31125	93374	22%
Inlet pump inspection	Every 5 years	1556	29569	7%
Inlet pump replacement	Every 25 years	31125	93374	22%
Gate & Combi-wall coating	Every 20 years	45000	180000	42%
		Total	**€425.886**	**100%**

And similarly for variant B, the maintenance costs are shown in table I25.

Table I 25: Maintenance costs – Variant B

Activity	Frequency	Costs per activity [€]	Costs during lifetime [€]	Contribution
Dock pump inspection	Every 5 years	1556	29569	5%
Dock pump replacement	Every 25 years	31125	93374	16%
Hydrojet inspection	Every 5 years	2046	40926	7%
Hydrojet replacement	Every 25 years	40926	122779	21%
Hydraulic motor inspection	Every 5 years	312	6231	1%
Hydraulic motor replacement	Every 25 years	6231	18694	3%
Gate driving system inspection	Every 5 years	1122	22443	4%
Gate driving system replacement	Every 25 years	22443	67330	12%
Gate & Combi-wall coating	Every 20 years	45000	180000	31%
		Total	**€581.346**	**100%**

Finally for Variant C, the maintenance costs are displayed in table I26.

Table I 26: Maintenance costs – Variant C

Activity	Frequency	Costs per activity [€]	Costs during lifetime [€]	Contribution
Dock pump inspection	Every 5 years	1556	29569	5%
Dock pump replacement	Every 25 years	31125	93374	16%

Hydraulic motor inspection	Every 5 years	312	5920	1%
Hydraulic motor replacement	Every 25 years	6231	18693.6	3%
Winch inspection	Every 5 years	3138	59627	10%
Winch replacement	Every 25 years	62765	188296	33%
Gate & Combi-wall coating	Every 20 years	45000	180000	31%
		Total	**€575.479**	**100%**

Appendix J: Multi Criteria Analysis details

This appendix gives all relevant background information for the multi criteria analysis, starting off with determining the weighting factors of the criteria which is done as follows. The criteria are compared in pairs, for each cell, a '0' or '1' indicates which of the two criteria is more important. After filling out the entire matrix, the scores per criteria are added up per row and the weighting factors can be determined based on these scores.

Table J 1: Weighting factor assessment

Criteria	A	B	C	D	E	Sum
Sustainability **A**		1	1	1	1	4
Return of Investment **B**	0		0	0	1	1
Ease of operation **C**	0	1		1	1	3
Ease of maintenance **D**	0	1	0		1	2
Constructability **E**	0	0	0	0		0

		Weighting factor	
A	8	8/21≈	35%
B	2	2/21≈	10%
C	6	6/21≈	30%
D	4	4/21≈	20%
E	1	1/21≈	5%
	Σ=21		Σ=100%

Ease of operation and sustainability are the most important criteria and are assigned a weight of 35% and 30% respectively, followed by ease of maintenance which is given a weighing factor of 20%, costs is then given a factor of 10% and finally constructability is given a factor of 5%.

The tables below give scores to each design element separately, for explanations chapter 6.3 can be consulted.
For the UCF, the scores are given below. Since ease of operation and ease of maintenance are not relevant for UCF design, all alternative are given a neutral score of 6.

Table J 2: UCF scores

		Design alternative			
Criteria	**Weight**	**A**	**B**	**C**	**D**
Sustainability	30%	8	9	3	9
Costs	10%	5	6	8	6
Ease of operation	30%	6	6	6	6
Ease of maintenance	25%	6	6	6	6
Constructability	5%	6	6	1	6
	Scores	**6.6**	**7.1**	**4.9**	**7.1**

For the sedimentation reduction strategies, the scores are given in table J3

Table J 3: Sedimentation reduction strategies scores

		Design alternative			
Criteria	**Weight**	**A**	**B**	**C**	**D**
Sustainability	30%	8	7	9	8
Costs	10%	6	6	8	6
Ease of operation	30%	8	7	4	8
Ease of maintenance	25%	8	4	7	8
Constructability	5%	5	5	7	5
	Scores	**7.7**	**6.2**	**6.9**	**7.7**

And finally for the gate type, the scores are given in table J4

Table J 4: Gate type scores

		Design alternative			
Criteria	**Weight**	**A**	**B**	**C**	**D**
Sustainability	30%	8	4	6	8
Costs	10%	7	3	8	7
Ease of operation	30%	5	7	7	5
Ease of maintenance	25%	9	4	5	9
Constructability	5%	8	5	6	8
	Scores	**7.2**	**4.9**	**6.3**	**7.2**

The scores given in chapter 6.3 are explained below.
For the sustainability criteria, variant B leads to the largest reduction compared to the base design and it therefore rewarded a 9. Variant A has the next best carbon footprint reduction and is in the same order of magnitude as Variant B and therefore scores an 8. Variant C only leads to a minor reduction and scores a 6. Variant D finally combines the most sustainable elements of each variant and is assumed to score similar to Variant B due to the large influence of the floor package, which explains the 9 score for Variant D.
For the required investments, Variant C clearly scores better than the other variants and therefore receives the highest score here. Variant A and D show similar performance but Variant B requires a marginally larger investment and therefore is assigned a 6.
For the ease of operation, Variant A and D contain the caisson gate which requires an external crane to remove the gate. This is a more time-consuming and difficult procedure that requires more human actions. On top of that, the pipe inlet gate needs to be opened and closed but this eventually leads to a faster operation of the dock since the water pressure can leave the chamber, enabling a swift docking procedure. Variant B contains the sliding gate which is a fast and automatic procedure but vibrations could make the opening and closing of the gate more tricky. The bubble screen doesn't need additional actions for operation but it does bring additional risks of malfunctioning or clogging of bubble screen system. For Variant C, the mitre gate system is another fast and easy to operate driving system. The only downside of the winches system is the slow docking procedure that this brings, but the operation of the winches is a simple process.
All in all, the removal of the caisson gate scores poorly for the ease of operation criteria, but this is largely compensated by the fast docking procedure. Variants B and C both have

automatic operation of the gate and therefore score a little bit higher. Variant C scores a little bit higher due to the low risks and automated processes.
For the ease of maintenance the caisson gate scores best since the gate can be completely removed to reapply the coating and no mechanical driving unit is present that would require maintenance. Furthermore, maintenance within the pipe can be assessed easily by closing off the pipe with gates. This leads to the best score for variants A and D for this criterion. The sliding gate of Variant B might be hard to access and frequent cleaning and unclogging of the hydro jets is needed. Mitre gates are expected to require less maintenance than a sliding gate but is harder to apply maintenance than for the caisson gate. The winches are easily accessible since they are located on the dock walls and the winch cords can be replaced easily. All in all, Variant B scores worst for this criteria with a 5 followed by Variant C with a score of 7. Variants A and D clearly score better with a 9.
For the constructability criteria, the UCF with rebars scores worst since it is by far the hardest to construct and never applied in practice. On top of that, mitre gate are commonly applied for locks but less common for dock gate since they typically have a larger width that complicates the design. The simplicity of the winch system compensates but still Variant C scores poorly for the constructability criteria with a 4. For Variants A and D, the gate installation is the most simple due to the lack of gate operating systems but the installation of the pipe is more complicated than other sedimentation reduction strategies. The hydro jet system is also not commonly applied and effective operation of the bubble screen could complicate the design process. All in all, the simplicity of the caisson gate design of variants A and D result in a score of 7 for constructability. Variant B scores a little bit worse with a 6 due to the complexity in the hydro jet design.

Appendix K: Dock operations at the current shipyard

This appendix aims to give an insight into the operation procedure at the current Damen shipyard as well as the floating docks that were present in the past.
In the current shipyard's ship lift docking procedure, the vessel's mooring lines are connected from the dock to the ship. Two tug boats then help to maneuver the vessel in the right position to enter the basin. Winches are located at the sides of the dock and the mooring lines get connected to the bollards on the vessel's deck and are tightened. While the vessel might also contain strong winches that could tighten mooring lines, these winches are often too powerful to ensure adequate mooring and thus the dock's winches are used to do so. In the meantime, the docking blocks are positioned appropriately conform the vessel hull shape to ensure a stable docking position for the vessel.
In the 1980's, four floating docks were in use, all originally manufactured in Sweden and purchased by the shipyard to increase the capacity of the shipyard. However, over the course of time a structural failure lead to the collapse of one of the floating docks. At that time, the docks were already near the end of their lifetime and so it was decided that all four docks were to be demolished. A picture of the dock failure can be seen in figure K1 below.

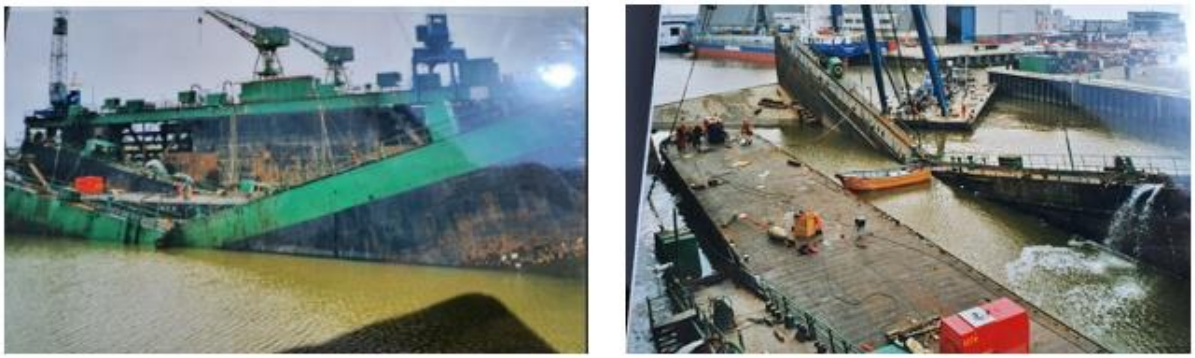

Figure K 1: Failure of the old floating dock at the Damen Shipyard

Appendix L: Location-specific design aspects

This appendix gives additional background information regarding the location specific design aspects such as sedimentation of the dock and nitrogen emissions near the intended construction location.

Located in the Wadden Sea, the port of Harlingen is known to suffer from high yearly sedimentation rates that reduce the effective depth of the harbour basin over time and subsequently complicate vessel navigation through the port. This means that expensive dredging works are necessary which needs to be prevented as much as possible (Deltares, 2013). Even though the expected location of the new dock and its entry are located relatively far downstream of the port entrance, local sedimentation can still be expected to be present. In general, this sedimentation is caused by three main processes, which are tidal filling and emptying, horizontal eddies and density-driven vertical flow (Winterwerp, 2005). From the mentioned causes, Deltares has found that for the specific case of the Port of Harlingen, the main drivers for siltation are the tidal filling and emptying of the port basin and the density-driven circulation (Deltares, 2013). This density difference can be driven by a horizontal gradient in salinity, temperature or sediment concentration (Vanlede, 2014). In our case, the dominant cause of the density-driven circulation is found to be the discharges of freshwater into the port of Harlingen. However, the effect of the tidal variation on these sedimentation processes that exist for the complete port of Harlingen are assumed to be limited at the location of the new dock. The location of the new dock is at a distance of approximately 3 kilometers from the entrance of the port, as visible on Figure L1 (Google Maps, 2022).

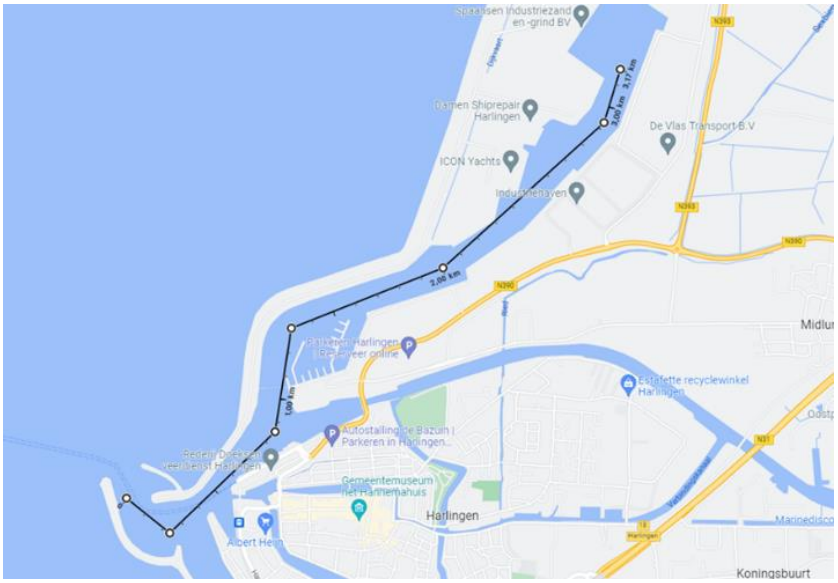

Figure L 1: Distance between the entrance of the Port of Harlingen and Damen Shiprepair, source: (Google Maps, 2022)

Research from Deltares shows that the effect of the sedimentation processes have already reached a minimum at a distance of approximately 1300 meters. This can be seen in Figure L2 below, at the peak of the tidal cycle, the sedimentation at the first harbor basin is at 0.1 g/L and therefore this value is assumed to be considerably lower at the location of the dock

(Deltares, 2013). The density-driven circulation is more likely to play a factor in the sedimentation of the port.

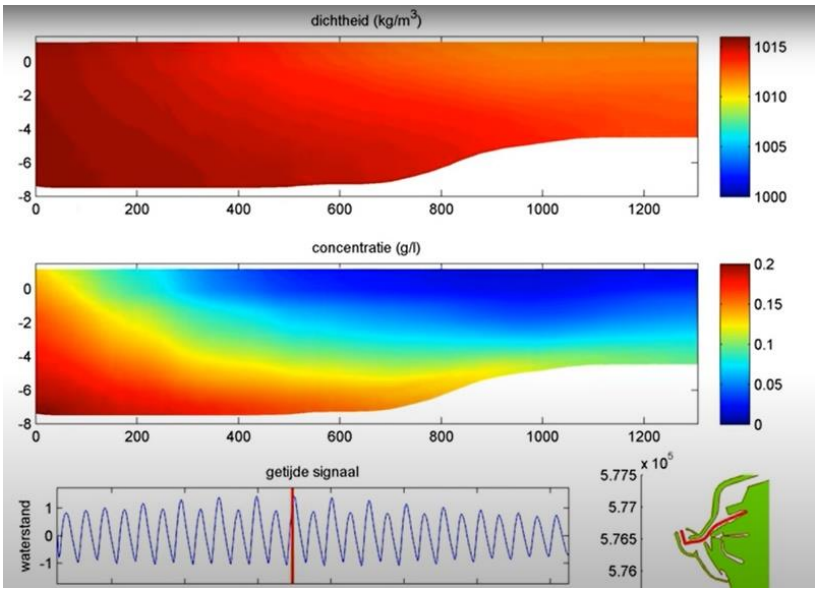

Figure L 2: Sediment concentration at tidal peak, source: (Deltares, 2013)

Various mitigation measures exist to reduce the amount of siltation, including a siltation trap or siltation screen. A siltation trap is a local deepening of the bed where sediments prefer to settle due to the reduced flow velocity caused by the locally increased water column that is present (El Hamdi, 2011). Silt screen can take various forms, most of which either will form a barrier for navigation (standing or hanging silt screen (Radermacher, 2013)), or will require a surplus of energy for operation, as for example an air bubble silt curtain (Cheng, 2021). For the siltation of the graving dock, the solution should possibly be searched in an efficient disposal of the inflowing silt, possibly by allowing an outflow of water from the backside of the dock when the vessel enters the dock that reduces the turbulence near the entrance of the dock chamber due to the reduced return flow.
An aspect that should also be considered when discussing the sedimentation of a dock is the opportunities for re-use of the silt upon dredging. Depending on the chemical and physical composition of the silt, it could potentially be used for the following uses:

- Engineering purposes like land reclamation or beach nourishment.
- Agricultural uses due to the typical fertile characteristics of the silt.
- Environmental enhancement, including the restoration of nature areas such as wetland.

It has to be mentioned that the local silt might be contaminated and additional costs for decontamination of the silt need to be included (Maher, 2013).

Another location specific design issue is the emissions of nitrogen. While nitrogen is naturally present in the atmosphere, it can cause problems when reacting with other substances. The present nitrogen problems are caused by the emission of nitrogen dioxide (NOx) after reacting with oxygen during combustion processes caused by for example road vehicles (cars, trucks), gas boilers and large industrial processes. The other harmful gas is ammonia (NH3) which is created when nitrogen reacts with hydrogen, as is the case in the agricultural sector through the evaporation of manure. In case large amounts of these gasses are emitted, it leads to an enhanced growth of certain specific plant species which results in deterioration of other species due to the competition among species in a habitat. This deterioration of diversity leads to a more limited food supply for animal species with overall harm to the flora and fauna in the Netherlands as a result (PH bouwadvies, 2021). Simultaneously, large concentrations in groundwater and surface water is detrimental for the water quality and the water life (Oenema, 2019).

For the construction of the graving dock, the emissions during the construction phase do not have to be considered when determining the environmental footprint of the dock for applying for a building permit but it should still be minimized in view of the other emission gasses. The guidelines SEB (Schoon en Emissieloos Bouwen) collect researches and initiatives, focusing on the reduction of emissions during the construction phase, that are under development or already in execution throughout the Netherlands. Aspects such as clean building machinery and zero-omission building logistics are discussed and serve as a possibility for the construction phase of the graving dock as well (SEB, 2021).

Appendix M: Dock components specification

This appendix gives background information regarding the most commonly applied dock gate types and explains the hydraulic operation of the two kinds of emptying/filling system.

Gate types

A short introduction of these most commonly applied gate types is given below:

- Mitre gates: Being one of the oldest gate types, they are most often used as lock gates or impounding gats in ports or docks. Their mode of operation is a rotation around hinges that are installed on the vertical axis (Royal Haskoning DHV, 2019). The main advantage of this gate type is its low cost and short opening time but downsides include the sensitivity for blockage by for example debris and ice (Molenaar, Locks, 2020). Figure M1 shows an example of this gate type (Allianz). Single leaf gates are comparable to mitre gates in terms of operation and characteristics, but are usually more applicable for locks or docks with a small width.

Figure 72: Mitre lock gates, source: (Allianz)

- Sector gates: These rotational gates can be applied in pairs or as a single gates and have the main advantages that they can retain water in two ways and they can be operated in case of a water head difference across the gate which makes them very applicable as lock gates or storm surge barriers but for docks these characteristics are not of importance. The large amount of material that is required during the construction of the gates makes them less favorable in comparison to other gate types (Molenaar, Locks, 2020). A well-known example of the application of sector gates in the Netherlands is the Maeslantkering.
- Lift gates: Using a vertical translational movement, lift gates are usually opened by means of winches and wire ropes that pull the gates upwards. This gate type requires little space for operation and are easy to control and repair. However, the limited air draught that is provided for the vessels in combination with the large and heavy superstructure that is needed for application of this gate type likely makes it less applicable for docks. Furthermore, deflection of the bottom of the gates under full loading conditions can cause difficulties with the roller tracks that guide the gate during operation (Molenaar, Locks, 2020).
- A sliding or rolling gate moves horizontally into a gate chamber in the lock wall during operation. The main advantages are the watertightness of the gate in closed condition and its easy operation and maintenance. On the downside, there is a possibility of jamming of the operational system of the gate during opening or closure of the gate and the fact that a large door recess area is necessary adjacent to the gate which increases the costs of this gate type.

- Caisson gates need to be completely removed in case of operation. This is usually done by using large cranes or other machinery but floating variants exist as well, which can be filled and pumped dry and removed by dragging them across the water surface. The ability for maintaining a considerable reverse hydrostatic head in combination with the lack of need for an operational system (which means no chance of malfunction during operation) and cheap and effective design means that this type of gate is common among shipping docks. On the other hand, additional equipment is necessary for removal or placement of the dock which increases the amount of preparation and time that is necessary for operation. This type of gate is present at the dock of Icon Yachts, that was mentioned before. The fact that the dock is used for construction of vessels means that the frequency with which the dock gate needs to be removed is relatively low and thus this gate type is very suitable for this dock. As mentioned before, in figure 4, this gate can be seen as well as the crane rails that are located on the outside of the dock so that the dock cranes can be used for removal or placement of the gates. In figure M2, the procedure of placement of a floating caisson dock can be seen, (Ravestein Shipyard & Construction Company, 2017)

Figure 73: Procedure of caisson gate placement, source: (Ravestein Shipyard & Construction Company, 2017)

Filling and emptying systems:

When the head filling system is subject to too large head differences, very turbulent water will be created which has an effect on the stability of the vessel inside the dock and the inflow of silt. From a hydraulic point of view, in case of flow through a gate, the available potential energy, function of $\sqrt{m * g * h}$ is transformed into kinetic energy, function of $\frac{1}{2} * m * v^2$ without very significant losses of energy. Stilling chambers can be included to increase the lift of head filling systems. It's typically located underneath the lock chamber floor and aims to dissipate as much of turbulent water energy as possible. Culverts are used to guide water from the open channel into the stilling basin, where it is distributed into the lock chamber and often flow breaking elements are constructed into the stilling chamber (for energy breaking purposes).

For the longitudinal inlet system, a certain energy head loss has to be taken into account for the intake of the culvert and a friction loss for the transportation of the flow through the culvert, additional losses due to bends in the culvert exist as well and in total, a significant amount of energy loss will be present. The culvert can be located in or adjacent to the lock wall, in, below or above the lock chamber floor.

Appendix N: Sustainable design alternative details

This appendix gives further background information regarding the 9R framework and illustrates how this can be applied in the design of the graving dock.

- Refuse (R0) in this case could mean to not construct a graving dock at all and try to increase Damen's capacity in a different way, for example by purchasing an already existing floating dock which has the same dimensions as the intended graving dock. Naturally the climate impact of this strategy would nearly be zero (except for the transport of the dock to the shipyard). However, the decision of constructing a new graving dock has already been made at an earlier stage and at a 'higher level' of decision making. For the purpose of this thesis, the designer therefore has no say in this and this strategy will therefore not be considered.
- Rethink (R1) could mean making the dock multi-functional and thereby making the product use more intensive. The roof of the hall can be used to place solar panels that generate energy for either the operation of the dock or for other purposes at the shipyard, or additional workplaces and offices can be placed within the dock hall.
- Reduce (R2) means to increase the efficiency in product manufacture or use by minimizing the amount of natural resources and materials. This strategy is closely linked to the Life Cycle Analysis, which will be treated later on in this chapter. Increasing the efficiency of the manufacturing process of products is more of a task for 'higher level' instances and lies outside the scope of this thesis but aiming to reduce the amount of natural resources offers a lot of possibilities for the design of the graving dock. Designing for Disassembly is one of them and allows structures to be easily disassembled at the end of their lifetime so that the elements which make up the structure can easily be removed and used for other purposes. The main issue here is ensure the structural performance of the dock. For example, the loads acting on a graving dock are usually significant and the inclusion of a hinge in the retaining wall which might make disassembly of the retaining wall easier could prove to be structurally impossible. Similarly, the use of a gravity wall consisting of separate interlocking concrete blocks might ease the deconstruction efforts for the wall but on the other hand it would increase the amount of concrete that is necessary. The use of sustainable building materials such as recycled steel or sustainable concrete solutions serve as another possibility that reduces the overall climate impact of the design. A permanent, steel fibre reinforced underwater concrete floor would reduce the need for multiple concrete floors and consequently reduce the amount of concrete necessary in the design. Choosing local manufacturers would reduce the emissions during the transport of the products and CO2-neutral machinery are other possibilities to implement the R2-strategy in the design of the graving dock.

For Reuse (R3), the element is still in good condition after disassembly and can directly be applied in a different project to fulfil its original function. For Repair (R4), Refurbish (R5) and Remanufacture (R6) an increasing amount of maintenance is required to bring the element back to the appropriate quality to fulfil the same function. Repurpose (R7) uses the discarded element or parts of the element in a new product with a different function. These strategies could also be applied to the design of the graving dock, for example by removing structural elements at the end of their lifetime and depending on the state of these elements, applying them in other projects.
For Recycle (R8) this includes process the material into obtain a similar or lower quality. For example, the concrete which will be used in the design of the graving dock can be downcycled into construction rubble or concrete bricks and create value in a different purpose than originally in the graving dock. Recovery (R9) includes the incineration of the building materials

and recovering energy as a result. These two strategies are common practice in the building sector but they retain the lowest value of the material.

The way that the environmental impact of a design is typically determined is by using software such as DuboCalc to perform an Life Cycle Assessment. The following paragraph summarizes the environmental impact categories and life cycle phases that the software takes into account.

DuboCalc takes 11 different impact categories into account which describe the various negative effects that the environment might experience during the lifetime of certain product. These Environmental Impact Categories are expressed in equivalent units. For example, not every greenhouse that is emitted during the manufacturing of a certain product is equally powerful and are therefore expressed in CO2-equivalent units, meaning that the amount of CH4 and N2O need to normalized to equivalent amounts of CO2 and therefore multiplied by a factor of 21 and 310 respectively (Jonkers, 2018).
DuboCalc takes the following 11 categories into account and assigns a so-called 'shadow price' to each of these categories to express the impact in terms of monetary value per unit equivalent (van 't Wout, Groot, Sminia, & Haas, 2010):

Table N 1: Environmental Impact Categories (van 't Wout, Groot, Sminia, & Haas, 2010)

	Category name	**Description**	**Unit**	**Weight factor (€ per unit)**
1	Global Warming Potential (GWP)	The amount of greenhouse gases which contribute to the anthropogenic greenhouse effect that are emitted during the lifetime of the product.	Kg CO_2 eq	0.05
2	Ozone layer Depletion Potential (ODP)	The amount of ozone depleting compounds that are emitted during the lifetime of the product.	Kg CFC-11 eq	30
3	Human Toxicity Potential (HTP)	The emissions of compounds which have an adverse effect on human health.	Kg 1,4-DB eq	0.09
4	Freshwater Aquatic Eco-Toxicity Potential (FAETP)	The emissions of compounds which have an adverse effect on organisms living in the aquatic freshwater environment.	Kg 1,4-DB eq	0.03
5	Marine Aquatic Eco-Toxicity Potential (MAETP)	The emission of compounds which have an adverse effect on organisms living in the aquatic saltwater environment.	Kg 1,4-DB eq	0.0001
6	Terrestrial Eco-Toxicity Potential (TETP)	The emission of compounds which have an adverse effect on organisms living in the terrestrial (land) environment.	Kg 1,4-DB eq	0.06
7	Photochemical Oxidation Potential (POCP)	The emission of compounds which form chemically reactive compounds after reacting with sunlight, that can be harmful for both human health and for nature.	Kg C_2H_4	2
8	Acidification Potential (AP)	The emissions of acidic compounds which can have detrimental effects on the natural environment and built environment.	Kg SO_2 eq	4
9	Eutrophication Potential (EP)	The emissions of excess nutrients (especially nitrogen and phosphorous compounds) which lead to excess quantities	Kg PO_4 eq	9

		of plants and algae, limiting the growth of other types of organisms.		
10	Abiotic Depletion Potential non-Fuel (ADP non-fuel)	The depletion of 'rare earth elements' such as minerals and ores.	Kg Sb eq	0.16
11	Abiotic Depletion Potential Fuel (ADP-fuel)	The depletion of fossil fuels.	Kg Sb eq	0.16

DuboCalc scores the performance of the various construction elements and processes for each of these Environmental Impact Categories during each individual stage of the element's life cycle so that an insight can be gained which phase contributes most to the ECI of the element and the structure as a whole. In this way, insight can be gained in which stage of the dock's lifetime the largest amount of environmental impact can be saved by implementing more sustainable alternatives. The stages that are identified in DuboCalc are the following:

- A1 – A3 Production stage:
  - A1: Raw material supply
  - A2: Transportation from excavation site to factory
  - A3: Manufacturing of the product
- A4 – A5 Construction stage:
  - A4: Transportation from factory to construction site
  - A5: Construction installation process
- B1 – B5: Use stage:
  - B1: Use
  - B2: Maintenance
  - B3: Repair
  - B4: Replacement
  - B5: Refurbishment
- B6 – B7 Energy use during life cycle:
  - B6: Energy use
  - B7: Water use
- C1 – C4: End-of-life stage C1-C4:
  - C1: Demolition Process
  - C2: Transport from construction site to waste plant
  - C3: Waste processing
  - C4: Disposal
- D: Remaining value: Re-use, recovery, recycling potential

Appendix O: Dock design requirements

This appendix elaborates on the specific dock design aspects that form the basis of the object chapter in chapter 4.1.

The dimensions of the dock are determined by the design vessel that the dock aims to handle. Eyeing the development in vessel dimensions over the past years, Damen Harlingen aims to be able to dock vessels with a capacity of 900-1250 TEU. The design vessel that is chosen for the design of the dock is based on the *Endeavor*, which is a container vessel that is built by Volharding Shipyard and is currently owned by JR Shipping BV. Exact information on this ship can be found in Appendix A, but this ship is characterized by a L.o.a. (Length over all) of 134.65 m, a beam of 21.5 meters and a draught (which is the distance from the bottom of the keel to the waterline) of 7 meters (Confeeder Shipping & Chartering, 2022). For the dimensions of the dock, extra space of approximately 5 meters is necessary on either side of the vessel when docked in order to make repair and maintenance works possible. The blocks on which the vessel will be placed need to be around 1,80 meters high so that personnel can access the bottom of the ship and a freeboard of 2 meters is applied for the height of the dock. This comes down to the following dimensions for the dock: a length of 150 meters, a width of 30 meters and a depth of 11.8 meters. As far as the facilities within the dock are concerned, an intermediate gate is required in order to split up the dock into multiple compartments so that multiple vessels can be handled simultaneously. An entrance ramp has to be constructed in order to make de dock accessible for equipment, machines and personnel. Damen Harlingen currently mainly uses aerial lifts to perform the maintenance works and so the slope of the entrance ramp and thus the space that is required for construction of the ramp will depend on the maximum slope that an aerial lift can handle, which is called the gradeability of the aerial lift. In practice, mainly a scissor lift or a telescopic boom lift are used to perform the maintenance works and after consulting the technical specifics of various types of aerial lift, it is found that the gradeability of the scissorlift is typically lower than that of a telescope boom lift. The governing gradeability is found to be 25% after consulting the current aerial lift supplier Verno. (PB Lifttechnik GmbH, 2022). For safety, a slope of 20 % should be applied in the design. When maintaining a dock chamber depth of 11.8 meters, this comes down to a entrance ramp length of 60 meters.

In case insufficient space is available for the construction of the entrance ramp, an alternative with overhead rail cranes can be chosen. The minimal requirements for this crane is a minimum of 2 cranes, each consisting of 2 trolley with a capacity of 20 t per trolley. Within the hall, sufficient space needs to be present on either side of the dock chamber so that either a forklift and/or a truck can access the dock for the delivery and transport of equipment and materials. 6 workspaces need to be present within the dock to facilitate the maintenance works, since electricians, carpenters, bank workers/fitters, painters and installers all need a workspace each and another spare workspace is required. The required dimensions of these workspaces are a length of 10 meters, a width of 8 meters and a height of 3.5 meters. An office area, from which the dock master can operate the dock needs to be present as well and is often build above the workplaces in practice.

The total height of the hall depends on the required lifting height for the cranes which is determined by the total height of the design vessel. For safety reasons, an exaggerated vessel height is chosen, namely by taking the height of the next largest JR Shipping vessel, the MV Elysee. Based on the dimensions of this ship, which can be seen in Appendix A, the total height of this vessel can be estimated to be 46 meters. When maintaining a clearance between the vessel and the crane of 1 meter and 3 meters between the crane and the top of the hall (space for the overhead crane beam and entrance path to perform maintenance), a total hall height between the dock chamber floor and the hall roof of 50 meters is necessary. A clearance of 40 meters above the hall floor is chosen. Thus, the hall has the following dimensions: A length of 155 m, a width of 50 meters and a height of 40 meters.

The requirements for the dock doors are mainly determined by the ability to keep the dock completely watertight, so minimization of the leakage discharge is crucial, and the possibility

to perform maintenance works to the door which is required every 5 years on average. For both the dock door and the filling/emptying system, speed of operation is a governing factor for this type of dock since it will mainly be used to perform works on damaged vessels that require a quick docking. The frequency of which the gate doors and filling/emptying systems need to be operated is considerably larger than for a dock that performs construction works and thus speed of operation plays a large role in choosing the optimal dock door.
Another requirement focuses on removing the inflowing sediment in a fast and effective way, since cleaning the dock floor is nowadays done manually, which delays the repair and maintenance works by a couple of days. This is unwanted since it leads to an increase in costs and reduces the capacity of the dock and so the requirement for the new dock is that a solution is found for removal of the inflowing sediment.
Finally, a solution must be found that enables the removal of the long propeller shaft of the vessel, which will be necessary for some construction works.

Appendix P: Stakeholder analysis

This appendix explains the decisions behind the scores for the stakeholder analysis, starting off with a definition of the terms ‘Interest’ and ‘Power’. The level of interest described how closely each stakeholder would want to monitor the progress of the project and this is mainly determined by the way in which the stakeholder is influenced, both in a positive and negative way. Examples of this influence are the effects of the dock to the environment, the job opportunities that are created and the potential boost to the local economy.
The amount of power that each stakeholder has is determined by its ability to make decisions or alter conditions that directly influence the project. For example, governmental institutes will have a large amount of power due to their right to hand out or withdraw permits. Local businesses might be interested in the increased opportunities for employment but they do not have the right to make any decisions. While the values for both of these parameters is estimated and thus leave room for discussion, the main aim of this stakeholder analysis is gain insights into the relative importance of each stakeholder and to summarize their role.

Damen Harlingen naturally is the main primary stakeholder in this project, as it acts as the client in the design and construction of the new graving dock. It serves as the investing party and has the major say in what the dock will look like, which facilities should be present and what the functions of the dock should be. Their interest in the project can be described as the need for an increased capacity that will be created by the construction of the dock. At the same time, Damen wants to minimize the costs as much as possible while complying with all the laws and regulations that are set out by other (governmental) stakeholders and it wants to create a certain support base within the group of stakeholders that is influenced by the presence of the new dock such as the neighboring companies within the port of Harlingen, the small and medium sized businesses in and around the Harlingen municipality, contractors and local residents. The interest in the project is naturally very high, this stakeholder’s power lies in determining the lay-out, facilities and overall design of the dock.

There are several governmental institutions that will have a say in the projects, each on a different scale, which all share the fact that they will act as a condition-creating party in the project. They will make sure that during the full design and construction process, all relevant laws are obeyed such as the ‘Wet milieubeheer’, which is the main environmental law on the protection of the existing nature (Rijkswaterstaat, 2022). The ‘Waterwet’ describes the main regulations regarding the quality of surface and ground waters, which is a very relevant topic for a graving dock due to the fact that waste waters are often present and need to be handled in an appropriate way. Besides monitoring whether all regulations all followed appropriately, the Harlingen municipality, wants to make sure that the new project fits into the zoning plan (bestemmingsplan) and the structural visions (structuurvisie) that exist. The most recent versions of these documents describes that the activities within the port should ‘be combined with the creation of jobs and value’ and that the acquisition of new assets should focus on ‘creating additional value to the port of Harlingen’. The municipality wants to develop the port into a versatile, safe, sustainable and smart port and the design of the new dock should fit these ideas (Arcadis, 2012). Furthermore, this stakeholder is interested in the boost to the local economy that the construction of the new dock might bring through the opportunities that are created for the small to medium sized businesses (the middle class) in and around the municipality. On the other hand, this party has some sort of a mediating function as the municipality would want to keep other stakeholders in the vicinity of the municipality, like the citizens, neighboring companies and environmental parties satisfied. It is therefore also important for this stakeholder that the nuisance to the environment that might be caused during the construction and use of the new dock are all obeying the regulations that exist. This stakeholder can be identified as both powerful, due to the rights to hand out and withdraw permits, and highly interested in the proceedings of the project.

The second governmental party that plays a role in this project is ‘Provinsje Fryslân’, together with ‘Wetterskip Fryslân’ which are the provincial government institution and provincial water board respectively. Many of the interests that this party has match those of the municipal party, in the sense that this party has interest in the boost of the local economy through increased employment opportunities that are created and the increase of the capacity of the Port of Harlingen. The role of this stakeholder with regards to the maintenance of environment is more extensive than for the municipality. Making sure the all environmental laws and the corresponding requirements with regards to emissions are followed is one of its main tasks, as well as handing out environmental permits that will play an essential role in the construction of the new dock due to its vicinity to the Wadden Sea. These tasks are carried out by the FUMO (Fryske Utfieringstsjinst Miljeu en Omjouwing), which is an executive organization created by the two aforementioned provincial institutes, that is responsible for the compliance of all environmental laws with regards to emissions that affect the air-, soil- and water quality as well as the acceptable noise emissions. It can be concluded that this stakeholder is powerful through its ability to withdraw permits and has high interest in the project.

The Waddenvereniging is a nature conservation organization that is committed to the protection of the Wadden Sea since its founding in 1965. On their website, the organization described itself as ‘private, independent and critical’, and ‘responding strongly to any development that takes place in or around the Wadden Sea’. The main interest in the project for this party is the effects that the realization of the new dock has on the conditions of the Wadden Sea, both in the short and long term. This stakeholder will be following the progress of this project closely since it influences a few of the ’10 major concerns’ that the organization describes on its website (Waddenvereniging, 2022). First of all, the organization sees danger in the large amount of navigation that takes place within the Wadden Sea on a daily basis. Accidents have happened in the past with container vessels and oil tankers and the Waddenvereniging is advocating for the prohibition of ‘environmentally dangerous shipping’ along the Wadden Sea. Furthermore, dredging of ports and shipping through the Wadden Sea leads to an increased turbidity of the water which is detrimental to algae growth and consequently the oxygen concentration in the water. Finally, the organization actively opposes the realizing of ‘polluting companies’ near the Wadden Sea. This stakeholder mainly aims to reach its goal by applying pressure/lobbying in local, regional and national governments and occasionally through legal opposition (Waddenvereniging, 2022). It can be concluded that this stakeholder will have great interest in the development and progress of the dock, but the amount of power can be considered to be relatively low since it doesn’t have the right to directly influence any decisions regarding the state of the project. This stakeholder would also be interested in extra tourism and awareness for the Wadden Sea area, so exploring possibilities to give back to the Wadden Sea through this way may prove to be worth it in order to keep this stakeholder satisfied.

The Port of Harlingen is responsible for maintaining the order in and regulating the use of the port, by imposing the so-called ‘Havenverordening’, which states rules that ensure the safety within the port itself. This party is therefore interested in the effect that the new dock will have on the use of the port, for example through the increased vessel intensity that will be created and the effects this has on the capacity of the port. The new dock should fit well into the existing port infrastructure and it should not intervene with the current regulations regarding the spatial distribution of the port, as is determined in the ‘Harbour Plan’ (Port of Harlingen, 2022). Similar to the earlier mentioned government institution, the role of the Port of Harlingen can be described to be of high interest and high power due to its condition-setting nature.

One of the secondary stakeholder are the inhabitants of Harlingen, whose main interest in the project is the creation of new employment opportunities by the realization of the dock, both during construction as well as a dock crew that handles the use of the dock during its lifetime. On the other hand, this stakeholder does not want to experience any nuisance in the form of noise, light or odor. While the port of Harlingen is relatively remote, there are no residential

areas in the vicinity of the new dock, it is still important to minimize the negative impact that the new dock might have on the inhabitants. In relative sense, both the interest in the project as well as the power that this stakeholder has can be described to be low.

Small and medium sized businesses in the area of Harlingen will be interested in the new employment opportunities and increase in economic development that the new dock might bring. For instance, the fact that additional vessel and operational crews will (temporarily) reside in Harlingen can bring an increase in revenue for these companies. The construction works can bring additional employment and revenue to the local contractors and construction companies. This stakeholder is considered to have a high interest in the project but a relatively low power.

The final stakeholder is the neighboring companies in the port of Harlingen, whose main interests is the fact that they don't want to experience nuisance from the presence of the new dock. The realization and operation of the new dock should not interfere with their own activities. This stakeholder will also be interested in the potential increase in revenue that is created. For example, a nearby crane rental company can be hired for the construction of the dock, which would both create a boost in revenues for this company and it would reduce the environmental impact of the construction phase by reducing the amount of transport that is needed. This stakeholder can described to be of low power but of medium to high interest in the project.

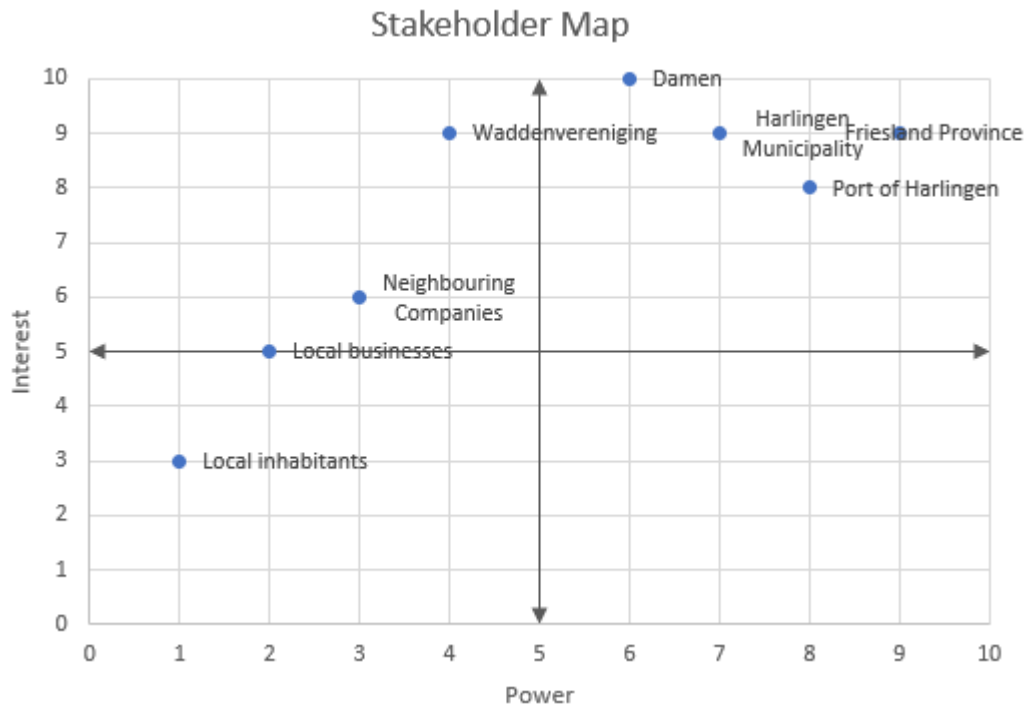

Figure P 1: Stakeholder map

Figure P1 shows the final stakeholder map.

Appendix Q: Dock head design

This appendix gives the design calculations behind the design of the dock head structure. The dock head structure will form the seat for the dock gate and has to be completely watertight. The structure will have a length of 12 meters, where the 2 meter wide gate is placed in the middle and so 5 meters of dock structure is placed on each side for stability purposes. Anchor piles are placed in 5 rows with a centre to centre distance of 3 meters, each row contains tension piles at a centre to centre distance of 2.4 meters and an edge distance of 1.8 meters which is in accordance with the tension pile plan of the dock chamber. The floor of the dock head is 1.5 meters thick and the walls have a thickness of 1 meter. A side view of the dock structure can be seen in figure Q1 below, including the governing water level on the outer side since this will be the design load situation.

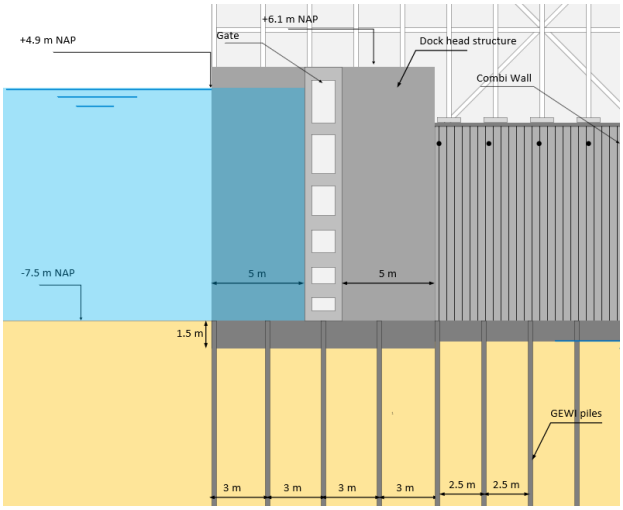

Figure Q 1: Dock head side view

The front view can be seen in Figure Q2.

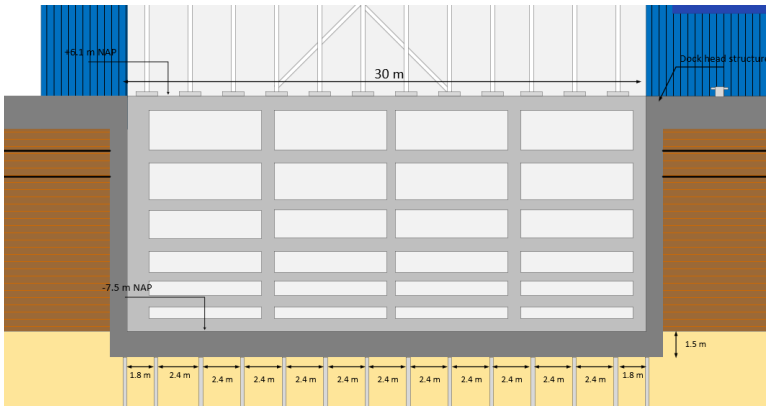

Figure Q 2: Dock head front view

The load on each tension pile row is determined by the stability of the dock head structure under the design load conditions, where the loads are the hydrostatic pressures acting on the gate, the upward water pressure underneath the structure, the self-weight of the gate and the self-weight of the dock head. The loading situation showing the hydrostatic loads on the structure can be seen in the figure underneath.

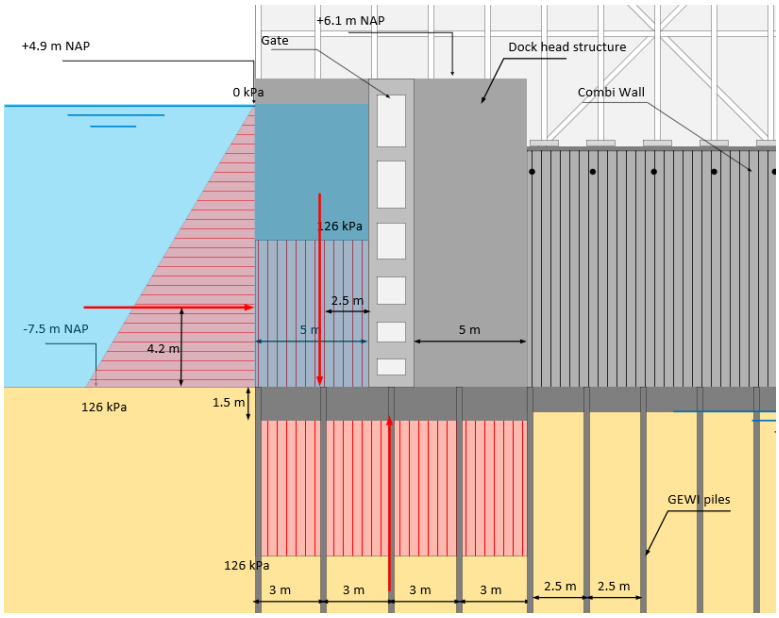

Figure Q 3: Hydrostatic loads on the dock head

Calculating the moments around the centre of the gate at the dock floor, the only forces causing a bending moment are the hydrostatic pressures acting on the outer side of the dock head.

Load	Value [kN/m']	Distance causing moment [m]	Moment [kNm/m']	Direction	Load type
Hydrostatic, left	$0.5*10*12.6^2$=794	4.2	3334	Right/clockwise	Variable
Hydrostatic left	5*10*12.6 = 630	3.5	2205	Down/counter clockwise	Variable
Upward water pressure	12*10*12.6 = 1512	-	-	Up	Variable
Gate s.w.	90	-	-	Down	Permanent
Dock head s.w.	425	-	-	Down	Permanent
ΣV	367 (Upward)	**ΣM**	1129 (Clockwise)		

The table shows the magnitude of all loads acting on the dock head, from which it can be concluded that an effective moment on the dock head in clockwise direction is present as well as an resulting upward load. The 5 rows of tension piles need to ensure both a rotational and vertical equilibrium, from the resulting forces on each pile row can be computed. The nett vertical loads is spread equally for each row resulting in a downward directed force of 367/5=73 kN/m'. For the rotational stability, each row is considered to contribute an equal bending moment, resulting in varying reaction forces per row, which can be seen in Figure Q4 below.

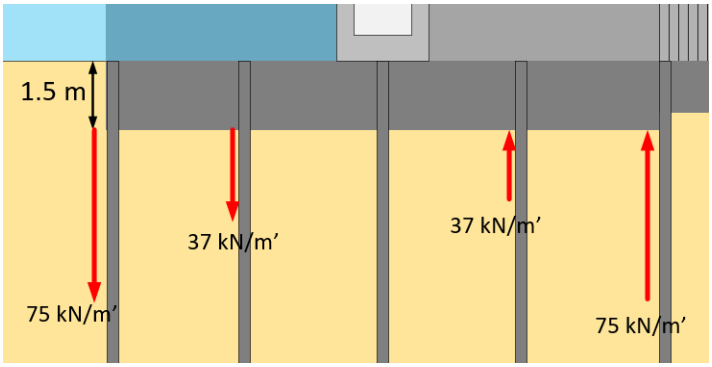

Figure Q 4: Reaction forces caused by moment

Combining these results in the final reaction forces in Figure Q5:

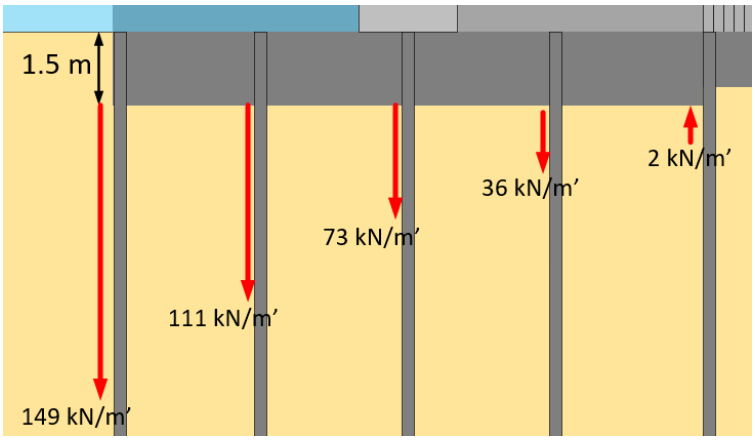

Figure Q 5: Total reaction forces (SLS)

After applying safety factor of 1.5 for variable loads and 1.35 for permanent load and performing the calculations again, the governing load on the tension pile row amounts to 238 kN/m' in downward direction meaning that the piles function as tension piles. Per pile the governing required load therefore amounts to 238*2.4=572 kN. This means that the maintained installation depth of -33 mNAP is sufficient and could even be reduced by a meter.

The horizontal equilibrium must be ensured by the frictional forces along the perimeter of the combiwall and the floor. The acting load is the hydrostatic force with a magnitude of roughly 800 kN/m' over a width of 30 meters. The resisting loads are determined using Rankine's model for soil pressures, which resulted in a resisting frictional force per m' of 780 kN/m' and since the length of the chamber is 5 times the width, it is concluded that the resisting force is larger than the acting force and so the horizontal equilibrium is guaranteed. Figure Q6 shows a screen shot of the calculation.

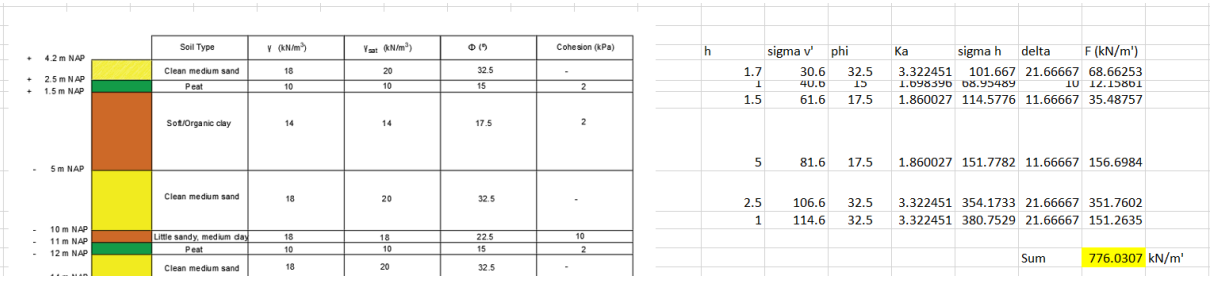

	Soil Type	γ (kN/m³)	γsat (kN/m³)	Φ (°)	Cohesion (kPa)
+ 4.2 m NAP					
	Clean medium sand	18	20	32.5	-
+ 2.5 m NAP	Peat	10	10	15	2
+ 1.5 m NAP					
	Soft/Organic clay	14	14	17.5	2
- 5 m NAP					
	Clean medium sand	18	20	32.5	-
- 10 m NAP					
- 11 m NAP	Little sandy, medium clay	18	18	22.5	10
- 12 m NAP	Peat	10	10	15	2
	Clean medium sand	18	20	32.5	-

h	sigma v'	phi	Ka	sigma h	delta	F (kN/m')	
1.7	30.6	32.5	3.322451	101.667	21.66667	68.66253	
1	40.6	15	1.698396	68.95489	10	12.15861	
1.5	61.6	17.5	1.860027	114.5776	11.66667	35.48757	
5	81.6	17.5	1.860027	151.7782	11.66667	156.6984	
2.5	106.6	32.5	3.322451	354.1733	21.66667	351.7602	
1	114.6	32.5	3.322451	380.7529	21.66667	151.2635	
					Sum	776.0307	kN/m'

Figure Q 6: Horizontal equilibrium calculation results

These results also form the basis for the strength and stiffness checks of the dock head floor, which takes the governing row of tension piles and the design load acting on it to calculate the required longitudinal and shear reinforcement and check the cracks and deformations. The loading scheme, M-line and V-line for both ULS and SLS conditions are shown in figure Q7 below.

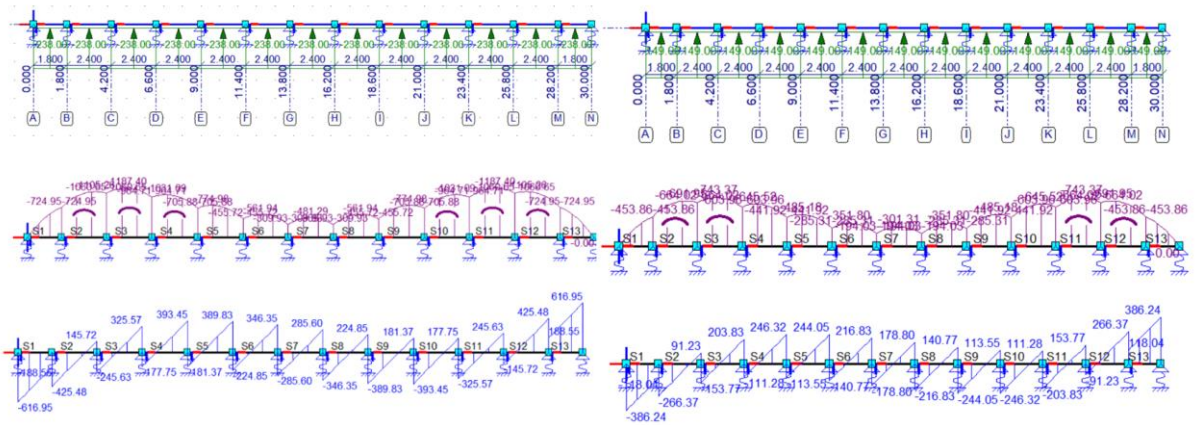

Figure Q 7: Loading schemes, M-lines and V-lines for ULS (left) and SLS conditions

For the ULS conditions, it is found that a φ20-100 configuration of longitudinal reinforcement is required in combination with φ12-200 configuration for the shear reinforcement. The cracking moment is not reach for SLS conditions and the maximum deflection is found to be 20 millimetres which is within the limits. All in all, this concludes the design of the dock head structure.